Cumulative Dissertation

On the Role of Trade-offs in Predator-Prey Interactions

for the degree of Dr. rer. nat.
Ecology

by Elias Ehrlich

Submitted to
Faculty of Science,
Institute of Biochemistry and Biology,
University of Potsdam

First supervisor:	**Evaluation**:
Prof. Dr. Ursula Gaedke	Prof. Dr. Ursula Gaedke
Second supervisor:	Prof. Dr. Thomas Kiørboe
Prof. Dr. Lutz Becks	Prof. Dr. Claus Rueffler

Potsdam, January 2019
Disputation: 08 April 2019

Published online at the
Institutional Repository of the University of Potsdam:
https://doi.org/10.25932/publishup-43063
https://nbn-resolving.org/urn:nbn:de:kobv:517-opus4-430631

Kumulative Dissertation

Trade-offs und ihre Bedeutung in Räuber-Beute Interaktionen

zur Erlangung des akademischen Grades Dr. rer. nat.
im Doktorstudium der Ökologie

von Elias Ehrlich

Eingereicht an der
Mathematisch-Naturwissenschaflichen Fakultät,
Institut für Biochemie und Biologie,
Universität Potsdam

Hauptbetreuerin:	**Begutachtung**:
Prof. Dr. Ursula Gaedke	Prof. Dr. Ursula Gaedke
Zweitbetreuer:	Prof. Dr. Thomas Kiørboe
Prof. Dr. Lutz Becks	Prof. Dr. Claus Rueffler

Potsdam, Januar 2019

Summary

Predation drives coexistence, evolution and population dynamics of species in food webs, and has strong impacts on related ecosystem functions (e.g. primary production). The effect of predation on these processes largely depends on the trade-offs between functional traits in the predator and prey community. Trade-offs between defence against predation and competitive ability, for example, allow for prey speciation and predator-mediated coexistence of prey species with different strategies (defended or competitive), which may stabilize the overall food web dynamics. While the importance of such trade-offs for coexistence is widely known, we lack an understanding and the empirical evidence of how the variety of differently shaped trade-offs at multiple trophic levels affect biodiversity, trait adaptation and biomass dynamics in food webs. Such mechanistic understanding is crucial for predictions and management decisions that aim to maintain biodiversity and the capability of communities to adapt to environmental change ensuring their persistence.

In this dissertation, after a general introduction to predator-prey interactions and trade-offs, I *first* focus on trade-offs in the prey between qualitatively different types of defence (e.g. camouflage or escape behaviour) and their costs. I show that these different types lead to different patterns of predator-mediated coexistence and population dynamics, by using a simple predator-prey model. In a *second* step, I elaborate quantitative aspects of trade-offs and demonstrates that the shape of the trade-off curve in combination with trait-fitness relationships strongly affects competition among different prey types: Either specialized species with extreme trait combinations (undefended or completely defended) coexist, or a species with an intermediate defence level dominates. The developed theory on trade-off shapes and coexistence is kept general, allowing for applications apart from defence-competitiveness trade-offs. *Thirdly*, I tested the theory on trade-off shapes on a long-term field data set of phytoplankton from Lake Constance. The measured concave trade-off between defence and growth governs seasonal trait changes of phytoplankton in response to an altering grazing pressure by zooplankton, and affects the maintenance of trait variation in the community. In a *fourth* step, I analyse the interplay of different trade-offs at multiple trophic levels with plankton data of Lake Constance and a corresponding tritrophic food web model. The results show that the trait and biomass dynamics of the different three trophic levels are interrelated in a trophic biomass-trait cascade, leading to unintuitive patterns of trait changes that are reversed in comparison to predictions from

bitrophic systems. *Finally*, in the general discussion, I extract main ideas on trade-offs in multitrophic systems, develop a graphical theory on trade-off-based coexistence, discuss the interplay of intra- and interspecific trade-offs, and end with a management-oriented view on the results of the dissertation, describing how food webs may respond to future global changes, given their trade-offs.

Zusammenfassung

Trophische Interaktionen sind von entscheidender Bedeutung für die Biodiversität in Ökosystemen und die daran gekoppelten Ökosystemfunktionen (z.B. Primärproduktion, Nährstoffkreislauf). Außerdem beeinflussen sie die Evolution und Populationsdynamiken von Arten. Die Wirkungsweise von trophischen Interaktionen auf diese Prozesse hängt dabei von den Trade-offs ab, denen Räuber und Beute z.B. auf Grund physiologischer Beschränkungen unterliegen. Als Trade-off wird die Kosten-Nutzen-Beziehung zwischen zwei oder mehr funktionellen Eigenschaften eines Organismus bezeichnet, so zum Beispiel das Einhergehen einer höheren Verteidigung gegen Fraß mit einer geringeren Konkurrenzfähigkeit um Ressourcen. Solche Trade-offs zwischen Verteidigung und Konkurrenzfähigkeit ermöglichen die Koexistenz von Beutearten mit verschiedenen Strategien (verteidigt oder konkurrenzfähig), was sich stabilisierend auf die gesamten Dynamiken im Nahrungsnetz auswirken kann. Obwohl die Annahme weit verbreitet ist, dass Trade-offs die Koexistenz von Arten fördern, mangelt es am Verständnis und an empirischen Nachweisen, wie sich die Vielzahl unterschiedlich geformter Trade-offs von Arten verschiedener trophischer Ebenen auf die Biodiversität, die Anpassung von funktionellen Eigenschaften und die Biomassedynamik in Nahrungsnetzen auswirkt. Solch ein Verständnis ist jedoch entscheidend für die Vorhersagen und Managemententscheidungen bezüglich des Erhalts von Biodiversität, die das Anpassungspotential von Artengemeinschaften an zukünftige Veränderung in der Umwelt und damit das Überdauern von Artengemeinschaften langfristig sicherstellt.

Die hier vorliegende Dissertation startet mit einer kurzen Einführung in die Rolle von Räuber-Beute-Beziehungen und Trade-offs in Ökosystemen. In einem *ersten* Schritt, lege ich den Fokus zunächst auf Trade-offs in Beutegemeinschaften zwischen qualitativ verschiedenen Verteidigungsmechanismen (z.B. Tarnung oder Fluchtverhalten) und -kosten, und zeige anhand von einfachen Räuber-Beute Modellen, wie sich diese Mechanismen hinsichtlich ihrer Wirkungsweise auf die Koexistenz und die Populationsdynamiken von Beutearten unterscheiden. Als *Zweites* konzentriert sich die Dissertation dann auf quantitative Aspekte der Trade-offs. So wird aufgezeigt, wie die Form der Trade-off-Kurve bei verschiedenen Beziehungen zwischen funktionellen Eigenschaften und der Fitness den Ausgang von Konkurrenzprozessen innerhalb von Beutegemeinschaften beeinflusst. Dabei kann es in Abhängigkeit von der Form der Trade-

off-Kurve entweder zu Koexistenz von spezialisierten Arten kommen (unverteidigt oder komplett verteidigt) oder aber zur Dominanz einer Art mit mittlerer Verteidigung. Der *dritte* Schwerpunkt dieser Arbeit liegt dann auf dem Test der Theorie zur Trade-off-Kurve und Koexistenz anhand von Langzeitfelddaten des Phytoplanktons im Bodensee. Es zeigt sich hierbei, dass der gefundene konkave Trade-off zwischen Verteidung und Wachstumsrate in Kombination mit einem sich verändernden Fraßdruck durch das Zooplankton die Anpassung von funktionellen Eigenschaften und den Erhalt von Variation dieser Eigenschaften innerhalb der Phytoplanktongemeinschaft steuert. In einem *vierten* Schritt, analysiere ich das Zusammenspiel von Trade-offs auf mehreren trophischen Ebenen, basierend auf Phyto- und Zooplanktondaten aus dem Bodensee und einem dafür entwickelten tritrophischen Nahrungsnetzmodell. Die Ergebnisse zeigen, dass die Dynamiken der funktionellen Eigenschaften und Biomassen durch eine Kaskade über die drei trophischen Ebenen hinweg gekoppelt sind, die zu unintuitiven Mustern in den Anpassungen der funktionellen Eigenschaften zwischen den Ebenen führt. In der generellen Diskussion bringe ich *abschließend* die Ideen zur Wirkung von Trade-offs in multitrophischen System in einen breiteren Kontext. Zudem entwickle ich eine generelle graphische Theorie zur Trade-off basierten Koexistenz in Abhängigkeit von der Fitnesslandschaft, diskutiere das mögliche Zusammenspiel von intra- und interspezifischen Trade-offs, und gebe schlussendlich einen Management-orientierten Einblick in die Relevanz der Ergebnisse dieser Dissertation für das Verhalten von Nahrungsnetzen im Zuge des Globalen Wandels unter der Wirkung von Trade-offs.

Contents

1 General introduction

1.1 The role of predator-prey interactions in ecosystems

In the vastness of the savanna or even in a tiny drop of water, living organisms struggle for their survival, like zebras being attacked by lions or bacteria being eaten by protists. Such *predator-prey interactions* are central components of almost every ecosystem. They interconnect species in food webs, govern the flow of energy among trophic levels and have strong impacts on ecosystem structure and functions (e.g. production or nutrient cycling). Climate change and anthropogenic stress (e.g. fishing) can alter predator-prey interactions with potentially devastating consequences for the ecosystem functions and human well-being (Petchey et al. 1999; Jackson et al. 2001; Tylianakis et al. 2008; Hoegh-Guldberg and Bruno 2010). Therefore, mechanistic understanding and predictions of how altered trophic interactions affect ecosystems are of fundamental importance for finding appropriate management decisions maintaining ecosystem functions under global change.

The pivotal role of predators in ecosystems often only becomes visible in their absence (e.g. predator extinction) or when invasive predators emerge, having strong impacts on *biodiversity* and related ecosystem functions (Doherty et al. 2016; Atwood and Hammill 2018). For example, in the coastal areas of Alaska, the absence of sea otters (*Enhydra lutris*) leads to the deforestation of huge kelp forests due to strong herbivory of sea urchins which are released from top-down control (Estes and Palmisano 1974; Estes and Duggins 1995). Hence, sea otters, as predators of sea urchins, are crucial for the maintenance of kelp forests and thus for the diversity of species relying on these unique habitats (Steneck et al. 2002). On the contrary, the invasion of the predatory brown tree snake (*Boiga irregularos*) on Guam has strongly reduced diversity in the avifauna (Savidge 1987). Native bird species on this island lacked coevolution with predators which prevented development of appropriate defence traits, rendering them highly vulnerable to predation by an invasive predator (Wiles et al. 2003). Consequently, this invasive snake with its broad prey spectrum has driven many bird species to extinction, which implicitly highlights the fundamental role of *trait adaptation* in predator-prey systems for the persistence of communities.

Predator-prey interactions do not only affect the survival of species, but also their

population dynamics. They may cause population cycles (May 1972) resulting in fluctuating availability of certain ecosystem functions (e.g. primary production or nutrient cycling), which can be seen in an example from the aquatic realm: In temperate, meso- and eutrophic lakes, water turbidity typically changes among the seasons. First, it increases in spring and then suddenly decreases in early summer, resulting in a 'clear-water phase', before it increases again during summer. These dynamics in water turbidity are caused by a predator-prey cycle between zooplankton and light-absorbing algae (Sommer et al. 2012), which reveals that predator-prey interactions can even modify the physical conditions in ecosystems.

These three examples on sea otters, an invasive snake and plankton demonstrate the high relevance of studying predator-prey interactions for multiple ecological and evolutionary disciplines, i.e. biodiversity research, conservation biology, trait-based ecology, evolutionary biology, community and population ecology. A mechanistic understanding of how predator-prey interactions shape their environment is crucial for ecosystem management, and demands the development of general theory in all these disciplines, holding preferably independent of the type of organism, that is, for lions as well as for protist.

1.2 Functional traits and trade-offs of predator and prey

The effect of trophic interactions on biodiversity, evolution and population dynamics depends on the strength of the interactions between predator and prey (McCann et al. 1998), which is determined by their functional traits. A functional trait is 'a well-defined, measurable property of organisms, usually measured at the individual level and used comparatively across species [...] that strongly influences organismal performance' (McGill et al. 2006). Prey performance (i.e. fitness) largely depends on predation-induced losses. Hence, under high grazing pressure, selection in prey typically favors functional traits attenuating the interaction strength, that is, defensive traits reducing the probability of being consumed. In contrast, selection in predators works towards the opposite, i.e. intensifying the interaction, and promotes offensive traits (counter-defences) increasing the probability of prey consumption. Usually, a beneficial change of one trait (e.g. defence) comes at the cost of a detrimental change of another trait (e.g. growth rate), due to energetic, physiological, genetic or resource allocation constraints (Stearns 1989). Such *trade-offs between functional traits* prevent the occurrence of a 'superspecies' being optimal regarding all traits (Kneitel and Chase 2004), for example, a completely defended prey with maximal competitiveness for all resources. Hence, these trade-offs are crucial

for coexistence and trait adaptation in predator-prey communities.

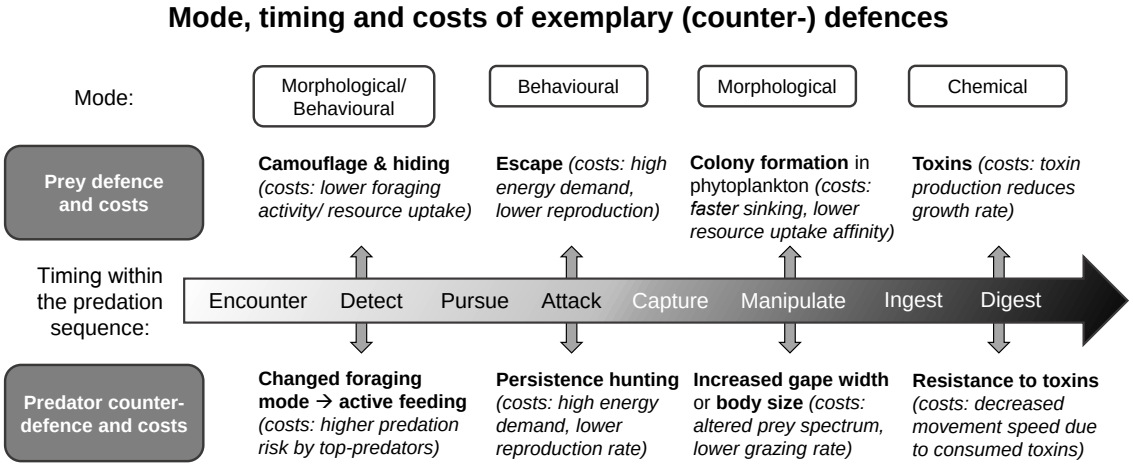

Figure 1.1: Mode, timing and costs of exemplary prey defences and corresponding counter-defences of the predator. Defence and counter-defence mechanisms can be classified into behavioural, morphological or chemical mechanisms (mode), and can act at different phases of the predation sequence (timing).

A huge variety of prey defence mechanisms with different costs exists. These mechanisms may act at different phases of the predation sequence (Weiss et al. 2012; Bateman et al. 2014), decreasing the probability of being encountered, detected, pursued, attacked, captured, manipulated, ingested or digested (Lima and Dill 1990). Plants and animals exhibit morphological or chemical defences, while typically animals (and some autotrophs, e.g. motile phytoplankton) have the additional option to defend by altering their behaviour (Boukal 2014; Pančić and Kiørboe 2018). Figure 1.1 displays several examples of defence mechanisms with different modes (behavioural, morphological, chemical), timing (phase of predation sequence) and costs. Alternative strategies of being resistant to predation are either to tolerate grazing by growing fast, which is only possible under high food supply for the prey (Koffel et al. 2018), or to call an enemy (parasite or consumer) of the predator, widely known from plants emitting volatiles (Kessler and Baldwin 2001). Predators show different strategies to overcome prey defence by changing their behaviour and morphology, or by chemical responses, e.g. to counter toxins (Karban and Agrawal 2002). Such counter-defence mechanisms are often specific to certain prey defence mechanisms and have specific costs (Brodie and Brodie 1990), for examples see Figure 1.1. In many cases, predator counter-defence against prey (e.g. active feeding) trades off with defence against a top-predator, implying a foraging-predation risk trade-off (Lima et al. 1985; Verdolin 2006; Kiørboe 2011), which indirectly links lower and upper trophic levels in food webs.

To classify such trade-offs, we can use three major trade-off characteristics: the type, the shape and the dimensionality (Fig. 1.2). Trade-offs differ in their type when they

involve different functional traits (Fig. 1.2), for example, two defence-growth trade-offs involving two different defence traits such as camouflage colouration or escape speed. As shown in Figure 1.1, a multitude of such different types of trade-offs exists in predator-prey systems. The way in which constraints link different traits to each other determines the shape of the trade-off (Fig. 1.2). For a trade-off between two traits (x and y), the shape may be convex ($\partial^2 y/\partial x^2 > 0$), linear ($\partial^2 y/\partial x^2 = 0$), concave ($\partial^2 y/\partial x^2 < 0$) or more complex with different implications for the direction of selection and coexistence of species (HilleRisLambers and Dieckmann 2003; de Mazancourt and Dieckmann 2004; Rueffler et al. 2004; Jones et al. 2009). Much theory is built on two-dimensional trade-offs (e.g. Sibly and Calow 1983; Abrams 2006; Våge et al. 2014), but they may even be multidimensional (Edwards et al. 2011), i.e. constraints link more than two functional traits (Fig. 1.2). For example, colony formation in phytoplankton may trade off with sinking rate and light affinity (Lürling and Van Donk 2000).

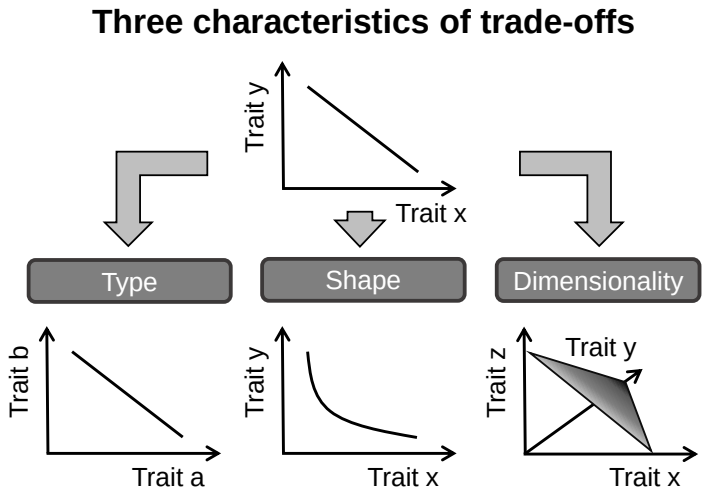

Figure 1.2: Trade-offs can be classified according to three different characteristics: the type describes which traits trade off, the shape specifies how the traits are related and the dimensionality determines how many traits are involved.

Furthermore, trade-offs between functional traits exist at different hierarchical levels (Litchman et al. 2015): At the individual level among organisms of the same species (intraspecific trade-offs) or among species in a community sharing similar constraints (interspecific trade-offs). Intraspecific trade-offs define the potential range of trait combinations accessible by phenotypic plasticity or evolution of species, and may allow for allopatric speciation by evolutionary branching (de Mazancourt and Dieckmann 2004; Rueffler et al. 2004). Interspecific trade-offs form a fundamental basis of species coexistence and determine how community composition changes under altered environmental conditions (Tilman 2000). Given interspecific trade-offs, no species can be optimal with respect to all traits leading to a diversification of strategies (Kneitel and

Chase 2004).

1.3 Biodiversity, predation and trade-offs

Around 3.5 billion years ago, the first living organisms on earth were bacteria. Biodiversity was low and trophic interactions among organisms likely did not exist at the beginning of life on earth. The evolution of predation started probably much later, but likely increased biodiversity on earth due to the wide range of possible niches arising from predator specialization on different prey species and from prey defending against such predation (Bengtson 2002). The occupation of these niches led to periods of strong evolutionary radiation, such as the cambrium explosion where many arthropod and mollusc species emerged (Marshall 2006). Numerous trophic interactions have evolved since that time, conglomerated in complex food webs. The resulting high biodiversity observed today positively correlates with many ecosystem functions and enhances the persistence of ecosystems under global change (Tilman et al. 2014; Soliveres et al. 2016; Acevedo-Trejos et al. 2018). This underlines the importance of studying biodiversity in food webs and the role of trade-offs promoting coexistence.

If multiple predators specialize on different resources (prey species), they may stably coexist (May 1974), i.e. each predator can invade back into the system in case of reduction to very low densities (Chesson 2000). Such stable coexistence is promoted by a trade-off between different resource use efficiencies. However, depending on the shape of the trade-off, generalists may occur and outcompete the specialists or coexist with them if resources are fluctuating (Abrams 2006; Rueffler et al. 2006). Even on one shared resource, two predator species are able to stably coexist under resource fluctuations if they face a 'gleaner-opportunist' trade-off (Abrams 2004). Such a trade-off implies relative non-linearity in the functional responses, meaning that one predator is superior (i.e. grazes faster) at low resource densities while the other is superior at high resource densities (Armstrong and McGehee 1980).

Numerous studies have aimed to reveal how predation shapes prey diversity and have produced partly contrasting results, i.e. predation may either enhance or decrease prey coexistence (reviewed in Chase et al. 2002). Given a trade-off between defence and competitive ability, predators are able to promote prey coexistence by suppressing the competitively superior prey which would outcompete the defended prey in predator absence. This coexistence mechanism is well-known as 'predator-mediated coexistence' (Abrams 1999; Ciros-Pérez et al. 2004), 'keystone predation' (Paine 1966; Menge et al. 1994; Leibold 1996) or 'killing the winner' (Thingstad 2000; Winter et al. 2010). Furthermore, predation promotes coexistence when the predator switches its preference always to the temporally dominant prey and disregards rare prey species (Murdoch 1969;

Abrams 1999; Prowe et al. 2012). However, if such switching behaviour and defence-competitiveness trade-offs are absent in the community or if defence is very costly in the face of poor resource conditions, predation decreases prey diversity and even accelerates extinction by increasing the overall mortality of prey (Proulx and Mazumder 1998; Chase et al. 2002). This holds especially for non-switching predators with a high generality (broad prey spectrum), which sustain a high grazing pressure on their favourite prey species even if it has a very low densities by additionally feeding on other species (Holt 1977). In mutlitrophic food webs, predators at higher trophic levels may also have cascading effects on the diversity of trophic levels below that of their prey (Donohue et al. 2017). For example, when carnivores reduce herbivore biomass, the diversity of primary producers may increase (Bruno and O'Connor 2005).

1.4 Trait adaptation in predator-prey systems

Biodiversity and the maintenance of trait variation provide the basis for future trait adaptation in food webs and their persistence under environmental change (Petchey et al. 1999). Trait adaptation can proceed on the species or community level, and may be restrained by intra- or interspecific trade-offs, respectively.

The two main mechanisms of intraspecific trait adaptation are evolution and phenotypic plasticity (Cortez 2011; Kovach-Orr and Fussmann 2012). Evolution may proceed from sorting of genotypes in species with standing genetic variation, genetic drift, from de novo mutations or recombination in sexually reproducing species. Predation is often a strong selective force driving evolution of prey defences (Reznick et al. 2008; Becks et al. 2010; Terhorst et al. 2010). Given an intraspecific trade-off, the increase in prey defence in response to predation is limited and may even reverses if predator densities drop to minimize costs imposed along other trait axes, e.g. competitiveness (Agrawal et al. 2012; DeMott and McKinney 2015). Research in the last two decades has shown that such back-and-forth evolutionary processes in the prey can happen on short, ecological time scales, which allows for eco-evolutionary feedbacks (Fussmann et al. 2003; Hairston et al. 2005; Becks et al. 2010). Evolution of the prey defence may entail evolution of predator counter-defences, resulting in an evolutionary arms race (Brodie and Brodie 1999; Cortez and Weitz 2014). The occurrence of these arms races depends on the relative speed of adaptation in predator and prey (van Velzen and Gaedke 2017). Empirical evidence of such coevolution is limited. Hiltunen and Becks (2014) observed coevolution of bacteria and ciliates in short-term microcosm experiments, while Palkovacs and Post (2008, 2009) observed such co-evolution even in the field, the gape width of landlocked alewifes evolved in response to size adaptation of crustacean zooplankton. As sustained prey defence is often costly, certain species show inducible defences, i.e. individuals

are phenotypically plastic (Agrawal 1998; Trussell and Nicklin 2002; Van Donk et al. 2011). This allows individuals to quickly respond to increasing or decreasing grazing pressure by inducing or reducing defence (e.g. colony formation) in order to optimize fitness along a trade-off (Ramos-Jiliberto 2003). However, phenotypic plasticity per se is often associated with additional costs for maintaining the sensory or regulatory machinery (DeWitt et al. 1998).

Describing the composition of communities or trophic levels in terms of functional traits, instead of taxonomy, is the core of trait-based approaches (McGill et al. 2006; Litchman and Klausmeier 2008; Litchman et al. 2013). Trait adaptation in communities in response to altered environmental conditions relies on sorting of species with different trait values, similar to the evolution of asexually reproducing species by genotype sorting. Invasion of species in a community context are equivalent to de novo mutations within species, and biomass-trait feedbacks among trophic levels behave similarly to eco-evolutionary feedbacks among predator and prey species. Therefore, concepts and theory on evolution of species can be partly transferred to the community level and backwards. Community trait adaptation has been shown, for example, for phytoplankton communities where high grazing pressure increased the frequency of defended species while interspecific trade-offs cause a reduction of that frequency at low predator densities and bottom-up control (Leibold 1999; Sommer et al. 2012). Kenitz et al. (2017) could even demonstrate co-adaptation between two trophic levels with multiple species at each trophic level (mobility in protists and foraging mode of predatory copepods). Tirok and Gaedke (2010) found similar patterns of co-adaptation between phytoplankton and ciliate communities. However, co-adaptation on multiple trophic levels in complex natural food webs remains underexplored.

1.5 Population dynamics

The way in which populations vary over time may determine the rhythm in which certain ecosystem functions increase or decrease (Lipson et al. 1999; Yang 2004; Cornulier et al. 2013). The population dynamics of a species may be stationary, cyclic or chaotic. These different types of population dynamics have strong implications for the predictability of ecosystem functions and for biodiversity. Given high amplitude cycles with low minima, species are threatened by stochastic extinctions (Pimm et al. 1988; Inchausti and Halley 2003), reducing biodiversity, which is not the case for stationary or temporally less variable dynamics. Fluctuations in population densities are driven either externally, e.g. via fluctuations in abiotic conditions, or internally, e.g. via biotic interactions (Berryman 2002).

Predator-prey cycles represent a famous example of such internally driven cycles.

These cycles can lead to a periodical release of previously fixed nutrients in ecosystems (Elser and Urabe 1999; Vanni 2002; Schmitz et al. 2010) and continuously alter the importance of competition in prey communities (Leibold 1996; Bohannan and Lenski 2000; Sommer et al. 2012). However, it depends on the productivity of a system whether predator-prey interactions cause cycles or not (May 1972; McCauley et al. 1999). An increasing productivity enhances cycles but does not necessarily increase predator biomass, which is known as the paradox of enrichment (Rosenzweig 1971). Given a certain temporal mean prey density, the average performance of a predator is lower under cycles in prey density compared to constant prey densities if the predator exhibits a saturating (type II) functional response (Abrams and Roth 1994). This phenomenon is known as Jensen's inequality (Jensen 1906).

Predator-prey cycles are often characterized according to the phase relationship between prey and predator, the period length and the amplitudes. The classic assumption is that predator densities follow prey densities with a quarter phase lag. However, the effect of stage structure (De Roos and Persson 2003), a third trophic level (Guill et al., *in prep.*) or trait adaptation may alter these phase relationships (Vos et al. 2004; Mougi and Iwasa 2010; Mougi 2012). For example, rapid evolution of prey defence is able to cause antiphase cycles with large period lengths, given a trade-off between defence and competitiveness (Yoshida et al. 2003; Becks et al. 2010; Hiltunen et al. 2014). Further outcomes of such prey evolution may be stationary dynamics or cryptic cycles (the predator cycles but not the prey), depending on the difference in the defence level among genotypes and the defence costs (Jones and Ellner 2007; Yoshida et al. 2007). Coevolution of predator and prey may even cause reversed cycles with the prey biomass following that of the predator, depending on the speed of adaptation and the trade-offs (Cortez and Weitz 2014; van Velzen and Gaedke 2018).

In natural food webs with many interacting species, population dynamics can be far more complex, depending on the food web structure (Ceulemans et al., *under review*). However, theory suggests that certain patterns hold independently of the type of food web. For example, weak trophic interactions often stabilize the population dynamics in food webs (McCann et al. 1998; Kondoh 2007), which may be promoted by trade-offs between defence and resource consumption (Kretzschmar et al. 1993; Abrams and Walters 1996). If prey increases in defence, the strength of interaction to its predator is low, but also the interaction to its resource is weak due to the low resource uptake rate coming along with higher defence.

To handle complexity in food webs, we can abstract from the species level and focus on the general dynamics of trophic levels. The dynamics of trophic levels can be affected by standing trait variation (species diversity), similar to how the population dynamics of one predator and one prey species are affected by genetic variation and evolution (genotype

diversity). Analogous to genotype sorting which alters population dynamics, dynamics of trophic levels are driven by species sorting (Abrams and Vos 2003). This may allow again a transfer of knowledge from the species to the community level.

1.6 Thesis overview

This thesis is divided into four publication-based chapters (Chapter 2-5) and examines how trade-offs between functional traits affect predator-prey interactions and shape i) coexistence, ii) trait adaptation and iii) population dynamics in food webs (Fig. 1.3). The chapters investigate these effects for two different characteristics of a trade-off, i.e. its type or shape (Fig. 1.2), or for trade-offs at multiple trophic levels (Fig. 1.3).

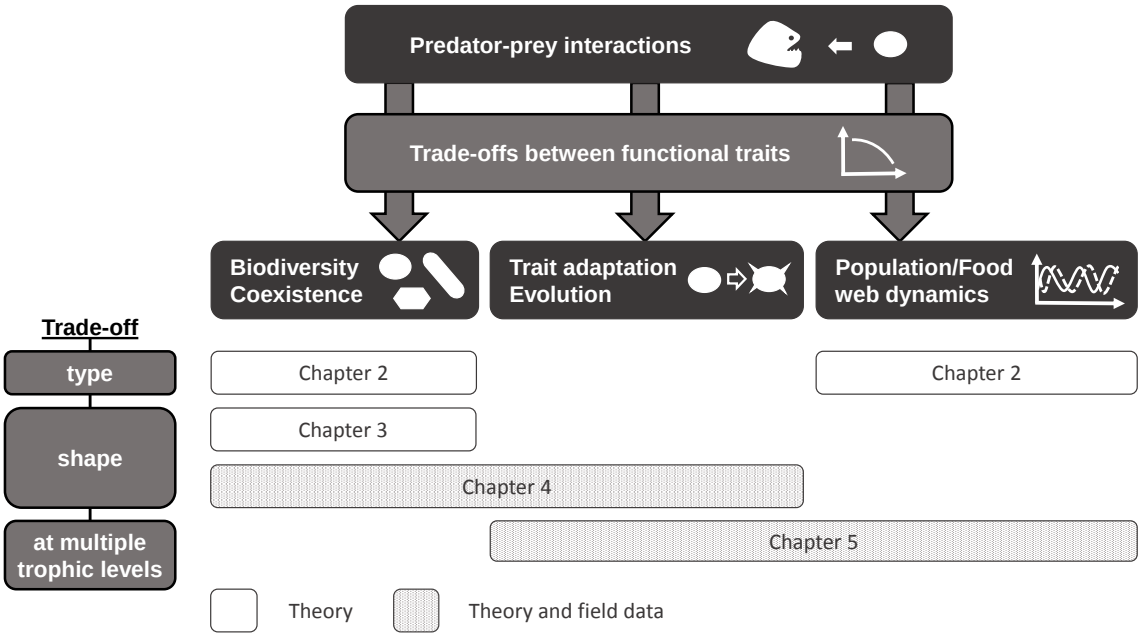

Figure 1.3: Thesis overview. The central question of this thesis is how trade-offs between functional traits affect the impacts of predator-prey interactions on three different ecological/evolutionary aspects, that is, biodiversity/coexistence, trait adaptation/evolution and population/food web dynamics. Each of the four chapters focusses on one or two of these aspects and examines how they depend on two different characteristics of a trade-off, i.e. its type and shape (Fig. 1.2, for dimensionality as a third characteristic see the general discussion), or on trade-offs at multiple trophic levels. The first two chapters (2, 3) are theoretical studies while Chapter 4 and 5 combine theory and analyses of long-term field data.

In *Chapter 2*, I explore how different types of prey trade-offs with different defence mechanisms and costs affect predator-mediated coexistence and population dynamics (steady-state or cycles) in a two-prey-one-predator system, based on mathematical analyses of a corresponding food web model (Fig. 1.4).

In *Chapter 3*, I develop a general theory on how trade-off shapes in combination with

different trait-fitness relationships determine species coexistence, and apply this theory to a predator-prey model with a defence-competitiveness trade-off in the prey (Fig. 1.4).

In *Chapter 4*, this theory on the effect of trade-off shapes on coexistence and trait adaptation is tested with long-term phytoplankton data from Lake Constance. To increase the understanding of the observed, seasonally changing dominance of different phytoplankton species facing a defence-growth trade-off, I performed numerical simulations of a food web model involving different phytoplankton species as prey and herbivorous zooplankton as predator (Fig. 1.4)

In *Chapter 5*, I present theory and analyse plankton field data (Lake Constance) on interrelated biomass-trait dynamics governed by trade-offs at multiple trophic levels. The observed dynamics are reproduced by a tritrophic food web model which involves the major functional groups of plankton (Fig. 1.4) and provides mechanistic insights on a trophic biomass-trait cascade that becomes apparent in the data.

In the *general discussion*, at first, I summarize ideas on the role of trade-offs in food webs as mediators of trophic cascades. Secondly, I develop a graphical theory on trade-off-based coexistence in different fitness landscapes, inspired by the investigations presented in Chapters 2-4, and include also trade-offs with higher dimensionality (Fig. 1.2). Thirdly, I extend the theory by additionally considering intraspecific trade-offs underlying an interspecific trade-off. Finally, I take a management-oriented view and draw conclusions on how trade-offs and predator-prey interactions govern the response of food webs to global changes.

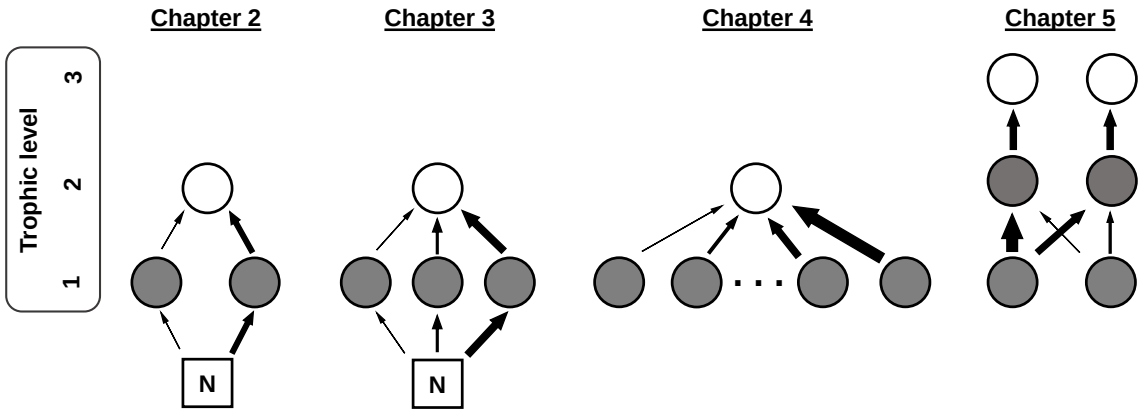

Figure 1.4: Overview on food web models used in the different chapters. The food webs involve species or functional groups (circles) at two or three trophic levels. The chapters focus on trade-offs at the first (prey), or at the first and the second trophic level (predator), as indicated by grey circles. Species or functional groups at the first trophic level either explicitly (box with N) or implicitly compete for a shared resource (no box). Arrows display trophic interactions and resource uptake, their thickness indicates the strength of these interactions.

Bibliography 1

Abrams, P. A. (1999). Is predator-mediated coexistence possible in unstable systems? *Ecology*, 80(2):608–621.

Abrams, P. A. (2004). When does periodic variation in resource growth allow robust coexistence of competing consumer species? *Ecology*, 85(2):372–382.

Abrams, P. A. (2006). Adaptive change in the resource-exploitation traits of a generalist consumer: the evolution and coexistence of generalists and specialists. *Evolution*, 60(3):427–439.

Abrams, P. A. and Roth, J. (1994). The responses of unstable food chains to enrichment. *Evolutionary Ecology*, 8(2):150–171.

Abrams, P. A. and Vos, M. (2003). Adaptation, density dependence and the responses of trophic level abundances to mortality. *Evolutionary Ecology Research*, 5:1113–1132.

Abrams, P. A. and Walters, C. J. (1996). Invulnerable Prey and the Paradox of Enrichment. *Ecology*, 77(4):1125–1133.

Acevedo-Trejos, E., Marañón, E., and Merico, A. (2018). Phytoplankton size diversity and ecosystem function relationships across oceanic regions. *Proceedings of the Royal Society B: Biological Sciences*, 285(1879):20180621.

Agrawal, A. A. (1998). Induced Responses to Herbivory and Increased Plant Performance. *Science*, 279(5354):1201–1202.

Agrawal, A. A., Hastings, A. P., Johnson, M. T. J., Maron, J. L., and Salminen, J.-P. (2012). Insect Herbivores Drive Real-Time Ecological and Evolutionary Change in Plant Populations. *Science*, 338(6103):113–116.

Armstrong, R. A. and McGehee, R. (1980). Competitive Exclusion. *The American Naturalist*, 115(2):151–170.

Atwood, T. B. and Hammill, E. (2018). The Importance of Marine Predators in the Provisioning of Ecosystem Services by Coastal Plant Communities. *Frontiers in Plant Science*, 9(September):1–7.

Bateman, A. W., Vos, M., and Anholt, B. R. (2014). When to Defend: Antipredator Defenses and the Predation Sequence. *The American Naturalist*, 183(6):847–855.

Becks, L., Ellner, S. P., Jones, L. E., and Hairston Jr., N. G. (2010). Reduction of adaptive genetic diversity radically alters eco-evolutionary community dynamics. *Ecology Letters*, 13(8):989–997.

Bengtson, S. (2002). Origins and Early Evolution of Predation. *Paleontological Society Papers*, 8(8):289–318.

Berryman, A. (2002). *Population Cycles: Causes and analyses*. Oxford University Press, Oxford (United Kingdom).

Bohannan, B. J. M. and Lenski, R. E. (2000). The Relative Importance of Competition and Predation Varies with Productivity in a Model Community. *The American Naturalist*, 156(4):329–340.

Boukal, D. S. (2014). Trait- and size-based descriptions of trophic links in freshwater food webs: current status and perspectives. *Journal of Limnology*, 73(s1):171–185.

Brodie, E. D. I. and Brodie, E. D. J. (1990). Tetrodotoxin Resistance in Garter Snakes: An Evolutionary Response of Predators to Dangerous Prey. *Evolution*, 44(3):651–659.

Brodie, E. D. I. and Brodie, E. D. J. (1999). Predator – Prey Arms Races: Asymmeterical selection on predators and prey may be reduced when prey are dangerous. *BioScience*, 49(July):557–568.

Bruno, J. F. and O'Connor, M. I. (2005). Cascading effects of predator diversity and omnivory in a marine food web. *Ecology Letters*, 8(10):1048–1056.

Chase, J. M., Abrams, P. A., Grover, J. P., Diehl, S., Chesson, P., Holt, R. D., Richards, S. A., Nisbet, R. M., and Case, T. J. (2002). The interaction between predation and competition: a review and synthesis. *Ecology Letters*, 5(2):302–315.

Chesson, P. (2000). Mechanisms of Maintenance of Species Diversity. *Annual Review of Ecology and Systematics*, 31(1):343–366.

Ciros-Pérez, J., Carmona, M. J., Lapesa, S., and Serra, M. (2004). Predation as a factor mediating resource competition among rotifer sibling species. *Limnology and Oceanography*, 49(1):40–50.

Cornulier, T., Yoccoz, N. G., Bretagnolle, V., Brommer, J. E., Butet, A., Ecke, F., Elston, D. A., Framstad, E., Henttonen, H., Hornfeldt, B., Huitu, O., Imholt, C., Ims, R. A., Jacob, J., Jedrzejewska, B., Millon, A., Petty, S. J., Pietiainen, H., Tkadlec, E., Zub, K., and Lambin, X. (2013). Europe-Wide Dampening of Population Cycles in Keystone Herbivores. *Science*, 340(6128):63–66.

Cortez, M. H. (2011). Comparing the qualitatively different effects rapidly evolving and rapidly induced defences have on predator-prey interactions. *Ecology Letters*, 14(2):202–209.

Cortez, M. H. and Weitz, J. S. (2014). Coevolution can reverse predator-prey cycles. *Proceedings of the National Academy of Sciences of the United States of America*, 111(20):7486–91.

de Mazancourt, C. and Dieckmann, U. (2004). Trade-Off Geometries and Frequency-Dependent Selection. *The American Naturalist*, 164(6):765–778.

De Roos, A. M. and Persson, L. (2003). Competition in size-structured populations: Mechanisms inducing cohort formation and population cycles. *Theoretical Population Biology*, 63(1):1–16.

DeMott, W. R. and McKinney, E. N. (2015). Use it or lose it? Loss of grazing defenses during laboratory culture of the digestion-resistant green alga Oocystis. *Journal of Plankton Research*, 37(2):399–408.

DeWitt, T. J., Sih, A., and Wilson, D. S. (1998). Costs and limits of phenotypic plasticity. *Trends in Ecology & Evolution*, 13(2):77–81.

Doherty, T. S., Glen, A. S., Nimmo, D. G., Ritchie, E. G., and Dickman, C. R. (2016). Invasive predators and global biodiversity loss. *Proceedings of the National Academy of Sciences*, 113(40):11261–11265.

Donohue, I., Petchey, O. L., Kéfi, S., Génin, A., Jackson, A. L., Yang, Q., and O'Connor, N. E. (2017). Loss of predator species, not intermediate consumers, triggers rapid and dramatic extinction cascades. *Global Change Biology*, 23(8):2962–2972.

Edwards, K. F., Klausmeier, C. A., and Litchman, E. (2011). Evidence for a three-way trade-off between nitrogen and phosphorus competitive abilities and cell size in phytoplankton. *Ecology*, 92(11):2085–2095.

Elser, J. J. and Urabe, J. (1999). The Stoichiometry of consumer-driven nutrient recycling: theory, observations, and consequences. *Ecology*, 80(3):735–751.

Estes, J. A. and Duggins, D. O. (1995). Sea Otters and Kelp Forests in Alaska: Generality and Variation in a Community Ecological Paradigm. *Ecological Monographs*, 65(1):75–100.

Estes, J. A. and Palmisano, J. F. (1974). Sea Otters: Their Role in Structuring Nearshore Communities. *Science*, 185(4156):1058–1060.

Fussmann, G. F., Ellner, S. P., and Hairston, N. G. (2003). Evolution as a critical component of plankton dynamics. *Proceedings of the Royal Society of London. Series B: Biological Sciences*, 270(1519):1015–1022.

Hairston, N. G., Ellner, S. P., Geber, M. A., Yoshida, T., and Fox, J. A. (2005). Rapid evolution and the convergence of ecological and evolutionary time. *Ecology Letters*, 8(10):1114–1127.

HilleRisLambers, R. and Dieckmann, U. (2003). Competition and predation in simple food webs: intermediately strong trade-offs maximize coexistence. *Proceedings of the Royal Society B: Biological Sciences*, 270(1533):2591–2598.

Hiltunen, T. and Becks, L. (2014). Consumer co-evolution as an important component of the eco-evolutionary feedback. *Nature Communications*, 5(1):5226.

Hiltunen, T., Hairston, N. G., Hooker, G., Jones, L. E., and Ellner, S. P. (2014). A newly discovered role of evolution in previously published consumer-resource dynamics. *Ecology Letters*, 17(8):915–923.

Hoegh-Guldberg, O. and Bruno, J. F. (2010). The Impact of Climate Change on the World's Marine Ecosystems. *Science*, 328(5985):1523–1528.

Holt, R. D. (1977). Predation, apparent competition, and the structure of prey communities. *Theoretical Population Biology*, 12(2):197–229.

Inchausti, P. and Halley, J. (2003). On the relation between temporal variability and persistence time in animal populations. *Journal of Animal Ecology*, 72(6):899–908.

Jackson, J. B. C., Kirby, M. X., Berger, W. H., Bjorndal, K. A., Botsford, L. W., Bourque, B. J., Bradbury, R. H., Cooke, R., Erlandson, J., Estes, J. A., Hughes, T. P., Kidwell, S., Lange, C. B., Lenihan, H. S., Pandolfi, J. M., Peterson, C. H., Steneck, R. S., Tegner, M. J., and Warner, R. R. (2001). Historical Overfishing and the Recent Collapse of Coastal Ecosystems. *Science*, 293(5530):629–637.

Jensen, J. L. W. V. (1906). Sur les fonctions convexes et les inéqualitiés entre les valeurs moyennes. *Acta Mathematica*, 30:175–193.

Jones, L. E., Becks, L., Ellner, S. P., Hairston Jr., N. G., Yoshida, T., and Fussmann, G. F. (2009). Rapid contemporary evolution and clonal food web dynamics. *Philosophical Transactions of the Royal Society B: Biological Sciences*, 364(1523):1579–1591.

Jones, L. E. and Ellner, S. P. (2007). Effects of rapid prey evolution on predator–prey cycles. *Journal of Mathematical Biology*, 55(4):541–573.

Karban, R. and Agrawal, A. A. (2002). Herbivore Offense. *Annual Review of Ecology and Systematics*, 33(1):641–664.

Kenitz, K. M., Visser, A. W., Mariani, P., and Andersen, K. H. (2017). Seasonal succession in zooplankton feeding traits reveals trophic trait coupling. *Limnology and Oceanography*, 62(3):1184–1197.

Kessler, A. and Baldwin, I. T. (2001). Defensive Function of Herbivore-Induced Plant Volatile Emissions in Nature. *Science*, 291(5511):2141–2144.

Kiørboe, T. (2011). How zooplankton feed: mechanisms, traits and trade-offs. *Biological Reviews*, 86(2):311–339.

Kneitel, J. M. and Chase, J. M. (2004). Trade-offs in community ecology: linking spatial scales and species coexistence. *Ecology Letters*, 7(1):69–80.

Koffel, T., Daufresne, T., Massol, F., and Klausmeier, C. A. (2018). Plant Strategies along Resource Gradients. *The American Naturalist*, 192(3):360–378.

Kondoh, M. (2007). Anti-predator defence and the complexity–stability relationship of food webs. *Proceedings of the Royal Society B: Biological Sciences*, 274(1618):1617–1624.

Kovach-Orr, C. and Fussmann, G. F. (2012). Evolutionary and plastic rescue in multitrophic model communities. *Philosophical Transactions of the Royal Society B: Biological Sciences*, 368(1610):20120084–20120084.

Kretzschmar, M., Nisbet, R., and Mccauley, E. (1993). A Predator-Prey Model for Zooplankton Grazing on Competing Algal Populations. *Theoretical Population Biology*, 44(1):32–66.

Leibold, M. A. (1996). A Graphical Model of Keystone Predators in Food Webs: Trophic Regulation of Abundance, Incidence, and Diversity Patterns in Communities. *The American Naturalist*, 147(5):784–812.

Leibold, M. A. (1999). Biodiversity and nutrient enrichment in pond plankton communities. *Evolutionary Ecology Research*, 1(1):73–95.

Lima, S. L. and Dill, L. M. (1990). Behavioral decisions made under the risk of predation: a review and prospectus. *Canadian Journal of Zoology*, 68(4):619–640.

Lima, S. L., Valone, T. J., and Caraco, T. (1985). Foraging-efficiency-predation-risk trade-off in the grey squirrel. *Animal Behaviour*, 33(1):155–165.

Lipson, D. A., Schmidt, S. K., and Monson, R. K. (1999). Links between Microbial Population Dynamics and Nitrogen Availability in an Alpine Ecosystem. *Ecology*, 80(5):1623–1631.

Litchman, E., Edwards, K. F., and Klausmeier, C. A. (2015). Microbial resource utilization traits and trade-offs: implications for community structure, functioning, and biogeochemical impacts at present and in the future. *Frontiers in Microbiology*, 06(APR):1–10.

Litchman, E. and Klausmeier, C. A. (2008). Trait-Based Community Ecology of Phytoplankton. *Annual Review of Ecology, Evolution, and Systematics*, 39(1):615–639.

Litchman, E., Ohman, M. D., and Kiørboe, T. (2013). Trait-based approaches to zooplankton communities. *Journal of Plankton Research*, 35:473–484.

Lürling, M. and Van Donk, E. (2000). Grazer-induced colony formation in Scenedesmus: are there costs to being colonial? *Oikos*, 88(1):111–118.

Marshall, C. R. (2006). Explaining the Cambiran "Explosion" of Animals. *Annual Review of Earth and Planetary Sciences*, 34(1):355–384.

May, R. M. (1972). Limit Cycles in Predator-Prey Communities. *Science*, 177(4052):900–902.

May, R. M. (1974). On the theory of niche overlap. *Theoretical Population Biology*, 5(3):297–332.

McCann, K., Hastings, A., and Huxel, G. R. (1998). Weak trophic interactions and the balance of nature. *Nature*, 395(6704):794–798.

McCauley, E., Nisbet, R. M., Murdoch, W. W., de Roos, A. M., and Gurney, W. S. C. (1999). Large-amplitude cycles of Daphnia and its algal prey in enriched environments. *Nature*, 402(6762):653–656.

McGill, B. J., Enquist, B. J., Weiher, E., and Westoby, M. (2006). Rebuilding community ecology from functional traits. *Trends in Ecology and Evolution*, 21(4):178–185.

Menge, B. A., Berlow, E. L., Blanchette, C. A., Navarrete, S. A., and Yamada, S. B. (1994). The Keystone Species Concept: Variation in Interaction Strength in a Rocky Intertidal Habitat. *Ecological Monographs*, 64(3):249–286.

Mougi, A. (2012). Unusual predator–prey dynamics under reciprocal phenotypic plasticity. *Journal of Theoretical Biology*, 305:96–102.

Mougi, A. and Iwasa, Y. (2010). Evolution towards oscillation or stability in a predator–prey system. *Proceedings of the Royal Society B: Biological Sciences*, 277(1697):3163–3171.

Murdoch, W. W. (1969). Switching in General Predators: Experiments on Predator Specificity and Stability of Prey Populations. *Ecological Monographs*, 39(4):335–354.

Paine, R. T. (1966). Food Web Complexity and Species Diversity. *The American Naturalist*, 100(910):65–75.

Palkovacs, E. P. and Post, D. M. (2008). Eco-evolutionary interactions between predators and prey: Can predator-induced changes to prey communities feed back to shape predator foraging traits? *Evolutionary Ecology Research*, 10(5):699–720.

Palkovacs, E. P. and Post, D. M. (2009). Experimental evidence that phenotypic divergence in predator foraging traits drives ecological divergence in prey communities. *Ecology*, 90(2):300–305.

Pančić, M. and Kiørboe, T. (2018). Phytoplankton defence mechanisms: traits and trade-offs. *Biological Reviews*, 93(2):1269–1303.

Petchey, O. L., McPhearson, P. T., Casey, T. M., and Morin, P. J. (1999). Environmental warming alters food-web structure and ecosystem function. *Nature*, 402(6757):69–72.

Pimm, S. L., Jones, H. L., and Diamond, J. (1988). On the Risk of Extinction. *The American Naturalist*, 132(6):757–785.

Proulx, M. and Mazumder, A. (1998). Reversal of grazing impact on plant species richness in nutrient-poor vs. nutrient-rich ecosystems. *Ecology*, 79(8):2581–2592.

Prowe, A. F., Pahlow, M., Dutkiewicz, S., Follows, M., and Oschlies, A. (2012). Top-down control of marine phytoplankton diversity in a global ecosystem model. *Progress in Oceanography*, 101(1):1–13.

Ramos-Jiliberto, R. (2003). Population dynamics of prey exhibiting inducible defenses: the role of associated costs and density-dependence. *Theoretical Population Biology*, 64(2):221–231.

Reznick, D. N., Ghalambor, C. K., and Crooks, K. (2008). Experimental studies of evolution in guppies: a model for understanding the evolutionary consequences of predator removal in natural communities. *Molecular Ecology*, 17(1):97–107.

Rosenzweig, M. L. (1971). Paradox of Enrichment: Destabilization of Exploitation Ecosystems in Ecological Time. *Science*, 171(3969):385–387.

Rueffler, C., Van Dooren, T., and Metz, J. (2004). Adaptive walks on changing landscapes: Levins' approach extended. *Theoretical Population Biology*, 65(2):165–178.

Rueffler, C., Van Dooren, T. J. M., and Metz, J. A. J. (2006). The Evolution of Resource Specialization through Frequency-Dependent and Frequency-Independent Mechanisms. *The American Naturalist*, 167(1):81–93.

Savidge, J. A. (1987). Extinction of an Island Forest Avifauna by an Introduced Snake. *Ecology*, 68(3):660–668.

Schmitz, O. J., Hawlena, D., and Trussell, G. C. (2010). Predator control of ecosystem nutrient dynamics. *Ecology Letters*, 13(10):1199–1209.

Sibly, R. and Calow, P. (1983). An Integrated Approach to Life-Cycle Evolution using Selective Landscapes. *Journal of Theoretical Biology*, 102:527–547.

Soliveres, S., van der Plas, F., Manning, P., Prati, D., Gossner, M. M., Renner, S. C., Alt, F., Arndt, H., Baumgartner, V., Binkenstein, J., Birkhofer, K., Blaser, S., Blüthgen, N., Boch, S., Böhm, S., Börschig, C., Buscot, F., Diekötter, T., Heinze, J., Hölzel, N., Jung, K., Klaus, V. H., Kleinebecker, T., Klemmer, S., Krauss, J., Lange, M., Morris, E. K., Müller, J., Oelmann, Y., Overmann, J., Pašalić, E., Rillig, M. C., Schaefer, H. M., Schloter, M., Schmitt, B., Schöning, I., Schrumpf, M., Sikorski, J., Socher, S. A., Solly, E. F., Sonnemann, I., Sorkau, E., Steckel, J., Steffan-Dewenter, I., Stempfhuber, B., Tschapka, M., Türke, M., Venter, P. C., Weiner, C. N., Weisser, W. W., Werner, M., Westphal, C., Wilcke, W., Wolters, V., Wubet, T., Wurst, S., Fischer, M., and Allan, E. (2016). Biodiversity at multiple trophic levels is needed for ecosystem multifunctionality. *Nature*, 536(7617):456–459.

Sommer, U., Adrian, R., De Senerpont Domis, L., Elser, J. J., Gaedke, U., Ibelings, B., Jeppesen, E., Lürling, M., Molinero, J. C., Mooij, W. M., van Donk, E., and Winder, M. (2012). Beyond the Plankton Ecology Group (PEG) Model: Mechanisms Driving Plankton Succession. *Annual Review of Ecology, Evolution, and Systematics*, 43(1):429–448.

Stearns, S. C. (1989). Trade-Offs in Life-History Evolution. *Functional Ecology*, 3(3):259–268.

Steneck, R. S., Graham, M. H., Bourque, B. J., Corbett, D., Erlandson, J. M., Estes, J. A., and Tegner, M. J. (2002). Kelp forest ecosystems: biodiversity, stability, resilience and future. *Environmental Conservation*, 29(4):436–459.

Terhorst, C. P., Miller, T. E., and Levitan, D. R. (2010). Evolution of prey in ecological time reduces the effect size of predators in experimental microcosms. *Ecology*, 91(3):629–636.

Thingstad, T. F. (2000). Elements of a theory for the mechanisms controlling abundance, diversity, and biogeochemical role of lytic bacterial viruses in aquatic systems. *Limnology and Oceanography*, 45(6):1320–1328.

Tilman, D. (2000). Causes, consequences and ethics of biodiversity. *Nature*, 405(6783):208–211.

Tilman, D., Isbell, F., and Cowles, J. M. (2014). Biodiversity and Ecosystem Function. *Annual Review of Ecology, Evolution, and Systematics*, 45:471–493.

Tirok, K. and Gaedke, U. (2010). Internally driven alternation of functional traits in a multispecies predator–prey system. *Ecology*, 91(6):1748–1762.

Trussell, G. C. and Nicklin, M. O. (2002). Cue sensitivity, inducible defense, and trade-offs in a marine snail. *Ecology*, 83(6):1635–1647.

Tylianakis, J. M., Didham, R. K., Bascompte, J., and Wardle, D. A. (2008). Global change and species interactions in terrestrial ecosystems. *Ecology Letters*, 11(12):1351–1363.

Våge, S., Storesund, J. E., Giske, J., and Thingstad, T. F. (2014). Optimal Defense Strategies in an Idealized Microbial Food Web under Trade-Off between Competition and Defense. *PLoS ONE*, 9(7):e101415.

Van Donk, E., Ianora, A., and Vos, M. (2011). Induced defences in marine and freshwater phytoplankton: a review. *Hydrobiologia*, 668(1):3–19.

van Velzen, E. and Gaedke, U. (2017). Disentangling eco-evolutionary dynamics of predator-prey coevolution: the case of antiphase cycles. *Scientific Reports*, 7(1):17125.

van Velzen, E. and Gaedke, U. (2018). Reversed predator-prey cycles are driven by the amplitude of prey oscillations. *Ecology and Evolution*, 8(12):6317–6329.

Vanni, M. J. (2002). Nutrient Cycling by Animals in Freshwater Ecosystems. *Annual Review of Ecology and Systematics*, 33(1):341–370.

Verdolin, J. L. (2006). Meta-analysis of foraging and predation risk trade-offs in terrestrial systems. *Behavioral Ecology and Sociobiology*, 60(4):457–464.

Vos, M., Kooi, B. W., DeAngelis, D. L., and Mooij, W. M. (2004). Inducible defences and the paradox of enrichment. *Oikos*, 105(3):471–480.

Weiss, L., Laforsch, C., and Tollrian, R. (2012). The taste of predation and the defences of prey. In *Chemical Ecology in Aquatic Systems*, volume 6, pages 111–126. Oxford University Press.

Wiles, G. J., Bart, J., Beck Jr., R. E., and Aguon, C. F. (2003). Impacts of the Brown Tree Snake: Patterns of Decline and Species Persistence in Guam's Avifauna. *Conservation Biology*, 17(5):1350–1360.

Winter, C., Bouvier, T., Weinbauer, M. G., and Thingstad, T. F. (2010). Trade-Offs between Competition and Defense Specialists among Unicellular Planktonic Organisms: the "Killing the Winner" Hypothesis Revisited. *Microbiology and Molecular Biology Reviews*, 74(1):42–57.

Yang, L. H. (2004). Periodical Cicadas as Resource Pulses in North American Forests. *Science*, 306(5701):1565–1567.

Yoshida, T., Ellner, S. P., Jones, L. E., Bohannan, B. J. M., Lenski, R. E., and Hairston Jr., N. G. (2007). Cryptic population dynamics: rapid evolution masks trophic interactions. *PLoS biology*, 5(9):e235.

Yoshida, T., Jones, L. E., Ellner, S. P., Fussmann, G. F., and Hairston Jr., N. G. (2003). Rapid evolution drives ecological dynamics in a predator-prey system. *Nature*, 424(6946):303–306.

Declaration of contributions

Chapter 2:

Published as: *Not attackable or not crackable - How pre- and post-attack defences with different competition costs affect prey coexistence and population dynamics*

Authors: Elias Ehrlich and Ursula Gaedke

Published in *Ecology and Evolution* (2018).

EE had the principal idea. EE and UG designed the study. EE did the mathematical and numerical analyses and wrote the manuscript, on which UG commented.

Chapter 3:

Published as: *Trait–fitness relationships determine how trade-off shapes affect species coexistence*

Authors: Elias Ehrlich, Lutz Becks and Ursula Gaedke

Published in *Ecology* (2017).

EE, LB and UG conceived the study. EE developed the mathematical approach and performed the analysis. EE wrote the manuscript under supervision of UG, and LB commented on it.

Chapter 4:

Submitted as: *The shape of a defence-growth trade-off governs seasonal trait dynamics in natural phytoplankton*

Authors: Elias Ehrlich*, Nadja J. Kath* and Ursula Gaedke
*These authors contributed equally

Submitted to *Ecology Letters* and rejected after peer-review. To be submitted again.

EE, NK and UG designed the study. NK performed the data analysis. EE developed the theory and did the numerical analysis of the model. EE wrote most of the manuscript to which NK and UG contributed.

Chapter 5:

Submitted as: *Coupled changes in traits and biomasses cascading through a tritrophic plankton food web*

Authors: Elias Ehrlich and Ursula Gaedke

Under review in *Proceedings of the Royal Society B: Biological Sciences*.

EE and UG conceived the study and developed the model. EE performed the data analysis and did the numerical analysis of the model. EE wrote the manuscript in consultation with UG.

Potsdam, 28^{th} January 2019

Elias Ehrlich: _____ Prof. Dr. Ursula Gaedke: _____

2 Trade-off types, prey coexistence and population dynamics

Manuscript title:

Not attackable or not crackable - How pre- and post-attack defences with different competition costs affect prey coexistence and population dynamics

Elias Ehrlich[1] and Ursula Gaedke[1]

1. Department of Ecology and Ecosystem Modelling, University of Potsdam, Am Neuen Palais 10, 14469 Potsdam, Germany.

Published as:

Ehrlich, E. and Gaedke, U. (2018). Not attackable or not crackable - How pre- and post-attack defences with different competition costs affect prey coexistence and population dynamics. *Ecology and Evolution*, 8 (13), 6625-6637.

Abstract

It is well-known that prey species often face trade-offs between defence against predation and competitiveness, enabling predator-mediated coexistence. However, we lack an understanding of how the large variety of different defence traits with different competition costs affect coexistence and population dynamics. Our study focusses on two general defence mechanisms, i.e., pre-attack (e.g., camouflage) and post-attack defences (e.g., weaponry) that act at different phases of the predator-prey interaction. We consider a food web model with one predator, two prey types and one resource. One prey type is undefended while the other one is pre- or post-attack defended paying costs either by a higher half-saturation constant for resource uptake or a lower maximum growth rate. We show that post-attack defences promote prey coexistence and stabilize the population dynamics more strongly than pre-attack defences by interfering with the predator's functional response: because the predator spends time handling 'non-crackable' prey, the undefended prey is indirectly facilitated. A high half-saturation constant as defence costs promotes coexistence more and stabilizes the dynamics less than a low maximum growth rate. The former imposes high costs at low resource concentrations but allows for temporally high growth rates at predator-induced resource peaks preventing the extinction of the defended prey. We evaluate the effects of the different defence mechanisms and costs on coexistence under different enrichment levels in order to vary the importance of bottom-up and top-down control of the prey community.

Introduction

Predation and competition for resources represent two major factors determining the survival of species at low and intermediate trophic levels (Sih et al. 1985). Hence, there is strong selection for increasing defence against predation and competitiveness. However, species optimizing one functional trait commonly have to pay costs regarding other traits due to physiological, energetic and genetic constraints (Stearns 1989). Trade-offs between defence and competitiveness have been frequently found in nature and may explain the high diversity of strategies along the gradient of being defended or highly competitive (Coley et al. 1985; Agrawal 1998; Hillebrand et al. 2000). Predation may enable coexistence of competing species facing a trade-off between defence and competitiveness. This mechanism is known as keystone predation (Paine 1966; Menge et al. 1994; Leibold 1996) or analogously as killing the winner in a microbial context (Thingstad 2000; Winter et al. 2010): a competitive superior species is suppressed by predation promoting the inferior but defended competitor which allows them to coexist. Several studies highlighted the importance of this predator-mediated coexistence in experimental and natural communities (e.g. Fauth and Resetarits 1991; McPeek 1998; Ciros-Pérez et al. 2004).

Species evolved a variety of defence strategies to reduce their predation risk ranging from camouflage, apparent dead, mimicry, aposematism, warning calls, weaponry, chemical defence to escape behaviour (Lima and Dill 1990; Endler 1991). These defence mechanisms interact in different ways with the predator. Some of them even hamper the predator, e.g., chemical defences, while others do not, e.g., camouflage, which may have strong implications for the occurrence of predator-mediated coexistence. Furthermore, the type of defence costs regarding competitiveness (resource uptake affinity or growth rate) plays a important role for coexistence. Theory already showed that predator-mediated coexistence crucially depends on the environmental conditions (Chase et al. 2002), e.g., the enrichment level (Leibold 1996; Proulx and Mazumder 1998; Genkai-Kato and Yamamura 1999), the prey switching behaviour of the predator (Murdoch 1969; Abrams and Matsuda 1993; Fryxell and Lundberg 1994), the magnitude of the trade-off between defence and competitiveness (Abrams 1999; Tirok and Gaedke 2010; Kasada et al. 2014) and the difference in the defence level and the competitiveness between the prey types (Jones and Ellner 2007; Becks et al. 2010; Ehrlich et al. 2017). However, the role of different defence mechanisms and competition costs in prey communities remains unclear but holds promise to be decisive for their coexistence and the occurring population dynamics. Here, we want to evaluate explicitly the effects of different defence mechanisms and compare the influence of different defence costs in terms of competitiveness on prey coexistence and population dynamics.

Following Bateman et al. (2014), we distinguish between two general types of defence mechanisms: pre-attack and post-attack defences that act at different phases of the predation sequence, i.e., prey encounter, detection, attack, capture, manipulation, consumption and digestion. A pre-attack defence implies that the predator does not attack the prey, e.g., because it senses the defence, the prey is camouflaged or avoids habitats where predators occur. A post-attack defence means that the prey is attacked but survives, e.g., due to weaponry, escape behaviour or robustness. In contrast to pre-attack defences, the predator invests time and energy to handle prey with a post-attack defence which reduces its potential to consume another undefended prey (see Tab. 2.1). Hence, a post-attack defended prey interferes with the functional response of the predator for edible prey which may result in a lower top-down control of the total prey community while pre-attack defended prey does not. Thus, we expect different coexistence patterns and population dynamics in dependence of the defence mechanism.

We also distinguish between two general cost types of the defence in respect to resource competition: either having a reduced performance at low resource concentrations or growing slower independent of the resource concentrations. Referring to the Monod equation (Monod 1950), this corresponds either to a higher half-saturation constant for resource uptake or a lower maximum growth rate. There is empirical evidence from phytoplankton and plant communities that both cost types are ecologically relevant (Agrawal 1998; Yoshida et al. 2004; Meyer et al. 2006; Lind et al. 2013). However, a comparison of how both cost types affect the prey community is still missing.

Previous studies on predator-mediated coexistence in diamond-shaped food web models often implicitly assumed pre-attack defences (Fryxell and Lundberg 1994; Abrams 1999; Yamauchi and Yamamura 2005) and considered either a higher half-saturation constant (Yoshida et al. 2003; Jones and Ellner 2007; Becks et al. 2010) or a lower maximum growth rate as costs (Abrams 1999; Yoshida et al. 2007; Kasada et al. 2014). In this study, we explicitly model pre-attack and post-attack defences and both cost types. The modelled diamond-shaped food web involves a basal resource, two competing prey types with a trade-off between defence and competitiveness, and one predator species. One prey type is undefended while the other type is defended either by a reduced probability of being attacked or a lower probability of being consumed when attacked. We consider defence as a continuous trait with values ranging from completely defended to nearly undefended. The costs for defence are either a higher half-saturation constant or a lower maximum growth rate. By varying the values of both traits of the defended prey independently, we generate different magnitudes of the trade-off quantifying the costs of being more or less defended. For each trait combination, we test for coexistence and check whether the populations cycle or are in steady state. This enables us to evaluate how the different traits promote maintenance of prey diversity

and stabilize the dynamics. We analyse these effects under different enrichment levels (different resource concentrations) in order to vary the relative importance of bottom-up and top-down control.

Methods

We consider a diamond-shaped food web model with one predator (P), two prey types (A_i) and one resource (N) limiting the growth of the prey. The two prey types face a trade-off: A_1 is defended but has costs in respect to resource competition while A_2 is undefended and highly competitive. The following model description is divided into four parts. At first, we present the different defence mechanisms of A_1 and derive the respective functional response of the predator. Second, we describe the different competition costs based on the resource-dependent growth function of the prey types. Third, we apply the model to a fully parametrized chemostat system and finally, we explain how to analyse the effect of the different defence mechanisms and costs on prey coexistence and the population dynamics for the considered system.

Defence mechanisms

The predator attacks the prey A_i with the probability p_i and then consumes the captured prey with the probability q_i. While A_2 is completely undefended ($p_2 = q_2 = 1$), A_1 is able to defend against predation at different phases of the predation sequence (Bateman et al. 2014). We distinguish between two general defence mechanisms: pre-attack defences ($p_1 < 1$) and post-attack defences ($q_1 < 1$). A third special defence mechanism where the prey is attacked and consumed ($p_1 = q_1 = 1$) but survives passing the digestive system of the predator is investigated in Appendix A.1.

According to Brodie et al. (1991), we assume that the defended prey is specialized only on one defence mechanisms, i.e., if $p_1 < 1$ then $q_1 = 1$ and vice versa, as investing in one strategy reduces the fitness advantage of the other. The main difference between the defence mechanisms lies in how they affect the predator's functional response. We consider a Holling type II functional response of the predator implying that it spends a certain handling time for each attacked prey individual before it is able to attack the next prey item. Thus, the rate of consumption of the predator saturates with increasing prey density. The handling time comprises the time for attacking and capturing the prey (T_a), and, if the prey is consumed, the time for manipulating and digesting it (T_m). The two-prey type version of the Holling's disk equation is then given by

$$F_i = \frac{a\, p_i\, q_i\, A_i}{1 + a p_1 (T_a + q_1 T_m) A_1 + a p_2 (T_a + q_2 T_m) A_2} \tag{2.1}$$

where a represents the encounter rate (Holling 1959; Rueffler et al. 2006; Bateman et al. 2014). It should be mentioned here that the attack probability p_i scales the encounter rate a in the presented version of the type II functional response (Eq. 2.1). Therefore, the product of a and p_i can be interpreted as the effective attack rate on A_i.

The key to understand the effects of the different defence mechanisms on the functional response of predator is the handling time spent per prey individual. A completely undefended prey individual demands the full handling time of the predator attacking and manipulating it, i.e., $T_a + T_m$ (Tab. 2.1a). A pre-attack defended prey individual with $p_1 = 0$ is not attacked and thus demands no handling time of the predator (Tab. 2.1b) allowing the predator to focus on the undefended prey. In contrast, for a post-attack defended prey individual with $q_1 = 0$, the predator invests the attack time T_a without making use out of it (Tab. 2.1c). The relative size of T_a compared to T_m determines how much the different prey types differ in their handling times. To approach this difference systematically, we replace T_a by $c_a T$ and T_m by $c_m T$ where T is the total handling time, c_a the fraction of T spent for attacking the prey and c_m the fraction of T invested into manipulation which can be replaced by $c_m = 1 - c_a$. This leads us to

$$F_i = \frac{a\, p_i\, q_i\, A_i}{1 + a p_1 (c_a T + q_1 (1 - c_a) T) A_1 + a p_2 (c_a T + q_2 (1 - c_a) T) A_2} \,. \tag{2.2}$$

If c_a has very low values, pre- and post-attack defences do not differ substantially in their effect on the predator while high values of c_a imply high differences in handling times needed for a pre- and post-defended prey (see Eq. A1 and Tab. 2.1).

Table 2.1: Comparison of the predator's handling time spent per prey individual and the resulting energy gain of the predator for an undefended prey (a) and for prey types with three different defence mechanisms (b-d). T_a represents the time needed for attacking and capturing a prey individual and T_m is the manipulation and digestion time spent after capturing the prey.

Defence mechanism		Handling time	Energy gain	Examples
a) Undefended ($p_2 = 1, q_2 = 1$)		$T_a + T_m$	yes	-
b) Pre-attack defence ($p_1 = 0, q_1 = 1$)		0	no	Camouflage, mimicry, aposematism, apparent dead
c) Post-attack defence ($p_1 = 1, q_1 = 0$)		T_a	no	Weaponry, escape behaviour, robustness, autotomy
d) Digestion resistance (see Appendix A.1)		$T_a + T_m$	no	Algae with thickened cell walls or snails surviving gut passage in predators

Defence costs with respect to competitiveness

An empirically well-established resource-dependent growth model is the Monod equation with the parameters maximum per capita growth rate β_i and half-saturation constant K_i, i.e., the resource concentration where the growth rate reaches half of the maximum (Monod 1950). The Monod equation is equivalent to a Holling type II functional response but is not restricted to predator-prey interactions and has been applied also to autotrophic organisms taking up nutrients (e.g., Yoshida et al. 2003; Becks et al. 2010; Raatz et al. 2017). The per capita growth rate of A_i in dependence of N is described by

$$G_i = \beta_i \frac{N}{K_i + N} \,. \tag{2.3}$$

We distinguish here between two general types of defence costs of A_1 with respect to competitiveness: a reduced growth rate at low but not at high resource concentrations ($K_1 > K_2$) or a lower growth rate independent of the resource concentration ($\beta_1 < \beta_2$). Both cost traits (K_1 and β_1) are relevant in nature and their implications can be understood based on two extreme cases. First, for very high resource concentrations ($N \gg K_1$), the per capita growth rate of A_1 reaches its maximum and is independent of the half-saturation constant ($G_1 = \beta_1$, see Eq. 2.3). Second, for very low resource concentrations ($N \ll K_1$), the per capita growth rate of A_1 is given by $G_1 = \frac{\beta_1}{K_1} N$ (see Eq. 2.3) and thus depends on both cost traits. According to that, $\frac{\beta_i}{K_i}$ can be interpreted as the slope of the growth function at very low N which is defined as the resource affinity. In the absence of mortality, the prey type with the higher resource affinity would be competitive superior (Button 1978;

Healey 1980; Smith et al. 2014). However, given a certain rate of natural mortality δ, the competitiveness depends on the equilibrium resource concentration N_i^* at which the gross growth rate equals the mortality, i.e., $G_i = \delta$ (Tilman 1982). Following Eq. 2.3, the equilibrium resource concentration of a prey type A_i in monoculture is given by

$$N_i^* = \frac{K_i}{\frac{\beta_i}{\delta} - 1} \,. \tag{2.4}$$

The undefended prey A_2 has a lower equilibrium resource concentration than the defended prey A_1 ($N_2^* < N_1^*$) and thus outcompetes A_1 in the absence of predation. We use the ratio N_2^*/N_1^* as a measure of relative competitiveness of A_1 which allows us to compare the effects of the different defence costs (higher K_1 or lower β_1) on competition. For costs arising from $K_1 > K_2$ ($\beta_1 = \beta_2$), N_2^*/N_1^* equals K_2/K_1. For costs originating from $\beta_1 < \beta_2$ ($K_1 = K_2$), it is given by $\frac{\beta_1 - \delta}{\beta_2 - \delta}$ (see Eq. 2.4).

Chemostat model

Here, we put the diamond-shaped food web model with the previously derived functional responses and growth functions into an ecologically relevant context. We consider a chemostat system which is characterized by a continuous inflow of medium with resources and outflow of medium with resources and organisms (Smith and Waltman 1995). The magnitude of the in- and outflow is described by the dilution rate δ which represents the mortality rate of the prey and the predator. The resource concentration in the supplied medium N_I determines the quantity of inflowing resources. An increase in N_I implies an enrichment of the system. The changes of the resource concentration and population densities over time are defined by the following differential equations

$$\begin{aligned}
\frac{dN}{dt} &= \delta\,(N_I - N) - \frac{1}{\chi}\,G_1 A_1 - \frac{1}{\chi}\,G_2 A_2 \\
\frac{dA_i}{dt} &= G_i A_i - F_i P - \delta A_i \\
\frac{dP}{dt} &= \chi_P F_1 P + \chi_P F_2 P - \delta P
\end{aligned} \tag{2.5}$$

with $i = 1, 2$. The parameter χ describes the prey's conversion efficiency of resources into prey individuals. The parameter χ_P describes the efficiency with which consumed prey individuals are converted into predator individuals. To reach a suitable parametrization, we refer our model to an empirically well-studied rotifer-algae system with *Brachionus calyciflorus* as a predator and different genotypes of *Chlamydomonas reinhardtii* as prey (Becks et al. 2010, 2012). For details on the values and units of the parameters and the state variables see Table B1. For the given system, A_1 and A_2 represent different genotypes

of the same algal species. However, mechanistically, there is no difference between analysing coexistence of different species or genotypes of an asexually reproducing species without horizontal gene transfer.

Table 2.2: Values and units of state variables and parameters used in the predator-prey chemostat model parametrized for a rotifer-algae system (Becks et al. 2010, 2012).

Param. / Variable	Value	Unit	Ref.
N	-	µmol N/l	-
A_i	-	ind./ml	-
P	-	ind./ml	-
N_I	80, 160 or 240	µmol N/l	TVC
δ	0.8	d^{-1}	TVC
χ	2.7×10^6	ind./µmol N	L. Becks, unpublished data
χ_P	170×10^{-6}	-	Becks et al. (2010)
a	0.073	ml/d	calculated from Becks et al. (2010)
T	9.091×10^{-5}	d	calculated from Becks et al. (2010)
c_a	0.5	-	NM
p_i	p_1 varied, $p_2 = 1.0$	-	L. Becks, unpublished data
q_i	q_1 varied, $q_2 = 1.0$	-	L. Becks, unpublished data
K_i	K_1 varied, $K_2 = 2.2$	µmol N/l	L. Becks, unpublished data
β_i	β_1 varied, $\beta_2 = 1.6$	d^{-1}	N. Woltermann, unpublished data

TVC: Typical values used in chemostat experiments with rotifers and algae as they enable sufficient rotifer densities but avoid light limitation (e.g., Yoshida et al. 2003; Becks et al. 2010). NM: No measurements available. For simplicity, we assume that the fraction of T spent for attacking and manipulating the prey is equal, i.e., $c_a = 0.5$ (sensitivity analysis in Appendix A.3).

Analysis of coexistence and population dynamics

The traits of the undefended prey A_2 are fixed. By varying the defence level and the defence costs of A_1 independently, we generate different slopes of the trade-offs. In order to understand the individual effects of the different traits, we vary only the value of one defence trait and one cost trait at a time. The other trait values are equal to those of A_2. This results in four different types of trade-offs (TO) which we consider: p-K-TO, q-K-TO, p-β-TO and q-β-TO. First, we analyse how the different defence mechanisms ($p_1 < p_2$ or $q_1 < q_2$) affect prey coexistence and the population dynamics, i.e., whether cycles or steady state occur. Secondly, we compare the effect of different costs of defence ($K_1 > K_2$ or $\beta_1 < \beta_2$) on these properties.

In order to find the coexistence regions in the trait space, we applied an analytical

approach of Jones and Ellner (2007) which calculates the condition for a coexistence equilibrium where all net growth rates equal zero. A following linear stability analysis of these equilibria informs about the population dynamics. A steady-state occurs in case of a stable equilibrium. For an unstable equilibrium, coexistence with cycling population densities is possible. To check the basin of attraction of the respective attractor, i.e., the range of possible initial conditions leading to it, we perform an invasion analysis. We check whether A_1 can invade a resident community with N, A_2 and P which reveals whether coexistence is also reached with very low population densities of A_1. For further details on the analysis see Appendix A.2. To investigate details of the population dynamics, we did numerical integrations for selected parameter combinations with the odeint solver of the SciPy package in Python (Jones et al. 2001). For all simulations shown in the main text, we use the same setting of initial population densities ($N = N_I$, $A_1 = A_2 = 10^5$ ind./ml, $P = 1$ ind./ml) and a simulation time of 60 days.

Results

General patterns of prey coexistence and population dynamics

To explain the patterns of coexistence and population dynamics in general, we focus initially on the trade-off (TO) between attack probability p, i.e., pre-attack defence, and half-saturation constant K (p-K-TO). We consider three different enrichment levels, i.e., $N_I = 80$, 160 and 240 µmol N/l, to reveal the sensitivity of these patterns to the productivity of the system (Fig. 2.1a-c).

For a low resource supply ($N_I = 80$ µmol N/l), the defended prey A_1 dies out and only the undefended prey A_2 survives if the relative competitiveness N_2^*/N_1^* (cf. methods, Eq. 2.4) of A_1 is very low, i.e., A_1 has a high half-saturation constant K_1 (Fig. 2.1a). For higher values of N_2^*/N_1^*, A_1 and A_2 may coexist. The range of possible N_2^*/N_1^* values enabling coexistence increases with a decreasing attack probability p_1 (Fig. 2.1a). At low values of p_1, both prey types coexist for relatively low N_2^*/N_1^* values and even for high N_2^*/N_1^* values close to 1 (very low defence costs). The latter case implies a very high fitness of A_1 since it has favourable values for both traits. However, such a highly defended A_1 cannot outcompete A_2 as long as its competitiveness is lower than that of A_2 ($N_2^*/N_1^* < 1$) because A_1 needs A_2 to maintain the predator P and thus its advantage of being defended. In the absence of P, A_1 would be inferior compared to A_2 as long as its competitiveness is slightly lower than that of A_2. At high values of p_1, A_1 can maintain P by itself for N_2^*/N_1^* close to 1 and thus outcompetes A_2 (Fig. 2.1a).

For low levels of resource supply ($N_I = 80$ µmol N/l), both prey types coexist in a steady state, i.e., the coexistence equilibrium is always stable (Fig. 2.1a). Furthermore, the

outcome of coexistence is independent of the initial conditions as the invasion boundary of A_1 is identical to the boundary of the region where coexistence equilibria exist, indicating that they are globally stable. This pattern changes if we enrich the system, i.e., increase N_I to 160 or 240 µmol N/l. A higher resource supply enhances the occurrence of cycles (Fig. 2.1b, c). The higher concentration of resources reduces the bottom-up control which promotes the fitness of A_1 as its disadvantage regarding competition for resources gets less important. Therefore, the part of the trait space where A_1 goes extinct decreases while the part where A_1 outcompetes A_2 strongly increases which alters also the trait space of coexistence (Fig. 2.1b, c). Moreover, the invasion boundary of A_1 is not identical to the boundary of coexistence equilibria any more, implying that even if a coexistence equilibrium exists, the two prey types may not coexist. In parts of the trait space below the invasion boundary of A_1 where the coexistence equilibrium is unstable, there is no attractor enabling coexistence and only A_2 survives (① in Fig. 2.1b, c). In the region where a locally stable coexistence equilibrium exists but A_1 cannot invade (② in Fig. 2.1b, c), either both prey types coexist or A_1 goes extinct depending on the initial conditions. Multistability occurs also at trait ranges above the region of coexistence equilibria where A_1 cannot invade A_2 (③ in Fig. 2.1b, c). Here, priority effects matter: either A_1 outcompetes A_2 when present at initially high densities or goes extinct when A_2 is initially dominant (for details on multistability see Appendix A.4).

The predator P survives in all trait areas stated above for all enrichment levels. It would only die out when a highly defended A_1 has a higher competitiveness than A_2 ($N_2^*/N_1^* > 1$) leading to the extinction of A_2, the only suitable food source of P in this case.

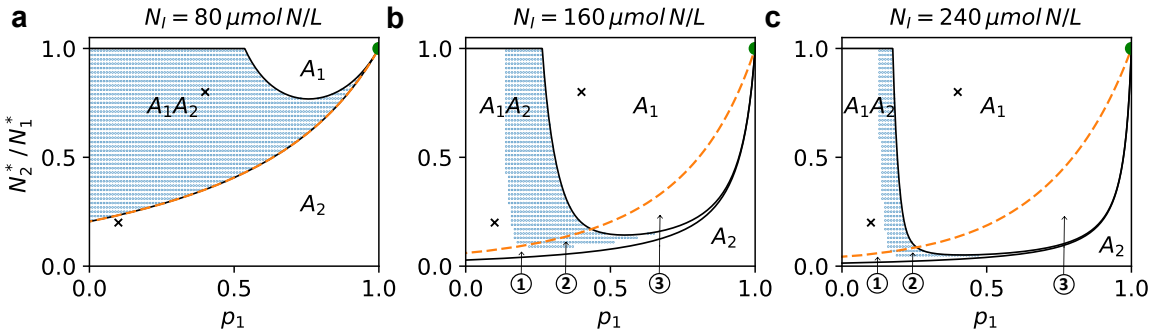

Figure 2.1: Prey coexistence and population dynamics for a trade-off (TO) between pre-attack defence, p, and half-saturation constant K (p-K-TO) under three levels of resource supply, i.e., $N_I = 80$, 160, 240 µmol N/l (a-c). The traits of the undefended prey A_2 are kept constant (green dot). The magnitude of the trade-off is changed by varying the attack probability p_1 and the half-saturation constant K_1 of the defended prey A_1 which determines its relative competitiveness N_2^*/N_1^* (cf. methods, Eq. 2.4). The capital letters display which prey types survive in the different parts of the trait space. The black lines enclose the part of the trait space where a coexistence equilibrium exists while blue dots mark where it is locally stable (steady state). The dashed orange line represents the invasion boundary above which A_1 can invade a resident community with A_2. The numbers indicate special cases which occur at intermediate and high enrichment levels (b, c): ① Only A_2 survives as the coexistence equilibrium is unstable and A_1 cannot invade, ② multistability between coexistence and survival of only A_2, ③ multistability between survival of A_1 and survival of A_2. The crosses mark trait combinations used in Fig. 2.5.

Comparison of different defence mechanisms

To demonstrate the effects of the different defence mechanisms on coexistence and population dynamics, we chose an intermediate resource supply ($N_I = 160$ µmol N/l) where coexistence with population cycles occurs and the defended prey A_1 is able to outcompete the undefended prey A_2 for a significant part of the trait space (Fig. 2.1b). The results for $N_I = 80$ and 240 µmol N/l are given in Appendix A.3 (Fig. A2, A3).

Comparing the different types of defence-competition trade-offs, we find qualitatively the same regions of coexistence in the trait space but with greatly differing importance (Fig. 2.2a-d). A post-attack defence ($p_1 = 1$, $q_1 < 1$) promotes coexistence more strongly than a pre-attack defence ($p_1 < 1$, $q_1 = 1$) and stabilizes the dynamics. This observation is independent of the type of costs for the defence (Fig. 2.2a-d). We elucidate the effects of the different defence mechanisms based on the comparison of the attack probability - half-saturation constant trade-off (p-K-TO, Fig. 2.2a) and the consumption probability - half-saturation constant trade-off (q-K-TO, Fig. 2.2c). The part of the trait space where the defended prey A_1 outcompetes the undefended prey A_2 is smaller for the q-K-TO while the coexistence region increases (Fig. 2.2a, c). The region where A_1 goes extinct remains constant. The changes in the coexistence patterns can be explained with the different growth functions of the predator P resulting from the different defence mechanisms. We consider two comparable levels of the different defences ($p_1 = 0.45$ or $q_1 = 0.45$) having

the same costs ($N_2^*/N_1^* = 0.5$). The population dynamics clearly reveal that the growth rate of P is higher for the p-K-TO compared to the q-K-TO although the amount of total available prey ($\sum p_i q_i A_i$) is slightly lower during the predator growing phase (Fig. 2.3a, b). The resulting higher biomass of P, i.e., the higher top-down control, in case of the p-K-TO drives the undefended prey A_2 to extinction (Fig. 2.3a).

More generally, the growth rates of P are equal for the p-K-TO and the q-K-TO in the absence of A_1 but they diverge for the different types of defences with an increasing density of the defended prey A_1 (Fig. 2.3c). With higher shares of A_1, the predator is increasingly handling 'non-crackable' prey for the q-K-TO which dampens its growth in comparison to the p-K-TO. At high densities of A_2, an increasing density of A_1 leads even to a reduction of growth in case of the q-K-TO while their is a slight increase in growth for the p-K-TO (Fig. 2.3c). When A_2 is absent, P dies out in case of the q-K-TO because the gross growth rate of P based on a post-attack defended A_1 lies below the mortality rate even for high densities of A_1 resulting in a negative net growth of P (Fig. 2.3c). Therefore, A_1 cannot outcompete A_2 as it needs A_2 to maintain the predator and thus its advantage in respect to defence. In addition, A_1 indirectly facilitates A_2 as it reduces the grazing loss of A_2 by keeping the predator handling 'non-crackable' food items (Fig. 2.3c). The described effects of the post-attack defence on predator growth result in the coexistence of both prey types for an extended trait space. These effects are absent in case of the pre-attack defence leading to the extinction of A_2. The lower growth rates of P in case of the q-K-TO explain also the more frequent occurrence of steady states (Fig. 2.2c). Cycles require sufficient deflections of population densities, i.e., high minima of prey densities, which are prevented due to the lower growth rates of P.

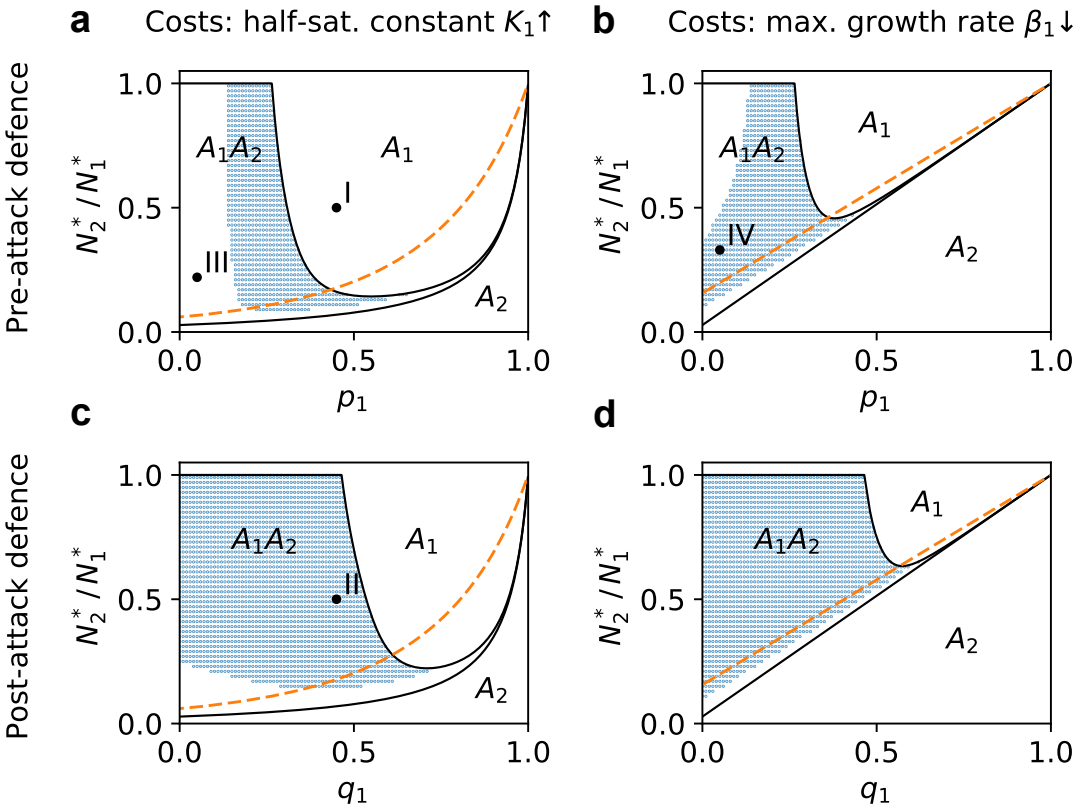

Figure 2.2: Comparison of different types of trade-offs between defence and resource competition regarding their effect on coexistence and population dynamics of a defended prey A_1 and an undefended prey A_2 at an intermediate resource supply ($N_I = 160$ µmol N/l). The trait values of A_1 are varied within the shown trait space. The defence occurs either prior to an attack by a predator via a lower attack probability p_1 (a, b) or after being attacked by a lower consumption probability q_1 (c, d). The costs of the defence are either a higher half-saturation constant K_1 (a, c) or a reduced maximum growth rate β_1 (b, d). Both cost traits affect the relative competitiveness N_2^*/N_1^* of A_1 compared to A_2 (cf. methods, Eq. 2.4). The capital letters display main regions in the trait space with different competition outcomes: Only the undefended prey survives (A_2), only the defended prey survives (A_1) or both prey types coexist (A_1A_2). Coexistence equilibria exist within the region surrounded by black lines while blue dots indicate where they are locally stable. The dashed orange line marks the invasion boundary of A_1. For further details on other regions with multistability see Fig. 2.1. The black dots with Roman numerals mark trait combinations for which population dynamics and growth functions are shown in Fig. 2.3 (I, II) and Fig. 2.4 (III, IV).

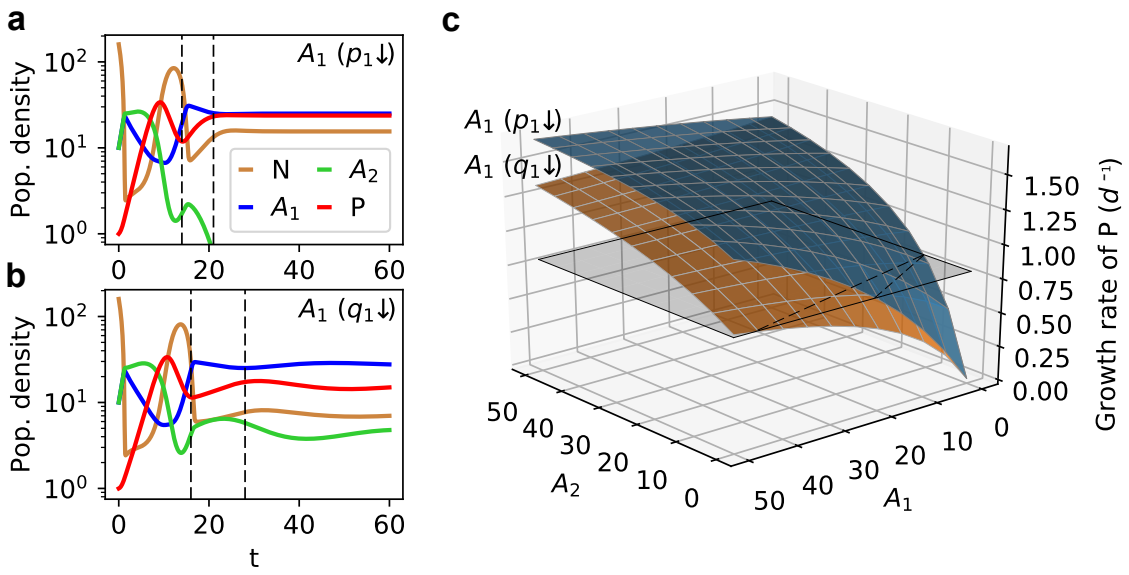

Figure 2.3: (a) Population dynamics for a pre-attack defence - half-saturation constant trade-off (trait combination I in Fig. 2.2a, $p_1 = 0.45$ and $K_1 = 4.4$ µmol N/l) and (b) a post-attack defence - half-saturation constant trade-off (trait combination II in Fig. 2.2c, $q_1 = 0.45$ and $K_1 = 4.4$ µmol N/l). The population densities of the resource N (µmol N/l), the two prey types A_i (10^4 ind./ml) and the predator P (ind./ml) are plotted over time t (d). The vertical dashed lines enclose one growing phase of P. (c) Per capita growth rate of P without mortality in dependence of the densities of the defended prey A_1 and the undefended prey A_2. The blue surface shows the growth function when A_1 is pre-attack defended (like in a) while the orange surface represents the growth function in case of a post-attack defended A_1 (like in b). The post-attack defence reduces the growth rate of P by keeping it unprofitably handling with defended prey individuals while there is no handling of pre-attack defended prey. The grey surface shows the dilution rate which represents the mortality of the predator. The black dashed lines illustrate where the growth rate of P equals its mortality, i.e., where its net growth rate is zero.

Comparison of different defence costs

We now compare the effects of different cost types based on the trade-off between attack probability and half-saturation constant (p-K-TO) or maximum growth rate (p-β-TO). A higher half-saturation constant K_1 rather than a lower maximum growth rate β_1 as defence costs allows the defended prey A_1 to survive even at lower values of relative competitiveness N_2^*/N_1^* and promotes cycles more strongly at high and intermediate defence levels, i.e., low and intermediate p_1 (Fig. 2.2a, b). The advantage of A_1 facing a p-K-TO and the altered stability of coexistence equilibria can be explained based on the population dynamics and growth functions of the prey types shown in Fig. 2.4 for the trait combinations (III, IV) marked in Fig. 2.2a, b. For the p-K-TO, the system cycles (Fig. 2.4a) while damped oscillation occur at the shown p-β-TO (Fig. 2.4b). The trait combinations III, IV are chosen as they lead to a similar level of resource concentrations and predator densities in the first growing phase of A_1 (marked phase in Fig. 2.4a, b). Despite the similar environmental conditions in this phase, A_1 reaches a much higher

growth rate for the p-K-TO than for the p-β-TO (Fig. 2.4a-c). In general, under (at least transient) cyclic conditions, A_1 increases in density when the predator strongly consumes A_2 leading to an increased resource availability (Fig. 2.4a, b). Accordingly, A_1 grows at a resource peak. At high resource concentrations, the growth function of A_1 is getting close to that of A_2 for the p-K-TO as they have the same maximum growth rate but it remains consistently lower in case of the p-β-TO (Fig. 2.4c). The higher growth rate of A_1 in case of the p-K-TO leads to more unstable equilibria and increases the occurrence of cycles compared to the p-β-TO. This explains also why A_1 survives also for a lower competitiveness N_2^*/N_1^* over a large range of p_1 values in case of the p-K-TO. Costs regarding K_1 can be seen as a more temporal disadvantage which only becomes relevant during pronounced resource depletion, i.e., bottom-up control. During top-down control (high predator densities), this disadvantage is less important since the resource conditions are good. The lower competitiveness of A_1 under resource depletion is counteracted by the relatively high growth rate at resource peaks enabling it to survive. We find basically the same effects of the different cost types when considering the other defence mechanism with the reduced consumption probability (q-K-TO and q-β-TO). However, the reduced occurrence of cycles in case of the β-costs is less evident as the post-attack defence mechanism is already stabilizing (Fig. 2.2c, d).

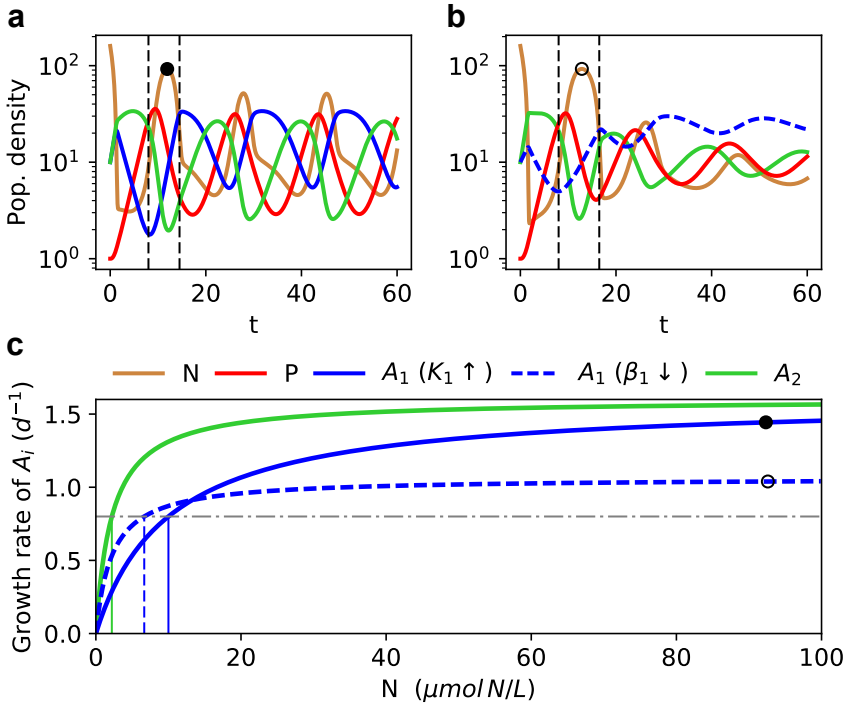

Figure 2.4: (a) Population dynamics for a trade-off between pre-attack defence and half-saturation constant (trait combination III in Fig. 2.2a) or (b) maximum growth rate (trait combination IV in Fig. 2.2b). The population densities of the resource N (µmol N/l), both prey types A_i (10^4 ind./ml) and the predator P (ind./ml) are plotted over time t (d). The pre-attack defended prey A_1 ($p_1 = 0.05$) has either a higher half-saturation constant ($K_1 = 10$ µmol N/l) (a) or a reduced maximum growth rate ($\beta_1 = 1.064\ d^{-1}$) (b) compared to the undefended prey A_2. The black dashed lines enclose one growing phase of A_1 at high resource concentrations (peak marked with dot) after strong grazing of A_2 by P. (c) Per capita growth rates of the prey types without mortality in dependence of the resource concentration are represented by the thick lines. The thin vertical green and blue lines show the resource concentration at equilibrium in monoculture N_i^* of each prey type where lower values of N_i^* imply higher competitiveness. The horizontal black dashed-dotted line represents the dilution rate, i.e., the mortality of the prey without the predator. The dots illustrate the realized growth rate of the respective defended prey at the resource peaks shown in (a, b).

The effect of the enrichment level

So far, we analysed how the different defence mechanisms and costs affect the proportion of the trait space leading to coexistence at a certain resource supply (Fig. 2.2). Now, we fix the trait values of both prey types but vary the enrichment level (N_I) to evaluate the maintenance of coexistence under altered environmental conditions. Pre-attack and post-attack defences differ in their implications for coexistence within a broad range of intermediate defence levels (Fig. 2.2). The type of costs is most relevant at high cost levels and intermediate to high defence levels (Fig. 2.2). Accordingly, we chose such trait combinations of the defended prey, i.e., an intermediate defence level with low costs and

a high defence level with high costs (marked in Fig. 2.1), to examine how the differences in coexistence patterns depend on the enrichment level (Fig. 2.5a, b). At an intermediate level of defence with low costs, coexistence is promoted by the post-attack defence in comparison to the pre-attack defence, independent of the type of costs (Fig. 2.5a). The post-attack defence allows the prey types to stably coexist over a wide range of enrichment levels from low to very high resource supplies while in case of the pre-attack defence coexistence is only possible for a low resource supply (Fig. 2.5a). Contrastingly, at a high level of defence and costs, the coexistence patterns diverge between the different cost types but are rather independent from the defence mechanism. Costs with respect to the half-saturation constant enable coexistence for lower and especially higher enrichment levels compared to costs regarding the maximum growth rate (Fig. 2.5b).

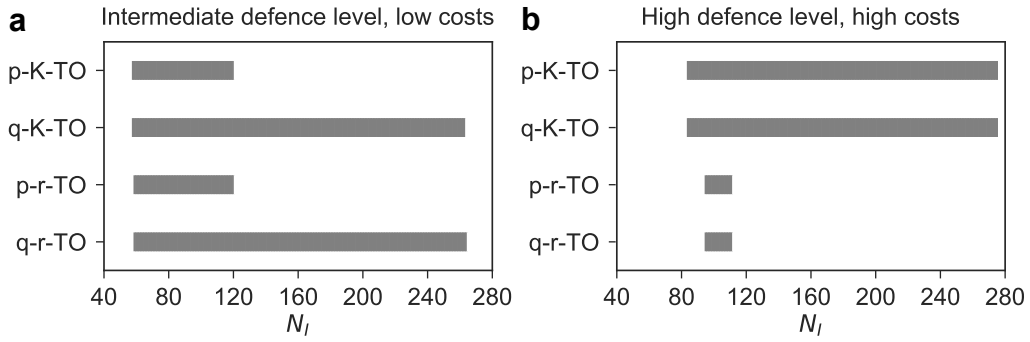

Figure 2.5: Coexistence of two prey types depending on the level of resource supply N_I (in µmol N/l), i.e., the enrichment level, for different trade-offs (TO) between pre-attack (p) or post-attack defence (q) and the half-saturation constant (K) or maximum growth rate (β). The bars indicate the range where both prey types stably coexist, implying that a coexistence equilibrium exists and the defended prey can invade the undefended prey. The defended prey has either (a) an intermediate defence level and low costs (p_1 or $q_1 = 0.4$, $N_2^*/N_1^* = 0.8$) or (b) a high defence level and high costs (p_1 or $q_1 = 0.1$, $N_2^*/N_1^* = 0.2$). These trait combinations are indicated in Fig. 2.1.

Sensitivity analysis

In Appendix A.3, we show how the coexistence and population dynamics of the prey types depend on the amount of the attack time relative to the manipulation time which is defined by c_a (fraction of total handling time spent for attacking). With higher values of c_a, the post-attack defence increasingly promotes coexistence and stabilizes the dynamics while the results for the pre-attack defence are independent of c_a (Appendix A.3: Fig. A4, A5). Furthermore, we check the sensitivity of our results with respect to the encounter rate a, the total handling time T, the conversion efficiency of the predator χ_P, the conversion efficiency of the prey χ, the resource concentration in the supplied medium N_I, the dilution rate δ, the maximum growth rate of the undefended prey β_2 and its half-saturation constant K_2. The general pattern that post-attack defences promote coexistence and stabilize the dynamics compared to pre-attack defences is independent of these parameter

values. The same holds for the observed pattern that costs regarding the half-saturation constant promote coexistence and the occurrence of cycles more strongly than costs with respect to the maximum growth rate (Appendix A.3: Fig. A6, A7 and A8). Obviously, the exact trait values for the occurrence of coexistence equilibria and their local stability depend on the values of all parameters.

Discussion

We compared the effects of pre-attack and post-attack defences with different costs in respect to resource competition on coexistence and population dynamics in a diamond-shaped food web. The post-attack defence promoted coexistence and stabilized the dynamics more than a pre-attack defence. Post-attack defended individuals damped the growth of the predator by keeping it handling them which indirectly facilitates the undefended prey. This mechanism enabled coexistence at trait combinations where the defended prey would outcompete the undefended one in case of a pre-attack defence. Costs regarding resource competition were either a higher half-saturation constant or a lower maximum growth rate. The former cost type promoted coexistence and cycling population densities more than a lower maximum growth rate by allowing the defended prey to realize high growth rates at temporally high resource concentrations which prevents its extinction even if it has a very low competitiveness.

The main difference between both defence mechanisms is that a post-attack defended prey affects the functional response of the predator consuming an undefended prey while a pre-attack defended prey does not. In a previous study of Grover (1995), inedible plants were generally described as interfering when they negatively affect the growth of the herbivore consuming an edible plant. This interference weakens the interaction between the predator and its prey. In food web theory, weak interactions are known to stabilize the population dynamics (McCann et al. 1998; McCann 2011). In fact, several authors (Kretzschmar et al. 1993; Grover 1995; Vos et al. 2001) showed that interfering inedible species stabilized dynamics in comparison to non-interfering inedible ones which resembles the effect observed in our study while they did not reveal the potential of interfering defended prey to enhance coexistence. This was not possible in their systems because the defended prey was completely inedible. Thus, it could not maintain the predator by itself and always had to coexist with the undefended prey. Contrastingly, we considered defence as a continuous trait. At low and intermediate defence levels, the defended prey is able to outcompete the undefended prey. The trait range where this competitive exclusion of the undefended prey occurred was strongly reduced by the post-attack defence while the trait range allowing coexistence increased in comparison to a non-interfering pre-attack defence due to indirect facilitation. The relevance of

our results is supported by empirical studies revealing that low to intermediate defence levels frequently occur in nature (White et al. 2011) and that defended prey types may outcompete undefended prey types even if they have costs for their defence (Kasada et al. 2014). The presented mechanism of indirect facilitation among prey species may provide an explanation why apparent competition, i.e., an increasing density of one prey species indirectly reduces the density of the other prey species via the predator (Holt 1977), is not always observed in nature (Chaneton and Bonsall 2000).

If attacking defended prey types hampers predator's growth, the question arises whether the predator adapts and entirely disregards the defended prey implying that post-attack defences become pre-attack defences. Pre-attack defences are also favourable from the point of view of the defended prey which is then able to better outcompete a competing undefended prey. Accordingly, predator and defended prey may evolve towards avoiding interactions with each other which would mean that being not attacked is the prevailing defence strategy. This reasoning is supported by the observation that many defended prey species show warning signals to deter the predator from attacking them (Blount et al. 2012; Stevens and Ruxton 2012) and that predators often show behavioural changes to avoid defended prey species (White et al. 2011; Xu et al. 2018). However, not attacking defended prey species implies a higher grazing pressure on undefended prey species which may reduce their population densities leading to the dominance of defended prey species. The resulting lack in food may cause predator attacks on the defended prey (Fryxell and Lundberg 1994; Barnett et al. 2007). However, if the defence of the prey is very effective, such prey switching behaviour of the predator is unlikely. Several studies highlighted the importance of the interplay between the predator's diet choice and the level of defence for prey coexistence and population dynamics (Abrams and Matsuda 1993; Fryxell and Lundberg 1994; Yamauchi and Yamamura 2005). Another argument for the occurrence of post-attack defences in nature is the inability of predators to discriminate between undefended and defended prey. This may hold especially for predators with nonselective feeding strategies, like e.g., filter feeding *Daphnia sp.* consuming filamentous algae (Peter and Lampert 1989). Furthermore, it strongly depends on the costs of the prey which defence mechanisms evolve (Bateman et al. 2014). Post-attack defences may evolve if pre-attack defences are very costly, e.g., if avoiding habitats with predators substantially lowers the possibility of resource acquisition (Verdolin 2006).

The used categorization into pre- and post-attack defences is based on mechanistic considerations regarding their effect on the invested handling time of the predator. Even if these categories are relevant for a broad range of defence mechanisms, they may not apply to every specific defence strategy. For example, several algal species are digestion-resistant, i.e., they are attacked and ingested by the zooplankton but survive the gut passage (Porter 1973; Meyer et al. 2006; Demott and McKinney 2015). The

same holds also for some species of aquatic snails eaten by mallards (van Leeuwen et al. 2012; Wada et al. 2012). Such digestion resistance may promote coexistence and stabilize the dynamics even more than post-attack defended prey (see Appendix A.1). Furthermore, toxicity of a prey may differ in the consequences on prey coexistence from the defence mechanisms considered here, especially when it interferes not only with the predator but also with the competitor (Hiltunen et al. 2012). However, for a large variety of defence strategies, e.g., aposematism, weaponry or mimicry, the used classification regarding the phase at which the defence interrupts the predation sequence is adequate. We distinguished between early (pre-attack) and late (post-attack) defences (Bateman et al. 2014). Of course, in nature there are gradients between pre- and post-attack defences, i.e., the handling of the predator aborts at different points in time which can be mimicked by varying the parameter c_a (see Appendix A.3). In the presented model, c_a was defined as the fraction of handling time invested in attacking prey. However, in a more general sense, c_a can be interpreted as the timing of a defended prey to abort the predation sequence relative to the total handling time, i.e., a large c_a corresponds to a late defence and vice versa. Therefore, the given equation of the predator's functional response for two prey types (Eq. A1) can be applied to multiple defence mechanisms acting at different phases of the predation sequence.

Hammill et al. (2015) provided first empirical evidence that inedible prey species promote persistence of edible ones based on an experiment with a flatworm feeding on ciliates. However, despite the wide-spread occurrence of post-attack defences, we found no study specifically analysing their effect on coexistence and comparing it to pre-attack defences. Thus, our research may serve as a starting point for future empirical studies on the maintenance of functional diversity within prey communities due to indirect facilitation of undefended prey species by post-attack defended prey species.

Quantifying defence costs is often difficult as it requires knowledge about the functional property of the prey which is influenced by an altered allocation of resources to implement the defence. Furthermore, the costs may be system specific and may vary depending on the environment (Siemens et al. 2002; Strauss et al. 2002), e.g., they may occur only when a competitor is present (van Velzen and Etienne 2015). We focussed on two major cost traits of defended prey types which describe their resource-dependent growth kinetics: a higher half-saturation constant which implies a reduced competitiveness at low resource concentration, and a lower maximum growth rate which reduces growth independent of the resource concentrations. Studies on plankton organisms revealed that trade-offs between maximum growth rates and defences frequently occur (Agrawal 1998; Meyer et al. 2006) but half-saturation constant-defence trade-offs were found as well (Yoshida et al. 2004; Becks et al. 2010). Furthermore, there is indication from phytoplankton organisms that the maximum growth rate and the half-saturation constant

are often positively correlated (Edwards et al. 2013; Litchman et al. 2015). Thus, Aksnes and Egge (1991) and Smith et al. (2014) suggested an alternative mechanistic formulation of nutrient-uptake kinetics for phytoplankton organisms which accounted implicitly for this correlation. They used the affinity, i.e., the slope of the uptake function at resource concentrations close to zero, instead of the half-saturation constant as a parameter describing the performance at low resource concentrations. However, the outcome would be similar: a lower affinity rather than a lower maximum growth rate as defence costs promotes coexistence and destabilizes the dynamics because it allows for temporally high growth rates of the defended prey at resource peaks.

In the context of plant communities, there is an ongoing debate on the costs of defences against herbivory. Several studies indicated that there is often no interspecific trade-off between defence and competitiveness as a higher resource supply adversely affected defended plants (Viola et al. 2010; Lind et al. 2013). In fact, Lind et al. (2013) demonstrated that defended plants are commonly the better competitor when resources are depleted but perform less well at high resource concentrations. Such multi-dimensional trade-offs may be included in future studies considering specific prey communities and their cost type/s of defence.

The coexistence of defended and undefended prey types critically depends on the relative importance of bottom-up and top-down control, i.e., the enrichment level of the system (Leibold 1996; Proulx and Mazumder 1998; Bohannan and Lenski 2000). Higher enrichment levels promote the defended prey as its disadvantage regarding resource competition gets less important relative to its advantage of being defended against predation. Thus, our insights on how the competitive exclusion of an undefended prey by an intermediately defended prey is prevented in case of post-attack defence may prevail more in systems with an intermediate or high resource supply (Fig. 2.5a). A high system productivity reduces also the potential extinction risk of the defended prey if the defence costs arise from a high half-saturation costs where resource peaks permit temporally high growth rates of the defended prey (Fig. 2.5b).

Acknowledgements

We thank Toni Klauschies, Lutz Becks and Thomas Kiørboe for fruitful discussions on the results, and Janne Hülsemann, Christopher Klausmeier and two anonymous reviewers for valuable comments on an earlier version of the manuscript. This research was funded by the German Research Foundation (DFG, GA 401/25-1).

Bibliography 2

Abrams, P. and Matsuda, H. (1993). Effects of adaptive predatory and anti-predator behaviour in a two-prey-one-predator system. *Evolutionary Ecology*, 7(3):312–326.

Abrams, P. A. (1999). Is predator-mediated coexistence possible in unstable systems? *Ecology*, 80(2):608–621.

Agrawal, A. A. (1998). Algal defense, grazers, and their interactions in aquatic trophic cascades. *Acta Oecologica*, 19(4):331–337.

Aksnes, D. and Egge, J. (1991). A theoretical model for nutrient uptake in phytoplankton. *Marine Ecology Progress Series*, 70(1):65–72.

Barnett, C., Bateson, M., and Rowe, C. (2007). State-dependent decision making: educated predators strategically trade off the costs and benefits of consuming aposematic prey. *Behavioral Ecology*, 18(4):645–651.

Bateman, A. W., Vos, M., and Anholt, B. R. (2014). When to Defend: Antipredator Defenses and the Predation Sequence. *The American Naturalist*, 183(6):847–855.

Becks, L., Ellner, S. P., Jones, L. E., and Hairston Jr., N. G. (2010). Reduction of adaptive genetic diversity radically alters eco-evolutionary community dynamics. *Ecology Letters*, 13(8):989–997.

Becks, L., Ellner, S. P., Jones, L. E., and Hairston Jr., N. G. (2012). The functional genomics of an eco-evolutionary feedback loop: linking gene expression, trait evolution, and community dynamics. *Ecology Letters*, 15(5):492–501.

Blount, J. D., Rowland, H. M., Drijfhout, F. P., Endler, J. A., Inger, R., Sloggett, J. J., Hurst, G. D. D., Hodgson, D. J., and Speed, M. P. (2012). How the ladybird got its spots: effects of resource limitation on the honesty of aposematic signals. *Functional Ecology*, 26(2):334–342.

Bohannan, B. J. M. and Lenski, R. E. (2000). The relative importance of competition and predation varies with productivety in a model community. *American Naturalist*, 156(4):329–340.

Brodie, E., Formanowicz, D., and Brodie, E. (1991). Predator avoidance and antipredator mechanisms: distinct pathways to survival. *Ethology Ecology & Evolution*, 3(1):73–77.

Button, D. (1978). On the theory of control of microbial growth kinetics by limiting nutrient concentrations. *Deep Sea Research*, 25(12):1163–1177.

Chaneton, E. J. and Bonsall, M. B. (2000). Enemy-mediated apparent competition: empirical patterns and the evidence. *Oikos*, 88(2):380–394.

Chase, J. M., Abrams, P. A., Grover, J. P., Diehl, S., Chesson, P., Holt, R. D., Richards, S. A., Nisbet, R. M., and Case, T. J. (2002). The interaction between predation and competition: A review and synthesis. *Ecology Letters*, 5:302–315.

Ciros-Pérez, J., Carmona, M. J., Lapesa, S., and Serra, M. (2004). Predation as a factor mediating resource competition among rotifer sibling species. *Limnology and Oceanography*, 49(1):40–50.

Coley, P. D., Bryant, J. P., and Chapin, F. S. (1985). Resource Availability and Plant Antiherbivore Defense. *Science*, 230(4728):895–899.

Demott, W. R. and McKinney, E. N. (2015). Use it or lose it? Loss of grazing defenses during laboratory culture of the digestion-resistant green alga Oocystis. *Journal of Plankton Research*, 37(2):399–408.

Edwards, K. F., Klausmeier, C. A., and Litchman, E. (2013). A Three-Way Trade-Off Maintains Functional Diversity under Variable Resource Supply. *The American Naturalist*, 182(6):786–800.

Ehrlich, E., Becks, L., and Gaedke, U. (2017). Trait-fitness relationships determine how trade-off shapes affect species coexistence. *Ecology*, 98(12):3188–3198.

Endler, J. A. (1991). Interactions between predators and prey. In *Behevioural Ecology: An Evolutionary Approach*, pages 169–196.

Fauth, J. E. and Resetarits, W. J. (1991). Interactions Between the Salamander Siren Intermedia and the Keystone Predator Notophthalmus Viridescens. *Ecology*, 72(3):827–838.

Fryxell, J. M. and Lundberg, P. (1994). Diet choice and predator-prey dynamics. *Evolutionary Ecology*, 8(4):407–421.

Genkai-Kato, M. and Yamamura, N. (1999). Unpalatable prey resolves the paradox of enrichment. *Proceedings of the Royal Society B: Biological Sciences*, 266(1425):1215–1219.

Grover, J. P. (1995). Competition, Herbivory, and Enrichment: Nutrient-Based Models for Edible and Inedible Plants. *The American Naturalist*, 145(5):746–774.

Hammill, E., Kratina, P., Vos, M., Petchey, O. L., and Anholt, B. R. (2015). Food web persistence is enhanced by non-trophic interactions. *Oecologia*, 178(2):549–556.

Healey, F. P. (1980). Slope of the Monod equation as an indicator of advantage in nutrient competition. *Microbial Ecology*, 5(4):281–286.

Hillebrand, H., Worm, B., and Lotze, H. (2000). Marine microbenthic community structure regulated by nitrogen loading and grazing pressure. *Marine Ecology Progress Series*, 204:27–38.

Hiltunen, T., Barreiro, A., and Hairston Jr., N. G. (2012). Mixotrophy and the toxicity of Ochromonas in pelagic food webs. *Freshwater Biology*, 57(11):2262–2271.

Holling, C. S. (1959). The Components of Predation as Revealed by a Study of Small-Mammal Predation of the European Pine Sawfly. *The Canadian Entomologist*, 91(05):293–320.

Holt, R. D. (1977). Predation, apparent competition, and the structure of prey communities. *Theoretical Population Biology*, 12(2):197–229.

Jones, E., Oliphant, T., and Peterson, P. (2001). SciPy: Open source scientific tools for Python, 2009.

Jones, L. E. and Ellner, S. P. (2007). Effects of rapid prey evolution on predator–prey cycles. *Journal of Mathematical Biology*, 55(4):541–573.

Kasada, M., Yamamichi, M., and Yoshida, T. (2014). Form of an evolutionary tradeoff affects eco-evolutionary dynamics in a predator–prey system. *Proceedings of the National Academy of Sciences*, 111(45):16035–16040.

Kretzschmar, M., Nisbet, R., and Mccauley, E. (1993). A Predator-Prey Model for Zooplankton Grazing on Competing Algal Populations. *Theoretical Population Biology*, 44(1):32–66.

Leibold, M. A. (1996). A Graphical Model of Keystone Predators in Food Webs: Trophic Regulation of Abundance, Incidence, and Diversity Patterns in Communities. *The American Naturalist*, 147(5):784–812.

Lima, S. L. and Dill, L. M. (1990). Behavioral decisions made under the risk of predation: a review and prospectus. *Canadian Journal of Zoology*, 68(4):619–640.

Lind, E. M., Borer, E., Seabloom, E., Adler, P., Bakker, J. D., Blumenthal, D. M., Crawley, M., Davies, K., Firn, J., Gruner, D. S., Stanley Harpole, W., Hautier, Y., Hillebrand, H., Knops, J., Melbourne, B., Mortensen, B., Risch, A. C., Schuetz, M., Stevens, C., and Wragg, P. D. (2013). Life-history constraints in grassland plant species: a growth-defence trade-off is the norm. *Ecology Letters*, 16(4):513–521.

Litchman, E., Edwards, K. F., and Klausmeier, C. A. (2015). Microbial resource utilization traits and trade-offs: implications for community structure, functioning, and biogeochemical impacts at present and in the future. *Frontiers in Microbiology*, 06(APR):1–10.

McCann, K., Hastings, A., and Huxel, G. R. (1998). Weak trophic interactions and the balance of nature. *Nature*, 395(6704):794–798.

McCann, K. S. (2011). *Food Webs (MPB-50)*, volume 50.

McPeek, M. A. (1998). The Consquences of Changing the Top Predator in a Food Web: A Comparative Experimental Approach. *Ecological Monographs*, 68(1):1.

Menge, B. A., Berlow, E. L., Blanchette, C. A., Navarrete, S. A., and Yamada, S. B. (1994). The Keystone Species Concept: Variation in Interaction Strength in a Rocky Intertidal Habitat. *Ecological Monographs*, 64(3):249–286.

Meyer, J. R., Ellner, S. P., Hairston, N. G., Jones, L. E., and Yoshida, T. (2006). Prey evolution on the time scale of predator-prey dynamics revealed by allele-specific quantitative PCR. *Proceedings of the National Academy of Sciences of the United States of America*, 103(28):10690–10695.

Monod, J. (1950). La technique de culture continue: theorie et applications. *Annals de l'Institut Pasteur*, 79:390–410.

Murdoch, W. W. (1969). Switching in General Predators: Experiments on Predator Specificity and Stability of Prey Populations. *Ecological Monographs*, 39(4):335–354.

Paine, R. T. (1966). Food Web Complexity and Species Diversity. *The American Naturalist*, 100(910):65–75.

Peter, H. and Lampert, W. (1989). The effect of Daphnia body size on filtering rate inhibition in the presence of a filamentous cyanobacterium. *Limnology and Oceanography*, 34(6):1084–1089.

Porter, K. G. (1973). Selective Grazing and Differential Digestion of Algae by Zooplankton. *Nature*, 244(5412):179–180.

Proulx, M. and Mazumder, A. (1998). Reversal of grazing impact on plant species richness in nutrient-poor vs. nutrient-rich ecosystems. *Ecology*, 79(8):2581–2592.

Raatz, M., Gaedke, U., and Wacker, A. (2017). High food quality of prey lowers its risk of extinction. *Oikos*, 126(10):1501–1510.

Rueffler, C., Van Dooren, T. J. M., and Metz, J. A. J. (2006). The Evolution of Resource Specialization through Frequency-Dependent and Frequency-Independent Mechanisms. *The American Naturalist*, 167(1):81–93.

Siemens, D. H., Garner, S. H., Mitchell-Olds, T., and Callaway, R. M. (2002). Cost of defense in the context of plant competition: Brassica rapa may grow and defend. *Ecology*, 83(2):505–517.

Sih, A., Crowley, P., McPeek, M., Petranka, J., and Strohmeier, K. (1985). Predation, Competition, and Prey Communities: A Review of Field Experiments. *Annual Review of Ecology and Systematics*, 16(1):269–311.

Smith, H. L. and Waltman, P. (1995). The theory of the chemostat: dynamics of microbial competition. *Cambridge Studies in Mathematical Biology*.

Smith, S. L., Merico, A., Wirtz, K. W., and Pahlow, M. (2014). Leaving misleading legacies behind in plankton ecosystem modelling. *Journal of Plankton Research*, 36(3):613–620.

Stearns, S. C. (1989). Trade-Offs in Life-History Evolution. *Functional Ecology*, 3(3):259.

Stevens, M. and Ruxton, G. D. (2012). Linking the evolution and form of warning coloration in nature. *Proceedings of the Royal Society B: Biological Sciences*, 279(1728):417–426.

Strauss, S. Y., Rudgers, J. A., Lau, J. A., and Irwin, R. E. (2002). Direct and ecological costs of resistance to herbivory. *Trends in Ecology and Evolution*, 17(6):278–285.

Thingstad, T. F. (2000). Elements of a theory for the mechanisms controlling abundance, diversity, and biogeochemical role of lytic bacterial viruses in aquatic systems. *Limnology and Oceanography*, 45(6):1320–1328.

Tilman, D. (1982). *Resource Competition and Community Structure*. Princeton University Press, Princeton, NJ.

Tirok, K. and Gaedke, U. (2010). Internally driven alternation of functional traits in a multispecies predator–prey system. *Ecology*, 91(6):1748–1762.

van Leeuwen, C. H. A., van der Velde, G., van Lith, B., and Klaassen, M. (2012). Experimental Quantification of Long Distance Dispersal Potential of Aquatic Snails in the Gut of Migratory Birds. *PLoS ONE*, 7(3):e32292.

van Velzen, E. and Etienne, R. S. (2015). The importance of ecological costs for the evolution of plant defense against herbivory. *Journal of Theoretical Biology*, 372:89–99.

Verdolin, J. L. (2006). Meta-analysis of foraging and predation risk trade-offs in terrestrial systems. *Behavioral Ecology and Sociobiology*, 60(4):457–464.

Viola, D. V., Mordecai, E. a., Jaramillo, A. G., Sistla, S. a., Albertson, L. K., Gosnell, J. S., Cardinale, B. J., and Levine, J. M. (2010). Competition-defense tradeoffs and the maintenance of plant diversity. *Pnas*, 107(40):17217–22.

Vos, M., Berrocal, S. M., Karamaouna, F., Hemerik, L., and Vet, L. E. M. (2001). Plant-mediated indirect effects and the persistence of parasitoid-herbivore communities.

Wada, S., Kawakami, K., and Chiba, S. (2012). Snails can survive passage through a bird's digestive system. *Journal of Biogeography*, 39(1):69–73.

White, J. D., Kaul, R. B., Knoll, L. B., Wilson, A. E., and Sarnelle, O. (2011). Large variation in vulnerability to grazing within a population of the colonial phytoplankter, Microcystis aeruginosa. *Limnology and Oceanography*, 56(5):1714–1724.

Winter, C., Bouvier, T., Weinbauer, M. G., and Thingstad, T. F. (2010). Trade-Offs between Competition and Defense Specialists among Unicellular Planktonic Organisms: the "Killing the Winner" Hypothesis Revisited. *Microbiology and Molecular Biology Reviews*, 74(1):42–57.

Xu, J., Nielsen, L. T., and Kiørboe, T. (2018). Foraging response and acclimation of ambush feeding and feeding-current feeding copepods to toxic dinoflagellates. *Limnology and Oceanography*.

Yamauchi, A. and Yamamura, N. (2005). Effects of defense evolution and diet choice on population dynamics in a one-predator-two-prey system. *Ecology*, 86(9):2513–2524.

Yoshida, T., Ellner, S. P., Jones, L. E., Bohannan, B. J. M., Lenski, R. E., and Hairston Jr., N. G. (2007). Cryptic population dynamics: rapid evolution masks trophic interactions. *PLoS biology*, 5(9):e235.

Yoshida, T., Hairston, N. G., and Ellner, S. P. (2004). Evolutionary trade-off between defence against grazing and competitive ability in a simple unicellular alga, Chlorella vulgaris. *Proceedings of the Royal Society B: Biological Sciences*, 271(1551):1947–1953.

Yoshida, T., Jones, L. E., Ellner, S. P., Fussmann, G. F., and Hairston, N. G. (2003). Rapid evolution drives ecological dynamics in a predator-prey system. *Nature*, 424(July):303–306.

3 Trade-off shapes, fitness and coexistence

Manuscript title:

Trait-fitness relationships determine how trade-off shapes affect species coexistence

Elias Ehrlich[1], Lutz Becks[2] and Ursula Gaedke[1]

1. Department of Ecology and Ecosystem Modelling, University of Potsdam, Am Neuen Palais 10, 14469 Potsdam, Germany.
2. Community Dynamics Group, Department of Evolutionary Ecology, Max Planck Institute for Evolutionary Biology, August-Thienemann-Str. 2, 24306 Plön, Germany.

Published as:

Ehrlich, E., Becks, L., and Gaedke, U. (2017). Trait-fitness relationships determine how trade-off shapes affect species coexistence. *Ecology*, 98(12), 3188–3198.

Abstract

Trade-offs between functional traits are ubiquitous in nature and can promote species coexistence depending on their shape. Classic theory predicts that convex trade-offs facilitate coexistence of specialized species with extreme trait values (extreme species) while concave trade-offs promote species with intermediate trait values (intermediate species). We show here that this prediction becomes insufficient when the traits translate non-linearly into fitness which frequently occurs in nature, e.g. an increasing length of spines reduces grazing losses only up to a certain threshold resulting in a saturating or sigmoid trait-fitness function. We present a novel, general approach to evaluate the effect of different trade-off shapes on species coexistence. We compare the trade-off curve to the invasion boundary of an intermediate species invading the two extreme species. At this boundary the invasion fitness is zero. Thus, it separates trait combinations where invasion is or is not possible. The invasion boundary is calculated based on measurable trait-fitness relationships. If at least one of these relationships is not linear, the invasion boundary becomes non-linear implying that convex and concave trade-offs not necessarily lead to different coexistence patterns. Therefore, we suggest a new ecological classification of trade-offs into extreme-favouring and intermediate-favouring which differs from a purely mathematical description of their shape. We apply our approach to a well-established model of an empirical predator-prey system with competing prey types facing a trade-off between edibility and half-saturation constant for nutrient uptake. We show that the survival of the intermediate prey depends on the convexity of the trade-off. Overall, our approach provides a general tool to make a priori predictions on the outcome of competition among species facing a common trade-off in dependence of the shape of the trade-off and the shape of the trait-fitness relationships.

Introduction

Understanding the mechanisms of species coexistence still poses a major challenge in ecology. Trade-offs between different functional traits provide an essential basis for coexistence by allowing differentiation of ecological strategies through diverging trait values among coexisting species (Tilman 2000). Because species are unable to optimize the values of all their traits at the same time due to physiological, energetic and genetic constraints, maximizing the value of one trait (e.g. defence against predation) generally implies costs regarding other traits (e.g. growth). Such trade-offs are common, occur for all types of species interactions, and may prevent the occurrence of a "superspecies" performing best under all conditions and outcompeting all others (Kneitel and Chase 2004).

The existence of a trade-off does not necessarily imply that different highly specialized species coexist. As firstly reported by Levins (1962, 1968), the species composition crucially depend on the shape of the trade-off between the traits. Assuming that fitness increases linearly with higher trait values, convex trade-offs imply that an intermediate value of one trait x comes with high fitness costs regarding the other trait y while the opposite holds for concave trade-offs (Fig. 3.1a). Accordingly, convex trade-offs which are mathematically defined by a positive second derivative ($\partial^2 y/\partial x^2$) were often called strong while concave trade-offs having a negative second derivative were named weak (Egas et al. 2004; Abrams 2006a; Rueffler et al. 2006). Previous theory commonly predicts that convex trade-offs select for extreme trait combinations (extreme species) while concave trade-offs promote species with intermediate trait values (intermediate species). This was shown for trade-offs of consumers using two different habitats/resources (Egas et al. 2004; Abrams 2006a), host trade-offs between growth rate and resistance against parasitism (Boots and Haraguchi 1999; Bowers and Hodgkinson 2001), trade-offs of pathogens transmitted to two different hosts (Gudelj et al. 2004) and prey trade-offs between reproduction/resource competition and vulnerability to predation (Day et al. 2002; Abrams 2003; Jones et al. 2009). In some of these studies, "convex" and "concave" were oppositely defined while we refer here to the mathematical definition mentioned before (see Fig. 3.1a).

Empiricists have made strong effort to measure trade-off curves (Benkman 1993; Schluter 1995; O'Hara Hines et al. 2004; Jessup and Bohannan 2008) and recently tested Levins' theory with competition experiments (Maharjan et al. 2013; Meyer et al. 2015). However, the consequences of different trade-off curves for the outcome of competition may strongly depend on the considered traits trading off and how they relate to fitness (de Mazancourt and Dieckmann 2004; Rueffler et al. 2004; Bowers et al. 2005; White and Bowers 2005; Hoyle et al. 2008). For specific cases, the prediction may hold that convex

trade-offs always favour extreme species while concave trade-offs promote intermediate species. In our paper, we abstract from specific cases and show that this distinction is insufficient when the traits translate non-linearly into fitness. To overcome this problem, we present a novel, general approach to evaluate consequences of different trade-off shapes for species coexistence based on measurable trait-fitness relationships. In order to do this, we calculate the invasion boundary of an intermediate species invading the two extreme species and compare the trade-off curve to it. This allows us to predict whether the extreme species will dominate for a given trade-off curve (invasion impossible) or whether an intermediate species will be part of the community (invasion possible). In addition, we evaluate when an intermediate species may stably coexist with one extreme species or both of them based on invasion criteria (Fig. 3.1b). Our approach is appropriate for systems without multi-stability implying that a species which is unable to invade can also not persist at high densities. Our results reveal that convex and concave trade-offs do often not imply different coexistence scenarios depending on the fitness functions. Therefore, we suggest a new classification of trade-offs into extreme-favouring (EF) and intermediate-favouring (MF) trade-offs which differs from a purely mathematical description of their shape. MF-trade-offs allow for the invasion of an intermediate species into the extreme species while EF-trade-offs do not.

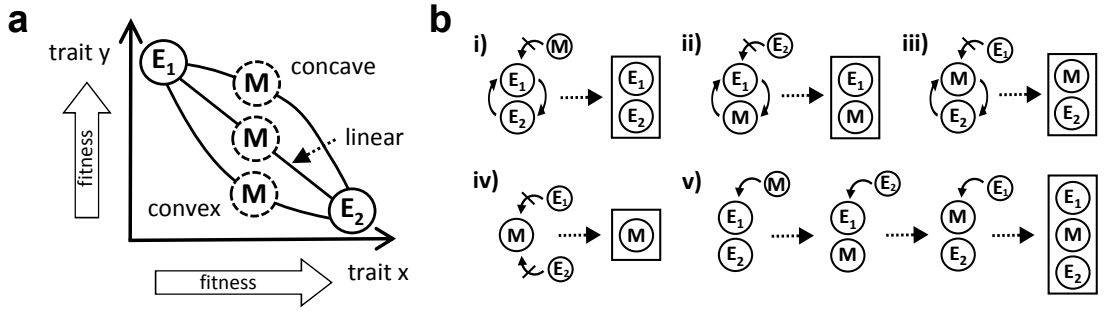

Figure 3.1: (a) Different shapes of a trade-off between trait x and trait y. The trait values of the extreme species E_1 and E_2 are fixed (solid circles) while the trait values of the intermediate species M (dashed circles) depend on the shape of the trade-off. (b) Coexistence analysis based on the invasion criterion. Assuming that the extreme species always coexist in the absence of M and no multi-stability occurs, five possible outcomes exist (i-v) which are illustrated behind the dashed arrows in the boxes. The necessary invasion tests are shown in front of the dashed arrows. Arrows indicate successful invasion paths while struck-through arrows represent impossible invasion paths. Two species coexist if they are mutual invasible and if they are non-invasible by the third species (i-iii). Only the intermediate species survives when both extreme species cannot invade it (iv). Coexistence of all three species occurs if each species can invade the others (v) (cf. general approach).

Previous studies often examined trade-off shapes in an evolutionary context with adaptive dynamics where organisms could gradually adapt their trait values and reached maximal fitness due to selection (de Mazancourt and Dieckmann 2004; Rueffler et al. 2004; White and Bowers 2005). Here, we take an ecological perspective and analyse sorting of species (or genotypes) with fixed trait values facing an interspecific (or intraspecific) trade-off. Thus, in contrast to the previously mentioned studies, the considered community does not necessarily has to be evolutionary attainable via local mutations from a monomorphic population but can be assembled, e.g. by immigration. Typically, trade-offs are regarded to be species-specific. However, also interspecific trade-offs are common in nature when organisms of different species share similar physiological constraints between functional traits (Tilman et al. 1982; Kneitel and Chase 2004), e.g. based on allometric relationships (Litchman et al. 2007). Mechanistically, there is no difference between competition of species facing an interspecific trade-off and sorting of genotypes of an asexually reproducing species with an intraspecific trade-off (assuming no horizontal gene transfer). In the following, we refer to species while the results are transferable to genotype sorting.

First, we introduce our general framework on how to calculate the shape of invasion boundaries based on given trait-fitness relationships and how to infer consequences of different trade-off shapes from that. We present illustrative cases where the invasion boundary is not linear but convex, concave or a combination of both. In the second part, we apply the general approach to a well-established model of an empirical predator-prey system with competing prey types facing a trade-off between edibility (probability of being attacked) and its half-saturation constant for nutrient uptake. We calculated the invasion boundary of an intermediate prey invading a defended extreme prey (low edibiblity) and a competitive extreme prey (low half-saturation constant) which was convex. Consequently, we found the same coexistence pattern for concave and slightly convex trade-offs lying above the invasion boundary. In addition to the analysis of stable coexistence, we considered the duration of co-occurrence in case of competitive exclusion which increased with trade-off curves getting closer to the invasion boundary as expected based on the theory on fitness equality (Hubbell 2001; He et al. 2012).

General approach

Trait-fitness relationships and the invasion boundary

We consider a general system of three competing species which face an interspecific trade-off between two functional traits x and y: two species with extreme trait values (E_1, E_2) and one intermediate species (M). We assume niche differentiation of E_1 and E_2, i.e. their

traits (x_1, y_1 and x_2, y_2) are fixed at the opposite extreme values of the trait range allowing them to stably coexist when M is absent. The aim of this approach is first to detect the invasion boundary of M invading a resident community of E_1 and E_2 (combinations of trait values x_M and y_M where the invasion fitness equals zero). The invasion boundary may be linear, convex, concave or a combination of convex and concave parts. This is described by the second derivative of one trait with respect to the other trait at the invasion boundary, i.e. $\frac{\partial^2 y_M}{\partial x_M^2}$. In the following paragraphs, we achieve a general representation of this second derivative based on terms describing how x_M and y_M translate into fitness.

To achieve a criterion for the invasion success of M, we consider its per capita growth rate which is defined as its fitness. The fitness can be written as a function f of its traits x_M and y_M, its population density M and the population densities of the extreme species E_1 and E_2:

$$\frac{1}{M}\frac{dM}{dt} = f(x_M, y_M, M, E_1, E_2) \; . \tag{3.1}$$

For simplicity, we incorporate no further environmental variables, e.g. fluctuating abiotic factors, resource concentration, parasite or predator density, which can be added when considering a specific system (but see below). The fitness of M may also depend on the traits of E_1 and E_2. However, to simplify the notation, we drop them out of the function in Eq. 3.1 as they are fixed at constant values. Furthermore, we call the traits of M simply x and y from now on.

The invasion fitness of M is defined as its long-term mean per capita growth rate at very low densities ($M \approx 0$) in a resident system of E_1 and E_2, i.e.

$$\left\langle \frac{1}{M}\frac{dM}{dt} \right\rangle = \langle f(x, y, 0, E_1, E_2) \rangle \; . \tag{3.2}$$

If the resident community is in a stable equilibrium, the angle brackets indicating the long-term mean can be omitted as the population densities are constant over time. In case of fluctuating densities, the mean is taken over one cycle. At the invasion boudary, $\langle f(x, y, 0, E_1, E_2) \rangle$ is equal to zero. In many cases, the traits affect different fitness components, e.g. growth based on resource consumption and loss due to predation. Therefore, we replace f by two additive functions f_x and f_y where each refers to one fitness component (for non-additive cases see Appendix B.1):

$$\langle f_x(x, 0, E_1, E_2) \rangle + \langle f_y(y, 0, E_1, E_2) \rangle = 0 \tag{3.3}$$

Trade-offs imply that the value of one trait depends on the value of another trait. Thus, y can be expressed as a function of x and Eq. 3.3 can be rearranged to $\langle f_y(y(x), 0, E_1, E_2) \rangle = -\langle f_x(x, 0, E_1, E_2) \rangle$ while differentiating both sides of this equation with respect to x yields

$\frac{\partial \langle f_y \rangle}{\partial y} \frac{\partial y}{\partial x} = -\frac{\partial \langle f_x \rangle}{\partial x}$ and thus

$$\frac{\partial y}{\partial x} = -\frac{\partial \langle f_x \rangle / \partial x}{\partial \langle f_y \rangle / \partial y} . \tag{3.4}$$

For simplicity, the arguments of f_x and f_y are not displayed any more. If $\partial y / \partial x$ is negative the invasion boundary has a negative slope and *vice versa*. The second derivative of y with respect to x describes the change of the slope of the invasion boundary along the gradient of x:

$$\frac{\partial^2 y}{\partial x^2} = \frac{\frac{\partial \langle f_x \rangle}{\partial x} \frac{\partial^2 \langle f_y \rangle}{\partial y^2} \frac{\partial y}{\partial x} - \frac{\partial^2 \langle f_x \rangle}{\partial x^2} \frac{\partial \langle f_y \rangle}{\partial y}}{\left(\frac{\partial \langle f_y \rangle}{\partial y} \right)^2} . \tag{3.5}$$

The invasion boundary is concave if $\partial^2 y / \partial x^2$ is negative, convex for positive values and linear when $\partial^2 y / \partial x^2 = 0$. Thus, Eq. 3.5 provides information about the shape of the invasion boundary. The individual terms of Eq. 3.5 or at least their signs are typically known or can be measured for specific systems: the signs of $\partial \langle f_x \rangle / \partial x$ and $\partial \langle f_y \rangle / \partial y$ describe whether an increasing trait value leads to a gain or a loss of fitness. The signs of $\partial^2 \langle f_x \rangle / \partial x^2$ and $\partial^2 \langle f_y \rangle / \partial y^2$ indicate whether this change in fitness accelerates or decelerates with increasing trait values.

Fig. 3.2 summarizes different cases of trait-invasion fitness relationships and the resulting directions and shapes of the invasion boundary based on Eq. 3.4 and 3.5. Case 1 represents the standard case with positive, linear trait-fitness relationships resulting in a linear invasion boundary ($\partial^2 y / \partial x^2 = 0$) with a negative slope ($\partial y / \partial x < 0$). As shown in case 2, the slope can be positive when one of the traits affects the fitness negatively ($\partial \langle f_x \rangle / \partial x < 0$ or $\partial \langle f_y \rangle / \partial y < 0$), e.g. an increasing value of natural mortality reduces fitness.

In the cases 3-5, we focus on different shapes of the invasion boundary instead of different directions and consider only traits with a positive effect on the invasion fitness, i.e. the slope is always negative. The invasion boundary is concave when one trait has an increasingly higher effect on the invasion fitness with increasing trait values, i.e. $\partial^2 \langle f_x \rangle / \partial x^2 > 0$ (case 3). As shown in case 4, it is convex when this effect is decreasingly higher ($\partial^2 \langle f_x \rangle / \partial x^2 < 0$). Case 5 reveals that an invasion boundary can consist of convex and concave parts. Such special shapes occur when the range of trait values determines whether the effect of one trait on the invasion fitness is increasingly or decreasingly higher with increasing trait values. A typical example of such a trait is the neck length of giraffes feeding on tree leaves. Below a certain threshold, the leaves are out of reach. Above the threshold, a longer neck increases fitness as they have access to a larger number of leaves. However, once a giraffe's neck is sufficiently long so that most of the leaves are within reach, a further increase in neck length does not lead any more to a higher fitness. The often spheroid shape of tree crowns causes the sigmoid shape of the

fitness function.

Case	$\langle f_x \rangle$	$\langle f_y \rangle$	$\frac{\partial \langle f_x \rangle}{\partial x}$	$\frac{\partial \langle f_y \rangle}{\partial y}$	$\frac{\partial y}{\partial x}$	$\frac{\partial^2 \langle f_x \rangle}{\partial x^2}$	$\frac{\partial^2 \langle f_y \rangle}{\partial y^2}$	$\frac{\partial^2 y}{\partial x^2}$	Invas. boundary
1	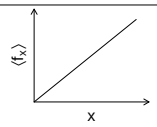	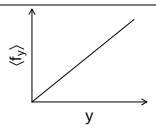	+	+	-	0	0	0	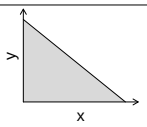
2	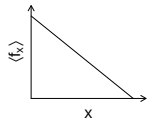	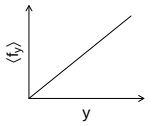	-	+	+	0	0	0	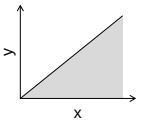
3	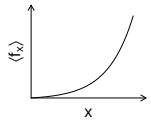	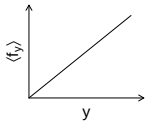	+	+	-	+	0	-	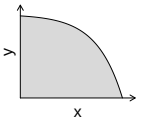
4	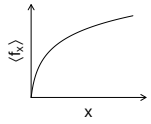	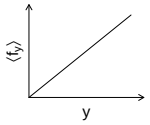	+	+	-	-	0	+	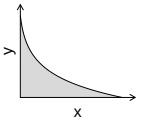
5	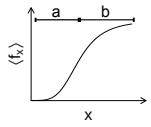	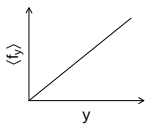	+	+	-	a) + b) -	0	a) - b) +	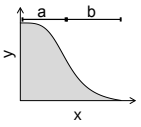
6	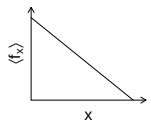	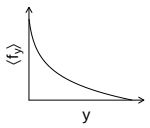	-	-	-	0	+	+	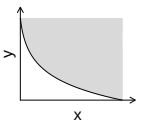

Figure 3.2: Invasion boundaries of the intermediate species M resulting from different cases how its traits x and y translate into its additive invasion fitness components $\langle f_x \rangle$ and $\langle f_y \rangle$. The sign of $\partial y / \partial x$ determines the direction of the invasion boundary while its shape depends on the sign of $\partial^2 y / \partial x^2$. The black curve in the last column represents the invasion boundary and grey (white) areas refer to trait combinations where the invasion of M is impossible (possible).

Case 6 is further evaluated in the example below when we apply this approach to a predator-prey system with a trade-off between prey edibility and its half-saturation constant for nutrient uptake. Higher values of both traits have a negative effect on the invasion fitness which implies again a negative slope of the invasion boundary but the assignment of areas in the trait space where invasion is possible or not is reversed as low values of both traits are beneficial. Moreover, the shape of the invasion boundary is convex and thus differs from the standard case because the trait y has a non-linear effect on fitness ($\partial^2 \langle f_y \rangle / \partial y^2 > 0$).

So far, we have shown cases where only one trait translates non-linearly into fitness. In Appendix B.1, we present the resulting invasion boundaries for cases where both traits affect the fitness non-linearly (Appendix B.1: Fig. B1). Moreover, we show invasion boundaries for cases where the fitness components f_x and f_y are multiplicative rather than

additive as assumed in Eq. 3.3. Remarkably, even for linear trait-fitness relationships the invasion boundary is non-linear when the fitness components are multiplicative (Appendix B.1: Fig. B2). Applying our approach to a general resource competition model with a trade-off between specialization on two different resources (Appendix B.2) reveals that the shape of the invasion boundary may depend on whether the residents cycle or are in steady-state which is line with previous results of Abrams (2006a).

Trade-off shapes, invasion boundaries and coexistence

To assess the effect of different trade-off shapes on coexistence, we compare the trade-off curve to the calculated invasion boundary. Both curves share the same terminal points, i.e. the trait combinations of the extreme species. Thus, a comparison of their shape allows direct conclusions on coexistence. We classify trade-offs as extreme-favouring (EF) when the invasion of an intermediate species is not possible leading to coexistence of only the extreme species and as intermediate-favouring (MF) if an intermediate species can invade the extreme species and becomes part of the community. We define a trade-off as neutral if it is identical to the invasion boundary. In Fig. 3.3, we show examples of different trade-off curves and the respective invasion boundary. In the standard case, the invasion boundary is linear implying that convex trade-offs are EF while concave trade-offs are MF (Fig. 3.3a). For concave invasion boundaries, EF-trade-offs can be convex, linear and slightly concave while only strongly concave trade-offs are MF (Fig. 3.3b). The assignment of EF- and MF-trade-offs can be reversed depending on whether both traits translate positively into fitness (Fig. 3.3c) or negatively (Fig. 3.3d). If the trade-off curve or the invasion boundary is a combination of convex and concave parts, the trade-off may be MF and EF depending on the considered trait range (Fig. 3.3e,f). Thus, depending on the trait combination of the intermediate species, it will be part of the community or not.

Assuming that E_1 and E_2 stably coexist in the absence of M, EF-trade-offs always lead to coexistence of the extreme species (Fig. 3.1b i) while there are several possibilities of coexistence in case of MF-trade-offs where M is part of the community. We use the invasion criterion (Chesson 2000) to test for the different coexistence scenarios. The invasion criterion states that two species stably coexist if each one is able to invade a system dominated by the other resident species (mutual invasibility). We extend this criterion to our three species system. Assuming no multi-stability, four outcomes of coexistence are possible for MF-trade-offs (Fig. 3.1b): ii) Coexistence of E_1 and M when E_1+M are mutual invasible and not invasible by E_2, iii) Coexistence of M and E_2 when M+E_2 are mutual invasible and not invasible by E_1, iv) Survival of only M if M is not invasible by E_1 and E_2, v) Coexistence of E_1, M and E_2 when E_1+E_2 is invasible by M, E_1+M by E_2 and M+E_2 by E_1. The three conditions for coexistence of all three species ensure that each species is able to increase after strong reduction in density. For example,

if E_1 is reduced to very low densities, it can invade the remaining community whereby it is not important whether the invasion occurs directly into M+E_2 or whether there is a step in between, e.g. E_2 decreases also to very low densities followed by the invasion of E_1 into M and then the invasion of E_2 into E_1+M. The conditions of case v) comprise all of these possible invasion paths.

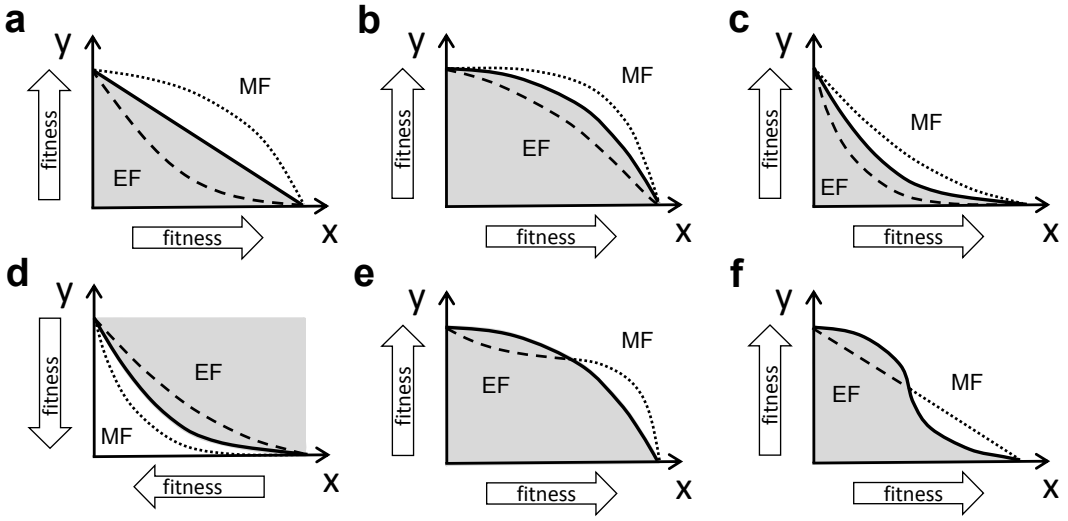

Figure 3.3: Trade-offs are extreme-favouring (EF) or intermediate-favouring (MF) depending on their shape, the invasion boundary of the intermediate species M (solid line) and the direction of fitness increase (arrows). Dashed lines highlight examples of EF-trade-offs while dotted lines indicate MF-trade-offs. Trait combinations of M (x,y) where M cannot (can) invade the extreme species are marked with grey (white). (a) Standard case with a linear invasion boundary where convex trade-offs are EF while concave ones are MF. Non-linear invasion boundaries lead to deviations from the standard case. (b) For concave invasion boundaries, even slightly concave trade-offs are EF. (c) Convex invasion boundaries allow slightly convex trade-offs to be MF. (d) Inverse trait-fitness relationships reverse the assignment of EF- and MF-trade-offs. (e,f) More complex shapes of the trade-off or the invasion boundary allow for EF and MF parts within one trade-off curve.

Applying the general approach to a predator-prey system

Model description

We applied the general framework to a model of an empirically well-studied chemostat system with the rotifer *Brachionus calyciflorus* as predator (B), different genotypes of the green algae *Chlamydomonas reinhardtii* as prey (E_1, M and E_2) and a limiting nutrient (N) for the algae. The algal genotypes face a trade-off between edibility for the predator, i.e. probability of being attacked, and the half-saturation constant for the uptake of

nutrients while we assume the other parameters to be identical (Becks et al. 2010, 2012). Some genotypes exhibit defence mechanisms (e.g. colony formation) which reduces their edibility but lowers also their affinity for nutrients (e.g. due to a lower diffusion velocity of nutrients through the matrix surrounding the colonies), i.e. increases their half-saturation constant (Becks et al. 2012, Woltermann & Becks, *unpublished data*). The trait values used in the model and stated below are based on Becks et al. (2010). The defended extreme prey E_1 has the lowest edibility ($p_1 = 0$) but the highest half-saturation constant ($K_1 = 8$ µmol N/l). The opposite holds for the competitive extreme prey E_2 ($p_2 = 1$, $K_2 = 2$ µmol N/l). We vary the trait values of the intermediate prey M between these extremes (p_M between 0 and 1, K_M between 2 and 8 µmol N/l).

The changes of the nutrient concentration and population densities over time are defined by the following differential equations

$$\begin{aligned}
\frac{dN}{dt} &= \delta\,(N_I - N) - \frac{r}{\chi}\frac{NM}{K_M + N} - \frac{r}{\chi}\sum_{i=1}^{2}\frac{NE_i}{K_i + N} \\
\frac{dM}{dt} &= M\left[r\frac{N}{K_M + N} - \frac{g\,p_M B}{K_B + p_M M + \sum p_i E_i} - \delta\right] \\
\frac{dE_i}{dt} &= E_i\left[r\frac{N}{K_i + N} - \frac{g\,p_i B}{K_B + p_M M + \sum p_i E_i} - \delta\right] \\
\frac{dB}{dt} &= B\left[\chi_B\frac{g\,(p_M M + \sum p_i E_i)}{K_B + p_M M + \sum p_i E_i} - \delta\right]
\end{aligned} \tag{3.6}$$

with $i = 1, 2$. The chemostat system is characterized by a continuous inflow of medium with nutrients at the concentration N_I and outflow of medium with nutrients and organisms. The magnitude of the inflow and the outflow is described by the dilution rate δ. The consumption of nutrients by the prey and the consumption of prey by the predator are described by a classical Holling-type II functional response (Monod's Equation). For further details on the parameters and their values see Appendix B.3: Table B1. In order to investigate the duration of co-occurrence and the population dynamics, we performed numerical integrations of this model with the lsoda solver of the deSolve package in R (Soetaert et al. 2010). In the simulations, we used the following initialization: $N = N_I$, $B = 1$ individual/ml and $E_1, M, E_2 = 10^5$ cells/ml. The simulations run for 200 days representing a relevant time scale for chemostat experiments. We determined the time until the first extinction event, i.e. the duration of co-occurrence, where the population density of one of the prey types falls below the extinction threshold (100 cells/ml), for each trait combination in a 1001×1001 grid covering the total trait space.

The invasion boundary of the intermediate prey

Here, we detect the shape of the invasion boundary of the intermediate prey M in a resident community of the defended extreme prey E_1 and the competitive extreme prey E_2. This specific system involves additionally nutrients N and the predator B. The invasion fitness of the intermediate prey ($M \approx 0$) equals

$$\left\langle \frac{1}{M}\frac{dM}{dt} \right\rangle = r\left\langle \frac{N}{K_M+N} \right\rangle - p_M \left\langle \frac{gB}{K_B+\sum p_i E_i} \right\rangle - \delta \,. \tag{3.7}$$

Remarkably, the non-linear effect of p_M in the denominator of the functional response term cancels out in the invasion fitness due to $M = 0$ (compare Eq. 3.6 and 3.7).

For simplicity, the traits of the intermediate prey are represented by p and K from now on. The traits affect different components of the invasion fitness which are additive (see Eq. 3.7). Therefore, the invasion fitness can be represented by two additive functions each depending on one trait and the respective population densities:

$$\langle f_p(p,0,E_1,E_2,B)\rangle = -p\left\langle \frac{gB}{K_B+\sum p_i E_i} \right\rangle - \delta \tag{3.8}$$

and

$$\langle f_K(K,N)\rangle = r\left\langle \frac{N}{K+N} \right\rangle . \tag{3.9}$$

By deriving the fitness terms in Eq. B19 and Eq. B20, we can infer how the traits of the intermediate prey translate into invasion fitness components which yields $\frac{\partial\langle f_p\rangle}{\partial p} < 0$, $\frac{\partial^2\langle f_p\rangle}{\partial p^2} = 0$, $\frac{\partial\langle f_K\rangle}{\partial K} < 0$ and $\frac{\partial^2\langle f_K\rangle}{\partial K^2} > 0$ (for details see Appendix B.4). This implies that the invasion fitness decreases linearly with higher p. With higher values of K, it decreases whereby the slope of that decrease becomes less negative. These relationships determine the shape of the invasion boundary. By applying the procedure explained above (see Eq. 3.3-3.5), we end up with the first and the second derivative of K with respect to p at the invasion boundary

$$\frac{\partial K}{\partial p} = -\frac{\partial\langle f_p\rangle/\partial p}{\partial\langle f_K\rangle/\partial K} < 0 \quad \text{and} \quad \frac{\partial^2 K}{\partial p^2} = \frac{\frac{\partial\langle f_p\rangle}{\partial p}\frac{\partial^2\langle f_K\rangle}{\partial K^2}\frac{\partial K}{\partial p} - \frac{\partial^2\langle f_p\rangle}{\partial p^2}\frac{\partial\langle f_K\rangle}{\partial K}}{\left(\frac{\partial\langle f_K\rangle}{\partial K}\right)^2} > 0 \,. \tag{3.10}$$

We can conclude that the slope of the invasion boundary for the traits p and K has a negative sign since the first derivative is negative (Eq. 3.10). Furthermore, the shape of the invasion boundary is convex, i.e. the second derivative is larger than zero (Eq. 3.10). As higher values of both traits are unfavourable, a EF-trade-off (invasion of M impossible)

occurs for trait combinations above the invasion boundary. This corresponds to case 6 shown in Fig. 3.2 and Fig. 3.3d.

Coexistence and co-occurrence of different prey types

The coexistence analysis described below is based on the invasibility criterion (Fig. 3.1b) and demands the calculation of invasion fitness and invasion boundaries which is documented in Appendix B.5. EF-trade-offs imply coexistence of the defended extreme prey E_1 and the competitive extreme prey E_2 as they cannot be invaded by the intermediate prey M (Fig. 3.1b case i, 3.4a, b). For MF-trade-offs, M can invade and thus different outcomes are possible (Fig. 3.1b case ii-iv, Fig. 3.4a, c-e): At low p_M values, M coexists with E_2 (Fig. 3.4a, c) where M represents an additional defended prey type which outcompetes the defended extreme prey E_1 by having the advantage of a lower half-saturation constant. In a narrow range of intermediate p_M values, neither E_1 nor E_2 can invade M since they are functionally not different enough from M. This leads to the survival of only M which is reasonably defended but can still sustain the predator and has a relatively low half-saturation constant (Fig. 3.4a, d). For high values of p_M, coexistence of E_1 and M occurs (Fig. 3.4a, e) where M outcompetes E_2 since it has also a relatively low half-saturation constant but a lower edibility compared to E_2.

Stable coexistence of three prey types demands that every prey type can invade the system of the two other prey types (Fig. 3.1b case v). This is precluded in our system due to the fact that the conditions for invasibility of $E_1 + E_2$ by M and of $E_1 + M$ by E_2 as well as $M + E_2$ by E_1 are mutually exclusive. Hence, the maximum number of stably coexisting prey types is two. However, all three prey types can co-occur for long periods (Fig. 3.4 c). The duration of co-occurrence increases for trait combinations closer to the invasion boundary (Fig. 3.4a-e). Exactly on the invasion boundary, i.e. for neutral trade-offs, none of the prey types is outcompeted due to fitness equality (Fig. 3.4a, f). This is called unstable coexistence as none of the prey types can invade the others because the invasion fitness equals zero. They only coexist if they are present at sufficiently high initial densities.

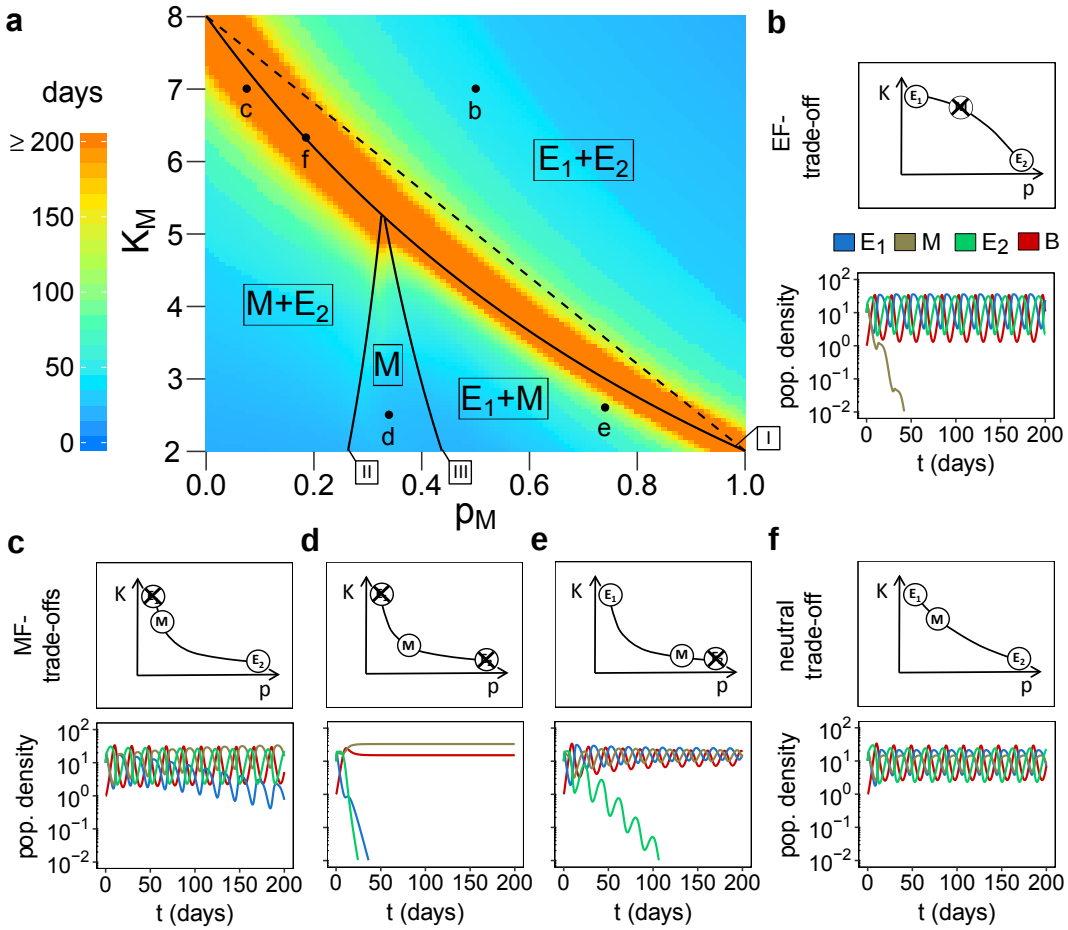

Figure 3.4: (a) Coexistence and duration of co-occurrence of the three prey types depending on the edibility p_M and the half-saturation constant K_M (µmol N/l) of the intermediate prey type M. The capital letters E_1, E_2 and M indicate which prey types coexist in the different regions framed by the solid lines representing the invasion boundaries (line I: M into E_1+E_2, II: E_2 into M, III: E_1 into M). The invasion boundary of M (line I) is convex and differs distinctly from the often assumed linear case (dashed line). The colour grid indicates the duration of co-occurrence (i.e. time until first extinction) which increases when getting closer to the invasion boundary of M. The dots labelled with small letters mark trait combinations for which potential shapes of the trade-off and the population dynamics of the prey types (10^4 cells/ml) and the predator B (individuals/ml) are shown in (b)-(f). The lower limit of the population density axis equals the extinction threshold of the prey types, 100 cells/ml. Trade-off curves are defined as extreme-favouring (EF), intermediate-favouring (MF) or neutral depending on whether they are above, below or identical to the invasion boundary of M.

Discussion

We developed a novel and general approach to analyse the consequences of different trade-off curves for coexistence based on measurable trait-fitness relationships. We revealed limitations of the common prediction that convex trade-offs favour species with extreme trait values while concave trade-offs enable survival of intermediate species.

These limitations arise from the implicit assumption of linear trait-fitness relationships implying that the invasion boundary of an intermediate species invading the extreme species is linear. Here, we infer the shape of the invasion boundary directly from the trait-fitness relationships and show that it is often non-linear. This holds when the relationship between at least one trait and the fitness is non-linear (Fig. 3.2, Fig. 3.4) or when the fitness components are non-additive (Appendix B.1). We show how information on the shape of the invasion boundary can be used to infer consequences of different trade-off curves for coexistence. Depending on the relative position of the trade-off curve to the invasion boundary, we classify trade-offs as extreme-favouring (EF, invasion of intermediate species not possible) or intermediate-favouring (MF, invasion possible) (Fig. 3.3). We apply our approach to an illustrative example of a predator-prey system with a trade-off between prey edibility and half-saturation constant for nutrients where the invasion boundary of an intermediate prey is convex.

The impacts of non-linear invasion boundaries on evolution were already highlighted by Rueffler et al. (2004) and de Mazancourt and Dieckmann (2004) who extended Levins' approach by allowing for density- and frequency-dependent fitness. They compared trade-off curves and invasion boundaries of mutant strategies in a monomorphic resident population to assess the direction of selection with gradual evolution. Rueffler et al. (2004) discussed under which conditions the invasion boundaries are non-linear but they did not specify their shape. For instance, non-linear invasion boundaries occur in stage-structured models when the traits are characteristic for different stages (Ebenman et al. 1996; Hoyle et al. 2008) and different resource competition models depending on the state of the resident community (Abrams 2006b; Abrams and Rueffler 2009). Further studies underline the importance of assessing the curvature of invasion boundaries for predicting evolutionary outcomes (Bowers et al. 2005; White and Bowers 2005). However, our study is the first which explicitly addresses the question of when the invasion boundary becomes convex, concave or has a more complex shape depending on the trait-fitness relationships (Fig. 3.2). Moreover, our approach is released from the limitation that coexistence has to be evolutionary attainable via local mutations. We consider coexistence within an existing pool of species with fixed trait values.

Our approach is based on the assumption that two extreme species facing a two-dimensional trade-off stably coexist in the absence of an intermediate species independent of the shape of the trade-off, i.e. they are mutual invasible. However, depending on the magnitude of the trade-off and the environment, only one extreme species may survive. For example, a defended prey cannot coexist with a fast-growing prey if the defence costs in terms of growth are very high (Abrams 1999; Kasada et al. 2014). Moreover, if the physiologically feasible trait range is very narrow, the extreme types may be too similar for stable coexistence. In such cases, we can adapt our approach and consider a resident

community of only one extreme species to check for the invasion of an intermediate species. In the previously described case with two coexisting resident extreme species, the trade-off curve and the invasion boundary shared the same terminal points (see Fig. 3.3). This needs not to be the case when only one resident extreme species is present. The trade-off curve and the invasion boundary still converge at the trait combination of the resident species which is neutrally invasible while at the other end of the trait range they may diverge. Nevertheless, it is possible to distinguish between EF- and MF-trade-offs just by detecting whether the trade-off curve lies below or above the invasion boundary of the intermediate species invading the one resident species.

We applied our general approach to an empirically well understood predator-prey chemostat system with a trade-off between prey edibility (probability of being attacked) and its half-saturation constant for nutrient uptake. We found that the invasion boundary of an intermediate prey invading the two extreme prey types was convex and had a negative slope. A subsequent invasion analysis (Fig. 3.1b) could explain the coexistence of different prey types (Fig. 3.4). Remarkably, for MF-trade-offs, the intermediate prey outcompeted both extreme prey types or stably coexisted with one of them depending on its trait values while stable coexistence of all three prey types is impossible in this system even under cycling population densities. This follows the general theorem stating that at most n species can coexist on n regulating variables (Meszéna et al. 2006), i.e. two different prey types can coexist based on one resource and one predator. However, previous theory revealed that fluctuating population densities may allow for a higher number of coexisting species. For example, Abrams (2006b) showed that two specialist and one generalist consumer can stably coexist on two resources for slightly convex trade-offs when the resources cycle asynchronously. This was possible due to the relative non-linearity arising from the different saturating functional responses of the consumers to the resources which promoted the fitness of the generalist. In models on interactions of prey species sharing one resource and a common predator, non-linear functional responses also promote cycles and allow for coexistence of two different prey strategies (Abrams and Matsuda 1997; Abrams et al. 1998; Abrams 1999; Yoshida et al. 2007). However, as shown in our study, relative non-linearities enabling stable coexistence of three prey strategies under fluctuating densities were not found in these predator-prey systems.

Three prey types cannot stably coexist but they may co-occur on long, ecologically relevant time scales when fitness differences are small, i.e. the trade-off is nearly neutral. Studies on the role of neutrality and nearly neutral trade-offs for maintaining functional diversity in natural communities have a long tradition in ecology (e.g. Hubbell 2001, 2005; Adler et al. 2007). High fitness equality extends the duration of co-occurrence and may increase the possibility of coexistence even if only weak stabilizing mechanisms are present (Chesson 2000; He et al. 2012; Pedruski et al. 2015). We argue here that nearly

neutral trade-offs and the resulting low differences in fitness may help to explain the partly observed high functional diversity in simple, short-term experimental systems like the predator-prey system considered in our study. Chemostat experiments mostly cover up to 100 generations (Becks et al. 2010; Hiltunen et al. 2014). Within this time scale, all prey types maintain empirically detectable population densities for nearly neutral trade-offs even if one prey type would die out in the long term (Fig. 3.4c). It should be mentioned here that the duration of co-occurrence depends not only on the degree of fitness equality but also on the extinction threshold and the initial population densities, e.g. low initial densities of an inferior competitor decrease the duration of co-occurrence.

So far, we focused on two-dimensional trade-offs. However, multiple traits may trade off in nature (e.g. Edwards et al. 2011) and our approach can be extended to multi-dimensional trade-offs. For example, a trade-off among three traits can be represented by a plane in a three-dimensional trait space. We can calculate the invasion boundary of an intermediate species invading the three possible extreme strategies. By comparing the planes of the trade-off and the invasion boundary, we can conclude whether the trade-off is EF or MF. Furthermore, there is the possibility that a trait affects more than one fitness component, e.g. the size of phytoplankton cells determines their growth, nutrient uptake, sedimentation and grazing losses (Litchman and Klausmeier 2008; Finkel et al. 2010). Accordingly, such traits were often called 'master traits'. Dividing a 'master trait' into the associated functional parameters like maximum growth rate, nutrient affinity, sedimentation velocity and vulnerability to predation leads us to individual fitness functions which can be handled with our approach.

Previous research has documented that trade-offs often tend to be EF and found specialization of strategies indicating high costs of intermediate strategies (Benkman 1993; Schluter 1995; O'Hara Hines et al. 2004; Mealor and Boots 2006). However, evidently, MF-trade-offs are also relevant, e.g. for trade-offs between stress tolerance and resource-dependent growth in different *Escherichia coli* strains (Maharjan et al. 2013). Empirical evidence for trade-offs consisting of EF and MF parts is currently lacking but development of theory on trade-off curves combining concave and convex parts, which have the potential to be EF and MF, has been intensified (Zu et al. 2011; Zu and Takeuchi 2012). Our approach contributes to this theoretical work and allows to assess consequences of more complex trade-off shapes. Furthermore, previous research showed that the shape of trade-offs may depend on the environment (Jessup and Bohannan 2008) which would allow for a continuous switching between EF and MF under fluctuating conditions. This also implies that neutral trade-offs may be of low relevance in natural systems because a trade-off curve identical to the invasion boundary is unlikely to prevail for extended periods of time. Nevertheless, nearly neutral trade-offs may be relevant. For instance, trait measurements on the edibility and maximum growth rate of different

phytoplankton species indicate a nearly linear trade-off (Wirtz and Eckhardt 1996). According to our study, the invasion boundary for these traits is linear as well (case 2 in Figure 3.2) suggesting that these phytoplankton species co-occur due to low fitness differences instead of strong niche differentiation.

Conclusion

We conclude that the common prediction that convex trade-offs promote species with extreme trait values while concave trade-offs favour species with intermediate trait values fails in case of non-linear trait-fitness relationships which frequently occur in nature. Our approach stating how the shape of a trade-off affects coexistence in dependence of the fitness functions overcomes this limitation and can be readily used in practice: establishing the trait-fitness relationships enables to calculate the invasion boundary of an intermediate species invading a community of species with extreme trait values. A comparison of this boundary with the shape of the trade-off allows to predict coexistence. This leads us to a new classification of trade-offs into extreme-favouring and intermediate-favouring which is more specific in terms of the ecological consequences than a purely mathematical description of their curvature, i.e. convex or concave.

Acknowledgments

We are grateful to Christian Guill for helpful recommendations on the mathematical analysis. We thank Ellen van Velzen, Claus Rueffler, Toni Klauschies, Noemi Woltermann and Michael Raatz for fruitful discussions on the results and Kevin Gross for valuable comments on an earlier version of the manuscript. This research was funded by the German Research Foundation (DFG, GA 401/25-1). L.B. was supported by the DFG's Emmy Noether Programme (BE 4135/3-1).

Bibliography 3

Abrams, P. A. (1999). Is predator-mediated coexistence possible in unstable systems? *Ecology*, 80(2):608–621.

Abrams, P. A. (2003). Can adaptive evolution or behaviour lead to diversification of traits determining a trade-off between foraging gain and predation risk? *Evolutionary Ecology Research*, 5(5):653–670.

Abrams, P. A. (2006a). Adaptive change in the resource-exploitation traits of a generalist consumer: the evolution and coexistence of generalists and specialists. *Evolution*, 60(3):427–439.

Abrams, P. A. (2006b). The Prerequisites for and Likelihood of Generalist-Specialist Coexistence. *The American Naturalist*, 167(3):329–342.

Abrams, P. A., Holt, R. D., and Roth, J. D. (1998). Apparent competition or apparent mutualism? Shared predation when populations cycle. *Ecology*, 79(1):201–212.

Abrams, P. A. and Matsuda, H. (1997). Prey Adaptation as a Cause of Predator-Prey Cycles. *Evolution*, 51(6):1742–1750.

Abrams, P. A. and Rueffler, C. (2009). Coexistence and limiting similarity of consumer species competing for a linear array of resources. *Ecology*, 90(3):812–822.

Adler, P. B., HilleRislambers, J., and Levine, J. M. (2007). A niche for neutrality. *Ecology Letters*, 10(2):95–104.

Becks, L., Ellner, S. P., Jones, L. E., and Hairston Jr., N. G. (2010). Reduction of adaptive genetic diversity radically alters eco-evolutionary community dynamics. *Ecology Letters*, 13(8):989–997.

Becks, L., Ellner, S. P., Jones, L. E., and Hairston Jr., N. G. (2012). The functional genomics of an eco-evolutionary feedback loop: linking gene expression, trait evolution, and community dynamics. *Ecology Letters*, 15(5):492–501.

Benkman, C. W. (1993). Adaptation to Single Resources and the Evolution of Crossbill (Loxia) Diversity. *Ecological Monographs*, 63(3):305–325.

Boots, M. and Haraguchi, Y. (1999). The Evolution of Costly Resistance in Host-Parasite Systems. *The American Naturalist*, 153(4):359–370.

Bowers, R. G. and Hodgkinson, D. E. (2001). Community Dynamics, Trade-offs, Invasion Criteria and the Evolution of Host Resistance to Microparasites. *Journal of Theoretical Biology*, 212(3):315–331.

Bowers, R. G., Hoyle, A., White, A., and Boots, M. (2005). The geometric theory of adaptive evolution: trade-off and invasion plots. *Journal of Theoretical Biology*, 233(3):363–377.

Chesson, P. (2000). Mechanisms of Maintenance of Species Diversity. *Annual Review of Ecology and Systematics*, 31(1):343–366.

Day, T., Abrams, P. A., and Chase, J. M. (2002). The Role of Size-Specific Predation in the Evolution and Diversification of Prey Life Histories. *Evolution*, 56(5):877–887.

de Mazancourt, C. and Dieckmann, U. (2004). Trade-Off Geometries and Frequency-Dependent Selection. *The American Naturalist*, 164(6):765–778.

Ebenman, B., Johansson, A., Jonsson, T., and Wennergren, U. (1996). Evolution of Stable Population Dynamics through Natural Selection. *Proceedings of the Royal Society B: Biological Sciences*, 263(1374):1145–1151.

Edwards, K. F., Klausmeier, C. A., and Litchman, E. (2011). Evidence for a three-way trade-off between nitrogen and phosphorus competitive abilities and cell size in phytoplankton. *Ecology*, 92(11):2085–2095.

Egas, M., Dieckmann, U., and Sabelis, M. W. (2004). Evolution Restricts the Coexistence of Specialists and Generalists: The Role of Trade-off Structure. *The American Naturalist*, 163(4):518–531.

Finkel, Z. V., Beardall, J., Flynn, K. J., Quigg, A., Rees, T. A. V., and Raven, J. A. (2010). Phytoplankton in a changing world: cell size and elemental stoichiometry. *Journal of Plankton Research*, 32(1):119–137.

Gudelj, I., van den Bosch, F., and Gilligan, C. A. (2004). Transmission rates and adaptive evolution of pathogens in sympatric heterogeneous plant populations. *Proceedings of the Royal Society B: Biological Sciences*, 271(1553):2187–2194.

He, F., Zhang, D.-Y., and Lin, K. (2012). Coexistence of nearly neutral species. *Journal of Plant Ecology*, 5(1):72–81.

Hiltunen, T., Ellner, S. P., Hooker, G., Jones, L. E., and Hairston Jr., N. G. (2014). Eco-Evolutionary Dynamics in a Three-Species Food Web with Intraguild Predation. *Advances in Ecological Research*, 50:41–73.

Hoyle, A., Bowers, R. G., White, A., and Boots, M. (2008). The influence of trade-off shape on evolutionary behaviour in classical ecological scenarios. *Journal of Theoretical Biology*, 250(3):498–511.

Hubbell, S. P. (2001). *The Unified Neutral Theory of Biodiversity and Biogeography*. Princeton University Press, Princeton.

Hubbell, S. P. (2005). Neutral theory in community of ecology and the hypothesis functional equivalence. *Functional Ecology*, 19(1):166–172.

Jessup, C. M. and Bohannan, B. J. M. (2008). The shape of an ecological trade-off varies with environment. *Ecology Letters*, 11(9):947–959.

Jones, L. E., Becks, L., Ellner, S. P., Hairston Jr., N. G., Yoshida, T., and Fussmann, G. F. (2009). Rapid contemporary evolution and clonal food web dynamics. *Philosophical Transactions of the Royal Society B: Biological Sciences*, 364(1523):1579–1591.

Kasada, M., Yamamichi, M., and Yoshida, T. (2014). Form of an evolutionary tradeoff affects eco-evolutionary dynamics in a predator–prey system. *Proceedings of the National Academy of Sciences*, 111(45):16035–16040.

Kneitel, J. M. and Chase, J. M. (2004). Trade-offs in community ecology: linking spatial scales and species coexistence. *Ecology Letters*, 7(1):69–80.

Levins, R. (1962). Theory of Fitness in a Heterogeneous Environment. I. The Fitness Set and Adaptive Function. *The American Naturalist*, 96(891):361–373.

Levins, R. (1968). *Evolution in changing environments*. Princeton University Press, Princeton.

Litchman, E. and Klausmeier, C. A. (2008). Trait-Based Community Ecology of Phytoplankton. *Annual Review of Ecology, Evolution, and Systematics*, 39(1):615–639.

Litchman, E., Klausmeier, C. A., Schofield, O. M., and Falkowski, P. G. (2007). The role of functional traits and trade-offs in structuring phytoplankton communities: scaling from cellular to ecosystem level. *Ecology Letters*, 10(12):1170–1181.

Maharjan, R., Nilsson, S., Sung, J., Haynes, K., Beardmore, R. E., Hurst, L. D., Ferenci, T., and Gudelj, I. (2013). The form of a trade-off determines the response to competition. *Ecology Letters*, 16(10):1267–1276.

Mealor, M. A. and Boots, M. (2006). An indirect approach to imply trade-off shapes: population level patterns in resistance suggest a decreasingly costly resistance mechanism in a model insect system. *Journal of Evolutionary Biology*, 19(2):326–330.

Meszéna, G., Gyllenberg, M., Pásztor, L., and Metz, J. A. (2006). Competitive exclusion and limiting similarity: A unified theory. *Theoretical Population Biology*, 69(1):68–87.

Meyer, J. R., Gudelj, I., and Beardmore, R. (2015). Biophysical mechanisms that maintain biodiversity through trade-offs. *Nature Communications*, 6(1):6278.

O'Hara Hines, R. J., Hines, W. G. S., and Robinson, B. W. (2004). A New Statistical Test of Fitness Set Data from Reciprocal Transplant Experiments Involving Intermediate Phenotypes. *The American Naturalist*, 163(1):97–104.

Pedruski, M. T., Fussmann, G. F., and Gonzalez, A. (2015). Predicting the outcome of competition when fitness inequality is variable. *Royal Society Open Science*, 2(8):150274.

Rueffler, C., Van Dooren, T., and Metz, J. (2004). Adaptive walks on changing landscapes: Levins' approach extended. *Theoretical Population Biology*, 65(2):165–178.

Rueffler, C., Van Dooren, T. J. M., and Metz, J. A. J. (2006). The Evolution of Resource Specialization through Frequency-Dependent and Frequency-Independent Mechanisms. *The American Naturalist*, 167(1):81–93.

Schluter, D. (1995). Adaptive Radiation in Sticklebacks: Trade-Offs in Feeding Performance and Growth. *Ecology*, 76(1):82–90.

Soetaert, K., Petzoldt, T., and Setzer, R. W. (2010). Package deSolve: Solving Initial Value Differential Equations in R. *Journal Of Statistical Software*, 33(9):1–25.

Tilman, D. (2000). Causes, consequences and ethics of biodiversity. *Nature*, 405(6783):208–211.

Tilman, D., Kilham, S. S., and Kilham, P. (1982). Phytoplankton Community Ecology: The Role of Limiting Nutrients. *Annual Review of Ecology and Systematics*, 13(1982):349–372.

White, A. and Bowers, R. G. (2005). Adaptive dynamics of Lotka-Volterra systems with trade-offs: the role of interspecific parameter dependence in branching. *Mathematical Biosciences*, 193(1):101–117.

Wirtz, K.-W. and Eckhardt, B. (1996). Effective variables in ecosystem models with an application to phytoplankton succession. *Ecological Modelling*, 92(1):33–53.

Yoshida, T., Ellner, S. P., Jones, L. E., Bohannan, B. J. M., Lenski, R. E., and Hairston Jr., N. G. (2007). Cryptic population dynamics: rapid evolution masks trophic interactions. *PLoS biology*, 5(9):e235.

Zu, J., Mimura, M., and Takeuchi, Y. (2011). Adaptive evolution of foraging-related traits in a predator-prey community. *Journal of Theoretical Biology*, 268(1):14–29.

Zu, J. and Takeuchi, Y. (2012). Adaptive evolution of anti-predator ability promotes the diversity of prey species: Critical function analysis. *Biosystems*, 109(2):192–202.

4 Testing theory on trade-off shapes with phytoplankton field data

---

Manuscript title:

The shape of a defence-growth trade-off governs seasonal trait dynamics in natural phytoplankton

Elias Ehrlich[1], Nadja J. Kath[1] and Ursula Gaedke[1]

1. Department of Ecology and Ecosystem Modelling, University of Potsdam, Am Neuen Palais 10, 14469 Potsdam, Germany.

Submitted as:

Ehrlich, E., Kath, N. J. and Gaedke, U. (2018). The shape of a defence-growth trade-off governs seasonal trait dynamics in natural phytoplankton. *Submitted to Ecology Letters and rejected after peer-review, to be submitted again*.

Abstract

Functional trait compositions of communities can adapt to altered environmental conditions ensuring community persistence. Theory predicts that the shape of trade-offs between traits crucially affects these trait dynamics, but its empirical verification from the field is missing. Here, we show how the shape of a defence-growth trade-off governs seasonal trait dynamics of a natural community, using high-frequency, long-term measurements of phytoplankton from Lake Constance. As expected from the lab-derived concave trade-off curve, we observed an alternating dominance of several fast-growing species with intermediate defence levels and gradual changes of the biomass-trait distribution due to seasonally changing grazing pressure. By combining data and modelling, we obtain mechanistic insights on the underlying fitness landscape, and show that low fitness differences can maintain trait variation along the trade-off curve. We provide firm evidence for a frequently assumed trade-off and conclude that quantifying its shape allows to understand environmentally driven trait changes within communities.

Introduction

Identifying trade-offs between functional traits of species is central to ecology because it provides a fundamental basis to understand species coexistence and the trait composition of natural communities (Tilman 2000). Trade-offs emerge through physiological, energetic, behavioural or genetic constraints (Stearns 1989) and can be detected within one species (Barry 1994; Yoshida et al. 2004) as well as on the community level among different species sharing similar individual-level constraints (Tilman et al. 1982; Litchman et al. 2007). Such interspecific trade-offs promote species diversity and guide the way of community trait changes under altered environmental conditions (Kneitel and Chase 2004).

Theory indicates that it is the shape of the trade-off curve between two traits which determines species coexistence and how trait values change in response to environmental forcing (Levins 1962; Rueffler et al. 2004; Abrams 2006). We summarize the theory and specify predictions in Box 4.1. While theory revealing the importance of the shape of the trade-off curve for coexistence and trait dynamics is well developed (de Mazancourt and Dieckmann 2004; Jones et al. 2009; Ehrlich et al. 2017), its empirical verification has been left far behind. Two studies successfully tested the theory in small-scale lab experiments assembling different bacterial strains (Maharjan et al. 2013; Meyer et al. 2015). However, respective approaches from the field are lacking, leaving open the question how the shape of the trade-off curve affects the trait composition of natural communities. In this article, we combine theory and long-term field data, and show how the shape of a classical defence-growth trade-off affects seasonal trait dynamics of phytoplankton in a large European lake.

Phytoplankton communities are well-suited for addressing this issue as important functional traits of phytoplankton have been measured in the lab revealing key trade-offs (Litchman and Klausmeier 2008; Pančić and Kiørboe 2018). Phytoplankton communities are extremely diverse spanning a large trait space (Weithoff 2003; Smith et al. 2005) indicating that trade-offs play a decisive role in maintaining trait variation. Furthermore, phytoplankton species have short generation times allowing for pronounced seasonal succession (Sommer et al. 2012). This offers the opportunity to observe species sorting in response to recurrently changing environmental conditions driving community trait dynamics.

Box 4.1: Theory on how the shape of a trade-off curve influences coexistence and trait dynamics

The trade-off curve is defined as the boundary of the set of feasible trait combinations, representing all possible phenotypes (Fig. 4.1, Rueffler et al. 2006). If the trade-off curve is convex, typically two specialized species coexist while all intermediate strategies are outcompeted in the long-term (given positive linear trait-fitness relationships, see Ehrlich et al. 2017) (Fig. 4.1a). If the trade-off curve is concave, only one species with intermediate trait values, determined by the present environmental conditions, is expected to survive in the long-term outcompeting all others (Fig. 4.1b). Nevertheless, on the short-term, more than one or two species may co-occur depending on the speed of competitive exclusion (Pedruski et al. 2015; Ehrlich et al. 2017) which is low for species with trait-combinations close to that of the species with maximal fitness and high for species at the unfavourable edge of the feasible trait space (Fig. 4.1a, b). Under directionally changing environmental conditions, the fitness maximum moves along a concave trade-off curve driving continued sorting of species with different trait values (Fig. 4.1b), e.g., an increasing grazing pressure promotes species with higher defence values at the cost of a decreasing maximum growth rate. In contrast, for convex trade-off curves, the fitness maxima usually stay at the extreme trait combinations (Fig. 4.1a) and only the biomass ratio between the specialized species is altered.

Previous trait-based studies on phytoplankton communities already quantified trade-offs among different resource utilization traits (Litchman et al. 2007) and revealed how the trait composition of phytoplankton communities in different lakes and a marine system depended on light and nutrient conditions (Edwards et al. 2013a,b). However, phytoplankton can be strongly top-down controlled selecting for phytoplankton defence, which was not considered in these studies but is likely to have a crucial effect on the seasonal trait dynamics (Sommer et al. 2012). Defence against predation often comes at the costs of a lower competiveness/ growth rate (Agrawal 1998; Pančić and Kiørboe 2018). This trade-off can mediate antagonistic effects of top-down and bottom-up control on the trait composition. A large body of theory assumes such a trade-off (Abrams 1999; Tirok and Gaedke 2010; Klausmeier and Litchman 2012). However, there is no study which quantifies the shape of this trade-off and uses this information in combination with theoretical insights on trade-off curves (see Box 4.1 and Fig. 4.1) to explain how predation and abiotic conditions drive the trait dynamics and variation of natural communities.

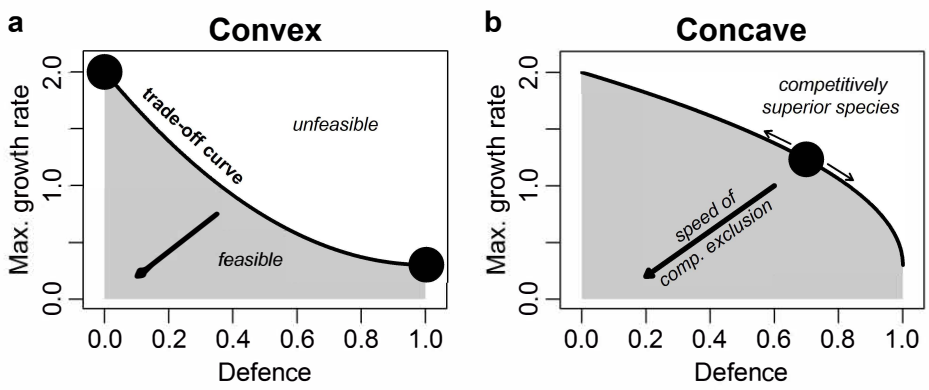

Figure 4.1: Competition outcome depending on the shape of the trade-off curve in a two dimensional trait space. The exemplary trade-off, shown here, is between defence against predation and maximum growth rate (d^{-1}). The trade-off curve (black line) represents the boundary between the set of feasible (grey area) and unfeasible trait combinations (white area). (a) A convex trade-off curve allows for coexistence of two specialized species with extreme trait values (marked by circles) while the other feasible trait combinations are outcompeted in the long-term. (b) A concave trade-off curve promotes a species with intermediate trait values (circle) finally outcompeting the other species where it depends on the present environmental conditions which intermediate strategy is of maximal fitness as indicated by the thin arrows. The speed of competitive exclusion increases in the direction towards the unfavourable edge of the feasible trait space (low trait values) which is indicated by the thick arrows (a, b).

Here, we combine theory and field data to show the importance of the shape of a trade-off between defence and maximum growth rate for the trait dynamics of a natural, co-evolved phytoplankton community. We use a comprehensive data set of large, deep, mesotrophic Lake Constance where strong trophic interactions, vertical mixing and resource depletion are important alternating forcing factors of phytoplankton (Gaedke 1998). The data set comprises 21 years of taxonomically resolved, high-frequency measurements of phytoplankton and their grazers as well as measurements of abiotic factors (vertical mixing intensity and phosphorous concentration) which all undergo a highly repetitive seasonal succession. The considered major functional traits were defence against predation, maximum growth rate and phosphate affinity. We expect that each trait is promoted by certain environmental conditions: 1. Species with high defence levels are favored by high grazing pressure. 2. High maximum growth rates are generally advantageous as they imply high growth capabilities and can compensate for high losses due to deep vertical mixing which removes phytoplankton from the favorable, euphotic zone. 3. A high phosphate affinity is promoted under phosphorous depletion. The species trait values were taken from lab measurements mainly conducted with Lake Constance plankton (Bruggeman 2011) revealing a concave trade-off between defence and maximum growth rate, while there was no significant correlation of these traits with phosphate affinity. To obtain mechanistic insights on the underlying fitness landscape guiding trait changes, we developed a model parametrized with the found trade-off curve.

We run numerical simulations to evaluate the favoured trait combinations and the speed of competitive exclusion of unfavorable trait combinations under different levels of grazing pressure, mimicking different seasonal field conditions. By linking theory, field data and modelling, we show that knowing the shape of the defence-growth trade-off is the key to understanding the ongoing trait changes and the maintenance of trait variation.

Material and methods

Study site and sampling

Upper Lake Constance (Bodensee) is a large (472 km^2), deep (mean depth = 101 m), warm-monomictic, mesotrophic lake bordered by Germany, Switzerland and Austria. It has a well-mixed epilimnion and a large pelagic zone (Gaedke et al. 2002). Lake Constance underwent reoligotrophication during which the total phosphorous concentration declined 4-fold from 1979 to 1996 leading to an annual phytoplankton biomass and production decline by 50% and 25%, respectively (Gaedke 1998). This had no major effects on the biomass-trait distribution reported here and is thus not further considered.

Plankton sampling was conducted weekly during the growing season and approximately fortnightly in winter, culminating in a time series of 853 phytoplankton biomass measurements from 1979 to 1999 (for details see https://fred.igb-berlin.de/Lakebase). Phytoplankton counts and cell volume estimates were obtained using Utermöhl (1958) inverted microscopy and were converted into biomass based on a specific carbon to volume relationship (Menden-Deuer and Lessard 2000). Measurements were taken from the uppermost water layer between 0 and 20 m depth which roughly corresponds to the epilimnion and the euphotic zone. In this study, we considered the 36 most abundant morphotypes of phytoplankton (constituting 92% of total phytoplankton biomass) comprising individual species or higher taxonomic units that are functionally identical or very similar under the functional classification employed here. This guaranteed a consistent resolution of phytoplankton counts across years. Zooplankton was sampled with the same frequency as phytoplankton. Data for all major herbivorous zooplankton groups (ciliates, rotifers, cladocerans and copepods) were available from 1987 to 1996.

Seasonal patterns

We subdivided the year into seven consecutive phases: late winter, early spring, late spring, clear-water phase (CWP), summer, autumn and early winter. Each phase was characterized by a well-defined combination of biotic and abiotic factors driving the phytoplankton community (Fig. 4.2): Strong vertical mixing implying high

phytoplankton losses from the euphotic zone occurred during winter and partly early spring. Grazing pressure was most important during the CWP and summer, and declined towards autumn. Nutrient depletion was most relevant in summer and autumn when vertical mixing, supplying nutrients from larger depths, was absent.

Trait data and trade-offs

The trait values for edibility, maximum growth rate and phosphate affinity of the 36 phytoplankton morphotypes were taken from Bruggeman (2011). Edibility was defined as the rate of prey consumption relative to the rate at which the favorite prey *Rhodomonas minuta* was consumed by *Daphnia* (Bruggeman 2011) which were very abundant prey and grazers in Lake Constance. We defined defence as $1-$ edibility. All morphotypes, their assigned trait data and taxonomy are listed in Appendix C.2. To detect potential pairwise trade-offs, we tested correlations between defence, maximum growth rate and phosphate affinity using the Spearman rank correlation.

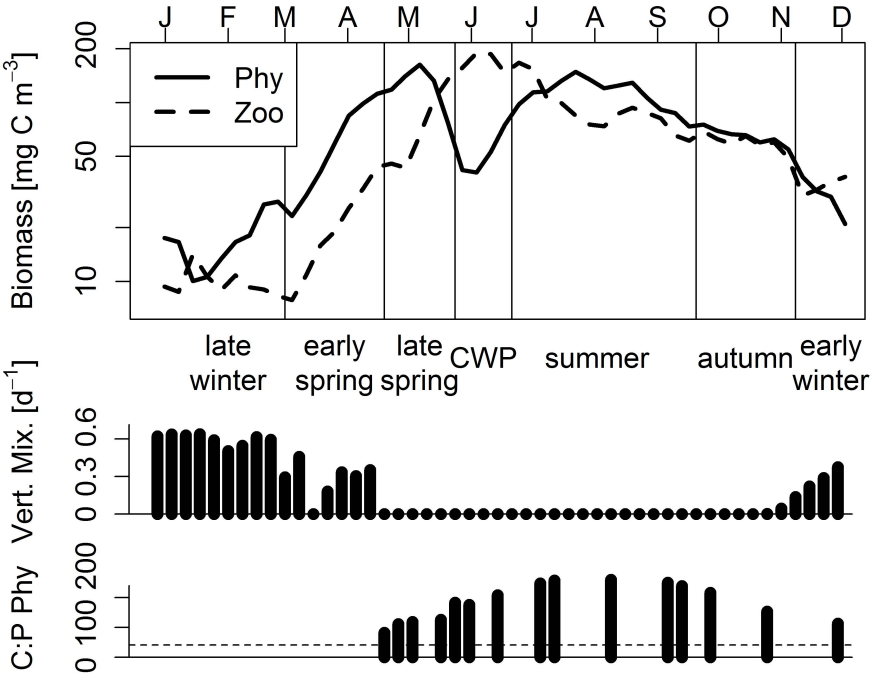

Figure 4.2: Inter-annual median biomass of phytoplankton (Phy) and herbivorous zooplankton (Zoo) in seven seasonal phases of a standardized year. The two bottom panels display the respective vertical mixing intensity which determines phytoplankton losses from the euphotic zone and the carbon to phosphorous (mass) ratio of phytoplankton indicating nutrient depletion (dashed line marks the Redfield ratio). For methodical details see Appendix C.1.

Model

We developed a simple model, based on Rosenzweig and MacArthur (1963), to show how the fitness landscape and the resulting biomass-trait distribution of a phytoplankton community differs under low (e.g., during early spring) and high grazing pressure (e.g., during summer). The model included N phytoplankton species which face a defence-growth trade-off, and one zooplankton group:

$$\begin{aligned}\frac{dP_i}{dt} &= r_i\left(1-\frac{\sum_{i=1}^{N}P_i}{K}\right)P_i - \frac{G(1-\delta_i)P_iZ}{H+\sum_{i=1}^{N}P_i} - m_P P_i \\ \frac{dZ}{dt} &= \varepsilon\frac{G\sum_{i=1}^{N}(1-\delta_i)P_i}{H+\sum_{i=1}^{N}P_i}Z - m_Z Z\end{aligned} \tag{4.1}$$

where P_i represents the biomass of phytoplankton species i, r_i the maximum growth rate, δ_i the defence against zooplankton, K the carrying capacity and m_P the natural mortality of phytoplankton. Z denotes the zooplankton biomass, G the maximum grazing rate, H the half-saturation constant, ε the conversion efficiency of phytoplankton biomass into zooplankton biomass and m_z the mortality of zooplankton (for a detailed parameter description see Appendix C.3). By changing m_z, we can vary the importance of grazing pressure where a low m_Z implies high zooplankton biomasses, that is, a high grazing pressure and vice versa. We assume a concave trade-off curve between r_i and δ_i, similar to the one found in the empirical data, and considered 184 different phytoplankton species with trait values spanning the whole feasible trait space. For details on the justification, parametrization, initialization and numerical integration of the model see Appendix C.3.

Results

The results section is divided into four parts: At first, we present insights on relevant trade-offs obtained from trait data for the morphotypes encountered in Lake Constance. Secondly, we describe the mean annual biomass-trait distribution of the phytoplankton community. Thirdly, we show how the biomass-trait distribution changes seasonally in response to altered environmental conditions. Finally, we compare the observed patterns with the model predictions.

Trade-offs

The 36 dominant morphotypes co-occurring in large, deep Lake Constance covered a large range of values in defence δ and maximum growth rate r (Fig. 4.3). In general, a low δ was accompanied by a high r and vice versa, leading to a significant, negative correlation between them ($\rho = -0.61$, $p = 10^{-5}$). The combination of high δ and

high r was not found, despite its potentially high fitness, suggesting a physiological or energetic constraint. Nevertheless, many species with intermediate δ and high r (and also high δ and intermediate r) occurred implying a concave trade-off curve (Fig. 4.3). Trait combinations of low to intermediate δ and small r being of low fitness were not found indicating past competitive exclusion. We tested also for correlations of δ or r with phosphate affinity which were not significant. In the following, we focus on the trait dynamics in δ and r but add information on phosphate affinity when useful.

Annual biomass-trait distribution

The mean annual biomass distribution within the trait space was obtained by weighting the morphotypes with their relative contribution to the total annual phytoplankton biomass (Fig. 4.3). The biomass was rather evenly distributed over the whole range of both traits with a maximum at intermediate to high values of δ and high r, caused by a cluster of different species of diatoms and chlorophytes. Considerable biomass occurs also at the extreme ends of the trait ranges (Fig. 4.3): *Rhodomonas* spp. with the lowest defence level and a high r constituted the highest annual share of biomass of an individual morphotype and occurred in almost every sample, and the highly defended but very slowly growing dinophytes exhibited intermediate mean annual relative biomasses. In general, for a given value of δ, the morphotypes with a higher r (i.e., higher fitness) dominated over those with lower r (Fig. 4.3). An exception to that was *Cryptomonas* spp. which only had an intermediate r despite its relatively low defence (δ=0.45) but the second highest mean annual relative biomass of an individual morphotype (Fig. 4.3). Remarkably, cryptomonads, chrysophytes, haplophytes and cyanobacteria generally had lower maximum growth rates compared to diatoms and chlorophytes given a certain defence level. For potential compensating advantages of these groups arising from further trait dimensions, see Discussion.

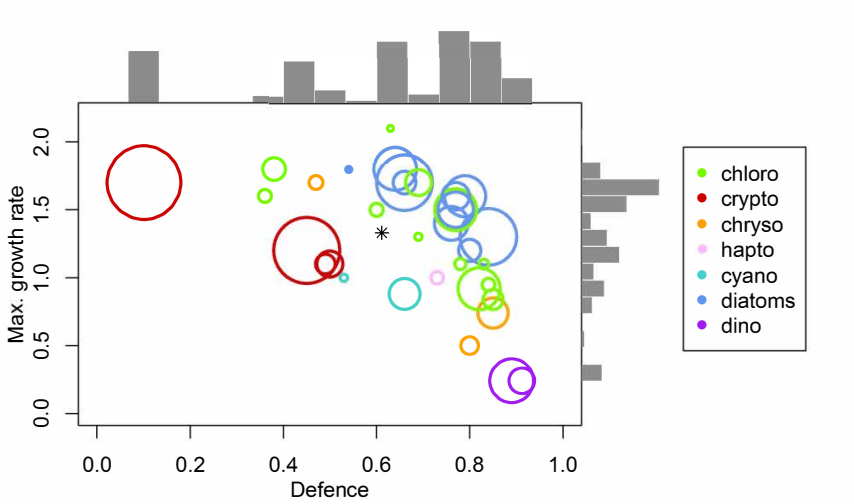

Figure 4.3: Defence δ and maximum growth rate r (d^{-1}) of the 36 most abundant phytoplankton morphotypes in Lake Constance. Colors indicate different taxonomic groups, i.e., chlorophyta, cryptomonads, chrysophytes, haptophytes, cyanobacteria, diatoms and dinophytes. The area of the circles is scaled by the mean annual relative biomass of the morphotypes. The asterisk marks the biomass-weighted community mean trait values ($\bar{\delta}$, $\bar{r}$). The bars display the relative biomass distribution along the two trait axes.

Seasonal trait dynamics

Independent of the season, a large body of biomass lays along the concave trade-off and not below (Fig. 4.4). The biomass distribution within the trait space varied seasonally (Fig. 4.4) in line with pronounced changes of the major forcing factors of phytoplankton development (Fig. 4.2). These community trait changes can be tracked by considering the community mean trait values ($\bar{\delta}$, $\bar{r}$) in the different seasonal phases, that is, the biomass-weighted average trait values among all morphotypes.

In late winter and early spring, vertical mixing and the resulting high loss rate were the dominant driver of the phytoplankton community in deep Lake Constance while grazing pressure and nutrient depletion were very low (Fig. 4.2). Morphotypes with high r being able to compensate for high losses dominated, whereas morphotypes with low r and high δ were almost absent (Fig. 4.4a, b). This is reflected in the community trait means (late winter: $\bar{\delta} = 0.51$, $\bar{r} = 1.56\,d^{-1}$; early spring: $\bar{\delta} = 0.52$, $\bar{r} = 1.57\,d^{-1}$). During late spring, grazing pressure increased (Fig. 4.2) but did not initiate a shift of the overall biomass distribution towards higher δ ($\bar{\delta} = 0.48$, $\bar{r} = 1.55\,d^{-1}$) (Fig. 4.4c). During the clear-water phase (CWP), the grazing pressure was at its annual maximum (Fig. 4.2). The mean community r decreased slightly ($\bar{r} = 1.35\,d^{-1}$) while the mean defence level did not change ($\bar{\delta} = 0.48$) despite the high grazing pressure (Fig. 4.4d), probably due to a delayed numerical response of highly defended but slowly growing morphotypes. In summer, nutrient depletion and grazing pressure were the dominant drivers of phytoplankton. The biomass shifted towards morphotypes with intermediate or high δ and accordingly low

r (Fig. 4e, $\bar{\delta} = 0.69$, $\bar{r} = 1.18\,d^{-1}$) but partially high phosphate affinity (Fig. 4.4e). In autumn, nutrient depletion and grazing were still mainly driving the phytoplankton community but declined compared to summer (Fig. 4.2). This resulted in a slight increase of morphotypes with lower δ and higher r ($\bar{\delta} = 0.62$, $\bar{r} = 1.28\,d^{-1}$) (Fig. 4.4f). In early winter, vertical mixing again represented the most important driver. Morphotypes with high r and intermediate δ contributed a high share to the total phytoplankton biomass (Fig. 4.4g, $\bar{\delta} = 0.56$, $\bar{r} = 1.40\,d^{-1}$).

The different morphotypes with intermediate or high δ dominating in different seasons had potentially different costs for their defence: In spring at deep vertical mixing and low nutrient depletion, the two dominant defended morphotypes had a high r but a very low phosphate affinity, while during summer with strong nutrient depletion and no deep vertical mixing, defended morphotypes had partly a more reduced r but a higher phosphate affinity (Fig. 4.4c, e). Hence, even if we found no significant correlation of δ or r with phosphate affinity within the whole community, some morphotypes may face a three-way trade-off. Nevertheless, the seasonal change in the community mean δ and r was stronger than for phosphate affinity (minimum during early spring: $215\,d^{-1}\,\mu mol^{-1}\,L$, maximum in autumn: $277\,d^{-1}\,\mu mol^{-1}\,L$) relative to the respective feasible trait range ($3.6 - 1600\,d^{-1}\,\mu mol^{-1}\,L$).

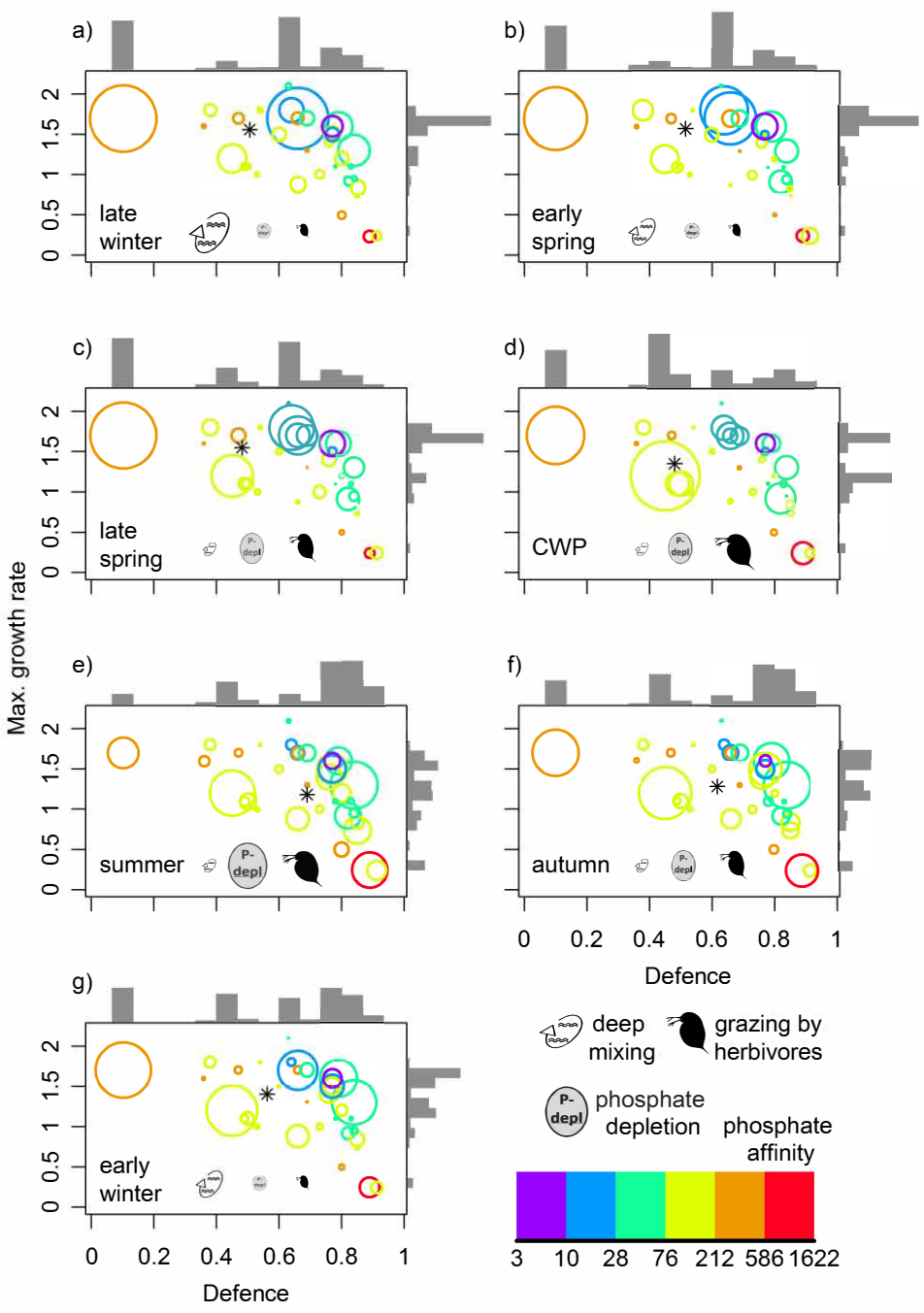

Figure 4.4: (a-g) Positions in the trait space of defence δ and maximum growth rate r (d^{-1}) and mean relative biomasses (scaling the area of the circles) of the 36 most abundant phytoplankton morphotypes in Lake Constance for the seven seasonal phases. The asterisks mark the respective biomass-weighted community mean trait values ($\bar{\delta}$, $\bar{r}$). Colors indicate the phosphate affinity ($d^{-1}\,\mu mol^{-1}\,L$) of the individual morphotypes. The icons represent the dominant drivers of the phytoplankton community (vertical mixing, phosphate depletion, grazing by herbivores) and their size indicates their relative importance for phytoplankton net growth in each phase. The bars display the relative biomass distribution along the two trait axes in each phase.

Model results

The model reproduced the general pattern in the empirical data, so that the favorable trait combinations shift from winter/spring (low grazing pressure) to summer/autumn (high grazing pressure) towards higher δ_i at the cost of a lower r_i (Fig. 4.4 a-f; 5a,b). For the given concave trade-off curve and set of trait combinations, the model predicted that two very similar species with intermediate δ_i but high r_i coexist in the long-term under low grazing pressure (Fig. 4.5a). Under high grazing pressure, the long-term outcome of the model was the survival of only one species with a high δ_i but intermediate r_i (Fig. 4.5a, b, for biomass dynamics see Appendix C.4). When considering the short-term results of the model being more in line with the time scale relevant for the data of the different seasons, we found that many species along the concave trade-off curve (especially close to the fitness maximum) survived the first 50 to 100 days (Fig. 4.5a, b), in accordance with the observations (Fig. 4.4a-g). This holds in particular under low grazing pressure (Fig. 4.5a,b). Overall, the time until extinction was shorter under high grazing pressure due to the high mortality caused by abundant grazers (Fig. 4.5a,b). In general, the speed of competitive exclusion increased (fitness decreased) towards the unfavourable edge of the trait space (low δ_i, low r_i) where the slope of the fitness decrease depended on the degree of grazing pressure. Under high grazing pressure the fitness gradient was more perpendicular to the defence axis than under low grazing pressure (Fig. 4.5a,b).

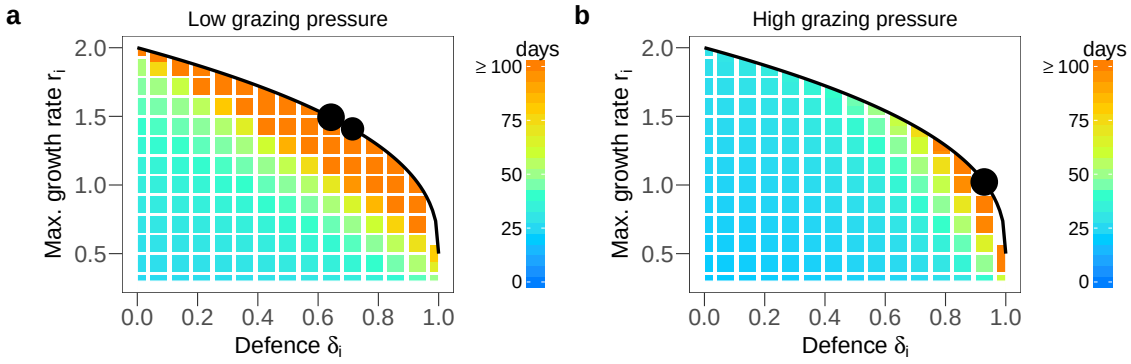

Figure 4.5: Model prediction on the competition outcome for a concave trade-off curve between defence δ_i and maximum growth rate r_i (black line) in the scenario of low grazing pressure on phytoplankton ($m_Z = 0.1\,d^{-1}$) mimicking conditions in winter and spring (a), and the scenario of high grazing pressure ($m_Z = 0.02\,d^{-1}$) during summer and autumn (b). The black dots denote the trait combinations of phytoplankton species which survive in the long-term, their size marks the mean relative biomass contribution between day 3000 and 4000 averaged among 100 simulations with randomized, different initial conditions (see Appendix C.3). The colour grid displays the average time until extinction of the different trait combinations in the short-term, that is, within the first 100 days of the simulations. Note that trait combinations of species with r_i-values below $0.3\,d^{-1}$ (i.e., below the rate of natural mortality) are not displayed.

Discussion

The 36 dominating phytoplankton morphotypes in Lake Constance faced a concave trade-off between defence and maximum growth rate. Theory predicts that concave trade-off curves promote species with intermediate strategies (see Box 4.1 and Fig. 4.1). Our data support this prediction as intermediately defended morphotypes with relatively high maximum growth rates constituted a high proportion of total annual phytoplankton biomass. Seasonal changes of the environmental conditions led to trait shifts in the phytoplankton community along the concave trade-off curve exactly as expected by the alternations in forcing factors. The model predicted a shift towards higher defence levels at the cost of lower maximum growth rates with increasing grazing pressure from spring to summer, as found in the data. Under constant conditions, the long-term outcome of the model was the survival of only one or two species with intermediate trait values. In contrast, we observed a high trait variation along the trade-off curve which can be explained by the short-term outcome of the model showing a slow competitive exclusion along the trade-off curve and shifting favorable trait combinations caused by seasonally changing conditions. The consideration of further trait dimensions such as phosphate affinity, which was not accounted for in the model, provide further explanation for the observed higher variation in defence and maximum growth rate. A high phosphate affinity, being relevant under nutrient depletion during summer, can compensate for low values of defence and maximum growth rate, and may allow the survival of the respective species.

The characterization of the trade-offs was based on trait data provided by Bruggeman (2011). He obtained trait values of the phytoplankton species from lab measurements and respective allometric calculations, mainly for the strains occurring in Lake Constance at the time of sampling. Uncertainties in trait values might arise from: 1.) Laboratory conditions which were not exactly the same as in the lake. 2.) Potential variation in the used allometric relationships (Taherzadeh et al. 2017). 3.) Phenotypic plasticity. However, all these uncertainties in the exact trait values were minor compared to the measured trait range. Hence, we argue that the lab-measured concave trade-off curve between defence and maximum growth rate adequately reflects the main trait composition of the phytoplankton community in Lake Constance.

Our model showed that, for a concave trade-off curve, two very similar species can stably coexist (Fig. 4.5a, Appendix C.4). This is in contradiction with theory predicting the survival of only one species (see Box 4.1 and Fig. 4.1b). The two species have intermediate strategies close to the fitness maximum and coexist based on stabilizing mechanisms arising from their slight difference in defence and growth. However, this community is not evolutionary stable (Edwards et al. 2018). Given gradual evolution, we

expect that one species would reach the exact fitness optimum via trait adaptation and outcompete the other for a concave trade-off curve (de Mazancourt and Dieckmann 2004; Rueffler et al. 2004). In nature, evolutionary processes do not always proceed gradually, i.e., with very small steps of trait adaptation, implying that reaching the exact fitness maximum can be unlikely. Hence, stable coexistence of similar but slightly different species close to the fitness maximum may be relevant in natural system.

In the model, only a low trait variation was maintained in the long-term based on a concave trade-off between defence and maximum growth rate. This is in contradiction with the empirical data showing a large trait variation including specialized species (highly defended or fast growing) and species having intermediate strategies. Abrams (2006) showed for a competition model that stable coexistence of two specialists using two different resources and one generalist is possible under asynchronous resource fluctuations. The species coexisted based on the relative non-linearity in their resource uptake functions. Such relative non-linearity enabling stable coexistence has not been found for the predator-prey model considered here. However, fitness-equalizing mechanisms may also promote species coexistence (Chesson 2000; Hubbell 2001). A fitness-equalizing trade-off implies that species with different trait values along the trade-off curve have equal fitness because the rate of loss determined by one trait (here: defence) and the rate of gain determined by the other trait (here: maximum growth rate) are exactly balancing (Ostling 2012). Trade-off curves are only fitness-equalizing for a specific shape equal to the shape of the fitness isoclines making fitness-equality improbable to occur in nature (Purves and Turnbull 2010). For the considered trade-off between defence and maximum growth rate, the fitness-equalizing case corresponds to a linear trade-off curve (Ehrlich et al. 2017, see colour gradient in Fig. 4.5 a,b) which was not found in the empirical data (see Fig. 4.3).

Even if the trade-off was not fitness-equalizing, we argue that low fitness differences along the concave trade-off curve allow for short-term coexistence due to slow competitive exclusion (see Fig. 4.5a, b). Given environmental fluctuations which continuously alter the selection regime, a low speed of competitive exclusion may promote coexistence even in the long-term (Huston 1979). In Lake Constance, the environmental conditions change seasonally and move the fitness maximum gradually along the trade-off curve from fast growing, intermediately defended species in early spring to slowly growing but more defended species in summer and then back in winter. Thus, several species along the trade-off curve have maximal fitness at different times of the year. This pattern of gradually moving fitness maxima is specific to concave trade-off curves and is not expected for convex ones (see Box 4.1, Fig. 4.1a and Appendix C.5). We argue that long-term coexistence of numerous phytoplankton species along the concave trade-off curve is possible based on: 1.) their high production under respective favorable

conditions, given their short generation times, 2.) their slow competitive exclusion under unfavorable conditions and 3.) their ability to form resting stages (Fryxell and of America 1983) causing a storage effect (Chesson 2000). Feasible but unfavorable trait combinations (i.e., low defence and low maximum growth rate) apart from the trade-off curve were quickly outcompeted in the model, providing an explanation for their absence in Lake Constance and in the whole data set of Bruggeman (2011) (see Appendix C.2).

The maintenance of a high trait variation in the lake was likely also promoted by further niche dimensions and respective traits which were not considered in the model. For instance, a high phosphate affinity is beneficial under strong nutrient depletion during summer and autumn, and may explain why the defended dinophytes survive despite their very high defence costs regarding the maximum growth rate (Fig. 4.3). The undefended *Rhodomonas* ssp. also had a high phosphate affinity which sheds light on its observed high biomasses and very regular occurrence in spite of its maximum growth rate not exceeding the one of intermediately defended species. In addition to that, *Rhodomonas* spp. is able to use additional light spectra based on the red accessory photopigment phycoerythrin allowing photosynthesis at greater depths which is relevant year round due to vertical mixing and self-shading. The same holds for *Cryptomonas* spp. which also reached high biomasses irrespectively of its low maximum growth rate relative to its defence level. The cyanobacteria (*Anabaena* spp. and *Oscillatoria* spp.) also produce additional photopigments and further increase their fitness by buoyance regulation which probably compensate for their relative low maximum growth rates compared to diatoms with similar defence levels. Diatoms seem to have maximal fitness regarding their defence and maximum growth rate. However, they face disadvantages due to the production of shells implying an additional silica demand and causing high sedimentation rates which lead to lower net growth rates than expected from their maximum growth rate. This is less relevant under intensive vertical mixing. Mixotrophy represents an additional niche dimension promoting the highly defended, bacterivorous *Dinobryon* spp. which exhibits a very low maximum growth rate but is able to obtain relevant amounts of phosphate from bacterivory under phosphorous depletion in Lake Constance (Kamjunke et al. 2006). In general, phytoplankton species of the same taxonomic group cluster within the trait space (Fig. 4.3) indicating shared ecological strategies among closely related species.

Lake Constance has successfully served as a model system for large open water bodies including marine ones (Gaedke 1992). It exhibits a typical seasonal plankton succession driven by vertical mixing, grazing and nutrient limitation (Sommer et al. 2012). These environmental factors are also main drivers of marine phytoplankton which is ecologically similar to freshwater phytoplankton and may face similar trade-offs (Kilham and Hecky 1988). Trade-offs between defence and growth are also relevant in terrestrial plant communities, for example, grasslands (Lind et al. 2013). Even independent from the

considered system with its environmental drivers and relevant trade-offs, our approach provides a general solution for obtaining mechanistic understanding of ongoing trait changes directly under field conditions.

Overall, to summarize, the identification of the major trade-off and its shape provided a remarkable key to understanding trait shifts and altering species composition in the phytoplankton community under seasonally changing environmental conditions. Although multiple trait dimensions might play a role, our results showed that defence and maximum growth rate represent key traits in Lake Constance where grazers are known to strongly impact phytoplankton net growth (Gaedke et al. 2002) and vertical mixing can cause high biomass losses from the euphotic zone (Gaedke et al. 1998). The maintenance of trait variation was linked to low fitness differences and the changing environment which continuously moved favorable trait combinations along the concave trade-off curve preventing competitive exclusion. Our study successfully explained major trait dynamics based on a model including only the two-dimensional, interspecific trade-off between defence and growth, and allowed to verify the theory on the shape of the trade-off curve in the field. Our findings revealed that the combination of trait and biomass data with simple models, involving the major trade-offs found in the data and information on their shape, represents a powerful approach to understanding trait dynamics and variation in natural communities.

Acknowledgements

Many thanks to Alexander Wacker, Alice Boit and Guntram Weithoff for very constructive comments on an earlier version of the manuscript. We thank Michael Raatz for fruitful discussions on the results. This research was funded by the German Research Foundation (DFG, GA 401/26-1/2).

Bibliography 4

Abrams, P. A. (1999). Is predator-mediated coexistence possible in unstable systems? *Ecology*, 80(2):608–621.

Abrams, P. A. (2006). The Prerequisites for and Likelihood of Generalist-Specialist Coexistence. *The American Naturalist*, 167(3):329–342.

Agrawal, A. A. (1998). Algal defense, grazers, and their interactions in aquatic trophic cascades. *Acta Oecologica*, 19(4):331–337.

Barry, M. J. (1994). The costs of crest induction for Daphnia carinata. *Oecologia*, 97(2):278–288.

Bruggeman, J. (2011). A phylogenetic approach to the estimation of phytoplankton traits. *Journal of Phycology*, 47(1):52–65.

Chesson, P. (2000). Mechanisms of Maintenance of Species Diversity. *Annual Review of Ecology and Systematics*, 31(1):343–366.

de Mazancourt, C. and Dieckmann, U. (2004). Trade-Off Geometries and Frequency-Dependent Selection. *The American Naturalist*, 164(6):765–778.

Edwards, K., Litchman, E., and Klausmeier, C. (2013a). Functional traits explain phytoplankton responses to environmental gradients accross lakes of the United States. *Ecology*, 94(7):1626–1635.

Edwards, K. F., Kremer, C. T., Miller, E. T., Osmond, M. M., Litchman, E., and Klausmeier, C. A. (2018). Evolutionarily stable communities: a framework for understanding the role of trait evolution in the maintenance of diversity. *Ecology Letters*, 21(12):1853–1868.

Edwards, K. F., Litchman, E., and Klausmeier, C. A. (2013b). Functional traits explain phytoplankton community structure and seasonal dynamics in a marine ecosystem. *Ecology Letters*, 16(1):56–63.

Ehrlich, E., Becks, L., and Gaedke, U. (2017). Trait-fitness relationships determine how trade-off shapes affect species coexistence. *Ecology*, 98(12):3188–3198.

Fryxell, G. A. and of America, P. S. (1983). *Survival Strategies of the Algae*. Cambridge Univ. Press, New York and London.

Gaedke, U. (1992). The size distribution of plankton biomass in a large lake and its seasonal variability. *Limnology and Oceanography*, 37(6):1202–1220.

Gaedke, U. (1998). The response of the pelagic food web to re-oligotrophication of a large and deep lake (L. Constance): Evidence for scale-dependent hierarchical patterns? *Archiv für Hydrobiologie*, 53:317–333.

Gaedke, U., Hochstädter, S., and Straile, D. (2002). Interplay between energy limitation and nutritional deficiency: Empirical data and food web models. *Ecological Monographs*, 72(2):251–270.

Gaedke, U., Ollinger, D., Straile, D., and Bäuerle, E. (1998). The impact of weather conditions on the seasonal plankton development. *Archiv fuer Hydrobiologie*, 53:565–585.

Hubbell, S. P. (2001). *The Unified Neutral Theory of Biodiversity and Biogeography*. Princeton University Press, Princeton.

Huston, M. (1979). A general hypothesis of species diversity. *The American Naturalist*, 113(1):81–101.

Jones, L. E., Becks, L., Ellner, S. P., Hairston Jr., N. G., Yoshida, T., and Fussmann, G. F. (2009). Rapid contemporary evolution and clonal food web dynamics. *Philosophical Transactions of the Royal Society B: Biological Sciences*, 364(1523):1579–1591.

Kamjunke, N., Henrichs, T., and Gaedke, U. (2006). Phosphorus gain by bacterivory promotes the mixotrophic flagellate Dinobryon spp. during re-oligotrophication. *Journal of Plankton Research*, 29(1):39–46.

Kilham, P. and Hecky, R. E. (1988). Comparative ecology of marine and freshwater phytoplankton1. *Limnology and Oceanography*, 33(4, part 2):776–795.

Klausmeier, C. A. and Litchman, E. (2012). Successional Dynamics in the Seasonally Forced Diamond Food Web. *The American Naturalist*, 180(1):1–16.

Kneitel, J. M. and Chase, J. M. (2004). Trade-offs in community ecology: linking spatial scales and species coexistence. *Ecology Letters*, 7(1):69–80.

Levins, R. (1962). Theory of Fitness in a Heterogeneous Environment. I. The Fitness Set and Adaptive Function. *The American Naturalist*, 96(891):361–373.

Lind, E. M., Borer, E., Seabloom, E., Adler, P., Bakker, J. D., Blumenthal, D. M., Crawley, M., Davies, K., Firn, J., Gruner, D. S., Stanley Harpole, W., Hautier, Y., Hillebrand, H., Knops, J., Melbourne, B., Mortensen, B., Risch, A. C., Schuetz, M., Stevens, C., and Wragg, P. D. (2013). Life-history constraints in grassland plant species: a growth-defence trade-off is the norm. *Ecology Letters*, 16(4):513–521.

Litchman, E. and Klausmeier, C. A. (2008). Trait-Based Community Ecology of Phytoplankton. *Annual Review of Ecology, Evolution, and Systematics*, 39(1):615–639.

Litchman, E., Klausmeier, C. A., Schofield, O. M., and Falkowski, P. G. (2007). The role of functional traits and trade-offs in structuring phytoplankton communities: scaling from cellular to ecosystem level. *Ecology Letters*, 10(12):1170–1181.

Maharjan, R., Nilsson, S., Sung, J., Haynes, K., Beardmore, R. E., Hurst, L. D., Ferenci, T., and Gudelj, I. (2013). The form of a trade-off determines the response to competition. *Ecology Letters*, 16(10):1267–1276.

Menden-Deuer, S. and Lessard, E. J. (2000). Carbon to volume relationships for dinoflagellates, diatoms, and other protist plankton. *Limnology and Oceanography*, 45(3):569–579.

Meyer, J. R., Gudelj, I., and Beardmore, R. (2015). Biophysical mechanisms that maintain biodiversity through trade-offs. *Nature Communications*, 6(1):6278.

Ostling, A. (2012). Do fitness-equalizing tradeoffs lead to neutral communities? *Theoretical Ecology*, 5(2):181–194.

Pančić, M. and Kiørboe, T. (2018). Phytoplankton defence mechanisms: traits and trade-offs. *Biological Reviews*, 93(2):1269–1303.

Pedruski, M. T., Fussmann, G. F., and Gonzalez, A. (2015). Predicting the outcome of competition when fitness inequality is variable. *Royal Society Open Science*, 2(8):150274.

Purves, D. W. and Turnbull, L. A. (2010). Different but equal: the implausible assumption at the heart of neutral theory. *Journal of Animal Ecology*, 79(6):1215–1225.

Rosenzweig, M. and MacArthur, R. (1963). Graphical representation and stability conditions of predator-prey interactions. *American Naturalist*, 97:209–223.

Rueffler, C., Van Dooren, T., and Metz, J. (2004). Adaptive walks on changing landscapes: Levins' approach extended. *Theoretical Population Biology*, 65(2):165–178.

Rueffler, C., Van Dooren, T. J. M., and Metz, J. A. J. (2006). The Evolution of Resource Specialization through Frequency-Dependent and Frequency-Independent Mechanisms. *The American Naturalist*, 167(1):81–93.

Smith, V. H., Foster, B. L., Grover, J. P., Holt, R. D., Leibold, M. A., and DeNoyelles, F. (2005). Phytoplankton species richness scales consistently from laboratory microcosms to the world's oceans. *Proceedings of the National Academy of Sciences*, 102(12):4393–4396.

Sommer, U., Adrian, R., De Senerpont Domis, L., Elser, J. J., Gaedke, U., Ibelings, B., Jeppesen, E., Lürling, M., Molinero, J. C., Mooij, W. M., van Donk, E., and Winder, M. (2012). Beyond the Plankton Ecology Group (PEG) Model: Mechanisms Driving Plankton Succession. *Annual Review of Ecology, Evolution, and Systematics*, 43(1):429–448.

Stearns, S. C. (1989). Trade-Offs in Life-History Evolution. *Functional Ecology*, 3(3):259–268.

Taherzadeh, N., Kerimoglu, O., and Wirtz, K. W. (2017). Can we predict phytoplankton community size structure using size scalings of eco-physiological traits? *Ecological Modelling*, 360:279–289.

Tilman, D. (2000). Causes, consequences and ethics of biodiversity. *Nature*, 405(6783):208–211.

Tilman, D., Kilham, S. S., and Kilham, P. (1982). Phytoplankton Community Ecology: The Role of Limiting Nutrients. *Annual Review of Ecology and Systematics*, 13(1982):349–372.

Tirok, K. and Gaedke, U. (2010). Internally driven alternation of functional traits in a multispecies predator–prey system. *Ecology*, 91(6):1748–1762.

Utermöhl, H. (1958). Zur Vervollkommnung der quantitativen Phytoplankton-Methodik. *Mitteilungen der Internationalen Vereinigung der Limnologie*, 9:1–38.

Weithoff, G. (2003). The concepts of 'plant functional types' and 'functional diversity' in lake phytoplankton - a new understanding of phytoplankton ecology? *Freshwater Biology*, 48(9):1669–1675.

Yoshida, T., Hairston, N. G., and Ellner, S. P. (2004). Evolutionary trade-off between defence against grazing and competitive ability in a simple unicellular alga, Chlorella vulgaris. *Proceedings of the Royal Society B: Biological Sciences*, 271(1551):1947–1953.

5 Trade-offs at multiple trophic levels of a food web

Manuscript title:

Coupled changes in traits and biomasses cascading through a tritrophic plankton food web

Elias Ehrlich[1], and Ursula Gaedke[1]

1. Department of Ecology and Ecosystem Modelling, University of Potsdam, Am Neuen Palais 10, 14469 Potsdam, Germany.

Submitted as:

Ehrlich, E., and Gaedke, U. (2019). Coupled changes in traits and biomasses cascading through a tritrophic plankton food web. *Under review in Proceedings of the Royal Society B: Biological Sciences*.

Abstract

Trait adaptation of predator and prey can strongly alter food web dynamics which has been shown for bitrophic systems. However, natural food webs are typically at least tritrophic, enabling indirect trait interactions with underexplored effects on these dynamics. Here, we demonstrate co-adaptation among three trophic levels in a natural plankton food web (Lake Constance) and in a corresponding model. We found highly recurrent seasonal biomass and trait dynamics, which were interrelated in a 'trophic biomass-trait cascade' and partly reversed compared to predictions from bitrophic systems: First, herbivores increased in counter-defence before phytoplankton defence increased. In contrast, trait adaptation of carnivores followed that of herbivores. By combining observations and model simulations, we explain the reversed trait dynamics at the two lower trophic levels with the top-down effect of carnivores and biomass-trait feedbacks between herbivores and phytoplankton. The model revealed that weakening carnivore predation leads to the predicted order, i.e. herbivore counter-defence follows upon phytoplankton defence. We conclude that trait adaptation between two trophic levels can be superimposed by the impact of a third trophic level. Thus, the analysis of pairwise trait adaptation can be misleading in natural food webs, while multitrophic trait-based approaches capture indirect biomass-trait interactions among trophic levels.

Introduction

Trophic interactions crucially affect the fitness of organisms in almost every ecosystem and thus have a high potential to drive trait changes in communities. High grazing pressure can select for defence against predation in prey communities, for example, increasing swimming speed, hiding or spine formation (Brodie et al. 1991). An enhanced defence level then leads to a strong selection of predator strategies to overcome prey defence, for example, by changing the feeding mode, increasing foraging activity or size (Boukal 2014), which in turn induces further changes in prey traits. Such trait feedbacks are known as the predator-prey arms race, being widely established in the context of coevolution of a single prey species and its predator (Dawkins and Krebs 1979; Brodie and Brodie 1999; Abrams 2000).

Here, we consider arms races in a broader context of co-adapting communities or trophic levels including several species with different trait values. Within these communities, trait changes emerges through sorting of species (Leibold et al. 1997), which alters the relative contribution of the species to the community biomass and thus the mean community trait value. Co-adaptation of communities and coevolution of species (in particular asexually reproducing species) are mechanistically similar. In both cases, selection alters the trait composition of trophic levels, acting either at the species or genotype level (Abrams and Vos 2003). Hence, theory on coevolution of predator and prey (Abrams 2000; Cortez and Weitz 2014; Yamamichi and Ellner 2016) can be transferred to the community context.

Previous theory predicts that the counter-defence trait of the predator follows the defence trait of the prey (Cortez and Weitz 2014; Velzen and Gaedke 2017), as visualized in conceptual Figure 5.1. Trade-offs play a central role in organizing these trait dynamics (Tien and Ellner 2012). For example, at low predator biomasses, prey defence decreases in order to minimize its costs regarding growth and at low defence levels, the predator decreases its counter-defence to optimize its grazing rate (Fig. 5.1). If trait and biomass dynamics proceed on similar time scales, they may mutually affect each other and produce feedbacks loops (Fig. 5.1), known as eco-evolutionary feedbacks in case of genetic trait changes (Fussmann et al. 2007; Post and Palkovacs 2009; Yamamichi and Ellner 2016) or biomass-trait feedbacks in a community context (Klauschies et al. 2016).

Most of the previous theory and empirical work focussed on co-adaptation of two trophic levels (Brodie and Brodie 1999; Post and Palkovacs 2009; Klauschies et al. 2016). A few studies successfully combined field data and modelling approaches, revealing that the observed trait dynamics matched with theoretical expectations (Tirok and Gaedke 2010; Kenitz et al. 2017). However, natural food webs usually comprise more than two trophic levels and each of them can interact with the others directly or indirectly via

changes in their biomasses or trait composition (Leibold et al. 1997; Abrams and Vos 2003; Schmitz et al. 2004, Ceulemans et al. *under review*). In this study, we want to address the question whether the predictions of previous theory concerning the dynamics of two co-adapting trophic levels (Fig. 5.1) hold also in a natural, multitrophic food web.

We use long-term data of large, deep Lake Constance with high-frequency biomass measurements of three trophic levels, namely phytoplankton, herbivorous and carnivorous zooplankton, and a corresponding tritrophic food web model (Fig. 5.2). We assign the species at each trophic level to two functional groups based on species-specific trait measurements (mainly body size) and well-known trophic relationships. An altered relative contribution of a functional group to the total biomass of the respective trophic level implies changes in the mean trait values of that level. We observed pronounced, highly recurrent changes in total biomasses and mean trait values of the trophic levels within a growing season, which were interrelated in a 'trophic biomass-trait cascade'. Remarkably, the order of trait changes between the two bottom trophic levels was reversed compared to predictions of previous theory on bitrophic systems: First, the herbivores increased in counter-defence before phytoplankton defence rose. The food web model reproduced the observed dynamics and showed that this reversed order was driven by the grazing impact of the third trophic level and biomass-trait feedbacks among the different trophic levels. Our results demonstrated that the analysis of pairwise trait adaptation can be misleading in natural food webs, while multitrophic trait-based approaches are suitable to obtain mechanistic understanding of community trait dynamics.

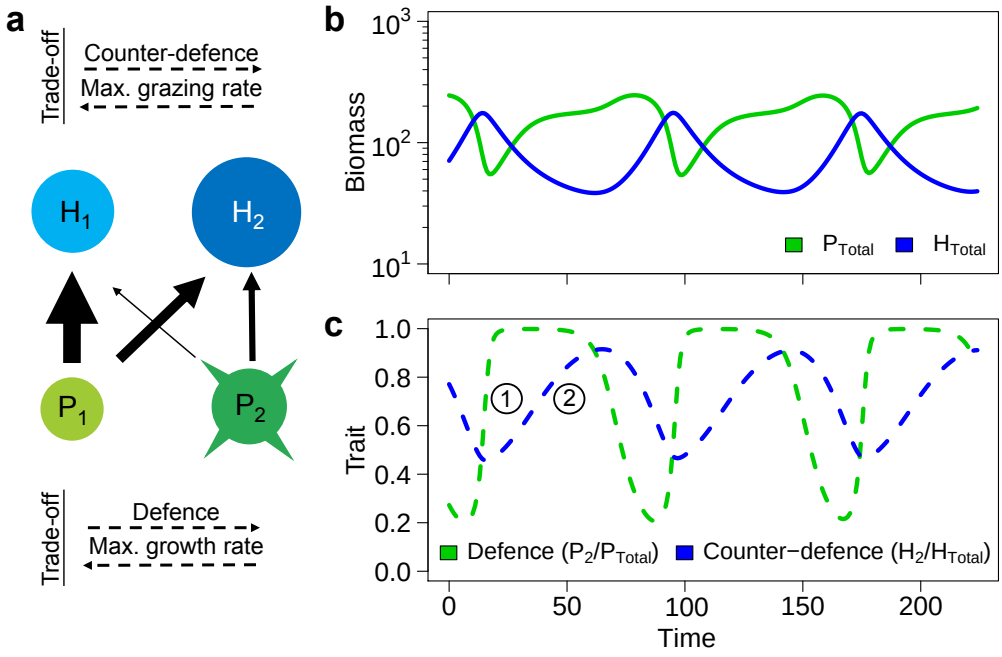

Figure 5.1: (a) Simple food web model of two co-adapting trophic levels, that is, primary producers P and herbivores H, and (b) their predicted biomass and (c) trait dynamics. (a) Each trophic level is divided into two types (genotypes, species or functional groups) reflecting trait differences: Undefended (P_1) and defended primary producers (P_2), and herbivores without (H_1) and with counter-defence (H_2). Defence trades off with maximum growth rate and counter-defence with maximum grazing rate (as indicated by dashed arrows). The strength of trophic interactions among the types is indicated by the thickness of the solid arrows. (b) The biomasses of the two trophic levels cycle, where P_{Total} denotes the total primary producer and H_{Total} the total herbivore biomass. (c) Cycles occur also in the traits with defence of primary producers increasing first ① followed by the counter-defence of herbivores ②. (b, c) Biomass and trait dynamics feedback on each other, for example, an increasing herbivore biomass initiate an increase of primary producer defence which, in turn, contributes to the decrease of herbivore biomass.

Methods

Study site and plankton data

Lake Constance (LC) is a temperate, large (472 km^2), deep (mean depth=101 m), warm-monomictic, meso-trophic lake north of the European Alps. Plankton data were collected weekly during the growing season and approximately every two weeks in winter from different depths. We used the data from the uppermost layer between 0 and 20 m depth, roughly corresponding to the epilimnion and euphotic zone. Plankton abundances were determined by microscopic counts and were converted to biomasses based on measurements of organism size and specific carbon to volume or length relationships. For details see Gaedke (1992) and literature cited therein, except for phytoplankton carbon conversion see Menden-Deuer and Lessard (2000).

We considered biomass data of phytoplankton, herbivorous and carnivorous zooplankton from 1987 to 1996, representing the main body of the first three trophic levels in the lake (Gaedke et al. 2002; Boit and Gaedke 2014). The biomass data were averaged across years using a biweekly resolution in order to obtain general insights on recurring seasonal patterns. We standardized the time axis relative to the onset of the clear-water phase (CWP) to account for interannual variability arising from differences in winter and early spring weather conditions (Tirok and Gaedke 2006). We excluded the winter season where mainly physical factors like irradience, vertical mixing and temperature determine plankton growth and focussed on the growing season with trophic interactions acting as main drivers of the plankton dynamics (Sommer et al. 2012). The growing season was defined here as the period from 12 weeks before the CWP to 20 weeks after the CWP, corresponding approximately to the period from March to early November.

Traits, trade-offs and functional groups

We distinguished between two functional groups at each of the three trophic levels based on species-specific lab measurements of traits characterizing the trophic interactions of the organisms and their competitiveness. Ensuing from this functional classification, we built a simplified food web comprising the major feeding links among these groups (Fig. 5.2). This allowed us to theoretically approach grazing-driven trait changes within each trophic level which can be tracked by shifts in the relative contribution of the functional groups. Phytoplankton was divided into well-edible P_1 and less-edible phytoplankton P_2 based on their longest linear dimension LLD (larger algae are less-edible), shape and colony formation (Knisely and Geller 1986). The phytoplankton faces an interspecific trade-off between defence and growth (Wirtz and Eckhardt 1996, Ehrlich et al. *submitted*). Hence, the lower edibility of P_2 for herbivores comes at the cost of a lower maximum weight-specific growth rate compared to P_1.

The herbivorous zooplankton was classified into small herbivores H_1, comprising ciliates (unicellular protists) and most of the rotifers (small, simply organized metazoans), and large herbivores H_2, consisting of the large rotifer *Asplanchna*, and herbivorous crustaceans (the waterflea *Daphnia*, another cladoceran *Bosmina* and the calanoid copepod *Eudiaptomus*). H_1 feeds almost entirely on well-edible algae. In contrast, H_2 has larger prey spectrum (i.e. generality) which covers also a considerable amount of the less-edible algae, implying a counter-defence (see Fig. 5.2). The counter-defence of large herbivores trades off with a lower weight-specific grazing rate compared to H_1 (de Castro and Gaedke 2008).

At the third trophic level, we distinguished between small carnivores C_1, made up of cyclopoid copepods, and large carnivores C_2, which were the cladocerans *Leptodora* and *Bythotrephes*. For simplicity, we assumed that C_1 feeds exclusively on H_1 and C_2 on H_2

(Fig. 5.2). In reality, C_1 is omnivorous as its juvenile stages consume also phytoplankton. However, the contribution of C_1 to phytoplankton grazing is minor (Tirok and Gaedke 2006). As we want to focus on the main feeding interactions driving trait changes, we disregard the link from phytoplankton to C_1.

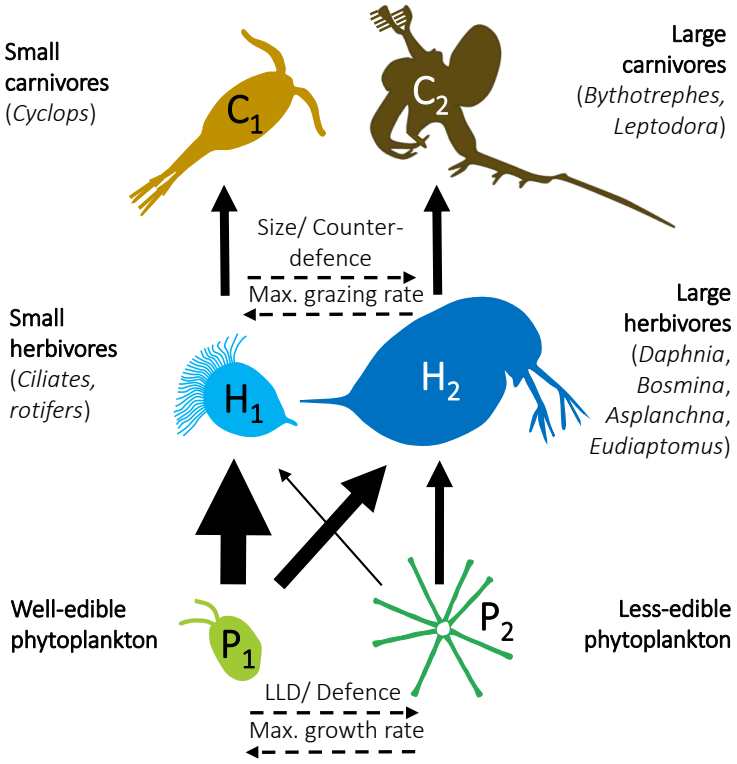

Figure 5.2: Modelled plankton food web with two functional groups at each of the three trophic levels considered. The top trophic levels (e.g. fishes) were not included here due to lacking data. Solid arrows represent trophic interactions where their thickness indicates the strength of the feeding link, given by the preference of the respective predator. Dashed arrows show the direction in which the respective trait values at the two bottom trophic levels increase.

Food web model

We set up a food web model comprising the main feeding links among the six previously described functional groups (Fig. 5.2). The population dynamics of P_1, P_2, H_1, H_2, C_1 and C_2 are given by

$$\begin{aligned}
\frac{dP_i}{dt} &= r_i P_i \left(1 - \frac{P_1 + P_2}{K}\right) - \sum_{j=1}^{2} \frac{G_j\, p_{ij} P_i H_j}{h + \sum_{i=1}^{2} p_{ij} P_i} \\
\frac{dH_j}{dt} &= \varepsilon \frac{G_j \sum_{i=1}^{2} p_{ij} P_i}{h + \sum_{i=1}^{2} p_{ij} P_i} H_j - a_j H_j C_j \\
\frac{dC_j}{dt} &= \varepsilon\, a_j H_j C_j - m_j C_j^2 \,.
\end{aligned} \tag{5.1}$$

The definitions, (initial) values and units of the state variable and parameters are provided in Table 5.1. We assume logistic growth of phytoplankton with symmetric competition between P_1 and P_2. Both phytoplankton groups share the same carrying capacity K but differ in their maximum weight-specific growth rate r_i and their edibility (probability of being attacked) for the different herbivores p_{ij} (Tab. 5.1). The grazing of herbivores on phytoplankton is described by a two-prey type Holling type II functional response. The herbivore groups differ in their maximum weight-specific grazing rates G_j and their preferences for the different phytoplankton groups which is reflected in the different p_{ij} values (Tab. 5.1). For simplicity, we assume equal half-saturation constants h for H_1 and H_2, and equal conversion efficiencies ε for H_1, H_2, C_1 and C_2.

To keep the model complexity at a minimum, we assume a linear functional response of carnivores, where the weight-specific attack rate a_j of C_1 is higher than for C_2. The carnivores are exposed to a density-dependent mortality rate which mimics, among others, grazing losses by fish predation. The weight-specific mortality rate is the product of the mortality rate m_j and the biomass of the respective carnivore group. That is, the weight-specific mortality rate increases linearly with increasing biomass. We assume that m_j is higher for large carnivores, as they are preferred by the dominant fish species (Straile and Hälbich 2000).

Mean temperatures in the uppermost 20 m vary from ca. 4 to 16 °C within the growing season which is described by

$$T = 6 \sin\left(1.4\,\pi \frac{t}{t_{end}} - 1.5\right) + 10 \tag{5.2}$$

in the model, fitting the measured temperature dynamics (Appendix D.1). We include a temperature-dependency in the maximum growth rates r_i of phytoplankton, the maximum grazing rates G_j of herbivores and the attack rate a_j of carnivores, as their metabolic activity is reduced at low temperatures. The temperature-dependent rates are given bv

$$\psi(T) = \psi_{T_{max}}\, Q_{10}^{\frac{T-T_{max}}{10^{\circ}\mathrm{C}}} \tag{5.3}$$

with $\psi \in \{r_i, G_j, a_j\}$ and $\psi_{T_{max}}$ being the respective rate at the maximum temperature within the growing season. We assume that phytoplankton and small herbivores exhibit a lower temperature sensitivity than the large herbivores and all carnivores which are predominantly crustaceans. Crustaceans are known to have a more strongly reduced performance at low temperature (Sommer et al. 2012) compared to unicellular organisms which corresponds to a higher Q_{10} (Tab. 5.1).

Table 5.1: State variables and parameters.

Var./ Par.	Definition	Value (at T_{max} for r_i, G_j, a_j)	Unit	Source
P_i	Biomass of phytoplankton group i	Initial: $P_1 = 12$, $P_2 = 8$	$mgCm^{-3}$	Own data*1
H_j	Biomass of herbivorous zooplankton group j	Initial: $H_1 = 4$, $H_2 = 5$	$mgCm^{-3}$	Own data*1
C_j	Biomass of carnivorous zooplankton group j	Initial: $C_1 = 10$, $C_2 = 0.1$	$mgCm^{-3}$	Own data*1
r_i	Max. weight-specific growth rate of P_i	$r_1 = 1.4$, $r_2 = 0.6$	d^{-1}	Bruggeman (2011)
K	Carrying capacity of P_i	400	$mgCm^{-3}$	Estimated from own data*1
p_{ij}	Edibility of P_i for H_j	$p_{11} = 1.0$, $p_{21} = 0.1$, $p_{12} = 1.0$, $p_{22} = 0.4$		Knisely and Geller (1986)
G_j	Max. weight-specific grazing rate of H_j	$G_1 = 1.2$, $G_2 = 0.6$	d^{-1}	Production to biomass ratios *2
h	Half-saturation constant	80	$mgCm^{-3}$	Estimated from own data*1
ε	Conversion efficiency	0.3		Straile (1997)
a_j	Weight-specific attack rate of C_j for H_j	$a_1 = 0.01$, $a_2 = 0.005$	$\frac{d^{-1}}{mgCm^{-3}}$	fitted
m_j	Mortality rate of C_j	$m_1 = 0.001$, $m_2 = 0.01$	$\frac{d^{-1}}{mgCm^{-3}}$	fitted
T_{max}	Max. temperature of growing season	16	°C	Measured (around early August)
Q_{10}	Temperature coefficient	For r_1, r_2, G_1: 1.5 For G_2, a_1, a_2: 2.5		Sherman et al. (2016) Burns (1969)
t_{end}	Period of growing season	225	d	Own data*1

*1 Measured biomasses (Fig. 5.3), for details see Boit and Gaedke (2014) and literature cited therein; *2 Obtained from direct measurements and a mass-balanced flow model developed for Lake Constance (Gaedke et al. 2002). The maximum production to biomass ratios, representing maximum weight-specific growth rates, were divided by the conversion efficiency ε to estimate maximum weight-specific grazing rates.

Results

The observed biomass and trait dynamics of phytoplankton, herbivorous and carnivorous zooplankton exhibit a pronounced seasonal succession and are highly repetitive among years (Fig. 5.3a-c). Rapid changes in biomasses and traits of all three trophic levels are interrelated and occur especially during spring and summer. In contrast to preliminary considerations (Fig. 5.1), the herbivore size (i.e. counter-defence) shifts prior to the increase of phytoplankton defence, which then goes along with a simultaneous shift in carnivore size (Fig. 5.3b, c). The food web model reproduces the observed dynamics and demonstrates that group-specific predation of carnivores may cause this reversed order of trait changes (Fig. 5.4a-c, 5.5). In the following, we first describe the observed biomass and trait dynamics. Subsequently, we link these patterns to our model results and present insights on mechanisms driving the order of trait changes.

Observations

Biomass dynamics

Starting from low biomasses at the beginning of the growing season, both phytoplankton and herbivore biomass strongly increase between week -12 and -6, i.e. 12 and 6 weeks before the clear-water phase (Fig. 5.3a). At the same time, the carnivores only slightly increase in biomass (Fig. 5.3a). Around week -6, the phytoplankton biomass reaches a maximum, corresponding to the spring bloom (169 $mgCm^{-3}$), while herbivorous biomass continues to increase (Fig. 5.3a). In early summer around week 0, the high herbivore biomass (185 $mgCm^{-3}$) causes a strong decrease and a distinct minimum of phytoplankton biomass (39 $mgCm^{-3}$), the so-called clear-water phase (CWP) (Fig. 5.3a). The carnivore biomass peaks prior to the CWP (67 $mgCm^{-3}$). After the CWP, the phytoplankton recovers and builds up a summer bloom around week 8 (144 $mgCm^{-3}$), while herbivore and carnivore biomasses are declining (Fig. 5.3a). In late summer and autumn, the previous biomass dynamics starting in spring repeat in a damped way and level off at the end of the growing season (Fig. 5.3a).

Trait dynamics

Shifts in the relative biomasses of functional groups imply changes in the mean trait values of the trophic levels; for example, an increasing amount of less-edible algae corresponds to an increasing mean longest linear dimension (LLD) of phytoplankton (Fig. 5.2). These two measures of the trait dynamics are generally in very good agreement for all three trophic levels (Fig. 5.3b, c). Minor deviations between them arise from intra-group variation (e.g. different less-edible phytoplankton species vary in their LLD) and

additional classification criteria of the functional groups (e.g. the shape of phytoplankton cells). In the following, we use mainly the relative biomasses of the functional groups to describe the trait dynamics, being directly comparable with the model results.

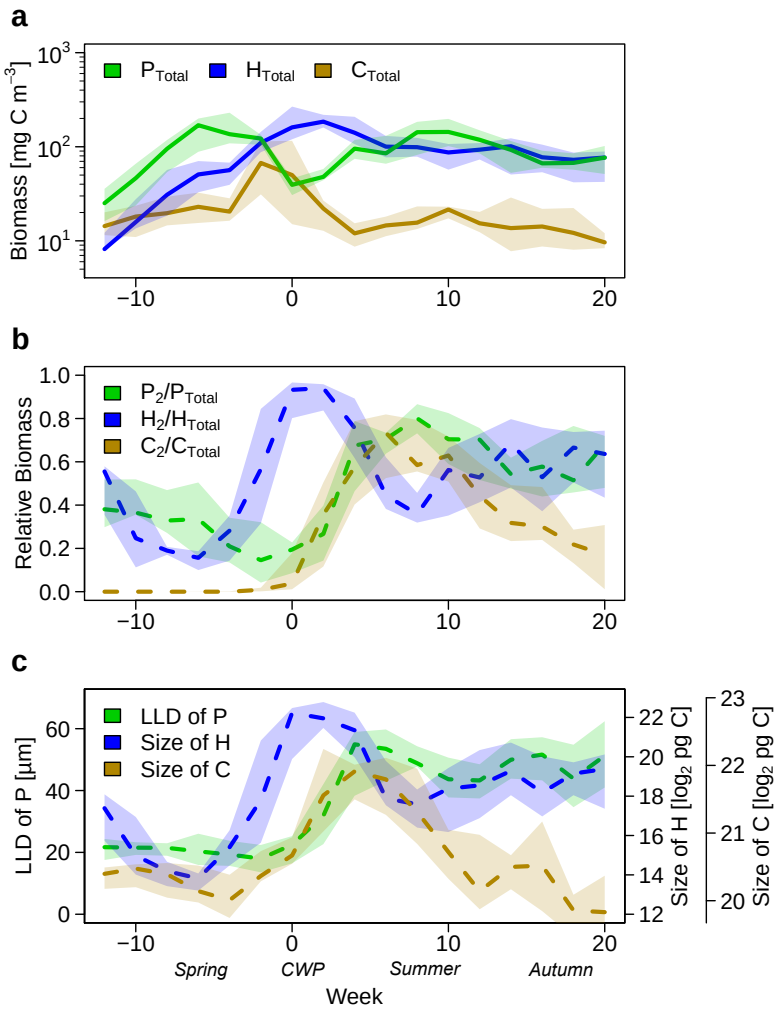

Figure 5.3: (a) Observed biomass and trait dynamics of the three trophic levels, displayed either (b) by the relative contribution of functional groups or (c) by the mean trait values. The data represent interannual medians from 1987 to 1996 in a biweekly resolution where the time dimension is scaled relative to the onset of the clear-water phase (CWP, week 0, at end of May or beginning of June). The shaded areas around the lines display the respective interquantile ranges. P_{Total} denotes the total phytoplankton biomass, H_{Total} the total herbivore biomass and C_{Total} the total carnivore biomass. Biomasses of less-edible phytoplankton, large herbivores and large carnivores are given by P_2, H_2 and C_2, respectively.

During spring, the phytoplankton community is increasingly dominated by fast-growing, well-edible species. The herbivore community is initially driven towards fast-grazing, small species (ciliates), being the preferred prey of small carnivores (cyclopoid copepods) (Fig. 5.2) which highly dominate the third trophic level at that time (Fig. 5.3b). Around week -6, the mean size of the herbivores starts to rapidly increase (more herbivorous cladocerans) during the phytoplankton spring bloom consisting mainly of

well-edible algae. The contribution of large herbivores, such as daphnids, increases from 16 % to 93 % (Fig. 5.3a, b). Subsequently, with the onset of the CWP (week 0), the amount of slowly growing less-edible species in the phytoplankton community strongly increases from 19 to 80 % (Fig. 5.3a, b). Simultaneously, the composition of the carnivore community shifts towards larger species (carnivorous cladocerans) from nearly 0 % to 73 % (Fig. 5.3b), which consume large herbivores (Fig. 5.2). In the further course of the growing season, the phytoplankton is dominated by less-edible species, while herbivore size first declines and then increases around the phytoplankton summer bloom (Fig. 5.3b). The contribution of large carnivores continuously decreases from week 6 onwards until the end of the growing season (Fig. 5.3b)

Food web model

Simulated biomass and trait dynamics

The simulated biomass and trait dynamics are generally in good agreement with the empirical data, especially during spring and summer (Fig. 5.3a,b, 5.4a,b). The model qualitatively reproduces the phytoplankton spring bloom during which the herbivore size (i.e. counter-defence for phytoplankton) rapidly increases after an initial decline. This shift in the herbivore community coincides with a peak of small carnivores, i.e. high C_{Total} and low C_2/C_{Total} (Fig. 5.3a,b, 5.4a,b), which preferentially feed on small herbivores (Fig. 5.2). The phytoplankton is well-edible at that time (low P_2/P_{Total}), suggesting that the increase of herbivore size is driven by the grazing impact of small carnivores rather than phytoplankton defence.

Similar to the data, simultaneous rapid increases of phytoplankton defence and carnivore size occur after that of herbivore size around the CWP, where herbivore biomass is maximal and phytoplankton biomass reaches a minimum (Fig. 5.3a,b, 5.4a,b). The model reveals that the grazing losses of well-edible phytoplankton are maximal at that time (Fig. 5.4c), driving the selection for phytoplankton defence (Fig. 5.4b). These grazing losses depend on the weight-specific grazing rates and the biomasses of the herbivores (Eq. 5.1). During the CWP, the high biomasses of large herbivores (Fig. 5.4a) compensate for their lower weight-specific grazing rates compared to small herbivores (Fig. 5.2) and impose maximal grazing losses on well-edible phytoplankton (Fig. 5.4c). This favours less-edible phytoplankton (Fig. 5.4b), even if it is partly consumed by large, counter-defended herbivores (Fig. 5.2). As observed, the herbivores then decrease in biomass at the time of low phytoplankton biomass, increased phytoplankton defence and higher biomasses of large carnivores (Fig. 5.3a,b, 5.4a,b), which graze on large herbivores (Fig. 5.2).

After the formation of the summer algal bloom, the observed and simulated dynamics

show slight differences. The relative biomasses of large herbivores and large carnivores tend to decrease in the data, while they remain high in the simulations (Fig. 5.3b, 5.4b). Generally, the model overestimates the relative biomasses of less-edible phytoplankton, large herbivores and large carnivores during summer and autumn (Fig. 5.3b, 5.4b).

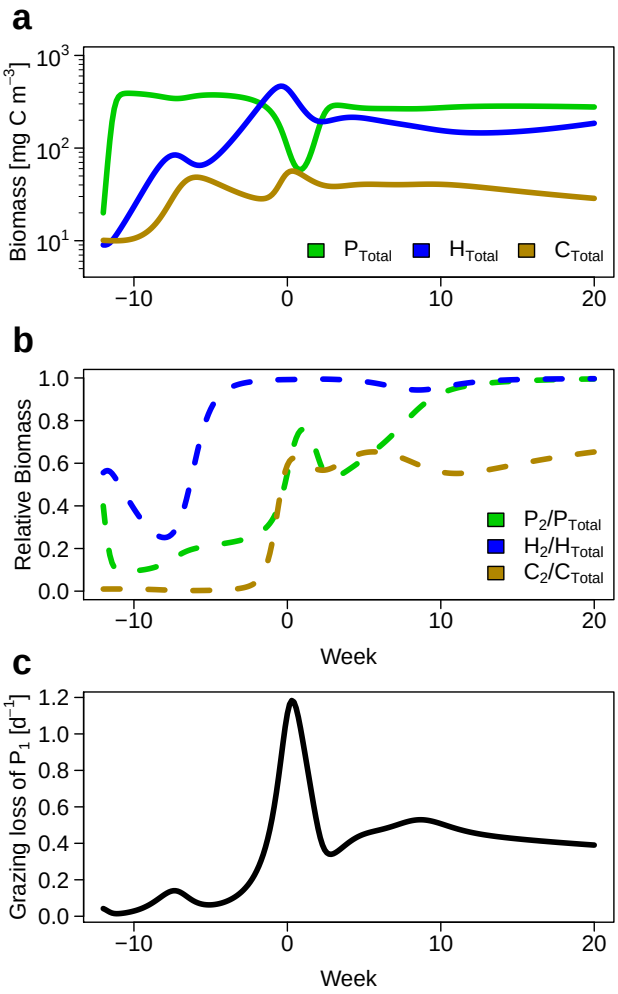

Figure 5.4: Numerical simulations of (a) biomass and (b) trait dynamics. (b) Trait changes are represented by changes in the biomass of a functional group (i.e. less-edible phytoplankton P_2, large herbivore H_2 and large carnivores C_2) relative to the total biomass of the respective trophic level (P_{Total}, H_{Total} or C_{Total}). Panel (c) displays the grazing-induced mortality rate of well-edible phytoplankton P_1. The increase of this grazing loss coincides with the increase of phytoplankton defence (P_2 / P_{Total}).

Testing the mechanism driving the order of trait changes

Here, we examine the mechanism underlying the pattern that herbivore size, i.e. counter-defence, increases prior to the increase of phytoplankton defence (Fig. 5.3b,c, 5.4b) which is reversed compared to predictions from bitrophic systems (Fig. 5.1). In Figure 5.5a-f, we vary the attack rate of small carnivores (a_1) in the model to test whether this reversed order is caused by a top-down control of small herbivores during spring, preventing

them from establishing a sufficiently high grazing pressure to induce trait changes in the phytoplankton.

Decreasing a_1 allows for a more pronounced biomass peak of small herbivores around week -7 (high H_{Total}, low H_2/H_{Total}) (Fig. 5.5c,d), due to the lower top-down control by carnivores, which hardly benefit from higher biomasses of their prey (Fig. 5.5e). In contrast to the observed dynamics (Fig. 5.3) and model simulations with the standard parametrization (Fig. 5.4), this initiates a pronounced decrease of phytoplankton biomass and an rapid increase in the relative biomass of less-edible algae (i.e. defence) already during spring (Fig. 5.5a,b), before the shift in herbivore size (i.e. counter-defence) occurs (Fig. 5.5d). The timing of the trait shifts in herbivores and carnivores hardly changes with the alternation of a_1 (Fig. 5.5d,f). Hence, at low attack rates (e.g. $a_1 = 10^{-2.5}$), the trait shifts at the three trophic levels occur consecutively starting with the first trophic level (Fig. 5.5b,d,f), as predicted by previous theory (Fig. 5.1).

Increasing a_1 does not alter the main pattern that herbivore counter-defence increases before phytoplankton defence and carnivore size but modifies the extent of trait changes (Fig. 5.5b,d,f).

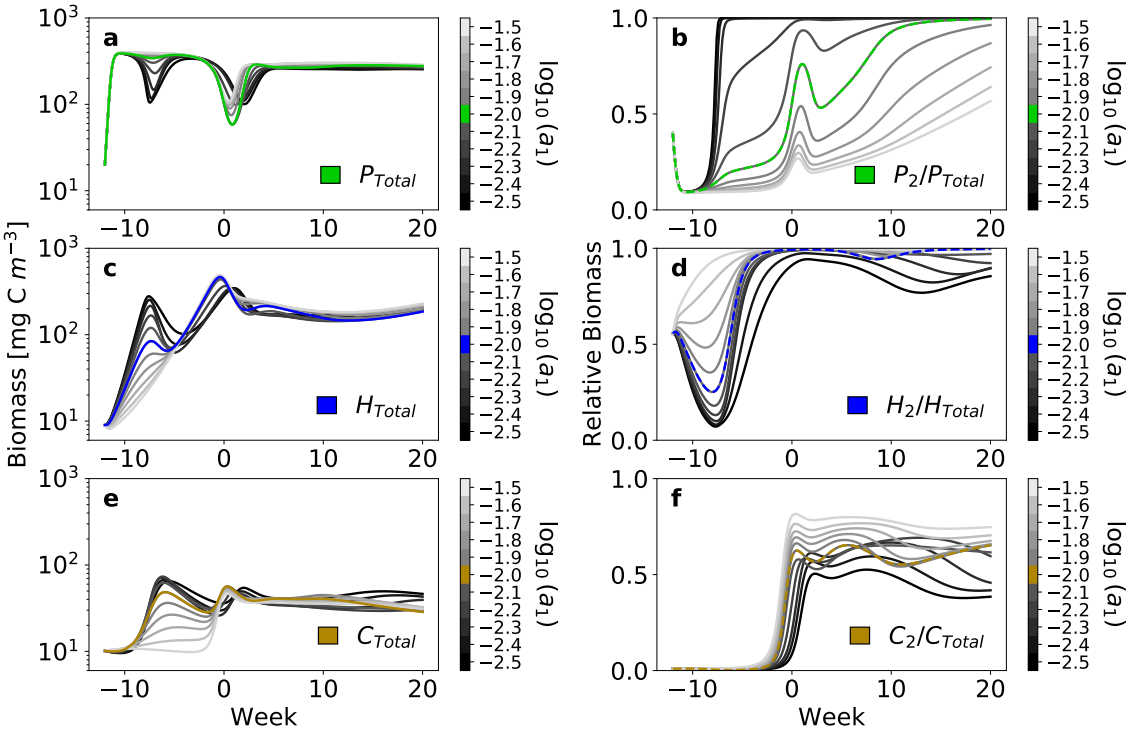

Figure 5.5: Sensitivity of biomass and trait dynamics of (a,b) phytoplankton, (c,d) herbivores and (e,f) carnivores to a varied attack rate of small carnivores (a_1). The greyish-black lines represent numerical simulations for different values of a_1, displayed at the bar. Coloured lines refer to the standard parametrization used before (i.e. $a_1 = 10^{-2}\,\frac{d^{-1}}{mgCm^{-3}}$).

Discussion

Our results provide first empirical evidence for rapid mutual biomass-trait adjustments among three trophic levels in a natural food web, using a long-term plankton data set of Lake Constance. The observed patterns of biomass and trait dynamics were highly repetitive among years (Fig. 5.3) and can be qualitatively reproduced by a simple food web model (Fig. 5.4a,b), which aggregates species into functional groups according to their trophic interactions (Fig. 5.2). The functional trait values of the different trophic levels changed in an unexpected order: First, herbivores became larger (late spring), implying the possibility to handle defended prey but at the cost of a lower maximum grazing rate, before phytoplankton became more defended (early summer). We explained this counter-intuitive pattern by group-specific predation of the third trophic level (Fig. 5.5). Small carnivores exert a top-down control on small herbivores during spring. This obviated the need for phytoplankton to defend until the herbivores increased in size, reducing predation by small carnivores. The resulting very high biomasses of the large herbivores during early summer imposed a high grazing pressure on phytoplankton (Fig. 5.4c) and made the algal defence then profitable, despite the lower weight-specific grazing rates of large herbivores compared to small ones. Hence, our results highlight that the understanding of trait dynamics in natural food webs demands insights on the interplay between traits and biomasses across multiple trophic levels.

Cyclopoid copepods, i.e. the small carnivores, are able to strongly graze on small herbivorous ciliates as they prevail in Lake Constance during spring (Wickham et al. 1995; Adrian and Schneider-Olt 1999). Indeed, the high production to biomass ratios of small herbivores during spring indicate high grazing losses (Gaedke et al. 2002). However, the long generation times of cyclopoids at low spring temperatures (Gillooly 2000) may hamper a fast numerical response imposing a strict top-down control on small herbivores (Tirok and Gaedke 2007). In addition to strong grazing by small carnivores, further potential explanations for the damped biomasses of small herbivores in spring, causing the reversed order of predator-prey adaptation, include: 1. Intra-guild predation: Large herbivores (*Daphnia* and *Eudiaptomus*) are able to prey also on small ciliates which was not implemented in the model but may contribute to the dampening of small herbivore growth (Wickham and Gilbert 1991; Adrian and Schneider-Olt 1999). 2. Interference competition: Ciliates and rotifers can be damaged by filter-feeding Daphnia when getting into their branchial chamber (Gilbert 1989; Wickham and Gilbert 1991). Furthermore, mutual intra-group adaptation within well-edible phytoplankton and ciliates may stabilizes the biomass dynamics in spring, preventing high peaks in ciliate biomasses and strong declines in well-edible phytoplankton (Tirok and Gaedke 2007, 2010). Independent of which of these mechanisms may dominate, we argue that small

herbivores bear an additional costs for their high grazing rates, that is, not only in respect to their reduced prey spectrum but also an ecological cost, emerging in the presence of predators, competitors or adaptation in prey (van Velzen and Etienne 2015).

The model captured the major characteristics of the observed biomass and trait dynamics well during spring and early summer, but overestimated the relative biomasses of less-edible algae, large herbivores and large carnivores from summer onwards. This implies that processes, which select towards the opposite trait directions (i.e. high edibility of algae, small size of herbivores and carnivores) during summer and autumn, are not sufficiently accounted for in the model. The following processes may be relevant: 1. Fish predation, especially on large carnivores (*Bythotrephes* and *Leptodora*) but also large herbivores (*Daphnia*), very likely contributes to the decrease of mean carnivore and herbivore size during summer (Luecke et al. 1990; Straile and Hälbich 2000). 2. The dormancy of small carnivores (cyclopoid copepods) during summer releases small herbivores from strong grazing pressure (Seebens et al. 2009) and thus may explain their higher observed biomasses. 3. Sedimentation causes an additional background mortality during summer stratification especially to less-edible phytoplankton, e.g. large diatoms (Sommer 1984), which may contribute to the observed higher amount of well-edible algae.

Apart from these processes, the considered model does not implement trait variation within the functional groups. For example, ciliates occurring in summer are known to reach larger sizes than ciliate species dominating in spring (Gaedke and Wickham 2004). Hence, they probably feed to some extent also on less-edible phytoplankton, providing a potential explanation why their observed biomasses exceed the model predictions. However, our model with its simple structure considering the trophic interactions among six fixed functional groups already reproduces the most striking patterns in the data, that is, the pronounced trait changes of three planktonic trophic levels during spring and early summer. Even excluding the implemented temperature sensitivity of the organisms only decreases the quantitative fit, but does not alter the overall pattern (Appendix D.2). Therefore, we argue that the observed order of trait changes and biomass peaks was largely driven by the considered trophic interactions (Fig. 5.2) and is robust against alternations in abiotic forcing. The low complexity of the model allows us to detect the reason why it reproduces the observed order of trait changes and to examine conditions reversing it (Fig. 5.5).

Changes in the traits at one trophic level may have cascading effects on the trait composition of adjacent trophic levels (Leibold et al. 1997). Kenitz et al. (2017) were the first to describe such interactions among trophic levels as a 'trophic trait cascade'. They considered two trophic levels, marine copepods feeding on protists, and found that the second trophic level adapted its feeding type in response to preceding changes in

motility of the first trophic level. In contrast, we found trait changes at the second trophic level which did not arise from adaptation to the trait composition of the first trophic level, but were driven by the third trophic level. Furthermore, we observed trait changes within the first trophic level (increase of defence) which do not match the altered herbivore trait composition (increased counter-defence). The increased defence of phytoplankton was likely caused by the higher biomass rather than the altered trait composition of herbivores, which escaped from carnivore predation by getting larger. This leads us to the concept of 'trophic biomass-trait cascades': Both biomass and trait changes can cascade through trophic levels and mutually affect each other, where trait alteration at one trophic level can be driven either by changes in traits or biomasses of adjacent trophic levels. Importantly, these changes in traits and biomasses can feedback on each other. Our results provide first empirical evidence for such biomass-trait feedbacks in a natural food web.

We conclude that, in multitrophic food webs, traits of intermediate trophic levels can be altered in an unintuitive way by superimposing effects of underlying and overlying trophic levels. This challenges the predictive power and applicability of models classically considering co-adaptation of only two trophic levels. In our study, the interaction of traits and biomasses among three trophic levels led to a reversed order of trait changes, being impossible to understand with a bitrophic view. Such reversed trait dynamics probably emerge in many natural food webs and may lead to misleading conclusions on how trait adaptation proceeds. This asks for multitrophic, trait-based approaches enhancing the understandability and predictability of trait changes in nature.

Acknowledgements

Many thanks to Alice Boit for constructive comments on an earlier version of the manuscript. We thank Toni Klauschies for fruitful discussions on the results. This research was funded by the German Research Foundation (DFG, GA 401/26-1/2).

Bibliography 5

Abrams, P. A. (2000). The evolution of predator-prey interactions: Theory and Evidence. *Annual Review of Ecology and Systematics*, 31(1):79–105.

Abrams, P. A. and Vos, M. (2003). Adaptation, density dependence and the responses of trophic level abundances to mortality. *Evolutionary Ecology Research*, 5:1113–1132.

Adrian, R. and Schneider-Olt, B. (1999). Top-down effects of crustacean zooplankton on pelagic microorganisms in a mesotrophic lake. *Journal of Plankton Research*, 21(11):2175–2190.

Boit, A. and Gaedke, U. (2014). Benchmarking successional progress in a quantitative food web. *PLoS ONE*, 9(2):e90404.

Boukal, D. S. (2014). Trait- and size-based descriptions of trophic links in freshwater food webs: current status and perspectives. *Journal of Limnology*, 73(s1):171–185.

Brodie, E., Formanowicz, D., and Brodie, E. (1991). Predator avoidance and antipredator mechanisms: distinct pathways to survival. *Ethology Ecology & Evolution*, 3(1):73–77.

Brodie, E. D. I. and Brodie, E. D. J. (1999). Predator – Prey Arms Races: Asymmeterical selection on predators and prey may be reduced when prey are dangerous. *BioScience*, 49(July):557–568.

Bruggeman, J. (2011). A phylogenetic approach to the estimation of phytoplankton traits. *Journal of Phycology*, 47(1):52–65.

Burns, C. W. (1969). Relation between filtering rate, temperature and body size in four species of daphnia. *Limnology and Oceanography*, 14(5):693–700.

Cortez, M. H. and Weitz, J. S. (2014). Coevolution can reverse predator-prey cycles. *Proceedings of the National Academy of Sciences of the United States of America*, 111(20):7486–91.

Dawkins, R. and Krebs, J. R. (1979). Arms races between and within species. *Proceedings of the Royal Society B: Biological Sciences*, 205:489–511.

de Castro, F. and Gaedke, U. (2008). The metabolism of lake plankton does not support the metabolic theory of ecology. *Oikos*, 117(8):1218–1226.

Fussmann, G. F., Loreau, M., and Abrams, P. A. (2007). Eco-evolutionary dynamics of communities and ecosystems. *Functional Ecology*, 21(3):465–477.

Gaedke, U. (1992). The size distribution of plankton biomass in a large lake and its seasonal variability. *Limnology and Oceanography*, 37(6):1202–1220.

Gaedke, U., Hochstädter, S., and Straile, D. (2002). Interplay between energy limitation and nutritional deficiency: Empirical data and food web models. *Ecological Monographs*, 72(2):251–270.

Gaedke, U. and Wickham, S. A. (2004). Ciliate dynamics in response to changing biotic and abiotic conditions in a large, deep lake (Lake Constance). *Aquatic Ecology*, 34:247–261.

Gilbert, J. J. (1989). The effect of Daphnia interference on a natural rotifer and ciliate community: Short-term bottle experiments. *Limnology and Oceanography*, 34(3):606–617.

Gillooly, J. F. (2000). Effect of body size and temperature on generation time in zooplankton. *Journal of Plankton Research*, 22(2):241–251.

Kenitz, K. M., Visser, A. W., Mariani, P., and Andersen, K. H. (2017). Seasonal succession in zooplankton feeding traits reveals trophic trait coupling. *Limnology and Oceanography*, 62(3):1184–1197.

Klauschies, T., Vasseur, D. A., and Gaedke, U. (2016). Trait adaptation promotes species coexistence in diverse predator and prey communities. *Ecology and Evolution*, 6(12):4141–4159.

Knisely, K. and Geller, W. (1986). Selective feeding of four zooplankton species on natural lake phytoplankton. *Oecologia*, 69(1):86–94.

Leibold, M. A., Chase, J. M., Shurin, J. B., and Downing, A. L. (1997). Species turnover and the regulation of trophic structure. *Annual Review of Ecology and Systematics*, 28:467–494.

Luecke, C., Vanni, M. J., Magnuson, J. J., Kitchell, J. F., and Jacobson, P. T. (1990). Seasonal regulation of Daphnia populations by planktivorous fish: Implications for the spring clear-water phase. *Limnology and Oceanography*, 35(8):1718–1733.

Menden-Deuer, S. and Lessard, E. J. (2000). Carbon to volume relationships for dinoflagellates, diatoms, and other protist plankton. *Limnology and Oceanography*, 45(3):569–579.

Post, D. M. and Palkovacs, E. P. (2009). Eco-evolutionary feedbacks in community and ecosystem ecology: interactions between the ecological theatre and the evolutionary play. *Philosophical Transactions of the Royal Society B: Biological Sciences*, 364(1523):1629–1640.

Schmitz, O. J., Krivan, V., and Ovadia, O. (2004). Trophic cascades: the primacy of trait-mediated indirect interactions. *Ecology Letters*, 7(2):153–163.

Seebens, H., Einsle, U., and Straile, D. (2009). Copepod life cycle adaptations and success in response to phytoplankton spring bloom phenology. *Global Change Biology*, 15(6):1394–1404.

Sherman, E., Moore, J. K., Primeau, F., and Tanouye, D. (2016). Temperature influence on phytoplankton community growth rates. *Global Biogeochemical Cycles*, 30(4):550–559.

Sommer, U. (1984). Sedimentation of principal phytoplankton species in Lake Constance. *Journal of Plankton Research*, 6(1):1–15.

Sommer, U., Adrian, R., De Senerpont Domis, L., Elser, J. J., Gaedke, U., Ibelings, B., Jeppesen, E., Lürling, M., Molinero, J. C., Mooij, W. M., van Donk, E., and Winder, M. (2012). Beyond the Plankton Ecology Group (PEG) Model: Mechanisms Driving Plankton Succession. *Annual Review of Ecology, Evolution, and Systematics*, 43(1):429–448.

Straile, D. (1997). Gross growth efficiencies of protozoan and metazoan zooplankton and their dependence on food concentration, predator-prey weight ratio, and taxonomic group. *Limnology and Oceanography*, 42(6):1375–1385.

Straile, D. and Hälbich, A. (2000). Life History and Multiple Antipredator Defenses of an Invertebrate Pelagic Predator, Bythotrephes longimanus. *Ecology*, 81(1):150.

Tien, R. J. and Ellner, S. P. (2012). Variable cost of prey defense and coevolution in predator-prey systems. *Ecological Monographs*, 82(4):491–504.

Tirok, K. and Gaedke, U. (2006). Spring weather determines the relative importance of ciliates, rotifers and crustaceans for the initiation of the clear-water phase in a large, deep lake. *Journal of Plankton Research*, 28(4):361–373.

Tirok, K. and Gaedke, U. (2007). Regulation of planktonic ciliate dynamics and functional composition during spring in Lake Constance. *Aquatic Microbial Ecology*, 49(1):87–100.

Tirok, K. and Gaedke, U. (2010). Internally driven alternation of functional traits in a multispecies predator–prey system. *Ecology*, 91(6):1748–1762.

van Velzen, E. and Etienne, R. S. (2015). The importance of ecological costs for the evolution of plant defense against herbivory. *Journal of Theoretical Biology*, 372:89–99.

Velzen, E. V. and Gaedke, U. (2017). Disentangling eco-evolutionary dynamics of predator-prey coevolution: the case of antiphase cycles. *Scientific Reports*, 7(1):17125.

Wickham, S. A. and Gilbert, J. J. (1991). Relative vulnerabilities of natural rotifer and ciliate communities to cladocerans: laboratory and field experiments. *Freshwater Biology*, 26:77–86.

Wickham, S. A., Limnologie, M.-p.-i., and Plon, D. (1995). Cyclops predation on ciliates: species-specific differences and functional responses. *Journal of Plankton Research*, 17(8):1633–1646.

Wirtz, K.-W. and Eckhardt, B. (1996). Effective variables in ecosystem models with an application to phytoplankton succession. *Ecological Modelling*, 92(1):33–53.

Yamamichi, M. and Ellner, S. P. (2016). Antagonistic coevolution between quantitative and mendelian traits. *Proceedings of the Royal Society B: Biological Sciences*, 283:20152926.

6 General discussion

In Chapters 2-5, I examined the influence of trade-offs on coexistence, trait adaptation and population dynamics in food webs. I showed that specific characteristics of a trade-off, like its type or its shape, are decisive for the composition and dynamics of food webs, and that trade-offs at multiple trophic levels govern the trait adaptation in complex food webs (for an overview of the main results, see Box 6.1). In this general discussion, I synthesize the obtained insights and extrapolate them to a broader global context.

Central to all thesis results (Box 6.1) was the analysis of which trait combinations from a given trait variation confined by trade-offs are positively selected in the community, that is, having maximal fitness. Such selection processes result in trait adaptation within communities, form the basis of coexistence (e.g. by disruptive selection) and impact population dynamics (e.g. cycles occur under alternating selection). The strategies of maximal fitness are defined by the characteristics of the underlying trade-off and the abiotic or biotic environment. In this thesis, the main focus was on selection within prey communities (Chapter 2-4, Chapter 5 considered additionally selection in predator communities). The considered, fitness-relevant environmental factors of a prey species were the concentration of its resource, competing prey species, biomasses and trait compositions of higher trophic levels, and abiotic factors influencing non-grazing mortality (e.g. the dilution rate or vertical mixing).

In the further course of this general discussion, I integrate general principles and develop theory on how the interplay of trade-offs and such environmental factors shape the fitness landscape and thus the composition and dynamics of food webs. At first, I explore the role of trade-offs as mediators of trophic biomass-trait cascades, by considering the time scale of trait adaptation and the biotic environmental setting driving trait changes. Secondly, I develop a general graphical theory on coexistence based on trade-offs, highlighting the importance of feedbacks among species and their environment which shape the fitness landscape. Here, I extend the theory also to trade-offs of higher dimensionality. In a third step, I discuss the potential interplay of intra- and interspecific trade-offs within this theoreticcal framework. Finally, I take a management-oriented perspective and upscale to broad global changes which affect the fitnss landscape of communities and may change their composition depending on the trade-offs of the species.

Box 6.1: Overview on main results

Chapter 2 - *Trade-off types, prey coexistence and population dynamics:*
Post-attack defence against predation (e.g. spine formation) promoted prey coexistence and stationary dynamics compared to pre-attack defences (e.g. hiding). Defence costs with respect to the half-saturation constant for resource uptake allowed for more coexistence and destabilized dynamics compared to costs regarding the maximum growth rate.

Chapter 3 - *Trade-off shapes, fitness and coexistence:*
A certain shape of the trade-off may imply different coexistence outcomes depending on which traits trade off and how they relate to fitness. This chapter provides an approach on how to predict these outcomes.

Chapter 4 - *Testing theory on trade-off shapes with phytoplankton field data:*
The theory was confirmed for a concave trade-off between defence and growth in phytoplankton. The concavity of the trade-off in combination with the seasonally changing grazing pressure (vertical mixing and nutrient depletion) governed the observed alternating dominance of phytoplankton species with different intermediate defence levels. The maintenance of trait variation in phytoplankton was explained with low fitness differences along the trade-off curve and changing environmental conditions promoting different species over time.

Chapter 5 - *Trade-offs at multiple trophic levels and food web dynamics:*
Biomass-trait dynamics of the three trophic levels were interrelated, resulting in trait dynamics being reversed compared to predictions from bitrophic systems: Counter-defence of herbivores increased before the rise of phytoplankton defence, despite its costs with respect to the grazing rate. This pattern became clear in the light of a trade-off-mediated trophic cascade driven by selective feeding of carnivores on herbivores.

6.1 Trade-offs as mediators of trophic cascades

Classic theory on trophic cascades predicts that an increased biomass of carnivores reduces the herbivore biomass and thus indirectly increases the biomass of primary producers (red arrows in Fig. 6.1) (Hairston et al. 1960; Paine 1980; Carpenter et al. 1985). However, when the trait composition of a trophic level is dynamic due to species sorting, evolution or phenotypic plasticity, other indirect effects of carnivores on primary producers are possible (Leibold et al. 1997; Werner and Peacor 2003; Ousterhout et al. 2018). As an example, I consider dynamic traits of herbivores, that is, defence against carnivores and grazing rate for primary producers, being linked via a predation risk-foraging trade-off (Schmitz et al. 2004). In this case, an increased carnivore biomass can drive selection towards higher herbivore defence values. Increased defence comes at the cost of a lower grazing rate, reducing the grazing pressure on primary producers (green arrows in Fig. 6.1). Such an indirect effect of carnivores on primary producers represents a trophic biomass-trait cascade which is mediated by the trade-off between defence and grazing rate.

The relative importance of the two described indirect effects (red and green arrows in Fig. 6.1) depends on the relative speed of changes in biomasses and traits (Schmitz et al. 2004). In case of a very low speed of trait changes (e.g via de novo mutations), biomass-biomass interactions among the trophic levels may have already altered the conditions in a way obviating the need of trait changes (e.g. declining carnivore biomass after reduction of herbivore biomass supersedes selection towards defence). In contrast, when trait changes proceed fast compared to biomass changes (e.g. by behavioural changes), they may hamper biomass-biomass interactions. For example, if a high carnivore biomass causes a fast increase of herbivore defence, this dampens the strength of trophic interaction between herbivores and carnivores (Fig. 6.1), and thus may prevent a decrease of herbivore biomass (Diehl et al. 2000). If changes in biomasses and traits act on similar time scales (e.g. trait adaptation by sorting of species or genotypes), both pathways of indirect effects may equally contribute.

The impact of the trait-mediated indirect effect (green arrows in Fig. 6.1) depends also on the fitness-determining environment and the shape of the trade-off, describing how costly the defence is (Creel and Christianson 2008). For example, high defence costs may hamper the selection for high defence in environments of low primary producer biomasses where the herbivore grazing performance needs to be high for survival and defence is of minor importance. Hence, the selection on traits in herbivores is driven from both sides (consumption of plants and grazing losses by carnivores), implying that this trait-mediated indirect effect (green arrows in Fig. 6.1) is regulated by the interplay between bottom-up and top-down control (Werner and Peacor 2003).

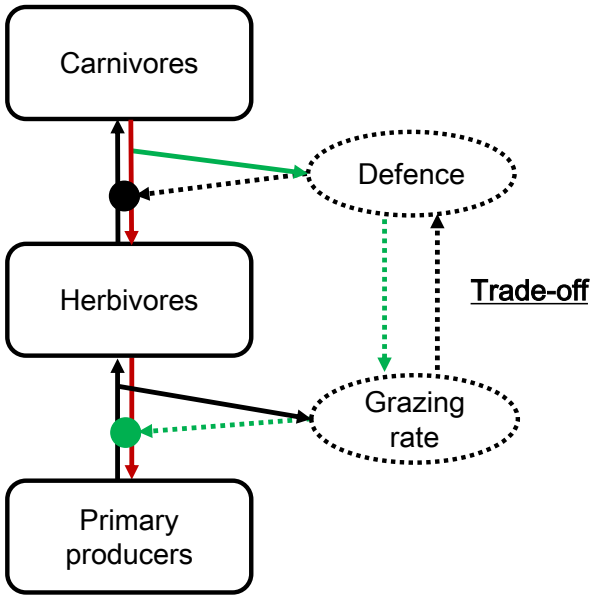

Figure 6.1: Direct effects among biomasses and traits in a tritrophic food web. Solid boxes represent biomasses and dashed ellipses herbivore traits which are interrelated in a trade-off. Solid arrows display direct effects driven by biomasses and dashed arrows illustrate effects driven by traits. The traits modulate the trophic interactions as indicated by the circles. In case of increased carnivore biomass, red-marked arrows show the classical trophic biomass cascade, i.e. carnivores reduce herbivore biomass which leads to higher biomass of primary producers. The set of green arrows denotes a trophic biomass-trait cascade, that is, an indirect effect of higher carnivore biomass on primary producer biomass via changes in herbivore traits. A higher carnivore biomass leads to an increased herbivore defence, which comes at the cost of a lower herbivore grazing rate and thus reduces the grazing pressure on primary producers.

6.2 Towards a graphical theory on trade-off-based coexistence

In this section, I generalize the theory on trade-off-based coexistence, introduced in Chapter 2, 3 and 4, with an extension of a graphical approach introduced by Levins (1962) in an evolutionary context. I focus mainly on two-dimensional trade-offs but explain also how to transfer the theory to multidimensional trade-offs.

The shape of the trade-off curve in combination with the fitness landscape determines coexistence of species with different strategies (de Mazancourt and Dieckmann 2004; Rueffler et al. 2006), for example, the co-occurrence of different breeding strategies, either producing few large or many small offsprings, in chondrichthyes and teleosts, respectively (Sibly et al. 2018). In a two-dimensional trait space, the fitness landscape can be represented by fitness isoclines, connecting trait combinations of equal fitness (Fig. 6.2) (Levins 1962; Sibly and Calow 1983; Rueffler et al. 2004). The fitness is defined here as the net per capita growth rate of a species with the given trait combination

(Metz et al. 1992). While constraints on the individual level (e.g. resource allocation) fix the shape of the trade-off curve, the shape of the fitness isoclines depends on the biotic and abiotic environment (Holloway et al. 1990; Geritz et al. 1998; Visser et al. 2008). For example, in the trait space spanned by defence and maximum growth rate, the slope of fitness isoclines changes with altered grazing pressure (Fig. 6.2). The trait combinations along the trade-off curve that reach the highest fitness isocline represent fitness maxima (Fig. 6.2). Species with such trait combinations are positively selected (Rueffler et al. 2004). Stably coexisting species must lie, in the long-term average, on the same maximally attainable fitness isocline, and grow until they both reach a mean fitness value of zero given negative density-dependence (i.e. the system reaches an attractor). Species below that fitness isocline are outcompeted in the long term.

For linear fitness isoclines, the graphical theory (Fig. 6.2) predicts the following:

1. Convex trade-off curves promote species with extreme trait combinations at the end of the trade-off curve (e.g. undefended and highly defended prey). Depending on the slope of the fitness isoclines, either only one of these extremes survives or both coexist (Fig. 6.2). Hence, according to Chapter 3, such a trade-off is extreme-favouring.

2. For linear trade-offs, either only one species with an extreme trait combination survives or many species along the trade-off curve are sustained (Fig. 6.2). These species have equal fitness for a slope of the fitness isoclines equal to that of the trade-off curve (Fig. 6.2).

3. Concave trade-offs allow only for one fitness maximum at an intermediate trait combination (where the fitness isocline is a tangent to the trade-off curve). Depending on the environment, i.e. the fitness landscape, species with different intermediate trait combinations along the trade-off curve survive (Fig. 6.2). Such a trade-off is called intermediate-favouring (Chapter 3).

Under constant environmental conditions (e.g. constant grazin pressure) implying a constant slope of the fitness isoclines, a concave trade-off leads to the lowest possible functional diversity, as the expected maximum number of fitness maxima is one (Fig. 6.2). However, such a concave trade-off may lead to the highest functional diversity, given external forcing (e.g. temperature dynamics altering grazing rate of predators) which continuously alters the slope of fitness isoclines: For each slope of fitness isoclines at a different point in time, a different trait combination has maximal fitness (Fig. 6.2) implying a potential for multiple temporal niches. These environmental changes needs to be frequent enough to prevent competitive exclusion (Huston 1979). In contrast, for convex and linear trade-offs, externally-forced changes in the environment mainly switches the fitness maxima from one extreme trait combination to the other (Fig. 6.2).

These insights can be transferred to a spatial context. Considering a spatial gradient of an environmental factor (e.g. nutrient concentration), the α-diversity, i.e. diversity at a local patch, may be highest for a convex or linear trade-off. However, the β-diversity, describing the trait variation in the whole meta-community, may be higher for concave trade-offs because at each patch a species with a different trait combination is of maximal fitness, matching the local conditions (given the spatially changing slope of the fitness isoclines).

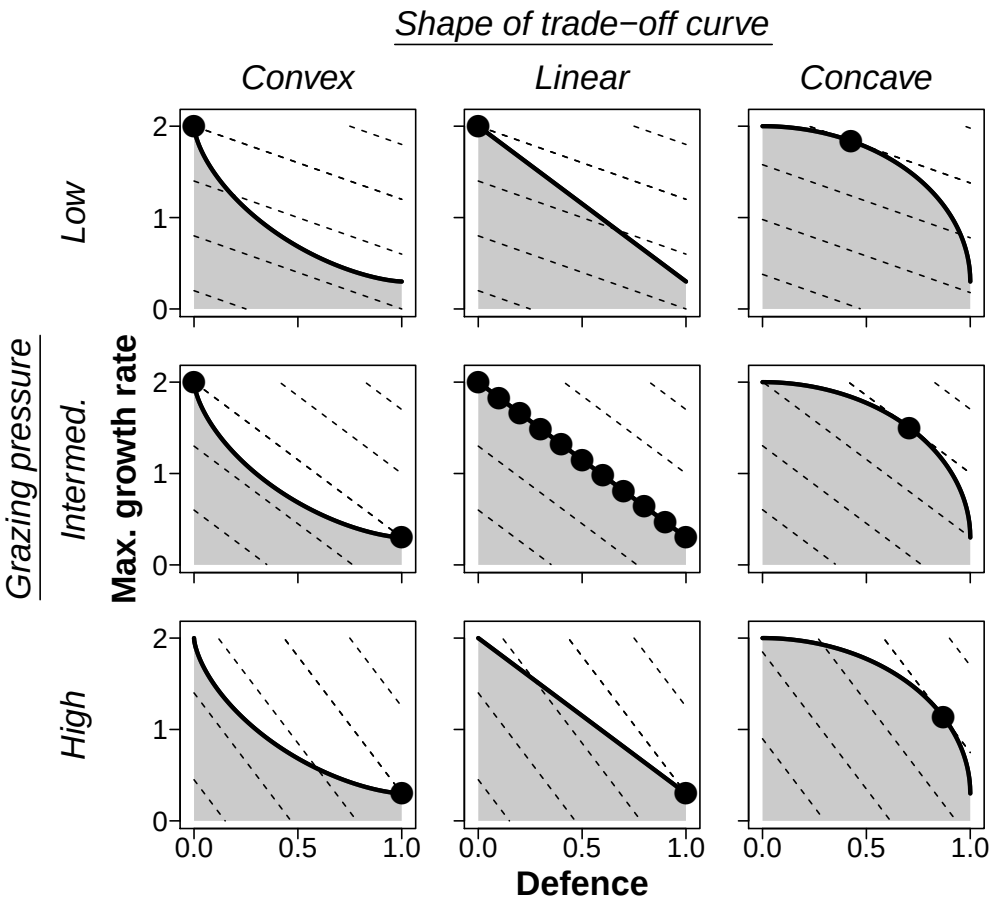

Figure 6.2: Graphical theory on fitness maxima, survival and coexistence of species depending on the shape of the trade-off and the environment which determines the fitness landscape. The shown example considers a trade-off between defence and maximum growth rate (d^{-1}) in a prey community with grazing pressure as a biotic environmental factor. The trade-off curve (thick solid line) represents the boundary of the set of feasible trait combinations (grey area) and may be convex, linear or concave. The fitness landscape is shaped by the grazing pressure (low, intermediate or high), resulting in different slopes of the fitness isoclines (dashed lines). The trait combinations reaching the highest fitness isocline are fitness maxima (dots). If two or more trait combinations are of maximal fitness in the long-term, the respective species with these trait combinations coexist, otherwise only one species survives.

Without changes in the environment, it seems unlikely that a fitness isocline exactly crosses both extreme trait combinations at the end of the trade-off curve, which is the

necessary condition for coexistence in case of convex or linear trade-off curves (see intermediate grazing pressure in Fig. 6.2). However, typically the organisms shape the environment by themselves. For example, an increase of undefended prey leads to high predator biomasses. The resulting higher grazing pressure alters the slope of the fitness isoclines and promotes the defended prey. Dominance of the defended prey, in turn, causes a decrease of predator biomass favouring the undefended prey and so forth.

To demonstrate how such dynamic interactions between species and their environment affect coexistence, I show numerical simulations for the predator-prey model presented in Chapter 2. This system allows for feedbacks among the different prey species A_i, nutrients N and the predator P. Instead of only two prey species, I consider 11 prey species facing a trade-off between defence d and maximum growth rate r. The trait combinations of these species are located on the trade-off curve, equally spaced along the defence axis between 0 (undefended) and 1 (completely defended). Defence is expressed in terms of digestion resistance.

First, I derive the equation describing the fitness isoclines. It should be mentioned here that, in contrast to Chapter 2 (Appendix A.1), d represents the defence value, that is, the probability of not being digested instead of the probability of being digested. The per capita growth rate of a prey species A_i is then given by

$$\frac{1}{A_i}\frac{dA_i}{dt} = r_i \frac{N}{K+N} - \frac{a(1-d_i)P}{1+aT\sum_{i=1}^{n} A_i} - \delta \,. \tag{6.1}$$

Along a fitness isocline, species with respective trait combinations have the same fitness W, that is, $W = \frac{1}{A_i}\frac{dA_i}{dt}$ for all species i on the fitness isocline. Solving for r_i, the relationship between the values of d_i and r_i leading to the same fitness W can be described by

$$r_i = \left[(1-d_i)\frac{aP}{1+aT\sum_{i=1}^{n} A_i} + \delta + W\right]\frac{K+N}{N} \,. \tag{6.2}$$

According to Eq. 6.2, the fitness isoclines are always linear. Different fitness isoclines (i.e. different W) have the same slope but differ in their intercept (Eq. 6.2). Based on Eq. 6.2, we can calculate the fitness isoclines under different environmental conditions, that is, different values of of P, A_i and N, determining their slope and intercept (Eq. 6.2).

The model simulations show that, for a convex trade-off between d_i and r_i, the two extreme species (undefended and completely defended prey) coexist in the long-term in a steady state and outcompete all intermediate species (Fig. 6.3a). The transient dynamics reveal how the different prey species alter the environment and thus the fitness landscape. High densities of the undefended prey lead to a high peak of the predator density (day 27) allowing for nutrient accumulation in the environment (Fig. 6.3a). This causes the

fitness isoclines to be more perpendicular to the defence axis (i.e. defence is most decisive for fitness) and leads to a temporal fitness maximum of the defended prey (Fig. 6.3b). In turn, the resulting high densities of the defended prey cause low predator densities and deplete the pool of nutrients (day 36, Fig. 6.3a). This leads to fitness isoclines being more perpendicular to the *r*-axis (i.e. defence is less decisive for fitness) and a temporal fitness maximum of the undefended prey (Fig. 6.3c). The described changes of the fitness isoclines (Fig. 6.3b, c) driven by one species promote the fitness of the other species, respectively. These species-driven changes of the fitness isoclines, which promote stable coexistence as the dominance of one species implies a fitness advantage for the other species, represent a graphical surrogate for stabilizing mechanisms, described in Chesson's coexistence theory (Chesson 2000).

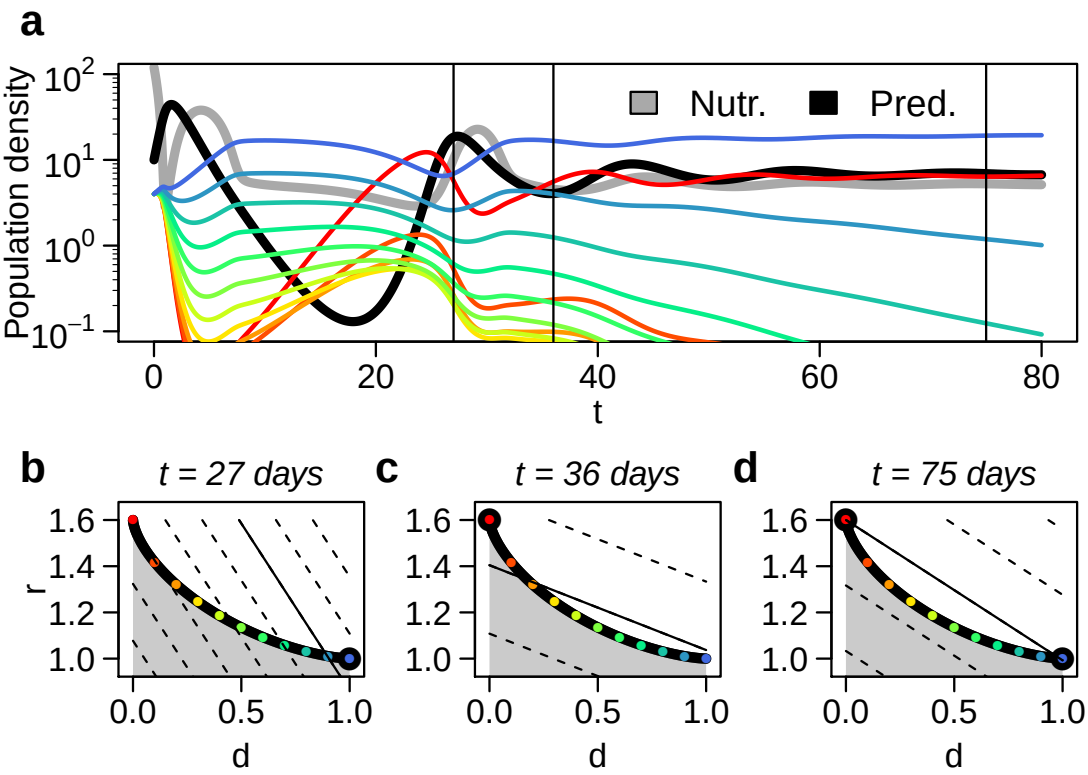

Figure 6.3: (a) Simulated population dynamics of nutrients (grey line), eleven prey species (coloured lines) and the predator (black line) for a convex trade-off between defence d and maximum growth rate r. (b-d) Different fitness maxima (black dots) at different points in time, marked by vertical lines in (a). Coloured dots mark trait combinations of the prey species whose dynamics are plotted in (a). The trade-off curve (thick solid line), which limits the feasible trait space (grey area), remains stationary. The slope of the fitness isoclines (thin dashed and solid lines) changes depending on the nutrient concentration and biomasses of prey and predator at the considered time (Eq. 6.2), resulting in different fitness maxima. The thin solid line represents the fitness isocline where fitness, i.e. the net pre capita growth rate (d^{-1}), is zero. Fitness isoclines below and above that one have negative or positive values, respectively. The fitness difference from one fitness isocline to the next is $0.2\,d^{-1}$.

In the further course of the simulations, damped oscillations occur in the population

dynamics (Fig. 6.3a). After these damped oscillations, the fitness isoclines finally stay at a slope where the fitness isocline of maximal attainable fitness exactly crosses the two extreme trait combinations (Fig. 6.3d, full asymptotic dynamics not shown). The maximum fitness is zero and thus the population densities stay constant (Fig. 6.3a,d). However, even under continued cycling of the populations (e.g. due to enrichment of the system), these prey species would coexist because, even if they temporally have different fitness, the mean long-term fitness is equal. Such coexistence is called stable coexistence (Chesson 2000), implying that even after strong reduction of a species, it recovers due to the described feedbacks between the species and its environment (stabilizing mechanisms).

However, the ability of these feedbacks or stabilizing mechanisms to promote coexistence has limits. For example, if the natural mortality rate of the predator (here dilution rate) is very high, even high densities of the undefended prey cannot supply sufficient predator densities that are necessary for a positive fitness of the defended prey. As a consequence, only the undefended prey survives even for convex trade-off curves with internally driven environmental changes.

The previously described stabilizing mechanisms are also observed for linear trade-offs, but here they lead to the coexistence of all eleven prey species (Fig. 6.4a-d). However, in contrast to the coexistence of only the undefended prey and the completely defended prey for a convex trade-off (Fig. 6.3a-d), this coexistence is not stable for all species. For example, a strong reduction of a defended prey would lead to higher biomasses of a similarly defended prey, which keeps the fitness isoclines in the same slope. Thus, the reduced defended prey has no advantage of being rare. It cannot increase again and stays at low densities. Such coexistence is called neutral or unstable coexistence, where the long-term biomass distribution of the species depends on their initial biomasses and is highly sensitive to stochasticity (Chesson 2000; Hubbell 2005; Purves and Turnbull 2010).

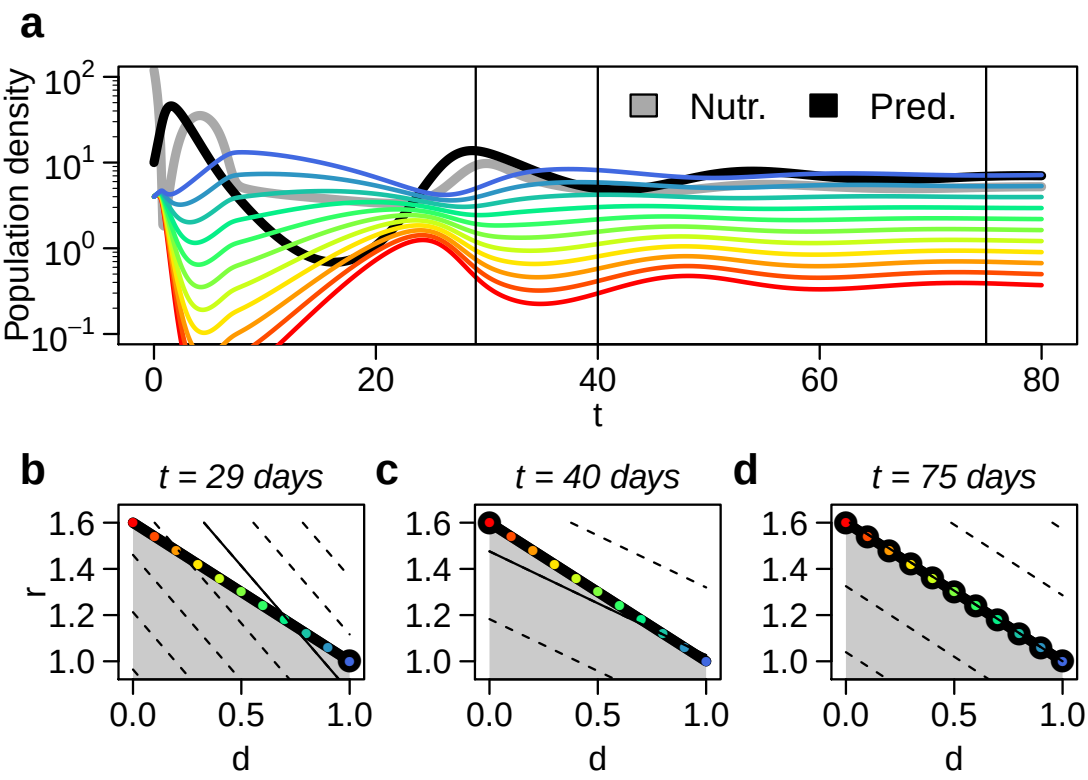

Figure 6.4: Same as in Fig. 6.3 but for a linear trade-off curve.

For concave trade-offs, I predicted earlier that only one species with intermediate trait combinations would survive (Fig. 6.2). However, in the numerical simulations, two similar prey species coexist, based on low stabilizing effects, i.e. one prey species is slightly more defended and benefits from high predator densities while the other functions as a fast-growing, undefended one (Fig. 6.5a-d). This coexistence is not evolutionary stable (Edwards et al. 2018). It vanishes when the full set of trait combinations would occur in the community, implying that also the trait combination of maximal fitness would be present, where the maximal attainable fitness isocline is tangent to the concave trade-off curve (a point on the trade-off curve between the two coexisting strategies). However, a species with exactly that trait combination may not occur under natural conditions, suggesting that this species coexistence for concave trade-offs may be relevant in nature as well. Nevertheless, the coexisting species are very similar in their trait values (Fig. 6.5d) implying a low functional diversity.

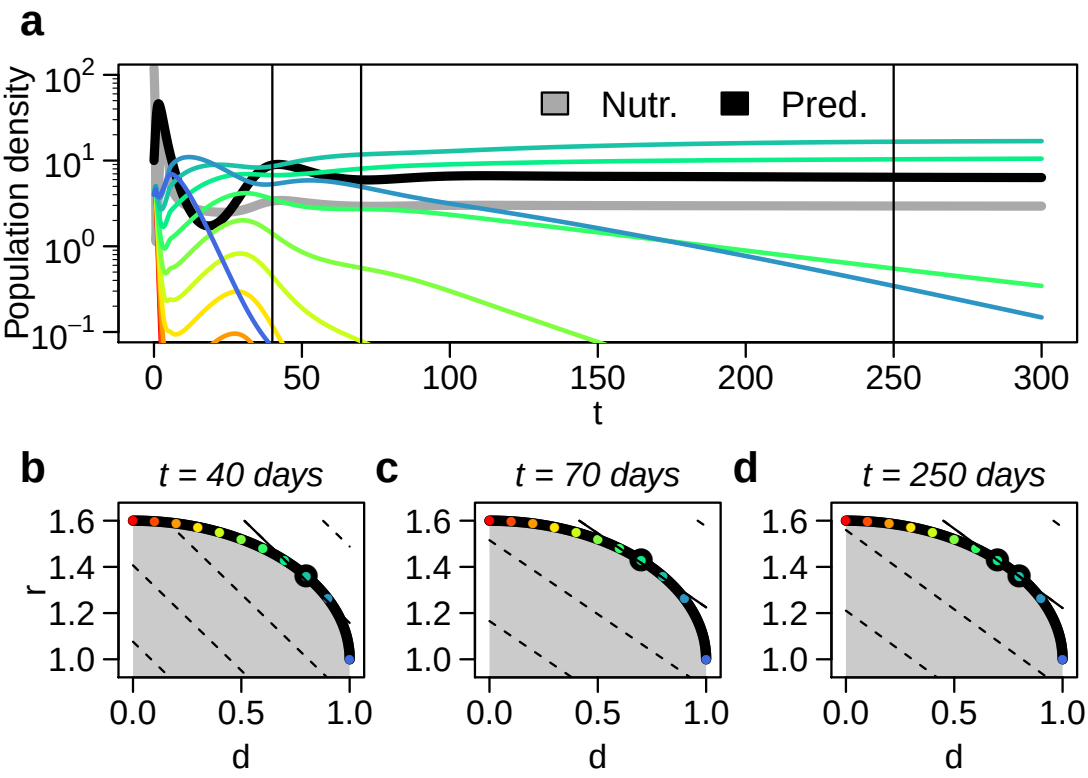

Figure 6.5: Same as in Fig. 6.3 but for a convex trade-off curve.

The coexistence found for example for the convex trade-off curve (Fig. 6.3a-d) was relying on feedbacks among the species and their abiotic and biotic environment (nutrients, predator). However, predator generation times (e.g. fish) may strongly differ from the generation times of the prey (e.g. zooplankton), which may prevent such feedbacks and changes in the fitness landscape. To illustrate the consequences of lacking feedbacks, I ran the simulations for the convex trade-off again with constant predator densities (Fig. 6.6a). The fitness isoclines stay at a rather constant slope over time (Fig. 6.6b-d). The undefended prey is always of maximal fitness (Fig. 6.6b-d) and outcompetes the others (Fig. 6.6a). Therefore, the potential for feedbacks between species and their environment (i.e. species-induced changes in the fitness landscapes) is crucial for stable coexistence. This may explain, for example, why the diversity of phytoplankton grazed by zooplankton with relatively short generation times is higher than the diversity of mesozooplankton (Jeppesen et al. 2000), which is grazed by fish with very long generation times lacking a fast numerical response to higher prey densities (Myers et al. 1999).

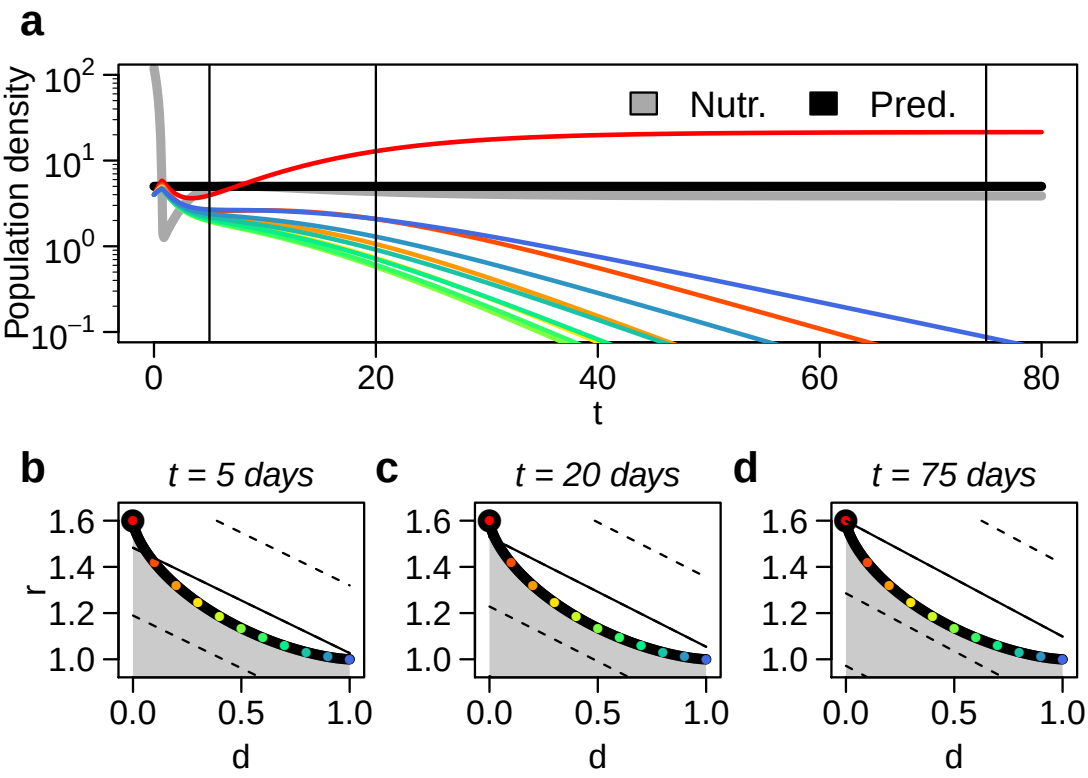

Figure 6.6: Similar to Fig. 6.3 but for simulations with constant predator densities.

The presented graphical approach works similarly for nonlinear fitness isoclines, but with predictions deviating from the previous ones: Convex, linear or concave trade-offs do not necessarily imply different outcomes of coexistence anymore. For example, slightly convex trade-off curves may promote a species with intermediate trait values given convex fitness isoclines, while trade-off curves with a higher convexity than that of the fitness isoclines still lead to coexistence of extreme species (Chapter 3). The trade-off leading to neutral coexistence may be convex or concave, instead of being linear. Furthermore, not only the slope but also the shape of the fitness isoclines may be flexible over time due to environmental changes. For example in a system of two specialists and one generalist exploiting two different resources (Abrams 2006), the fitness isoclines are linear under constant conditions but have more complex shapes under cycling resource concentrations, which allows for stable coexistence of all three consumer species (Appendix B.2).

The theory provided in this section can also be transferred to three-dimensional trade-offs where trade-offs and fitness isoclines represent planes in a 3-D trait space (Fig. 6.7). The difference in the number of coexisting species between different trade-off shapes may increase with a higher dimensionality: A convex trade-off plane (positive second derivatives in all trait directions) may lead to the coexistence of three different strategies (Fig. 6.7a), while a concave trade-off plane (negative second derivatives in all trait directions) may result in the survival of only one species with intermediate trait values (Fig. 6.7b).

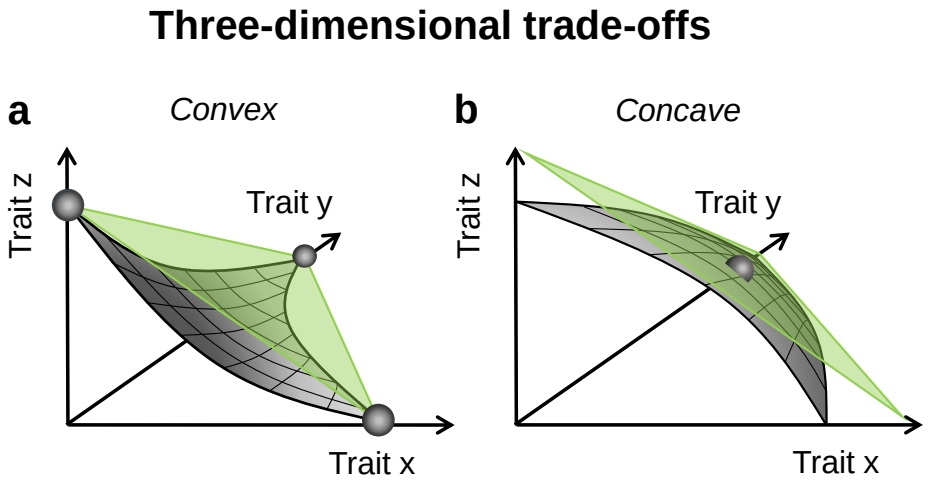

Figure 6.7: Trade-offs among three functional traits represent planes (grey) in a three-dimensional trait space. Convex (a) and concave (b) trade-off planes differ in the number and position of possible fitness maxima (grey spheres) for linear fitness isocline planes (green).

6.3 The interplay of intra- and interspecific trade-offs

So far, I focused mainly on interspecific trade-offs within a community where all species share similar individual constraints, e.g. a trade-off between defence and growth rate in phytoplankton (Chapter 4). However, the body structure and metabolic machinery of each species is often unique, implying that constraints likely differ among species and that evolution of species leads to different trade-off curves (Roff et al. 2002; Litchman et al. 2015). Hence, each species may face a different intraspecific trade-off with a different range of feasible trait combinations. These intraspecific trade-offs determine the trait variation of organisms within a species and govern its evolution or phenotypic plasticity, i.e. trait optimization along trade-off curves.

Here, I extend the theory on trade-off-based coexistence by examining the joint influence of different intraspecific trade-offs and an overarching interspecific trade-off. Figure 6.8 displays different combinations of convex or concave interspecific and intraspecific trade-offs. If the interspecific trade-off and the intraspecific trade-offs are convex, trait combinations at the end of the interspecific trade-off curve may have maximal fitness (Fig. 6.8a). For a convex interspecific trade-off and concave intraspecific trade-offs, the trait combinations of maximal fitness are also highly separated but not at the end of the feasible trait range (Fig. 6.8b). The general pattern that concave interspecific trade-off lead to fitness maxima at intermediate trait combinations is not affected by the shape of the intraspecific trade-offs (Fig. 6.8c, d). However, instead of only one fitness maximum, there are potentially more fitness maxima attained by different species, depending on the species-level trade-offs (Fig. 6.8c, d). The illustrated cases (Fig. 6.8a-d) represent examples demonstrating the substantial increase of possible outcomes if

different intraspecific trade-offs underly an overarching interspecific trade-off.

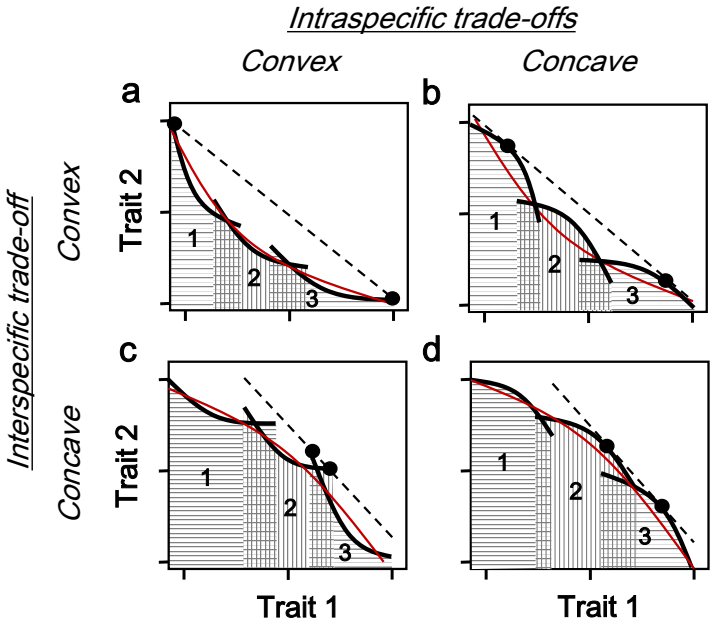

Figure 6.8: Combinations of intraspecific trade-offs (black solid lines) of three species (1-3) and an overarching interspecific trade-off (red line), which can be measured across species. The feasible trait ranges of the different species below the trade-off curves (differently patterned by grey lines) may overlap. Both intra- and interspecific trade-offs are either convex or concave, which leads to different fitness maxima (black dots) depending on the fitness isocline with the maximum attainable fitness (dashed line).

6.4 Global change, the response of food webs, and the influence of trade-offs

From a mechanistic point of view, global changes like anthropogenic habitat fragmentation, fishing or climate change can be interpreted as changes in the fitness landscape of ecological communities or food webs. The shape of trade-offs between functional traits determines the response of communities to such altered fitness landscapes, as explained in section 6.2.

For example, if climate change continuously decreases precipitation in a certain region, plants are selected for drought resistance, which may trade off with other traits, like shade tolerance (Smith and Huston 1989). The continuous change in conditions may lead to a consecutive replacement of species by more and more drought resistant ones, which would be the expectation for concave trade-offs (Fig. 6.2). However, if the trade-off is convex, species replacement may work differently. First, under humid conditions, the shade-tolerant species without drought resistance dominates. With decreasing precipitation, the other extreme species (shade-intolerant and very drought resistant) will

increase progressively in relative biomass until it completely replaced the shade-tolerant one (cf. Fig. 6.2).

Furthermore, higher temperatures caused by climate change can lead to higher feeding rates of predators (Englund et al. 2011). This may rise the importance of defence mechanisms and associated trade-offs in food webs. In terms of the fitness landscape, such increased grazing pressure corresponds to changes in the slope of fitness isoclines favouring high defence levels, as presented in Figure 6.2. Undefended, competitive species and defended species may still coexist but the relative contributions of defended prey to community biomasses may increase. However, the warming-induced increase of metabolic rates of predators (i.e. respiration losses) tends to exceed the increase of feeding rates, which weakens trophic interactions (Rall et al. 2010; Fussmann et al. 2014). Thus, climate change can also have the opposite effect on the fitness landscape and decreases the importance of defence.

At the same time, eutrophication due to fertilization in agriculture may decrease potential defence costs in autotrophs. This may facilitate defence-favouring changes in the fitness landscape and provides an explanation for the increasing occurrence of harmful blooms of defended algae, like cyanobacteria which benefit from higher phosphorus concentrations (Conley et al. 2009; Wang et al. 2010; Chislock et al. 2013). Such algal blooms can further alter the environment in a way that is beneficial for them. After an algal bloom, dead phytoplankton cells sink towards the sediment. The decomposition of this mass of dead organic matter by bacteria strongly reduces the oxygen content in the benthic zone which can lead to the extinction of benthic organisms (Chislock et al. 2013). This results in further decomposition and release of phosphorus from the sediment, fertilizing future algal blooms (Conley et al. 2009).

Humans selectively remove certain groups of organisms at low (e.g. deforestation), intermediate or high trophic levels (e.g. fishing) from ecosystems, which alters the trait composition of these trophic levels. For example, fast-growing forb species replace tree populations under deforestation (Uhl and Jordan 1984) or jellyfish species substitute fish in their role as plankton grazers in face of overfishing (Daskalov et al. 2007; Richardson et al. 2009). The altered trait composition of these trophic levels may have strong cascading effects towards the other trophic levels depending on their trade-offs (Fig. 6.1) and can fundamentally alter ecosystem functions such as primary production.

Plastic pollution represents another anthropogenic threat to marine and freshwater ecosystems, strongly affecting trophic interactions. Seabirds confuse floating macroplastic debris with their prey, which reduces their grazing performance and increases their mortality, due to constipation by plastic debris and the influence of associated toxins (Ryan 1987; Wilcox et al. 2015). Many other aquatic organisms, like fish and especially mussels, are strongly affected as well (Farrell and Nelson 2013;

Rochman et al. 2013). Even mesozooplankton and protists ingest microplastic (Cole et al. 2013). All these organisms spend time for handling plastic particles which indirectly facilitate their respective actual prey (similar to the effect of post-attack defended or digestion resistant prey, described in Chapter 2) (Carson 2013). The measured concentrations of microplastic have already reached the same order of magnitude as plankton concentrations in some regions of the ocean (Moore et al. 2001). Thus, the confusion, constipation and poisoning of all these predators by plastic particles may strongly weaken trophic interactions in aquatic food webs, which may counteract the higher feeding rates caused by climate change. The resulting reduced trophic transfer efficiency from low to high trophic levels may have devasting consequences for ecosystem functions and human well-being. Species may adapt to these plastic concentrations, for example, by changing their feeding mechanisms to selectively disregard plastic particles, which depends on the costs of such trait adaptations regarding other functional traits, i.e. the underlying trade-offs.

To maintain biodiversity and ecosystem functions, management in conservation biology, applied ecology, politics, agriculture and economics should aim for strategies preventing self-facilitating changes in ecosystems (e.g. harmful algal blooms). Such changes cause nonlinear and cascading changes in food webs and potentially result in losses of ecosystems functions. Strategies to prevent abrupt losses of ecosystem functions include a stronger limitation of fertilization, an improved garbage management, climate change mitigation, sustainable fishing/ lumbering and targeted protection of keystone predators. However, many global changes proceed inexorably, which increases the importance of human strategies to adapt to altered compositions of ecosystems. To assess, how communities respond to certain environmental changes, it is fundamental to quantify trade-offs between functional traits. Only on the basis of these trade-offs, we can mechanistically understand ongoing trait changes in communities and predict future community composition to develop future management strategies.

Bibliography 6

Abrams, P. A. (2006). Adaptive change in the resource-exploitation traits of a generalist consumer: the evolution and coexistence of generalists and specialists. *Evolution*, 60(3):427–439.

Carpenter, S. R., Kitchell, J. F., and Hodgson, J. R. (1985). Cascading Trophic Interactions and Lake Productivity. *BioScience*, 35(10):634–639.

Carson, H. S. (2013). The incidence of plastic ingestion by fishes: From the prey's perspective. *Marine Pollution Bulletin*, 74(1):170–174.

Chesson, P. (2000). Mechanisms of Maintenance of Species Diversity. *Annual Review of Ecology and Systematics*, 31(1):343–366.

Chislock, M. F., Doster, E., Zitomer, R. A., and Wilson, A. E. . (2013). Eutrophication: Causes, Consequences, and Conttrols in Aquatic Ecosystems. *Nature Education Knowledge*, 4(4):10.

Cole, M., Lindeque, P., Fileman, E., Halsband, C., Goodhead, R., Moger, J., and Galloway, T. S. (2013). Microplastic Ingestion by Zooplankton. *Environmental Science & Technology*, 47(12):6646–6655.

Conley, D. J., Paerl, H. W., Howarth, R. W., Boesch, D. F., Seitzinger, S. P., Havens, K. E., Lancelot, C., and Likens, G. E. (2009). Controlling Eutrophication: Nitrogen and Phosphorus. *Science*, 323(5917):1014–1015.

Creel, S. and Christianson, D. (2008). Relationships between direct predation and risk effects. *Trends in Ecology and Evolution*, 23(4):194–201.

Daskalov, G. M., Grishin, A. N., Rodionov, S., and Mihneva, V. (2007). Trophic cascades triggered by overfishing reveal possible mechanisms of ecosystem regime shifts. *Proceedings of the National Academy of Sciences*, 104(25):10518–10523.

de Mazancourt, C. and Dieckmann, U. (2004). Trade-Off Geometries and Frequency-Dependent Selection. *The American Naturalist*, 164(6):765–778.

Diehl, S., Cooper, S. D., Kratz, K. W., Nisbet, R. M., Roll, S. K., Wiseman, S. W., and Jenkins, Jr., T. M. (2000). Effects of Multiple, Predator-Induced Behaviors on Short-term Producer-Grazer Dynamics in Open Systems. *The American Naturalist*, 156(3):293–313.

Edwards, K. F., Kremer, C. T., Miller, E. T., Osmond, M. M., Litchman, E., and Klausmeier, C. A. (2018). Evolutionarily stable communities: a framework for understanding the role of trait evolution in the maintenance of diversity. *Ecology Letters*, 21(12):1853–1868.

Englund, G., Öhlund, G., Hein, C. L., and Diehl, S. (2011). Temperature dependence of the functional response. *Ecology Letters*, 14(9):914–921.

Farrell, P. and Nelson, K. (2013). Trophic level transfer of microplastic: Mytilus edulis (L.) to Carcinus maenas (L.). *Environmental Pollution*, 177:1–3.

Fussmann, K. E., Schwarzmüller, F., Brose, U., Jousset, A., and Rall, B. C. (2014). Ecological stability in response to warming. *Nature Climate Change*, 4(3):206–210.

Geritz, S. A., Kisdi, É., Meszéna, G., and Metz, J. A. (1998). Evolutionarily singular strategies and the adaptive growth and branching of the evolutionary tree. *Evolutionary Ecology*, 12(1):35–57.

Hairston, N. G., Smith, F. E., and Slobodkin, L. B. (1960). Community Structure, Population Control, and Competition. *The American Naturalist*, 94(879):421–425.

Holloway, G. J., Sibly, R. M., and Povey, S. R. (1990). Evolution in Toxin-Stressed Environments. *Functional Ecology*, 4(3):289.

Hubbell, S. P. (2005). Neutral theory in community of ecology and the hypothesis functional equivalence. *Functional Ecology*, 19(1):166–172.

Huston, M. (1979). A general hypothesis of species diversity. *The American Naturalist*, 113(1):81–101.

Jeppesen, E., Peder Jensen, J., Søndergaard, M., Lauridsen, T., and Landkildehus, F. (2000). Trophic structure, species richness and biodiversity in Danish lakes: changes along a phosphorus gradient. *Freshwater Biology*, 45(2):201–218.

Leibold, M. A., Chase, J. M., Shurin, and, J. B., and Downing, A. L. (1997). Species Turnover and the Regulation of Trophic Structure. *Annual Review of Ecology and Systematics*, 28(1):467–494.

Levins, R. (1962). Theory of Fitness in a Heterogeneous Environment. I. The Fitness Set and Adaptive Function. *The American Naturalist*, 96(891):361–373.

Litchman, E., Edwards, K. F., and Klausmeier, C. A. (2015). Microbial resource utilization traits and trade-offs: implications for community structure, functioning, and biogeochemical impacts at present and in the future. *Frontiers in Microbiology*, 06(APR):1–10.

Metz, J. A., Nisbet, R. M., and Geritz, S. A. (1992). How should we define 'fitness' for general ecological scenarios? *Trends in Ecology and Evolution*, 7(6):198–202.

Moore, C., Moore, S., Leecaster, M., and Weisberg, S. (2001). A Comparison of Plastic and Plankton in the North Pacific Central Gyre. *Marine Pollution Bulletin*, 42(12):1297–1300.

Myers, R. A., Bowen, K. G., and Barrowman, N. J. (1999). Maximum reproductive rate of fish at low population sizes. *Canadian Journal of Fisheries and Aquatic Sciences*, 56(12):2404–2419.

Ousterhout, B. H., Graham, S. R., Hasik, A. Z., Serrano, M., and Siepielski, A. M. (2018). Past selection impacts the strength of an aquatic trophic cascade. *Functional Ecology*, 32(6):1554–1562.

Paine, R. T. (1980). Food Webs: Linkage, Interaction Strength and Community Infrastructure. *Journal of Animal Ecology*, 49(3):666–685.

Purves, D. W. and Turnbull, L. A. (2010). Different but equal: the implausible assumption at the heart of neutral theory. *Journal of Animal Ecology*, 79(6):1215–1225.

Rall, B. C., Vucic-Pestic, O., Ehnes, R. B., Emmerson, M., and Brose, U. (2010). Temperature, predator-prey interaction strength and population stability. *Global Change Biology*, 16(8):2145–2157.

Richardson, A. J., Bakun, A., Hays, G. C., and Gibbons, M. J. (2009). The jellyfish joyride: causes, consequences and management responses to a more gelatinous future. *Trends in Ecology & Evolution*, 24(6):312–322.

Rochman, C. M., Hoh, E., Kurobe, T., and Teh, S. J. (2013). Ingested plastic transfers hazardous chemicals to fish and induces hepatic stress. *Scientific Reports*, 3(1):3263.

Roff, D. A., Mostowy, S., and Fairbairn, D. J. (2002). The evolution of trade-offs: Testing predictions on response to selection and environmental variation. *Evolution*, 56(1):84–95.

Rueffler, C., Van Dooren, T., and Metz, J. (2004). Adaptive walks on changing landscapes: Levins' approach extended. *Theoretical Population Biology*, 65(2):165–178.

Rueffler, C., Van Dooren, T. J. M., and Metz, J. A. J. (2006). The Evolution of Resource Specialization through Frequency-Dependent and Frequency-Independent Mechanisms. *The American Naturalist*, 167(1):81–93.

Ryan, P. G. (1987). The effects of ingested plastic on seabirds: Correlations between plastic load and body condition. *Environmental Pollution*, 46(2):119–125.

Schmitz, O. J., Krivan, V., and Ovadia, O. (2004). Trophic cascades: the primacy of trait-mediated indirect interactions. *Ecology Letters*, 7(2):153–163.

Sibly, R. and Calow, P. (1983). An Integrated Approach to Life-Cycle Evolution using Selective Landscapes. *Journal of Theoretical Biology*, 102:527–547.

Sibly, R. M., Kodric-Brown, A., Luna, S. M., and Brown, J. H. (2018). The shark-tuna dichotomy: why tuna lay tiny eggs but sharks produce large offspring. *Royal Society Open Science*, 5(8):180453.

Smith, T. and Huston, M. (1989). A Theory of the Spatial and Temporal Dynamics of Plant Communities. *Vegetatio*, 83(1/2):49–69.

Uhl, C. and Jordan, C. F. (1984). Succession and Nutrient Dynamics Following Forest Cutting and Burning in Amazonia. *Ecology*, 65(5):1476–1490.

Visser, A. W., Mariani, P., and Pigolotti, S. (2008). Swimming in turbulence: zooplankton fitness in terms of foraging efficiency and predation risk. *Journal of Plankton Research*, 31(2):121–133.

Wang, X., Qin, B., Gao, G., and Paerl, H. W. (2010). Nutrient enrichment and selective predation by zooplankton promote Microcystis (Cyanobacteria) bloom formation. *Journal of Plankton Research*, 32(4):457–470.

Werner, E. E. and Peacor, S. D. (2003). A Review of Trait-Mediated Indirect Interactions in Ecological Communities. *Ecology*, 84(5):1083–1100.

Wilcox, C., Van Sebille, E., and Hardesty, B. D. (2015). Threat of plastic pollution to seabirds is global, pervasive, and increasing. *Proceedings of the National Academy of Sciences*, 112(38):11899–11904.

Curriculum vitae

Elias Ehrlich

Dept. Ecology and Ecosystem Modelling, Instit. for Biochemistry and Biology,
Faculty of Science, University of Potsdam
Address: Am Neuen Palais 10, 14469 Potsdam, Germany
Email: eehrlich@uni-potsdam.de | Telephone: +49 331 977 1975

DATE OF BIRTH
15/04/1989

FAMILY STATUS
Married (since 2015), one child (born 2018)

EDUCATION

Since 08/2015	**PhD: Ecology** University of Potsdam | Potsdam, Germany Supervisors: Ursula Gaedke and Lutz Becks
04/2016 - 03/2018	**Part-time studies on practical computer science** FernUniversität Hagen | Hagen, Germany Courses on data structures, algorithms, imperative programming and object-orientated programming (20 ECTS)
10/2012 - 06/2015	**MSc: Ecology, Evolution and Conservation** University of Potsdam | Potsdam, Germany Thesis Title: 'Trade-offs between defense and competitiveness govern eco-evolutionary dynamics in predator-prey models' Final grade: 1.0 ('passed with distinction', best possible mark)

10/2009 - 09/2012	**BSc: Life Science** University of Potsdam	Potsdam, Germany Thesis Title: 'Einfluss eines Fischsterbens im Winter und Effekt von allochthonem Material auf die Dynamik funktioneller Gruppen im Plankton von eutrophen Flachwasserseen' Final grade: 1.5 ('very good')

AWARDS

10/2015	**'Jacob-Jacobi-Preis'**, Leibniz-Kolleg Potsdam For the best final Master's degree in 2014/2015 of the Faculty of Science of the University of Potsdam
10/2012 - 03/2015	**Scholarship**, Studienstiftung des deutschen Volkes (German Academic Scholarship Foundation)

EMPLOYMENT HISTORY

Since 08/2015	**Academic Employee** University of Potsdam	Potsdam, Germany DFG Priority Program 'Flexibility matters: Interplay between trait diversity and ecological dynamics using aquatic communities as model systems (DynaTrait)'
10/2012 - 02/2015	**Academic Tutor** and **Research Assistant** University of Potsdam	Potsdam, Germany • Tutorials on Ecology for life scientists and biology students (teacher training) • Data analysis and modelling in a project on phytoplankton diversity • Set up of software for parallel computation, optimization of simulation speed of models • Literature work for lectures in Ecology

TEACHING AND OUTREACH

- Bi-weekly tutorials on Ecology, University of Potsdam (winter term 2014, 2015, 2016)

- Lecture on dimensionality reduction of population models in 'Theoretical Ecology II', University of Potsdam (2017)
- Lecture on microplastic in the oceans offered to public audience. 'Ein Meer aus Plastik', Potsdamer Tag der Wissenschaft (2015, 2016, 2017 and 2018)
- Interactive presentation on the ecological footprint and sustainability for children. 'Eine Erde für Alle!', Potsdamer Tag der Wissenschaft (2015, 2016, 2017 and 2018)
- Several lectures on principles of scientific work and on sustainability offered to school classes (2012-2017)
- Interview on microplastic in the oceans. 'Besser kein Plastik', Portal - Das Potsdamer Universitätsmagazin, Potsdam, March 2016, p. 7
- Interview on plastic in the oceans. 'Ein gigantischer Plastikteppich', Märkische Allgemeine (MAZ), Potsdam, 29 April 2015, p. V1
- Interview on the ecological footprint. 'Wie der Eisbär beim Energiesparen hilft', Märkische Allgemeine (MAZ), Potsdam, 10 June 2014, p. 17

ADDITIONAL SKILLS

- Teaching, Tutoring and Presenting (based on experiences from acting)
- Software: R; Python; Matlab; Mathematica; C/C++; Latex
- Languages: German (first language), English (UNIcert III), French (basics)

CONFERENCE CONTRIBUTIONS

- Talk: 'Not attackable or not crackable - How pre- and post-attack defenses with different competition costs affect prey coexistence and population dynamics' (2018). Annual DynaTrait Meeting, Potsdam, Germany
- Talk: 'Trait-fitness relationships determine how trade-off shapes affect species coexistence' (2018). Models in Population Dynamics, Ecology, and Evolution (MPDEE'18), Leicester, UK
- Poster: 'Key properties of trade-offs affecting coexistence and population dynamics' (2017). Workshop on trait-based approaches to ocean life, Bergen, Norway
- Poster: 'Seasonal trait coupling of phyto- and zooplankton in Lake Constance - data and models' (2017). International DynaTrait Conference, Hannover, Germany
- Talk: 'Trait-fitness relationships determine how trade-off shapes affect species coexistence' (2017). International DynaTrait Conference, Hannover, Germany

- Talk: 'Multidimensional Trade-offs and Coexistence' (2016). Experimental Evolution & Community Dynamics Minisymposium, Plön, Germany
- Talk: 'Multidimensional Trade-offs and Coexistence' (2016). Annual DynaTrait Meeting, Potsdam, Germany
- Poster: 'The shape of trade-offs determines long- and short-term maintenance of functional diversity' (2016). European Conference on Mathematical and Theoretical Biology (ECMTB), Nottingham, UK
- Poster: 'Linear trade-offs between defence and growth maintain intraspecific trait variation in prey' (2015). Annual DynaTrait Meeting, Hannover, Germany
- Talk: 'Biodiversity effects in phytoplankton communities - combining experiments and modelling' (2013). Annual meeting of the German Limnological Society (DGL) and of the Ecological Society of Germany, Austria and Switzerland (GfÖ), Potsdam, Germany

INVITED TALK

- Talk: 'Trait-fitness relationships determine how trade-off shapes affect species coexistence' (2017) at the Centre for Ocean Life, Copenhagen, Denmark

PEER REVIEWS

- Peer reviewed for Ecological Monographs, Freshwater Biology and Functional Ecology

List of publications

PUBLISHED

Ehrlich, E., and Gaedke, U. (2018). Not attackable or not crackable - How pre- and post-attack defenses with different competition costs affect prey coexistence and population dynamics. *Ecology and Evolution*, 8 (13), 6625-6637

Ehrlich, E., Becks, L., and Gaedke, U. (2017). Trait-fitness relationships determine how trade-off shapes affect species coexistence. *Ecology*, 98 (12): 3188-3198.

SUBMITTED

Ehrlich, E., Kath, N. J. (shared first author) and Gaedke, U. (2018). The shape of the trade-off between defence and growth governs seasonal trait dynamics in a phytoplankton community. *Submitted to Ecology Letters and rejected after peer-review, to be submitted again.*

Ehrlich, E., and Gaedke, U. (2019). Coupled changes in traits and biomasses cascading through a tritrophic plankton food web. *Submitted to Proceedings of the Royal Society B: Biological Sciences, under review*.

Eigenständigkeitserklärung

Hiermit versichere ich, die vorliegende Dissertation selbstständig und nur unter Verwendung der von mir angegebenen Quellen und Hilfsmittel verfasst zu haben. Sowohl sinngemäß als auch wörtlich entnommene Inhalte wurden als solche kenntlich gemacht. Die Arbeit hat in dieser oder vergleichbarer Form noch keinem anderen Prüfungsgremium vorgelegen.

Datum: _____ Unterschrift: _____

Danksagung

Die Betreuung
Ein großes Dankeschön möchte ich Ursula Gaedke aussprechen für die umfangreiche Betreuung, ausgiebige Debatten, das entgegengebrachte Vertrauen in mich und meine Ideen, die Beratung und Unterstützung in der beruflichen Entwicklung, den ehrlichen Austausch bei Problemen und die stete Hilfsbereitschaft.

Das Projekt
Ursula Gaedke und Lutz Becks danke ich für das Ermöglichen der Promotion, Noemi Woltermann für die gute Zusammenarbeit und der DFG für die Finanzierung des Projekts (GA 401/25-1). Außerdem möchte ich Friederike Prowe für den vertrauensvollen Austausch mit ihr als Mentorin danken.

Die vorliegende Arbeit
Herzlich danken möchte ich Michael Raatz und Xenia Fahrentholz für das sehr konstruktive Korrekturlesen, sowie Slawa Suchin für Tipps rund um das effektivere Schreiben.

Die Arbeitsatmosphäre
Ein liebes Dankeschön richte ich an: Meine weltbeste/n Bürokollegen/in Michael Raatz, Ruben Ceulemans und Tamara Thieser für ein stets offenes Ohr und den Spaß auf der Arbeit; Stefan Saumweber für die Hilfe und den Humor bei technischen Problemen; Toni Klauschies für anregende und spaßbringende Diskussionen; Ellen van Velzen und Christian Guill für die fachliche Hilfe; Nadja Kath für konstruktive Teamsitzungen; Alice Boit und Alexander Wacker für gute Ratschläge; Alle Kolleg*innen für die wirklich schöne Arbeitsatmosphäre und unvergessliche Mensagänge.

Die Unterstützung
Meinen Groß-/ Eltern, Geschwistern und Freunden möchte ich ganz besonders danken für ihre Unterstützung, das Daumendrücken und die geteilte Freude.

Für Alles
Stefanie danke ich von Herzen für alles, was sich schwer in Worte fassen lässt – das

Verständnis und die Motivation, das gemeinsame Genießen all der schönen Momente während dieser Zeit, und die unerschütterliche, äußerst kraftgebende Unterstützung in schweren Phasen. Ein besonderes Dankeschön gilt nun schließlich auch August, der mich in der letzten Phase der Promotion mit seiner unbekümmerten Art und seinem Lächeln aufmunterte und motivierte.

Appendices

Appendix A - Chapter 2

A.1. Digestion resistance

Species may defend at different points of the predation sequence (sequence of encounter, attacking, capturing, manipulating, ingestion, digestion). In the main text, we distinguished between defences preventing attacks (low attack probability p_i) and those operating subsequent to attacks by reducing the consumption probability q_i. Empirical studies revealed that certain species may defend themselves even after being ingested by surviving the gut passage, e.g., aquatic snails eaten by birds (van Leeuwen et al. 2012; Wada et al. 2012) or phytoplankton species with thickened cell walls consumed by different zooplankton species (Porter 1973; Meyer et al. 2006; Demott and McKinney 2015). To implement such a digestion resistance into the functional response of the predator, we introduce the digestion probability d_i of the prey. We define a prey only as digestion resistant if it passes the digestive system of the predator alive. The probability of surviving the gut passage after being consumed is given by $1-d_i$. Low-quality prey, which is killed by consumption but mainly excreted afterwards, is not regarded as defended/digestion resistant. Such food-quality effects would be implemented by a low conversion efficiency of the predator rather than a low d_i (Raatz et al. 2017).

We consider a Holling type II functional response F_i of the predator for the prey A_i. It should be mentioned that, by including the digestion probability d_i into the functional response, F_i represents the rate of prey digestion instead of prey consumption

$$F_i = \frac{a\, p_i\, q_i\, d_i\, A_i}{1 + a p_1 (c_a T + q_1 (1-c_a) T) A_1 + a p_2 (c_a T + q_2 (1-c_a) T) A_2} \,. \qquad \text{(A1)}$$

A predator invests even more time in handling a digestion resistant A_1 compared to a post-attack defended A_1 (see Tab. 2.1 in the main text), i.e., not only the attack time T_a ($c_a T$) but also the manipulation time T_m ($(1-c_a)T$). Thus, the indirect facilitation of A_2 by A_1 increases and the coexistence region is enlarged in comparison to a post-attack defence (Fig. 2.2 and A1). The effects of digestion resistance and post-attack defences are equal if the main part of the handling time is needed for attacking ($c_a \approx 1$).

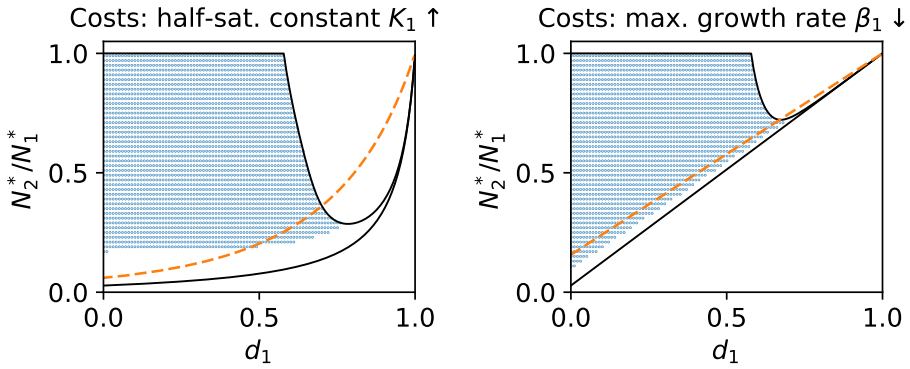

Figure A1: Coexistence and population dynamics of a digestion resistant prey A_1 and an undefended prey A_2 in dependence of the digestion probability d_1 of A_1 and its half-saturation constant for resource uptake K_1 or its maximum growth rate β_1. The trait values of A_2 are kept constant. The y-axis represents the relative competitiveness N_2^*/N_1^* of A_1 compared to A_2. The resource supply is set to N_I=160 µmol N/l. The black lines enclose the region where a coexistence equilibrium exists and blue dots mark where it is locally stable. The dashed orange line represents the invasion boundary of A_1 invading a resident community with A_2 (invasion is possible above the line).

A.2. Coexistence equilibria, linear stability analysis and invasion boundary

The calculation of coexistence equilibria, the linear stability analysis and the calculation of the invasion boundary are based on Jones and Ellner (2007). These calculations demand a rescaling of the model. At the end of the calculations, the traits are transferred back into their original units (prior to rescaling) to present the results in the main text.

Rescaling and reducing the dimensions of the predator-prey model

The analysed predator-prey model is given by

$$\begin{aligned}
\frac{dN}{dt} &= \delta\,(N_I - N) - \sum_{i=1}^{2} \frac{\beta_i}{\chi}\,\frac{N A_i}{K_i + N} \\
\frac{dA_i}{dt} &= A_i \left[\beta_i \frac{N}{K_i + N} - \frac{a\,p_i q_i d_i P}{1 + a\sum p_i (c_a T + q_i (1 - c_a) T)\,A_i} - \delta\right] \\
\frac{dP}{dt} &= P \left[\chi_P \frac{a \sum p_i q_i d_i A_i}{1 + a\sum p_i (c_a T + q_i (1 - c_a) T)\,A_i} - \delta\right]
\end{aligned} \tag{A2}$$

with $i = 1, 2$. In addition to the model presented in the main text (Eq. 2.2), we included also the digestion probability d_i (see Appendix A.1). To allow for analytical calculations, we rescale the model with the following substitutions

$$\begin{aligned}
&\tau = \delta t,\ S = \frac{N}{N_I},\ x_i = \frac{A_i}{\chi N_I},\ y = \frac{P}{\chi_P \chi N_I}, \\
&g = \frac{\chi_P}{\delta T},\ k_P = \frac{1}{\chi N_I a T},\ k_i = \frac{K_i}{N_I},\ r_i = \frac{\beta_i}{\delta}.
\end{aligned} \tag{A3}$$

The rescaling ensures that all variables and parameters are dimensionless.

The following equations represent the rescaled model

$$\begin{aligned}
\dot{S} &= 1 - S - \sum_{i=1}^{2} \frac{r_i S x_i}{k_i + S} \\
\dot{x_i} &= x_i \left[\frac{r_i S}{k_i + S} - \frac{g\,p_i q_i d_i y}{k_P + \sum p_i\,(c_a + q_i (1 - c_a))\,x_i} - 1\right] \\
\dot{y} &= y \left[\frac{g \sum p_i q_i d_i x_i}{k_P + \sum p_i\,(c_a + q_i (1 - c_a))\,x_i} - 1\right].
\end{aligned} \tag{A4}$$

The derivatives over time t ($\frac{dN}{dt}$, $\frac{dA_i}{dt}$, $\frac{dB}{dt}$) are transformed into derivatives over τ ($\dot{S}$, $\dot{x_i}$ and $\dot{y}$). The sum of the population densities $\sum = S + x_1 + x_2 + y$ is changing over time in

dependence of the rate of change of its components

$$\dot{\sum} = \dot{S} + \dot{x}_1 + \dot{x}_2 + \dot{y} \tag{A5}$$

Inserting the Eq. A4 into Eq. A5 results in

$$\begin{aligned} \dot{\sum} &= 1 - S - x_1 - x_2 - y \\ \dot{\sum} &= 1 - \sum \end{aligned} \tag{A6}$$

$\dot{\sum}$ becomes zero when $\sum$ gets close to one implying that $\sum = 1$ is an equilibrium (Jones and Ellner 2007). Thus, in the long-term, $\sum$ has a constant value of one meaning that the joint capacity of the populations S, x_1, x_2 and y in the chemostat system is one. Considering long-term dynamics allows the following substitution for the resource density by inserting $\sum = 1$ into $\sum = S + x_1 + x_2 + y$ and rearranging this equation

$$S = 1 - x_1 - x_2 - y\,. \tag{A7}$$

Thus, the resource density can be represented by a function of the densities of the prey types and the predator (Eq. A7) allowing for a dimensional reduction of the model (Jones and Ellner 2007). The rescaled, reduced model is represented by the following equations

$$\begin{aligned} \dot{x}_i &= x_i \left[\frac{r_i (1 - x_1 - x_2 - y)}{k_i + (1 - x_1 - x_2 - y)} - \frac{g\, p_i q_i d_i y}{k_P + \sum p_i (c_a + q_i(1 - c_a)) x_i} - 1 \right] \\ \dot{y} &= y \left[\frac{g \sum p_i q_i d_i x_i}{k_P + \sum p_i (c_a + q_i(1 - c_a)) x_i} - 1 \right]. \end{aligned} \tag{A8}$$

Coexistence equilibrium

One goal of this study is to find the conditions for coexistence of both prey types. Without a loss of generality, we explain our method based on the attack probability-maximum growth rate trade-off (p-β-TO) where the prey types do not differ in their consumption probability, digestion probability and their half-saturation constant, i.e., we assume that $q_1 = q_2 = 1$, $d_1 = d_2 = 1$ and $k_1 = k_2 = k$. One condition for coexistence is the existence of an equilibrium ($\dot{x}_1$, $\dot{x}_2$ and $\dot{y}$ equal to zero) where all population densities are positive. This kind of equilibrium is called coexistence equilibrium (Jones and Ellner 2007). Equilibrium population densities are marked with a tilde. By inserting $\dot{y} = 0$ into Eq. A8 the expression for the total attackable prey density at equilibrium ($\widetilde{Q} = \sum p_i \widetilde{x_i}$) is derived as

$$\widetilde{Q} = \frac{k_P}{g - 1} \;\Leftrightarrow\; \frac{g}{k_P + \widetilde{Q}} = \frac{1}{\widetilde{Q}} \tag{A9}$$

The substitution $S = 1 - x_1 - x_2 - y$ simplifies the further analysis (Eq. A7). The solution for the equilibrium predator density for $\dot{x}_1 = 0$ is

$$\widetilde{y} = \frac{\widetilde{Q}}{p_1}\left[\frac{(r_1 - 1)\widetilde{S} - k}{k + \widetilde{S}}\right] \tag{A10}$$

and for $\dot{x}_2 = 0$

$$\widetilde{y} = \frac{\widetilde{Q}}{p_2}\left[\frac{(r_2 - 1)\widetilde{S} - k}{k + \widetilde{S}}\right] \tag{A11}$$

These solutions (Eq. A10 and A11) have to be equal. Equating both terms results in

$$\widetilde{S} = \frac{(1 - \frac{p_1}{p_2})\,k}{\frac{p_1}{p_2} - \frac{p_1}{p_2}r_2 + r_1 - 1} \tag{A12}$$

$\widetilde{S}$ corresponds to the equilibrium resource density. The total prey density in equilibrium $\widetilde{X}$ $(= \widetilde{x_1} + \widetilde{x_2})$ is obtained by inserting $\widetilde{S}$ (Eq. A12) and $\widetilde{y}$ (Eq. A10 or A11) into $\widetilde{X} = 1 - \widetilde{S} - \widetilde{y}$. As explained in Jones and Ellner (2007), the equilibrium prey population densities $\widetilde{x_1}$ and $\widetilde{x_2}$ can be represented as

$$\begin{bmatrix} \widetilde{x_1} \\ \widetilde{x_2} \end{bmatrix} = \frac{1}{p_2 - p_1}\begin{bmatrix} p_2\widetilde{X} - \widetilde{Q} \\ \widetilde{Q} - p_1\widetilde{X} \end{bmatrix} \tag{A13}$$

Due to the coexistence condition stating that equilibrium population densities have to be positive ($\widetilde{x_1}$ and $\widetilde{x_2} > 0$) and remembering that $p_1 < p_2$ it follows from Equation A13 that $p_1\widetilde{X} < \widetilde{Q} < p_2\widetilde{X}$ (Jones and Ellner 2007). This term can be rearranged to

$$p_1 < \frac{\widetilde{Q}}{\widetilde{X}} < p_2 \tag{A14}$$

The Inequation A14 defines one condition for the coexistence equilibrium where $\frac{\widetilde{Q}}{\widetilde{X}}$ can be considered as a density-weighted mean attack probability of the prey types. The attack probability of the defended prey is smaller and the attack probability of the undefended prey is larger than this density-weighed mean attack probability when there is a coexistence equilibrium.

In the following, we derive the boundaries of the coexistence equilibrium region in the trait space of p_1 and r_1. At the first boundary of the coexistence equilibrium region, the costs of the defended prey exceed a certain level (low r_1) so that its equilibrium population density becomes zero ($\widetilde{x_1} = 0$). Hence, the equilibrium of the undefended prey and the predator is equal to that of the corresponding mono-prey system ($\overline{x_2}$, $\overline{y_2}$) at this boundary.

According to that, the equilibrium condition $\dot{x}_1 = 0$ yields

$$0 = \frac{r_1\,(1-\overline{x_2}-\overline{y_2})}{k+(1-\overline{x_2}-\overline{y_2})} - \frac{g\,p_1\,\overline{y_2}}{k_P+p_2\,\overline{x_2}} - 1 \tag{A15}$$

which can be rearranged to

$$r_1 = \left[\frac{g\,p_1\,\overline{y_2}}{k_P+p_2\,\overline{x_2}}+1\right]\frac{k+(1-\overline{x_2}-\overline{y_2})}{1-\overline{x_2}-\overline{y_2}} \tag{A16}$$

For each p_1, the corresponding r_1 at this boundary is obtained by inserting $\overline{x_2}$ and $\overline{y_2}$ into Equation A16. The equilibrium densities of the mono-prey system ($\overline{x_2}$, $\overline{y_2}$) can be derived from $\dot{y} = 0$, that is,

$$\overline{x_2} = \frac{k_P}{p_2\,(g-1)} \tag{A17}$$

and $\dot{x}_2 = 0$

$$\overline{y_2} = \frac{1}{2}\left[\nu - \sqrt{\nu^2 - 4\,r_2\,\overline{x_2}}\right] - \overline{x_2} \tag{A18}$$

$$\text{with} \quad \nu = k+1+r_2\,\overline{x_2}$$

The second boundary of the coexistence equilibrium region, where low defence costs prevent coexistence (high r_1), can be divided into two parts which meet at a p_1-value of $p^* = \frac{k_P\,/\,(g-1)}{1-k\,/\,(r_2-1)}$ (first part: $p_1 < p^*$, second part: $p_1 > p^*$) (Jones and Ellner 2007). For $p_1 < p^*$ and $r_1 > r_2$, the undefended prey goes extinct due to the higher competitiveness of the defended prey. The predator dies out as well as the defended prey represents no adequate food source (low attack probability p_1). Accordingly, the first part of the boundary ($p_1 < p^*$) is where the maximum growth rate of the defended prey becomes equal to that of the undefended prey

$$r_1 = r_2 \tag{A19}$$

For $p_1 > p^*$ and appropriately high r_1 values, the undefended prey goes extinct even if it has a higher maximum growth rate than the defended prey. The defended prey is able to maintain the predator due to its relatively high attack probability. In the presence of the predator, the defended prey is able to outcompete the undefended prey ($\widetilde{x_2} = 0$) for low

defence costs. Inserting $\widetilde{x_2} = 0$ into the equilibrium condition $\dot{x}_2 = 0$ yields

$$0 = \frac{r_2\left(1-\overline{x_1}-\overline{y_1}\right)}{k+\left(1-\overline{x_1}-\overline{y_1}\right)} - \frac{g\,p_2\,\overline{x_1}}{k_P + p_1\,x_1} - 1 \tag{A20}$$

The equilibrium densities of the mono-prey system $(\overline{x_1}, \overline{y_1})$ depend on p_1 and r_1. They can be obtained from $\dot{y} = 0$

$$\overline{x_1} = \frac{k_P}{p_1\left(g-1\right)} \tag{A21}$$

and $\dot{x}_1 = 0$

$$\overline{y_1} = \frac{1}{2}\left[\omega - \sqrt{\omega^2 - 4\,r_1\,\overline{x_1}}\right] - \overline{x_1} \tag{A22}$$

$$\text{with} \quad \omega = k + 1 + r_1\,\overline{x_1}$$

The r_1 for a certain p_1 at which $\overline{x_1}$ and $\overline{y_1}$ fulfill Equation A20 is called ϕ. By combining the solutions of both parts, that is, $p_1 < p^*$ and $p_1 > p^*$, we reach the general definition of the second boundary of the coexistence equilibrium region:

$$r_1 = \min[r_2, \phi] \tag{A23}$$

where ϕ is a function of p_1. For $p_1 < p^*$, the corresponding ϕ gets higher than r_2. In this case, the minimum function (Equation A23) ensures that the definition of the first part of this boundary holds (Equation A19).

Linear stability analysis

Another goal of this study is to identify the dynamics potentially occurring in this predator-prey system. A linear stability analysis enables to distinguish between locally stable equilibria (i.e. steady-state) and locally unstable equilibria (e.g. existence of stable limit cycles). Therefore, we analyse the local stability of the coexistence equilibrium. We refer here exemplary again to the p-β-TO and assume that $d_1 = d_2 = 1$ and $k_1 = k_2 = k$. The further steps are based on the study of Jones and Ellner (2007). The Jacobian matrix at the coexistence equilibrium J is generated by computing the necessary partial derivatives for the rescaled, reduced model (Eq. A8).

$$J = \begin{pmatrix} \frac{\partial \dot{x}_1}{\partial x_1} & \frac{\partial \dot{x}_1}{\partial x_2} & \frac{\partial \dot{x}_1}{\partial y} \\ \frac{\partial \dot{x}_2}{\partial x_1} & \frac{\partial \dot{x}_2}{\partial x_2} & \frac{\partial \dot{x}_2}{\partial y} \\ \frac{\partial \dot{y}}{\partial x_1} & \frac{\partial \dot{y}}{\partial x_2} & \frac{\partial \dot{y}}{\partial y} \end{pmatrix} \Bigg|_{x_1=\widetilde{x_1}, x_2=\widetilde{x_2}, y=\widetilde{y}}$$

$$= \begin{pmatrix} \widetilde{x_1}\,[u_{x_1} - p_1^2 \widetilde{y}\widetilde{v}'] & \widetilde{x_1}\,[u_{x_1} - p_1 p_2 \widetilde{y}\widetilde{v}'] & \widetilde{x_1}\,[u_{y_1} - p_1 \widetilde{v}] \\ \widetilde{x_2}\,[u_{x_2} - p_1 p_2 \widetilde{y}\widetilde{v}'] & \widetilde{x_2}\,[u_{x_2} - p_2^2 \widetilde{y}\widetilde{v}'] & \widetilde{x_2}\,[u_{y_2} - p_2 \widetilde{v}] \\ p_1 \widetilde{y}\widetilde{w}' & p_2 \widetilde{y}\widetilde{w}' & 0 \end{pmatrix} \tag{A24}$$

$$= \begin{pmatrix} a & b & c \\ d & e & f \\ g & h & i \end{pmatrix}$$

with

$$\begin{aligned} u_{x_1} = u_{y_1} &= -\frac{r_1 k}{(k+1-\widetilde{X}-\widetilde{y})^2} \\ u_{x_2} = u_{y_2} &= -\frac{r_2 k}{(k+1-\widetilde{X}-\widetilde{y})^2} \\ \widetilde{v} &= \frac{g}{k_P + \widetilde{Q}} \\ \widetilde{v}' &= -\frac{g}{(k_P + \widetilde{Q})^2} \\ \widetilde{w}' &= -\frac{g\,k_P}{(k_P + \widetilde{Q})^2} \end{aligned} \tag{A25}$$

The roots of the characteristic polynomial of J are the eigenvalues λ of J. If all eigenvalues have negative real parts then the equilibrium is locally stable. The general equation of characteristic polynomials for a 3×3 dimensional matrix is

$$p(\lambda) = \det(\lambda I - J) = \lambda^3 + c_2 \lambda^2 + c_1 \lambda + c_0 = 0 \tag{A26}$$

The coefficients of the characteristic polynomial are

$$\begin{aligned} c_0 &= -(a\,e\,i + b\,f\,g + c\,d\,h - g\,e\,c - h\,f\,a - i\,d\,b) = -\det(J) \\ c_1 &= a\,e + a\,i + e\,i - d\,b - g\,c - h\,f \\ c_2 &= -(a + e + i) = -\text{trace}(J) \end{aligned} \tag{A27}$$

The small letters in the definition of the coefficients represent the elements of the Jacobian matrix shown in Equation A24. The coefficient c_0 is equal to the negative determinant of J while c_2 equals the negative trace of J (Jones and Ellner 2007). The Routh-Hurwitz stability criterion (May 1974) is used for revealing whether the coexistence equilibrium is locally stable. According to this criterion, all eigenvalues (roots of the characteristic polynomial, Eq. A26) have negative real parts when the following conditions hold

$$\begin{aligned} I)\ & c_0 > 0 \\ II)\ & c_1 > 0 \\ III)\ & c_2 > 0 \\ IV)\ & c_1 c_2 > c_0\,. \end{aligned} \tag{A28}$$

Invasion boundary

Here we derive the invasion boundary of the defended prey A_1 invading a resident community of the undefended prey A_2 and the predator P. This demands no rescaling of the model. Hence, we refer to the original model (Eq. A2). We explain the calculation again based on the p-β-TO where $q_1 = q_2 = 1$, $d_1 = d_2 = 1$ and $K_1 = K_2 = K$. The invasion fitness of A_1 which is defined as the long-term mean per capita growth rate at very low densities ($A_1 \approx 0$) is given by

$$\left\langle \frac{1}{A_1}\frac{dA_1}{dt} \right\rangle = \beta_1 \left\langle \frac{N}{K+N} \right\rangle - p_1 \left\langle \frac{aP}{1+a\,p_2\,(c_a T + (1-c_a)T)\,A_2} \right\rangle - \delta \tag{A29}$$

where long-term means are indicated by angle brackets. At the invasion boundary, the invasion fitness equals zero, i.e.

$$0 = \beta_1 \left\langle \frac{N}{K+N} \right\rangle - p_1 \left\langle \frac{aP}{1+a\,p_2\,T\,A_2} \right\rangle - \delta\,. \tag{A30}$$

This can be rearranged to

$$\beta_1 = \frac{p_1 \left\langle \frac{aP}{1+a\,p_2\,T\,A_2} \right\rangle + \delta}{\left\langle \frac{N}{K+N} \right\rangle} \tag{A31}$$

which yields the relationship between the maximum growth rate β_1 and the attack probability p_1 of the defended prey at its invasion boundary. The long-term means of the densities of the resident community N, A_2 and P (Eq. A31) have to be computed numerically over one cycle of the residents.

A.3. Sensitivity analysis

Here, we examine the sensitivity of the results to altered parameter values. We show that the general pattern, that post-attack defences promote coexistence and stable dynamics more strongly than pre-attack defences and that a higher half-saturation K_1 enhances the occurrence of coexistence and destabilizes the dynamics compared to a lower maximum growth rate β_1, is largely independent from distinct parameter values (Fig. A2-A8).

First, we test how the results depend on the resource supply N_I (Fig. A2, A3). For a low level of resource supply ($N_I = 80$ µmol N/L), differences between the two defence mechanisms in coexistence patterns are low, but significant for different defence costs (Fig. A2). The population dynamics are overall stable for such a low resource supply independent of the defence and its costs (Fig. A2). Increasing the resource supply to $N_I = 240$ µmol N/L reveals large differences in coexistence patterns and population dynamics for the different types of defences and costs (Fig. A3).

Second, we consider the fraction of the predator handling time spent for attacking the prey c_a. With increasing values of c_a, a post-attacked defended prey demands higher handling times while a pre-attack defended prey is not handled by the predator. Thus, the patterns of coexistence and population dynamics for pre- and post-attack defences diverge when c_a increases (Fig. A4). The results for a pre-attack defence are independent of c_a (Fig. A5). In contrast, in case of a post-attack defence, a higher c_a steadily enhances coexistence and promotes the occurrence of stable dynamics up to a value around 0.35. Above this values, the fraction of locally stable coexistence equilibria does not increased any more (Fig. A5).

For the other parameters, a recurring pattern can be observed which is generally independent from the type of defence and costs. With increasing values of the encounter rate a, the conversion efficiency of the predator χ_P, the conversion efficiency of the prey χ and the resource supply N_I, the occurrence of coexistence equilibria initially increases but declines above a certain value while the fraction of locally stable coexistence equilibria which initially equals one is continuously decreasing (Fig. A6). Decreasing values of the total handling time T and the dilution rate δ initially increase the occurrence of coexistence equilibria but then decrease it below a certain value. The fraction of locally stable coexistence equilibria initially decreases with lower values of T and δ but then starts to increase again especially for lower values of T.

Independent of the defence mechanism and the cost type, a higher maximum growth β_2 of the undefended prey slightly enhances coexistence and promotes steady-state dynamics (Fig. A7). A similar trend can be observed for a lower half-saturation constant K_2 of the undefended prey in case of post-attack defences while it is slightly the opposite trend for pre-attack defences (Fig. A8).

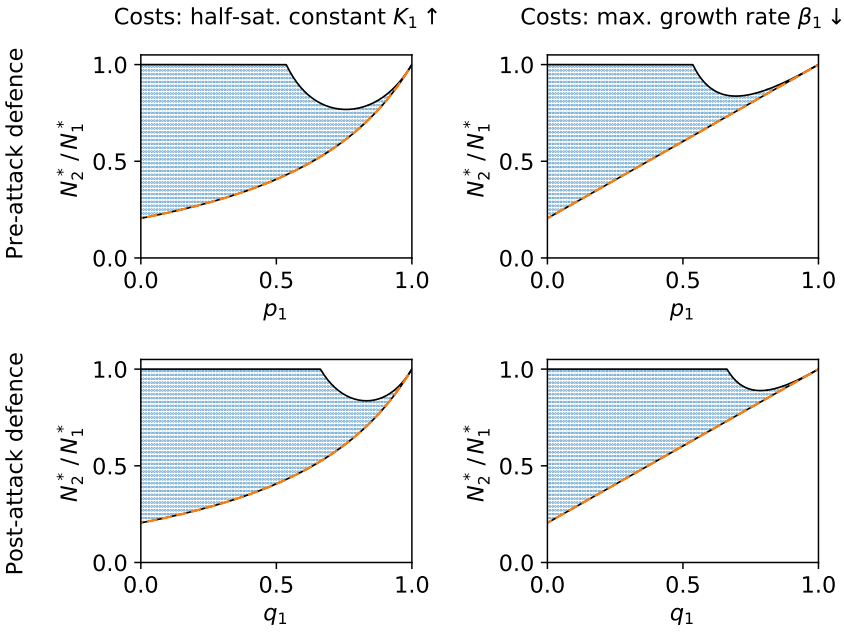

Figure A2: Low resource supply, $N_I = 80$ µmol N/l. Coexistence equilibria of the defended prey A_1 and the undefended prey A_2 in dependence of the defence mechanism (top: attack probability $p_1 < 1$, bottom: consumption probability $q_1 < 1$) and the defence costs (left: higher half-saturation constant K_1, right: lower maximum growth rate β_1). The y-axis represents the relative competitiveness of A_1 (see main text). The black lines enclose the region where a coexistence equilibrium exists and blue dots mark where it is locally stable. The dashed orange line represents the invasion boundary above which A_1 can invade a resident community with A_2.

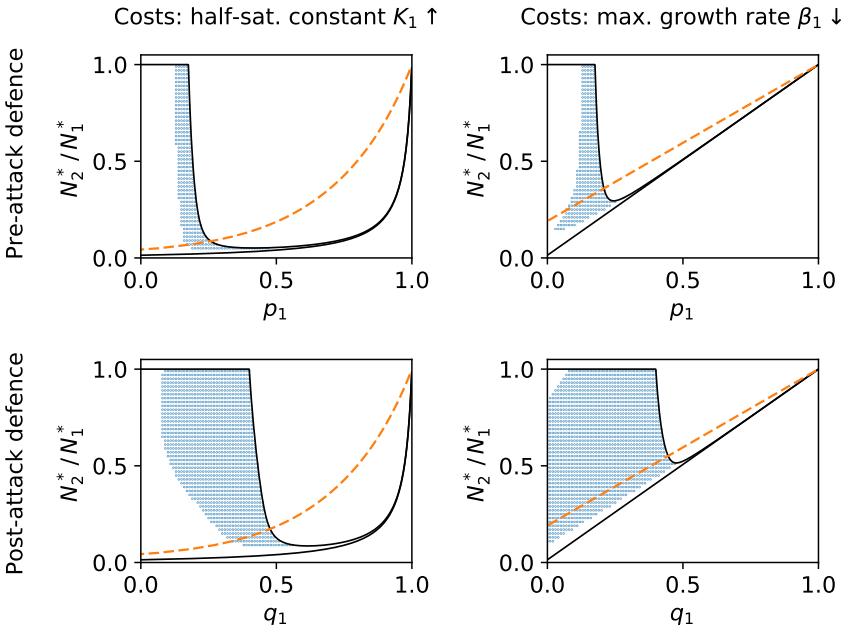

Figure A3: High resource supply, $N_I = 240$ µmol N/l. Coexistence equilibria of the defended prey A_1 and the undefended prey A_2 in dependence of the defence mechanism (top: attack probability $p_1 < 1$, bottom: consumption probability $q_1 < 1$) and the defence costs (left: higher half-saturation constant K_1, right: lower maximum growth rate β_1). The y-axis represents the relative competitiveness of A_1 (see main text). The black lines enclose the region where a coexistence equilibrium exists and blue dots mark where it is locally stable. The dashed orange line represents the invasion boundary above which A_1 can invade a resident community with A_2.

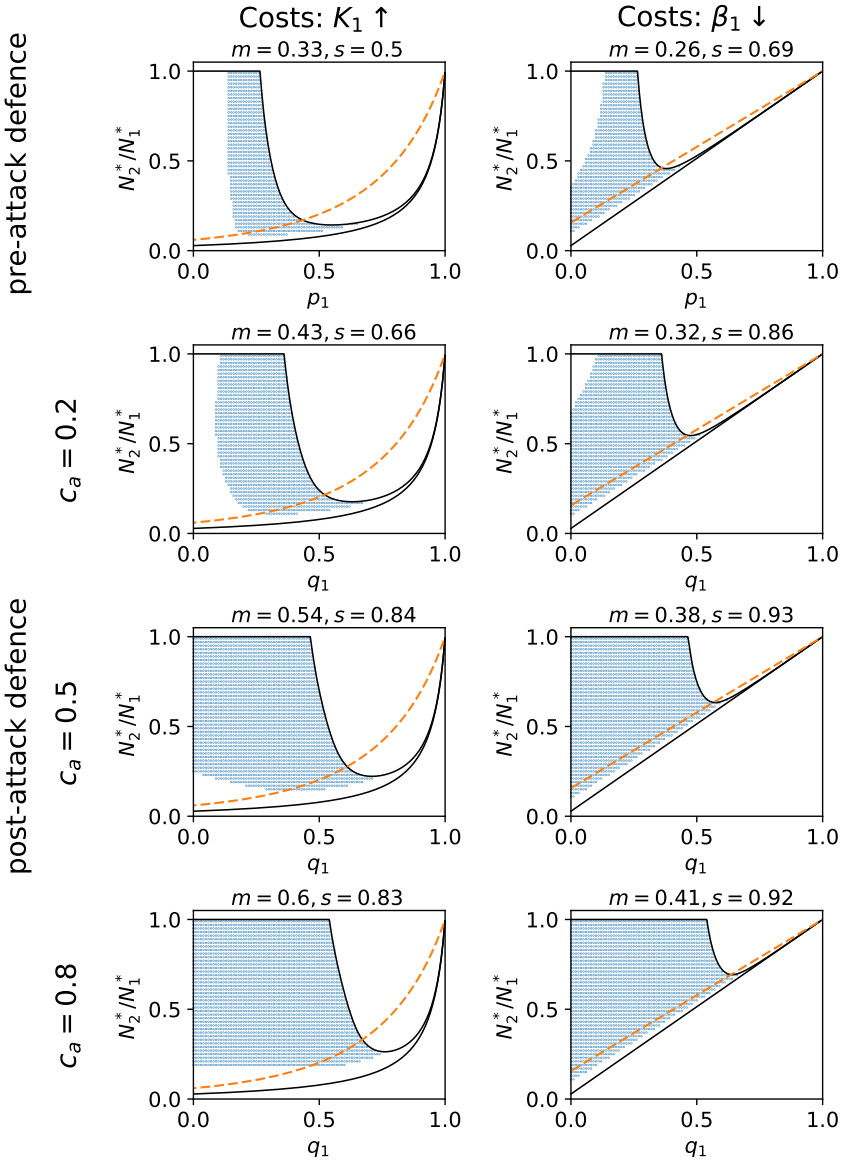

Figure A4: Coexistence equilibria of the defended prey A_1 and the undefended prey A_2 in dependence of the defence level (top panel: attack probability $p_1 < 1$, three bottom panels: consumption probability $q_1 < 1$) and the defence costs (left: higher half-saturation constant K_1, right: lower maximum growth rate β_1) for $N_I = 160$ µmol N/l. The y-axis represents the relative competitiveness of A_1 (see main text). The results for the post-attack defence depend on the fraction of the predator's handling time spent for attacking the prey c_a which increases from top to bottom. The black lines enclose the region where a coexistence equilibrium exists and blue dots mark where it is locally stable. m gives the fraction of the total trait space where a coexistence equilibrium exists while s indicates the fraction of the coexistence equilibria which are locally stable. The dashed orange line represents the invasion boundary above which A_1 can invade a resident community with A_2.

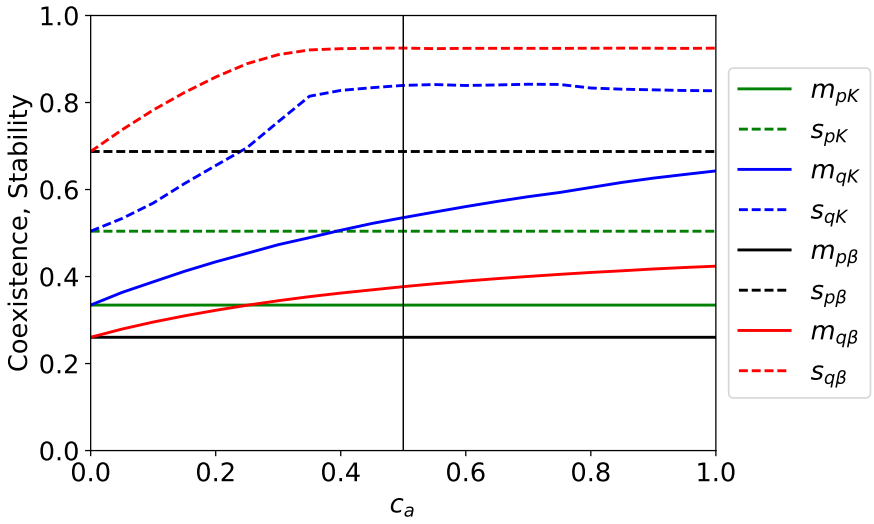

Figure A5: Coexistence equilibria and their local stability in dependence of the fraction of handling time spent for attacking the prey c_a. The vertical line marks the value of c_a used in the main text. m indicates the fraction of the total trait space where a coexistence equilibrium exists and s gives the amount of locally stable coexistence equilibria (see Fig. A4). The subscript letters refer to the considered defence trait (attack probability p or consumption probability q) and the cost trait (half-saturation constant K or maximum growth rate β).

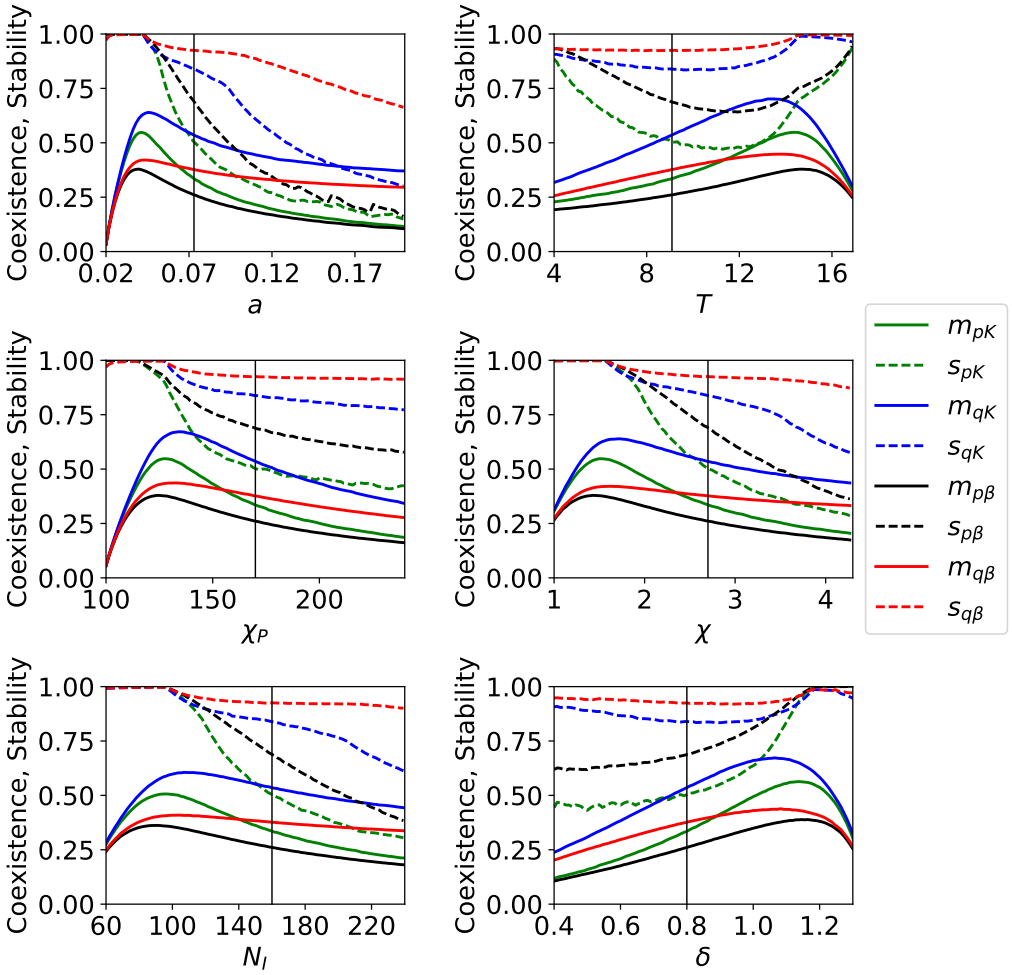

Figure A6: Coexistence equilibria and their local stability in dependence of (a) the encounter rate a (ml/d), (b) the total handling time T ($10^{-5}\,d$), (c) the predator's conversion efficiency χ_P (10^{-6}), (d) the conversion efficiency of the prey χ (10^6 ind./µmol N), (e) the resource concentration in the supplied medium N_I (µmol N/l), and (f) the dilution rate δ (d^{-1}). The vertical lines mark the parameter values used in the main text. m indicates the fraction of the total trait space where a coexistence equilibrium exists and s gives the amount of locally stable coexistence equilibria (see Fig. A4). The subscript letters refer to the considered defence trait (attack probability p or consumption probability q) and the cost trait (half-saturation constant K or maximum growth rate β).

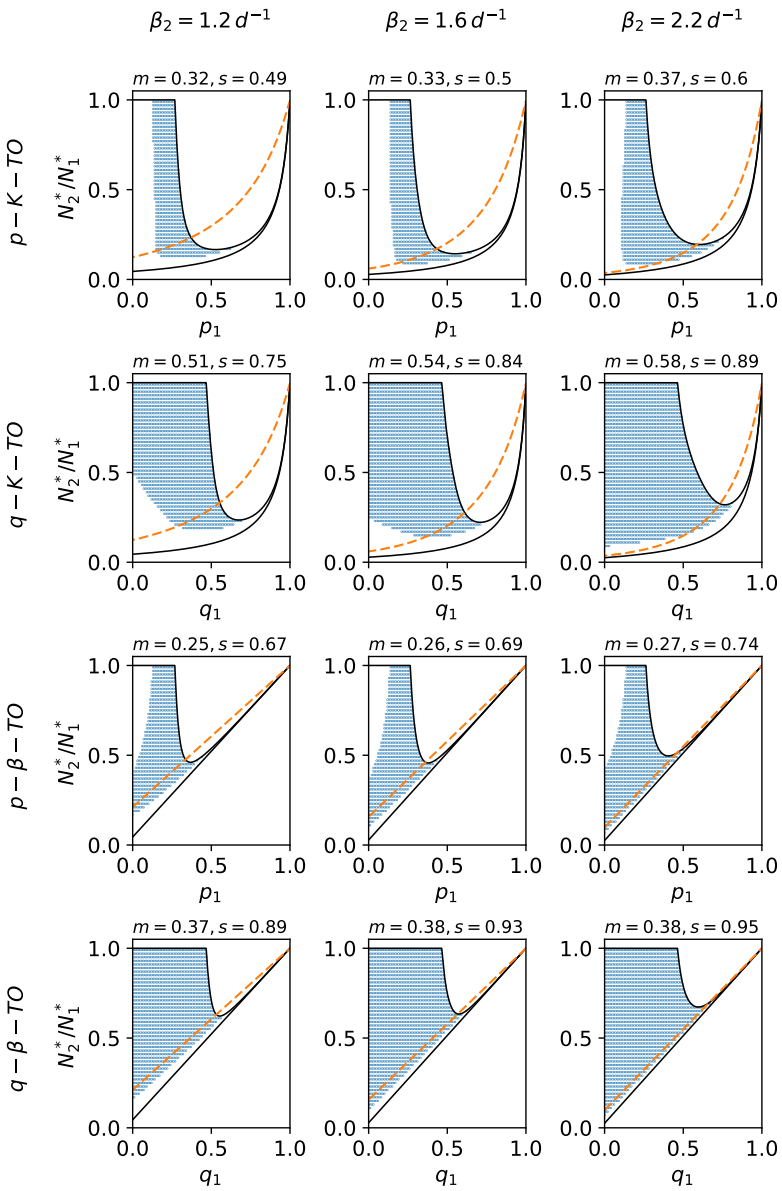

Figure A7: Coexistence equilibria of the defended prey A_1 and the undefended prey A_2 in dependence of the defence level (pre-attack defence with attack probability $p_1 < 1$ or post-attack defence with consumption probability $q_1 < 1$) and the defence costs (higher half-saturation constant K_1 or lower maximum growth rate β_1) for different maximum growth rates of the undefended prey β_2 (1.2, 1.6 or 2.2 d^{-1}). N_I is set to 160 µmol N/l. The black lines enclose the region where a coexistence equilibrium exists and blue dots mark where it is locally stable. m indicates the fraction of the total trait space where a coexistence equilibrium exists and s gives the amount of locally stable coexistence equilibria. The dashed orange line represents the invasion boundary above which A_1 can invade a resident community with A_2.

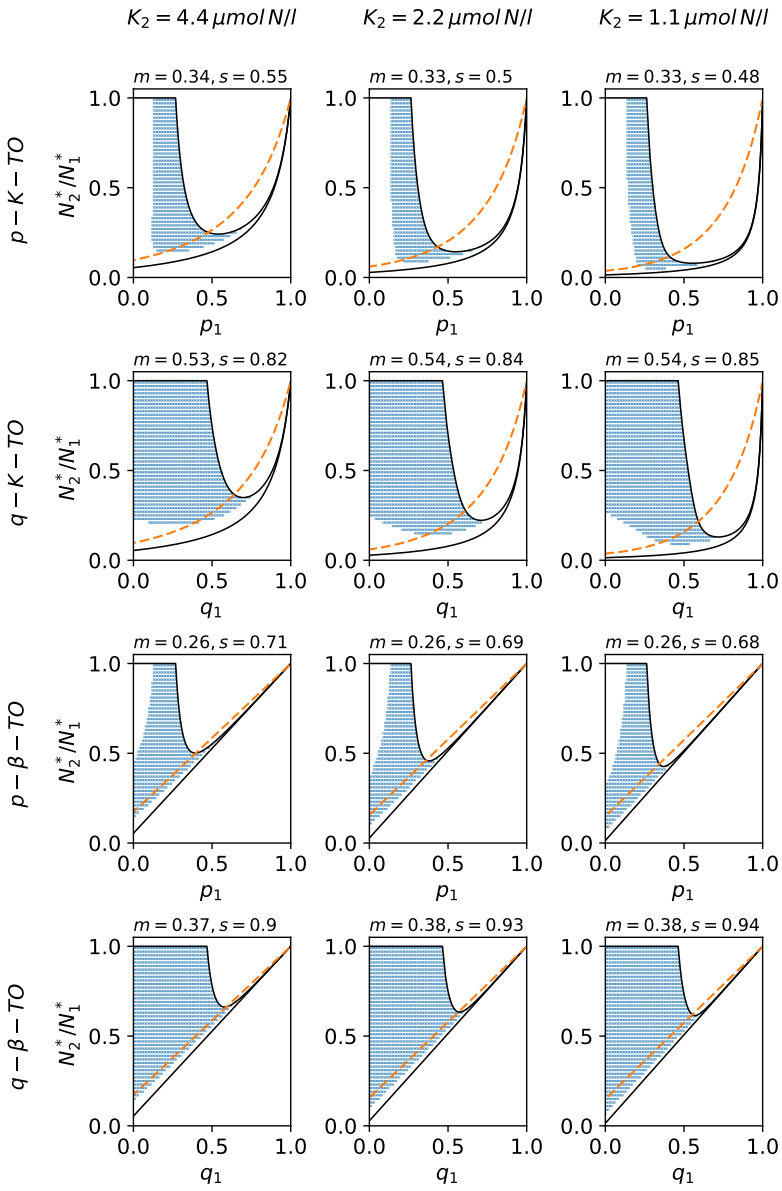

Figure A8: Coexistence equilibria of the defended prey A_1 and the undefended prey A_2 in dependence of the defence level (pre-attack defence with attack probability $p_1 < 1$ or post-attack defence with consumption probability $q_1 < 1$) and the defence costs (higher half-saturation constant K_1 or lower maximum growth rate β_1) for different values of the half-saturation constant of the undefended prey K_2 (4.4, 2.2 or 1.1 µmol N/l). N_I is set to 160 µmol N/l. The black lines enclose the region where a coexistence equilibrium exists and blue dots mark where it is locally stable. m indicates the fraction of the total trait space where a coexistence equilibrium exists and s gives the amount of locally stable coexistence equilibria. The dashed orange line represents the invasion boundary above which A_1 can invade a resident community with A_2.

A.4. Multistability

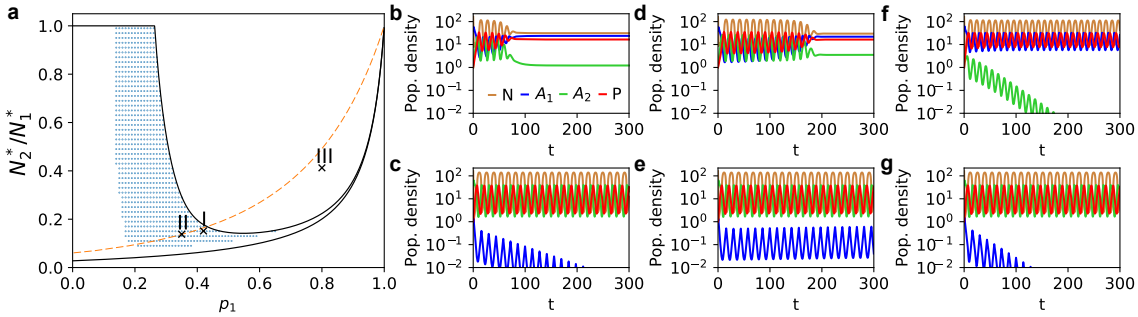

Figure A9: (a) Coexistence equilibria (within black lines), their stability (blue dots indicate local stability) and the invasion boundary of the defended prey A_1 invading a resident community with the undefended prey A_2 (dashed orange line) for a trade-off between attack probability and half-saturation constant. Multistability occurs at trait ranges where A_1 cannot invade but survives for high initial population densities. The trait combination I lies in a region where either both prey types coexist (b) or A_1 goes extinct (c) while in case of coexistence (trait combination II), the population densities are in steady state (d) or cycle (e) depending on the initial conditions. At the trait combination III either only A_1 survives (e) or is outcompeted (f). (b-g) Population dynamics with nutrients N, the two prey types A_i and the predator P. The initial densities of N (160 µmol N/l) and P (1 ind./ml) are kept constant. The initial density of A_1 is either 40×10^4 ind./ml (b, d, f) or 1×10^4 ind./ml (c, e, g) and *vice versa* for A_2.

Bibliography A

Demott, W. R. and McKinney, E. N. (2015). Use it or lose it? Loss of grazing defenses during laboratory culture of the digestion-resistant green alga Oocystis. *Journal of Plankton Research*, 37(2):399–408.

Jones, L. E. and Ellner, S. P. (2007). Effects of rapid prey evolution on predator–prey cycles. *Journal of Mathematical Biology*, 55(4):541–573.

May, R. (1974). *Stability and complexity in model ecosystems*. Princeton University Press.

Meyer, J. R., Ellner, S. P., Hairston, N. G., Jones, L. E., and Yoshida, T. (2006). Prey evolution on the time scale of predator-prey dynamics revealed by allele-specific quantitative PCR. *Proceedings of the National Academy of Sciences of the United States of America*, 103(28):10690–10695.

Porter, K. G. (1973). Selective Grazing and Differential Digestion of Algae by Zooplankton. *Nature*, 244(5412):179–180.

Raatz, M., Gaedke, U., and Wacker, A. (2017). High food quality of prey lowers its risk of extinction. *Oikos*, 126(10):1501–1510.

van Leeuwen, C. H. A., van der Velde, G., van Lith, B., and Klaassen, M. (2012). Experimental Quantification of Long Distance Dispersal Potential of Aquatic Snails in the Gut of Migratory Birds. *PLoS ONE*, 7(3):e32292.

Wada, S., Kawakami, K., and Chiba, S. (2012). Snails can survive passage through a bird's digestive system. *Journal of Biogeography*, 39(1):69–73.

Appendix B - Chapter 3

B.1. Invasion boundaries of M when both traits have non-linear effects on fitness and fitness components are non-additive

Both traits affect fitness non-linearly

Case	$\langle f_x \rangle$	$\langle f_y \rangle$	$\frac{\partial \langle f_x \rangle}{\partial x}$	$\frac{\partial \langle f_y \rangle}{\partial y}$	$\frac{\partial y}{\partial x}$	$\frac{\partial^2 \langle f_x \rangle}{\partial x^2}$	$\frac{\partial^2 \langle f_y \rangle}{\partial y^2}$	$\frac{\partial^2 y}{\partial x^2}$	Invasion boundary
1	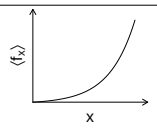	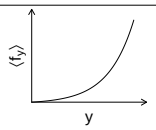	+	+	-	+	+	-	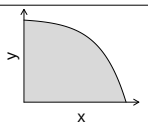
2	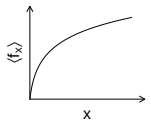	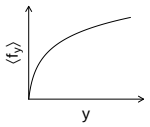	+	+	-	-	-	+	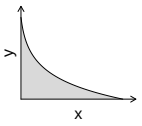
3	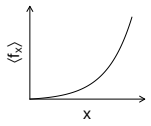	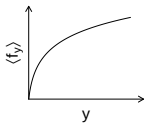	+	+	-	+	-	?	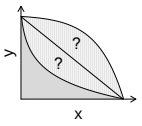

Figure B1: Invasion boundaries of the intermediate species M resulting from different cases where both its traits x and y translate non-linearly into its additive invasion fitness components $\langle f_x \rangle$ and $\langle f_y \rangle$. The sign of $\partial y / \partial x$ determines the direction of the invasion boundary while its shape depends on the sign of $\partial^2 y / \partial x^2$. The black curve in the last column represents the invasion boundary and grey (white) areas refer to trait combinations where M cannot (can) invade. A question mark indicates that the shape of the invasion boundary depends on the absolute values of the invasion fitness derivatives. In a certain range of trait combinations the invasibility is not clarified which is indicated by the grey-dotted area.

Non-additive fitness components

Here, we describe how to determine the direction and the shape of the invasion boundary of an intermediate species M invading the extreme species E_1 and E_2 for the traits x and y in case of non-additive fitness components f_x and f_y. We assume that they are multiplicative but the approach works also for more complex cases. The invasion fitness of the intermediate species ($M \approx 0$) is given by

$$\left\langle \frac{1}{M} \frac{dM}{dt} \right\rangle = \left\langle f_x(x,0,E_1,E_2) \cdot f_y(y(x),0,E_1,E_2) + c(0,E_1,E_2) \right\rangle . \qquad \text{(B1)}$$

Since f_x and f_y are multiplicative, they represent together either a growth or loss term. Therefore, we introduce a further fitness component c which represents the missing growth or loss term and depends on none of the traits involved in the trade-off. The

invasion boundary implies

$$0 = \left\langle f_x(x,0,E_1,E_2) \cdot f_y(y(x),0,E_1,E_2) + c(0,E_1,E_2) \right\rangle . \tag{B2}$$

This is derived with respect to x, i.e.

$$0 = \left\langle \frac{\partial (f_x \cdot f_y + c)}{\partial x} \right\rangle \tag{B3}$$

which yields

$$0 = \left\langle \frac{\partial f_x}{\partial x} f_y + f_x \frac{\partial f_y}{\partial y} \frac{\partial y}{\partial x} \right\rangle . \tag{B4}$$

Since $\partial y / \partial x$ is independent of time, Eq. B4 can be rearranged to

$$\frac{\partial y}{\partial x} = -\frac{\left\langle \frac{\partial f_x}{\partial x} f_y \right\rangle}{\left\langle \frac{\partial f_y}{\partial y} f_x \right\rangle} \tag{B5}$$

which describes the direction of the invasion boundary. The following second derivative determines the shape of the invasion boundary:

$$\frac{\partial^2 y}{\partial x^2} = -\frac{(F_1 + F_2) F_3 - F_4 (F_5 + F_6)}{(F_3)^2} \tag{B6}$$

with

$$F_1 = \left\langle \frac{\partial^2 f_x}{\partial x^2} f_y \right\rangle , \qquad F_2 = \left\langle \frac{\partial f_x}{\partial x} \frac{\partial f_y}{\partial y} \frac{\partial y}{\partial x} \right\rangle , \qquad F_3 = \left\langle \frac{\partial f_y}{\partial y} f_x \right\rangle , \tag{B7}$$
$$F_4 = \left\langle \frac{\partial f_x}{\partial x} f_y \right\rangle , \qquad F_5 = \left\langle \frac{\partial^2 f_y}{\partial y^2} \frac{\partial y}{\partial x} f_x \right\rangle , \qquad F_6 = \left\langle \frac{\partial f_y}{\partial y} \frac{\partial f_x}{\partial x} \right\rangle .$$

To conclude, we achieved a representation of the direction and the shape of the invasion boundary based on how the fitness components depend on the trait values as described in the main text (see general approach). In contrast to the additive case (Eq. 3.4, 3.5), they depend also on the sign of f_x and f_y. In Figure B2, we show invasion boundaries for different trait-fitness relationships where f_x and f_y refer to a growth term ($f_x > 0$ and $f_y > 0$). Remarkably, the invasion boundary is non-linear even if the traits translate linearly into the fitness components (case 1 in Figure B2).

Case	f_x	f_y	$\frac{\partial f_x}{\partial x}$	$\frac{\partial f_y}{\partial y}$	$\frac{\partial y}{\partial x}$	$\frac{\partial^2 f_x}{\partial x^2}$	$\frac{\partial^2 f_y}{\partial y^2}$	$\frac{\partial^2 y}{\partial x^2}$	Invasion boundary
1	+ 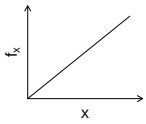	+ 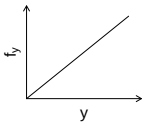	+	+	-	0	0	+	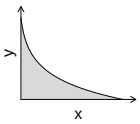
2	+ 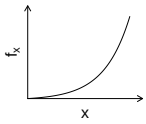	+ 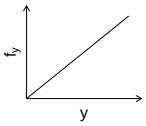	+	+	-	+	0	?	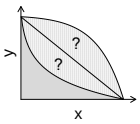
3	+ 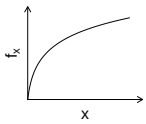	+ 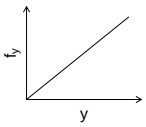	+	+	-	-	0	+	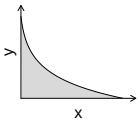

Figure B2: Invasion boundaries of M for different cases how its traits x and y translate into the multiplicative invasion fitness components f_x and f_y. The sign of $\partial y/\partial x$ determines the direction of the invasion boundary while its shape depends on the sign of $\partial^2 y/\partial x^2$. The black curve in the last column represents the invasion boundary and grey (white) areas refer to trait combinations where the invasion of M is impossible (possible). A question mark indicates that the shape of the invasion boundary depends on the absolute values of the invasion fitness components and their derivatives. In a certain range of trait combinations the invasibility is not clarified which is indicated by the grey-dotted area.

B.2. Application of the general approach to a resource competition model

Here, we apply our approach to a resource competition model that inspired previous ideas on the effects of different shapes of trade-offs on consumer coexistence (Abrams 2006). This example was chosen to demonstrate that the curvature of the invasion boundary may depend on the state of the resident community. The considered system consists of two resources (R_1, R_2) and three consumer species (two resource specialists E_1, E_2 and one generalist M) which face a trade-off between the traits of specialization on R_1 (x_i) and R_2 (y_i). E_1 is efficient in using R_1 but unable to use R_2 ($x_1 = 1$, $y_1 = 0$) while the opposite holds for E_2 ($x_2 = 0$, $y_2 = 1$). M is able to use both resources and has intermediate trait values ($0 < x < 1$, $0 < y < 1$). We check for which trait combinations M can invade a resident system of R_1, R_2, E_1 and E_2 and calculate the shape of the invasion boundary to infer effects of different trade-off shapes on coexistence. Previous theory predicts that the invasion boundary is linear for stable equilibria of the resident system allowing M to survive only for concave trade-offs. In contrast, asynchronous population cycles of the resident community promote M leading to its survival also for slightly convex trade-offs. This implies that the shape of the invasion boundary itself is convex and depends on the densities of the residents.

Here, we test these predictions with our approach of calculating the shape of the invasion boundary based on trait-fitness relationships. The per capita growth rate of M is given by

$$\frac{1}{M}\frac{dM}{dt} = \frac{b\left(xC_1R_1 + y(x)C_2R_2\right)}{1 + h\left(xC_1R_1 + y(x)C_2R_2\right)} - d \tag{B8}$$

where b represents the conversion efficiency, C_i the attack rate on R_i, h the handling time and d the per capita death rate of M. At the invasion boundary the long-term mean per capita growth rate of M at very low densities ($M \approx 0$) is equal to zero, i.e.

$$0 = \left\langle \frac{b\left(f_x + f_y\right)}{1 + h\left(f_x + f_y\right)} - d \right\rangle \tag{B9}$$

with the two non-additive fitness components each depending on one of the traits involved in the trade-off: $f_x = xC_1R_1$ and $f_y = y(x)C_2R_2$. We derive Eq. B9 with respect to x which yields

$$0 = \left\langle \frac{\frac{\partial f_x}{\partial x} + \frac{\partial f_y}{\partial y}\frac{\partial y}{\partial x}}{F^2} \right\rangle \tag{B10}$$

with $F = 1 + h\left(f_x + f_y\right)$. Rearranging this equations leads us to the first derivative of the

invasion boundary

$$\frac{\partial y}{\partial x} = -\frac{\left\langle (\frac{\partial f_x}{\partial x})/F^2 \right\rangle}{\left\langle (\frac{\partial f_y}{\partial y})/F^2 \right\rangle} \tag{B11}$$

which is always negative, implying that the invasion boundary has a negative slope in the trait space of x and y. The second derivative is then given by

$$\frac{\partial^2 y}{\partial x^2} = \frac{V-U}{\left\langle (\frac{\partial f_y}{\partial y})/F^2 \right\rangle^2} \tag{B12}$$

with

$$U = \left\langle \left[\frac{\partial^2 f_x}{\partial x^2} F - \frac{\partial f_x}{\partial x} 2h(\frac{\partial f_x}{\partial x} + \frac{\partial f_y}{\partial y}\frac{\partial y}{\partial x}) \right] /F^3 \right\rangle \cdot \left\langle (\frac{\partial f_y}{\partial y})/F^2 \right\rangle \tag{B13}$$

and

$$V = \left\langle \left[\frac{\partial^2 f_y}{\partial y^2}\frac{\partial y}{\partial x} F - \frac{\partial f_y}{\partial y} 2h(\frac{\partial f_x}{\partial x} + \frac{\partial f_y}{\partial y}\frac{\partial y}{\partial x}) \right] /F^3 \right\rangle \cdot \left\langle (\frac{\partial f_x}{\partial x})/F^2 \right\rangle . \tag{B14}$$

Since both second derivatives of the fitness components ($\frac{\partial^2 f_x}{\partial x^2}$ and $\frac{\partial^2 f_y}{\partial y^2}$) are zero, it simplifies to

$$U = -\left\langle \left[\frac{\partial f_x}{\partial x} 2h(\frac{\partial f_x}{\partial x} + \frac{\partial f_y}{\partial y}\frac{\partial y}{\partial x}) \right] /F^3 \right\rangle \cdot \left\langle (\frac{\partial f_y}{\partial y})/F^2 \right\rangle \tag{B15}$$

and

$$V = -\left\langle \left[\frac{\partial f_y}{\partial y} 2h(\frac{\partial f_x}{\partial x} + \frac{\partial f_y}{\partial y}\frac{\partial y}{\partial x}) \right] /F^3 \right\rangle \cdot \left\langle (\frac{\partial f_x}{\partial x})/F^2 \right\rangle . \tag{B16}$$

In case of a stable equilibrium of the residents, the second derivative of the invasion boundary equals

$$\frac{\partial^2 y}{\partial x^2} = \frac{-\left[\frac{\partial f_y}{\partial y} 2h(\frac{\partial f_x}{\partial x} + \frac{\partial f_y}{\partial y}\frac{\partial y}{\partial x}) \right] /F^3 \cdot (\frac{\partial f_x}{\partial x})/F^2 + \left[\frac{\partial f_x}{\partial x} 2h(\frac{\partial f_x}{\partial x} + \frac{\partial f_y}{\partial y}\frac{\partial y}{\partial x}) \right] /F^3 \cdot (\frac{\partial f_y}{\partial y})/F^2}{\left\langle (\frac{\partial f_y}{\partial y})/F^2 \right\rangle^2} \tag{B17}$$

which simplifies to

$$\frac{\partial^2 y}{\partial x^2} = 0 . \tag{B18}$$

Thus, we show with our approach considering trait-fitness relationships that the invasion boundary of M is linear for a stable equilibrium of the resident community. This implies different coexistence patterns for convex and concave trade-offs which is in line with Abrams (2006). Under cyclic conditions, the sign of the second derivative of the invasion

boundary (Eq. B12) depends on the fluctuating densities of the residents determining the values of the long-term means (Eq. B15, B16). In general, based on the results of Abrams (2006), we would assume that the invasion boundary is convex ($\frac{\partial^2 y}{\partial x^2} > 0$) when cycles occur. However, we cannot rule out other cases, i.e. linear or concave invasion boundaries.

B.3. Parameter definitions and values

Table B1: Parameter definitions and values used in the predator-prey model which is based on a rotifer-algae chemostat system.

Parameter	Description	Value	Ref.
N_I	Nutrient concentration in supplied medium	160 µmol N/l	TEC
δ	Chemostat dilution rate	0.8 d^{-1}	TEC
r	Max. growth rate of the algae	1.6 d^{-1}	NW
χ	Algal conversion efficiency	2.7×10^6 cells/µmol N	LBB
χ_B	Rotifer conversion efficiency	170 rotifers/10^6 cells	LB
g	Max. rotifer grazing rate	0.011×10^6 cells/rotifer/d	LB
K_B	Rotifer half-saturation constant	0.15×10^6 cells/ml	LB

NW: Estimated from batch culture experiments (Noemi Woltermann, unpublished data). TEC: Chosen according to typical experimental conditions. LBB: Estimated from batch culture experiments (Lutz Becks, unpublished data). LB: Becks et al. (2010).

B.4. First and second derivations of the invasion fitness with respect to the edibility p and the half-saturation constant K

The invasion fitness of the intermediate species ($M \approx 0$) invading the two extreme species (E_1 and E_2) can be represented by two additive functions $\langle f_p \rangle + \langle f_K \rangle$ each depending on one trait and the respective population densities:

$$\left\langle f_p(p,0,E_1,E_2,B) \right\rangle = -p \left\langle \frac{gB}{K_B + \sum p_i E_i} \right\rangle - \delta \tag{B19}$$

and

$$\langle f_K(K,N) \rangle = r \left\langle \frac{N}{K+N} \right\rangle . \tag{B20}$$

By derivating Eq. B19 and B20, we can infer how the traits of M translate into invasion fitness components which yields

$$\begin{aligned} \frac{\partial \langle f_p \rangle}{\partial p} &= -\left\langle \frac{gB}{K_B + \sum p_i E_i} \right\rangle, \qquad \frac{\partial^2 \langle f_p \rangle}{\partial p^2} = 0, \\ \frac{\partial \langle f_K \rangle}{\partial K} &= -r \left\langle \frac{N}{(K+N)^2} \right\rangle, \qquad \frac{\partial^2 \langle f_K \rangle}{\partial K^2} = r \left\langle \frac{N(2K+2N)}{(K+N)^4} \right\rangle . \end{aligned} \tag{B21}$$

Because all traits and the population densities have positive values, this results in the following relationships: $\frac{\partial \langle f_p \rangle}{\partial p} < 0$, $\frac{\partial^2 \langle f_p \rangle}{\partial p^2} = 0$, $\frac{\partial \langle f_K \rangle}{\partial K} < 0$ and $\frac{\partial^2 \langle f_K \rangle}{\partial K^2} > 0$.

B.5. Calculation of invasion boundaries

Two resident species

We derive here the invasion boundary of the intermediate prey M invading a resident community with the two extreme prey types E_1 and E_2. The population density of the invader is close to zero ($M \approx 0$). Its invasion fitness equals

$$\left\langle \frac{1}{M}\frac{dM}{dt} \right\rangle = r \left\langle \frac{N}{K_M + N} \right\rangle - p_M \left\langle \frac{gB}{K_B + \sum p_i E_i} \right\rangle - \delta \,. \tag{B22}$$

At the invasion boundary, the invasion fitness is equal to zero which yields

$$0 = r \left\langle \frac{N}{K_M + N} \right\rangle - p_M \left\langle \frac{gB}{K_B + \sum p_i E_i} \right\rangle - \delta \tag{B23}$$

while rearranging leads to

$$p_M = \frac{r \left\langle \frac{N}{K_M+N} \right\rangle - \delta}{\left\langle \frac{gB}{K_B+\sum p_i E_i} \right\rangle} \,. \tag{B24}$$

From Eq. B24, we can calculate the combinations of p_M and K_M of the invasion boundary. When there is no stable equilibrium of the resident community (N, E_1, E_2, B), the long-term means indicated by angle brackets (see Eq. B24) have to be calculated over one cycle of the residents. The procedure described above (Eq. B22-B24) can be used also for calculating the invasion boundaries of E_1 invading $M + E_2$ and E_2 invading $E_1 + M$.

One resident species

Here, we derive the invasion boundary of an extreme species (E_i with i=1 or 2) invading M. The invasion fitness of E_i is given by

$$\left\langle \frac{1}{E_i}\frac{dE_i}{dt} \right\rangle = r \left\langle \frac{N}{K_i + N} \right\rangle - p_i \left\langle \frac{gB}{K_B + p_M M} \right\rangle - \delta \,. \tag{B25}$$

At the invasion boundary, the invasion fitness equals zero, i.e.

$$0 = r \left\langle \frac{N}{K_i + N} \right\rangle - p_i \left\langle \frac{gB}{K_B + p_M M} \right\rangle - \delta \,. \tag{B26}$$

The long-term mean per capita growth rate of the resident M is also zero as it is in the asymptotic phase, i.e.

$$0 = r \left\langle \frac{N}{K_M + N} \right\rangle - p_M \left\langle \frac{gB}{K_B + p_M M} \right\rangle - \delta \,. \tag{B27}$$

Rearrangement leads to the equation

$$\left\langle \frac{g\,B}{K_B + p_M\,M} \right\rangle = \frac{1}{p_M}\left(r \left\langle \frac{N}{K_M + N} \right\rangle - \delta \right) . \tag{B28}$$

Replacing the mean functional response term of the predator in Eq. B26 according to Eq. B28 yields

$$0 = r \left\langle \frac{N}{K_i + N} \right\rangle - \frac{p_i}{p_M}\left(r \left\langle \frac{N}{K_M + N} \right\rangle - \delta \right) - \delta . \tag{B29}$$

For limit cycles of M and B, the terms $\left\langle \frac{N}{K_i+N} \right\rangle$ and $\left\langle \frac{N}{K_M+N} \right\rangle$ in Eq. B29 have to be found numerically. At a stable equilibrium, $\left\langle \frac{N}{K_i+N} \right\rangle$ and $\left\langle \frac{N}{K_M+N} \right\rangle$ can be replaced by $\frac{N^*}{K_i+N^*}$ and $\frac{N^*}{K_M+N^*}$ where N^* represents the equilibrium nutrient concentration with the value

$$N^* = \frac{N_I - \frac{r}{\delta\,\chi}\,M^* - K_M}{2} + \sqrt{\left(\frac{\frac{r}{\delta\,\chi}\,M^* + K_M - N_I}{2} \right)^2 + N_I\,K_M} \tag{B30}$$

and M^* is the equilibrium density of the resident:

$$M^* = \frac{K_B}{\left(\frac{\chi_B\,g}{\delta} - 1\right)\,p_M} . \tag{B31}$$

By applying a root finding function to Eq. B29, we determine the trait combinations (p_M, K_M) of the invasion boundary of E_i invading M.

Bibliography B

Abrams, P. A. (2006). Adaptive change in the resource-exploitation traits of a generalist consumer: the evolution and coexistence of generalists and specialists. *Evolution*, 60(3):427–439.

Becks, L., Ellner, S. P., Jones, L. E., and Hairston Jr., N. G. (2010). Reduction of adaptive genetic diversity radically alters eco-evolutionary community dynamics. *Ecology Letters*, 13(8):989–997.

Appendix C - Chapter 4

C.1. Methodical details

Classification of seasonal phases

We subdivided the year into 7 consecutive phases to minimize inter-annual variability due to different climatic conditions. These phases are late winter, early spring, late spring, clear water phase, summer, autumn and early winter (Fig. 4.2). The start and end of each phase was not a fixed calendar date but was determined for each year based upon independent physical (vertical mixing, temperature, water transparency), chemical (soluble reactive phosphorous concentration) and biological parameters (phytoplankton and zooplankton biomass, chlorophyll concentration and species composition) (Rocha et al. 2012). Each period is associated with a different well-defined forcing regime. (i) First, during late winter deep mixing and low irradiance lead to a decrease of phytoplankton biomass to the annual minimum level. (ii) Early spring is characterized by unstable stratification, variable underwater light climate, low grazing pressure and high, non-limiting nutrient concentrations which enables the first growth of algae and some grazers interrupted by mixing events. (iii) During late spring algal biomass further increases with the onset of thermal stratification which reduces nutrient concentrations. The high biomass of mostly small, edible algae promotes growth of different groups of micro- and meso-zooplankton. Grazing pressure mostly by ciliates increases. (iv) As a consequence, phytoplankton biomass strongly declines, resulting in the clear water phase, which is characterized by the strongest grazing pressure throughout the year, mainly caused by meso-zooplankton. Nutrient concentrations reincrease during the clear water phase due to remineralization and with decreased grazing pressure, the summer phytoplankton bloom starts. (v) Summer is marked by severe nutrient depletion leading to strong competition within the phytoplankton community, and the relevance of different zooplankton groups (ciliates, rotifers, cladocerans and copepods) with different feeding strategies and grazing on different groups of phytoplankton. (vi) An increase of the mixing depth as autumn begins leads to a minor reduction of algal biomass and replenishing of nutrients from deeper water. The increase in nutrients may give rise to an autumn phytoplankton and crustacean maximum, paralleled by shifts in algal species composition. (vii) Early winter starts around mid of November and is characterized by an increasing intensity of deep mixing and low irradiance.

Standardized time

The duration of the seasonal phases varied among years. To account for this meteorological year-to-year variation, we aligned the sampling dates to a standardized time axis. First, each sampling date (e.g. day 25 in phase ii in 1986) was scaled relative to the duration of the respective phase in that year (e.g. phase ii lasts 50 days in 1986) resulting in the relative sampling day (e.g. $25/50$). Multiplying the relative sampling day with the inter-annual mean duration of the respective phase (e.g. 46 days) yields the standardized day number of that sampling date (e.g. $25/50 \cdot 46 = 23$). Based on this method each sampling date can be assigned to a certain week in a standardized year. To display the seasonal biomass dynamics (shown in Fig. 4.2), we took the inter-annual median of the biomass data for every standardized week and then smoothed the data by averaging the medians of two adjacent weeks (moving average).

Mean relative biomasses

To evaluate the relative importance of a phytoplankton morphotype over the 21 years of sampling, we derived its mean annual relative biomass as follows: First, we calculated the relative biomass of each morphotype for every sampling date. Second, we averaged these relative biomasses among all dates within each year which yields the corresponding annual relative biomass of each morphotype. Finally, we derived the mean of these annual relative biomasses across years. This procedure reduces the influence of outliers at single dates, and gives equal weight to all sampling dates per year and all years which partly differed in their total biomass and sampling resolution. The relative importance of each morphotype during distinct seasonal phases (e.g. early spring) were computed accordingly by considering only the relative biomasses of the dates within that phase. The calculated mean relative biomasses allowed to infer the respective biomass-trait distributions since each morphotype represented a specific trait combination.

C:P ratio

We used the cellular carbon to phosphate mass ratio of phytoplankton (C:P) as an indicator for nutrient depletion which was measured at the standard sampling site in 1995 (Hochstädter 2000). The cellular C:P is more informative than the ambient phosphorous concentration in the water as phytoplankton can store phosphorous. Furthermore, most phytoplankton species can take up substantial amounts of phosphorous even at concentrations below the detection limit as they prevail in Lake Constance throughout summer. Vertical mixing intensity The vertical mixing intensity, determining the underwater light climate and losses of phytoplankton to the aphotic zone, was inferred from a one-dimensional hydrodynamic K - ε turbulent exchange model (Bäuerle et al.

1998; Gaedke 1998) and expressed as net exchange rate from the uppermost layer (0-8 m) to the deepest layer (20-100 m). It is closely related to the observed phytoplankton net growth during spring.

C.2. Trait data

Table C1: Morphotype number and name, its assigned trait values of defence, maximum growth rate r (d^{-1}) and phosphate affinity ($d^{-1}\,\mu mol^{-1}\,L$) according to Bruggeman (2011) and its taxonomic group of all 36 dominant phytoplankton morphotypes in Lake Constance. Two morphotypes (*Navicula* spp. and *Cymbella ventricosa*/*C. prostrata*) were not listed by Bruggeman (2011). Hence, we used trait values of the nearest genus for them (*Nitzschia* ssp. for both) having a similar longest linear dimension, cell volume and colony formation.

Morphotype number	Morphotype name	Defence	r	Phosphate affinity	Taxonomic group
1	*Anabaena* spp.	0.66	0.88	94.0	cyanobacteria
2	*Asterionella formosa*	0.79	1.6	56.0	diatoms
3	*Aulacoseira* spp.	0.77	1.5	18.0	diatoms
4	*Ceratium hirundinella*	0.89	0.24	1600.0	dinophytes
5	*Chlamydomonas* spp.	0.38	1.8	170.0	chlorophyta
6	*Chlorella* spp. & *Microcystis* spp.	0.69	1.7	45.0	chlorophyta
7	*Chrysochromulina parva*	0.73	1.0	160.0	haptophytes
8	*Cosmarium* spp.	0.84	0.95	72.0	chlorophyta
9	*Cryptomonas marssonii*	0.49	1.1	190.0	cryptomonads
10	*Cryptomonas rostratiformis*	0.5	1.1	200.0	cryptomonads
11	*Cryptomonas* spp.	0.45	1.2	140.0	cryptomonads
12	*Cyclotella* spp.	0.77	1.6	3.6	diatoms
13	*Cymbella ventricosa* & *C. prostrata*	0.54	1.8	150.0	diatoms
14	*Diatoma* spp.	0.76	1.4	210.0	diatoms
15	*Dinobryon* spp.	0.85	0.74	110.0	chrysophytes
16	*Erkenia subaequiciliata*	0.47	1.7	220.0	chrysophytes
17	*Eudorina elegans*	0.78	1.1	32.0	chlorophyta
18	*Fragilaria crotonensis*	0.84	1.3	50.0	diatoms
19	*Mallomonas* spp.	0.8	0.5	340.0	chrysophytes
20	*Mougeotia* spp.	0.77	1.5	87.0	chlorophyta
21	*Navicula* spp.	0.54	1.8	150.0	diatoms
22	*Nitzschia* spp.	0.54	1.8	150.0	diatoms
23	*Oocystis* spp.	0.6	1.5	190.0	chlorophyta

24	*Oscillatoria* spp.	0.53	1.0	99.0	cyanobacteria
25	*Pandorina morum*	0.82	0.92	46.0	chlorophyta
26	*Pediastrum* spp.	0.69	1.3	310.0	chlorophyta
27	*Peridinium* spp.	0.912	0.24	130.0	dinophytes
28	*Phacotus* spp.	0.34	1.6	430.0	chlorophyta
29	*Rhodomonas* spp.	0.1	1.7	550.0	cryptomonads
30	*Scenedesmus* spp.	0.63	2.1	45.0	chlorophyta
31	*Sphaerocystis schroeteri*	0.83	1.1	57.0	chlorophyta
32	*Staurastrum* spp.	0.85	0.84	150.0	chlorophyta
33	*Stephanodiscus neoastraea*	0.66	1.7	22.0	diatoms
34	*Stephanodiscus* spp.	0.64	1.8	13.0	diatoms
35	*Synedra* spp.	0.66	1.7	420.0	diatoms
36	*Tabellaria fenestrata*	0.8	1.2	210.0	diatoms

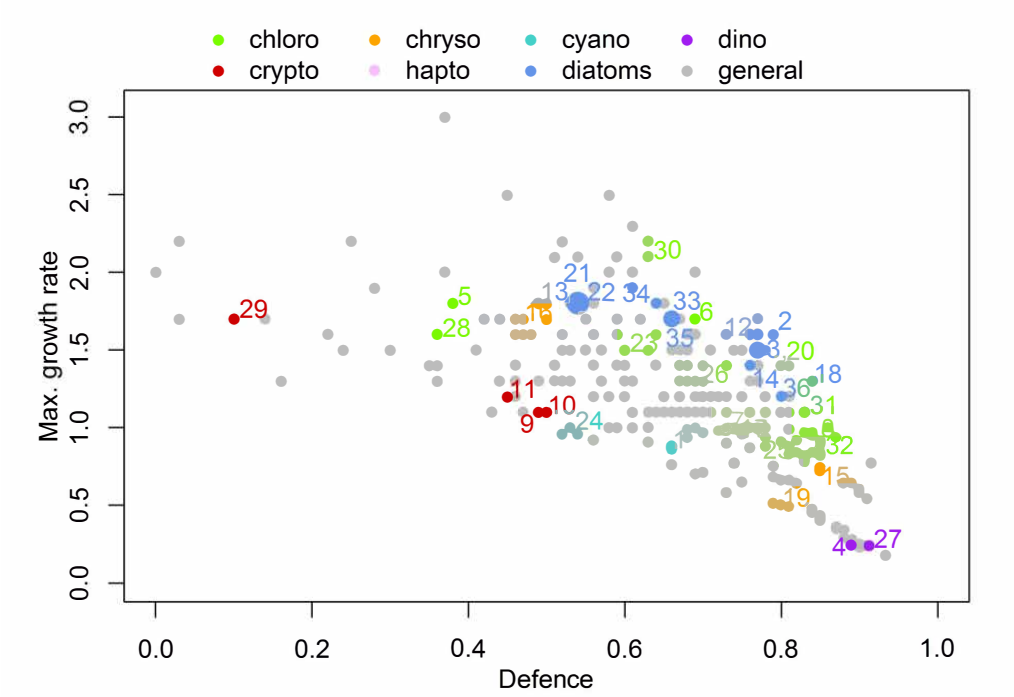

Figure C1: Defence δ and maximum growth rate r (d^{-1}) of the 36 most abundant phytoplankton morphotypes in Lake Constance (colored dots) and of all other phytoplankton morphotypes/species available at Bruggeman (2011) (grey dots). Colors indicate different taxonomic groups, i.e. chlorophyta, chrysophytes, cyanobacteria, dinophytes, cryptomonads, haptophytes and diatoms. The numbers refer to morphotype names listed in Table C1. Larger dots indicate that two or more morphotypes share the same trait combination.

C.3. Model description

The model

The following model equations describe the biomass dynamics of N phytoplankton species P_i and one zooplankton group Z:

$$\begin{aligned}\frac{dP_i}{dt} &= r_i\left(1-\frac{\sum_{i=1}^{N}P_i}{K}\right)P_i - \frac{G(1-\delta_i)P_iZ}{H+\sum_{i=1}^{N}P_i} - m_PP_i \\ \frac{dZ}{dt} &= \varepsilon\frac{G\sum_{i=1}^{N}(1-\delta_i)P_i}{H+\sum_{i=1}^{N}P_i}Z - m_ZZ\end{aligned} \tag{C1}$$

For simplicity, we assume logistic growth of phytoplankton with symmetric competition among all species to describe light- and nutrient-based growth. The phytoplankton species differ in their maximum growth rates r_i but share the same carrying capacity K and natural mortality m_P. Hence, the species with the highest r_i, performing well at high resource availability, is also the superior competitor under strong resource depletion (total phytoplankton biomass $\sum_{i=1}^{N}P_i$ close to K) in the model. The grazing of zooplankton on phytoplankton is described by a Holling type II function with the maximum grazing rate G and the half-saturation constant H. Phytoplankton species have different values of defence δ_i against zooplankton. We assume that defended phytoplankton cells also demand handling time of the predator equal to that of undefended phytoplankton but without energy gain because unselective feeders, which dominate in Lake Constance, are probably not able to discriminate between them and attack both (Ehrlich and Gaedke 2018). Accordingly, δ_i gives the probability of not being consumed (i.e. not ingested or digested) and surviving when attacked with values ranging between 0 (undefended) and 1 (completely defended). The probability of being consumed is then given by $(1-\delta_i)$, which scales the maximum grazing rate (see Eq. C1) and corresponds to the 'edibility', typically used in a limnetic context (Bruggeman 2011). The conversion efficiency of consumed phytoplankton into zooplankton biomass ε is assumed to be equal among the phytoplankton species. m_z represents the zooplankton mortality.

Trade-off curve

The trade-off curve between defence and maximum growth rate is given by the function

$$r_i = b(1-\delta_i)^a + c \tag{C2}$$

where a denotes the shape parameter, b the slope parameter and c the maximum growth rate of a completely defended species. If $a < 1$, the trade-off curve is concave. $a > 1$ gives a convex trade-off curve and $a = 1$ a linear one. We assume a concave trade-off

curve with $a = 0.4$, $b = 1.5\ d^{-1}$ and $c = 0.5 d^{-1}$ approximately reflecting the trade-off curve found in the trait data.

Parametrization and initialization

We considered different phytoplankton species with trait values spanning the whole feasible trait space. We determined the species trait values according to the following procedure: First, we defined a 15x15 grid of trait combinations covering the whole trait space (δ_i between 0 and 1, r_i between 0.0 and 2.0 d^{-1}). Second, we extracted only the feasible trait combinations below the trade-off curve. Third, we added 15 trait combinations exactly on the trade-off curve, equally spaced along the whole defence axis, which resulted in a total number of 184 trait combinations representing different phytoplankton species ($N = 184$). Based on measurements conducted at Lake Constance (Gaedke and Straile 1994; Gaedke 1998; Gaedke et al. 2002), we parametrized the model as follows: $K = 400 mg C m^{-3}$, $G = 1.3 d^{-1}$, $H = 80 mg C m^{-3}$, $\varepsilon = 0.3$, $m_P = 0.3 d^{-1}$, and $m_Z = 0.1 d^{-1}$ (spring scenario, low grazing pressure) or $m_Z = 0.02 d^{-1}$ (summer scenario, high grazing pressure). We initialized the model with random values from a uniform distribution between 0.1 and 4 $mg C m^{-3}$ for each P_i and between 1 and 20 $mg C m^{-3}$ for Z.

Numerical integration

The numerical integrations of the model were done with the lsoda solver of the deSolve package in R (Soetaert et al. 2010). We run the simulations for 4000 days and calculated the mean biomasses of the last 1000 days to detect the phytoplankton species dominating in the long-term. Furthermore, we checked which species survive in the short-term, that is, within the first 100 days. The extinction threshold was set to 10^{-4} $mg C m^{-3}$. We performed 100 simulations with different random initial conditions and averaged the mean biomasses and the time until extinction among all simulations.

C.4. Phytoplankton biomass dynamics

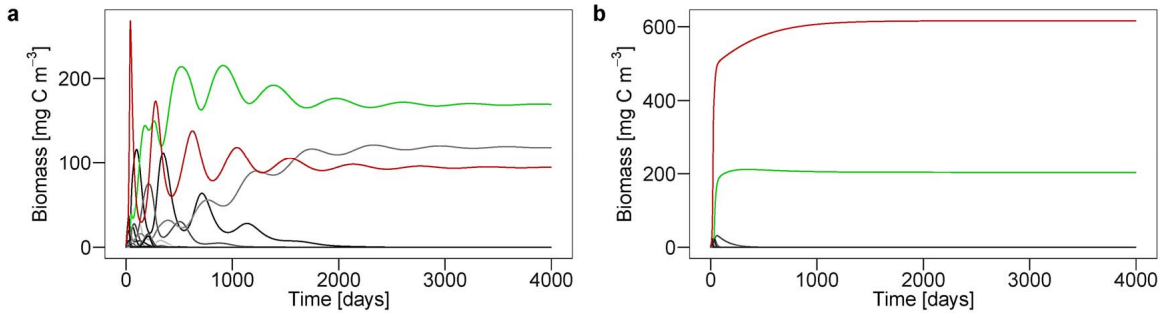

Figure C2: Simulated long-term biomass dynamics under low (a) and high grazing pressure (b) for one sample of randomized initial conditions. Grey and green lines represent phytoplankton species with different trait combinations where the green line marks the most dominant one. The red line corresponds to herbivorous zooplankton.

C.5. Convex trade-off curve

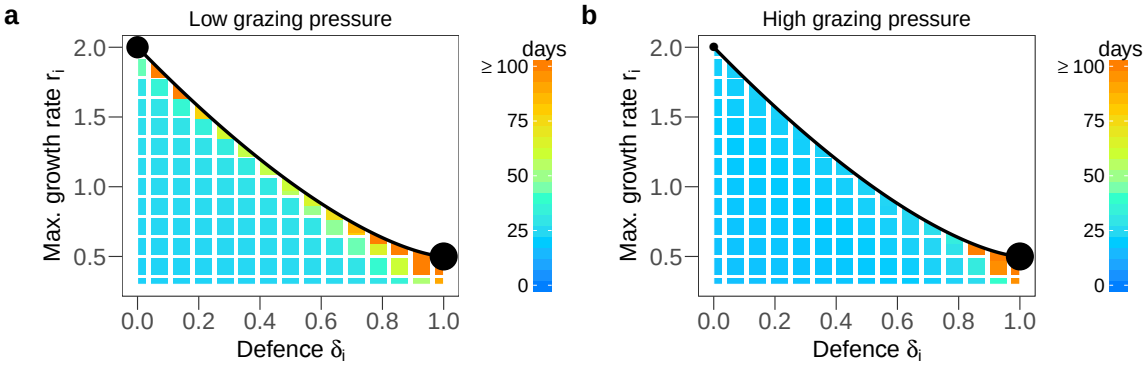

Figure C3: Model prediction on the competition outcome for a convex trade-off curve ($a = 1.5$) between defence δ_i and maximum growth rate r_i (black line) under (a) low grazing pressure on phytoplankton ($m_Z = 0.1\,d^{-1}$) and (b) high grazing pressure ($m_z = 0.02\,d^{-1}$). The black dots denote the trait combinations of phytoplankton species which survive in the long-term (fitness maxima), their size marks the mean relative biomass contribution between day 3000 and 4000 averaged among all simulations with randomized, different initial conditions. The colour grid displays the average time until extinction of the different trait combinations in the short-term, that is, within the first 100 days of the simulations. Note that trait combinations of species with r_i-values below 0.3 d^{-1} (i.e. below the rate of natural mortality) are not displayed.

Bibliography C

Bäuerle, E., Ollinger, D., and Ilmberger, J. (1998). Some meteorological, hydrological and hydrodynamical aspects of Upper Lake Constance. *Arch. Hydrobiol. Spec. Issues Advanc. Limnol.*, 53:31–83.

Bruggeman, J. (2011). A phylogenetic approach to the estimation of phytoplankton traits. *Journal of Phycology*, 47(1):52–65.

Ehrlich, E. and Gaedke, U. (2018). Not attackable or not crackable-How pre- and post-attack defenses with different competition costs affect prey coexistence and population dynamics. *Ecology and Evolution*, 8(13):6625–6637.

Gaedke, U. (1998). Functional and taxonomical properties of the phytoplankton community: Interannual variability and response to re-oligotrophication. *Archiv fuer Hydrobiologie*, 53:119–141.

Gaedke, U., Hochstädter, S., and Straile, D. (2002). Interplay between energy limitation and nutritional deficiency: Empirical data and food web models. *Ecological Monographs*, 72(2):251–270.

Gaedke, U. and Straile, D. (1994). Seasonal changes of trophic transfer efficiencies in a plankton food web derived from biomass size distributions and network analysis. *Ecological Modelling*, 75-76:435–445.

Hochstädter, S. (2000). Seasonal changes of C:P ratios of seston, bacteria, phytoplankton and zooplankton in a deep, mesotrophic lake. *Freshwater Biology*, 44(3):453–463.

Rocha, M. R., Vasseur, D. A., and Gaedke, U. (2012). Seasonal Variations Alter the Impact of Functional Traits on Plankton Dynamics. *PLoS ONE*, 7(12):e51257.

Soetaert, K., Petzoldt, T., and Setzer, R. W. (2010). Package deSolve: Solving Initial Value Differential Equations in R. *Journal Of Statistical Software*, 33(9):1–25.

Appendix D - Chapter 5

D.1. Temperature dynamics

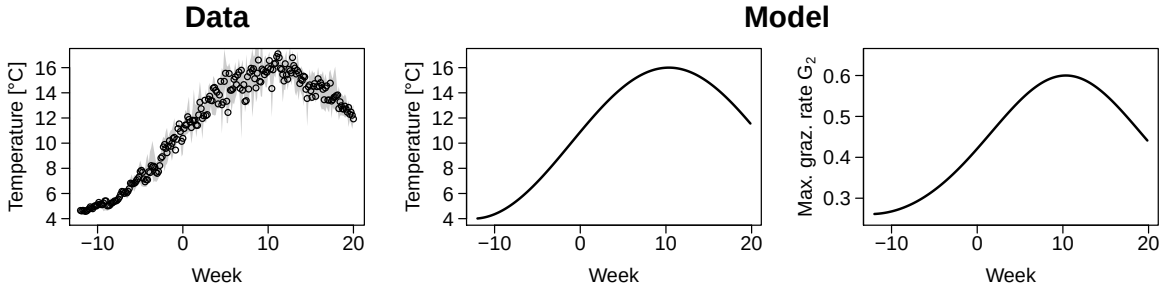

Figure D1: Interannual median and the respective interquantile range of daily temperature measurements from 1987 to 1996, simulated temperature dynamics and change of the maximum grazing rate of H_2 in dependence of the temperature.

D.2. Model simulations without temperature dynamics

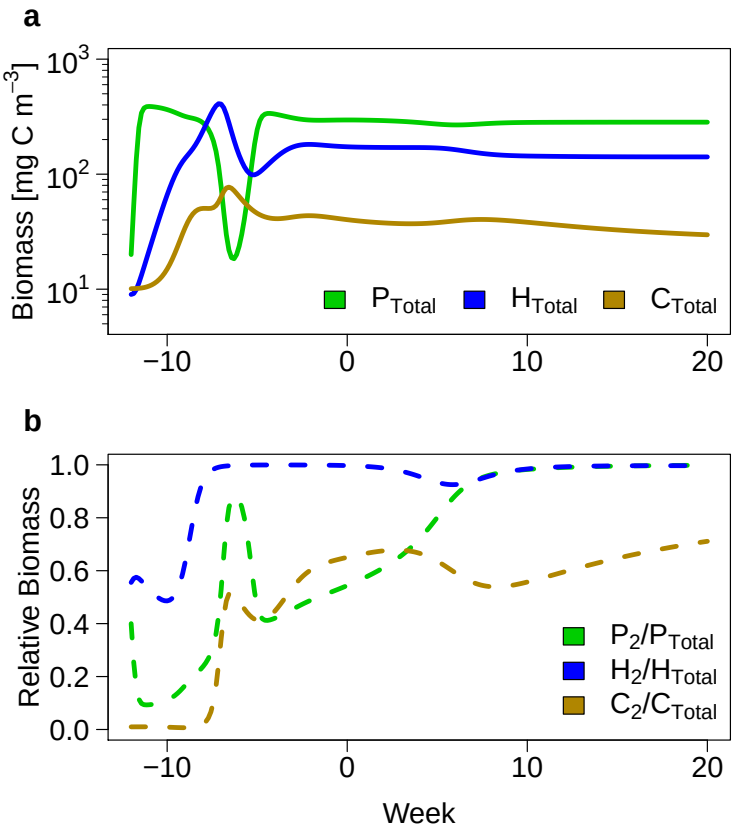

Figure D2: Numerical simulations of biomass (a) and trait dynamics (b) for the model without temperature dependency in growth, grazing and attack rates. P_{Total} denotes the total phytoplankton biomass, H_{Total} the total herbivore biomass, C_{Total} the total carnivore biomass, P_2 the biomass of less-edible phytoplankton, H_2 the biomass of large herbivores and C_2 the biomass of large carnivores.